Contribution to the Coordination of MPC Strategies for Distributed Systems, Applied to the Electric Power Production

John Sandoval-Moreno

UNIVERSITÉ DE GRENOBLE

THÈSE

pour obtenir le grade de

DOCTEUR DE L'UNIVERSITÉ DE GRENOBLE

Spécialité : **Automatique et Productique**

Arrêté ministériel : 7 août 2006

Présentée par
John Anderson SANDOVAL MORENO

Thèse dirigée par **Gildas BESANÇON** et
codirigée par **John MARTÍNEZ**

préparée au sein du **GIPSA-Lab**
dans **l'École Doctorale Électronique Électrotechnique Automatique Traitement du Signal (EEATS).**

Contribution à la Coordination de Commandes MPC pour Systèmes Distribués, Appliqués à la Production d'Énergie.

Thèse soutenue publiquement le **28 Novembre 2014**,
devant le jury composé de:

M. Didier GEORGES
Professeur, Grenoble-INP, Président
M. Sorin OLARU
Professeur, Supelec, Rapporteur
M. Gilney DAMM
Maître de Conférences, Université d'Evry Val d'Essonne, Rapporteur
M. Carlos OCAMPO MARTINEZ
Maître de Conférences, Universidad Politécnica de Catalunya, Examinateur
M. Gildas BESANÇON
Professeur, Grenoble-INP, Directeur de thèse
M. John MARTÍNEZ
Maître de Conférences, Grenoble-INP, Co-Directeur de thèse

Acknowledgments

I would like to thank the jury members of this thesis, specially to Mr. Didier Georges (Grenoble-INP) for being the president of the jury. In the same way, I would like to extend my gratitude to Mr. Sorin Olaru (Supelec) and Mr. Gilney Damm (Universitè d'Evry Val d'Essone), that dedicated their time and attention for writing the reports of this work, as well as Mr. Carlos Ocampo (Universidad Politécnica de Catalunya) for having evaluated this thesis.

To my directors, Mr. Gildas Besançon and Mr. John Martínez, both teachers and researchers at Grenoble-INP for guiding me during this years. The work with you has been really enriching, giving me the constant motivation to follow the scientific work during the rest of my life. Many thanks for your patience, support and non scientific talks, during coffee-pauses and other opportunities such such conferences, group integrations, casual meetings and so on.

I also address my acknowledgement to the staff of GIPSA-Lab, and the professors of the laboratory, in special to Mr. Oliver Sename, Mr. Christian Commault and Ms. Alina Voda for all their collaboration during my stance at GIPSA-Lab. Also, thanks to my colleagues of GIPSA-Lab: Tahar, Soheib, Simona, Humberto, Rogelio, Federico, Abraham, Juan, Uziel, Mihail, along others that have crossed with me in the lab.

To my friends, always present Ignacio Rubio, Felipe Castillo, Maria Rivas, Valentina Ciarla, I owe you more than you think. Gracias amigos por estar presentes y hablar de todo y de nada. Esas experiencias me han ayudado a ver la vida de otra forma y a seguir adelante. Mil y mil gracias.

Finally, my words are not enough for recognize to my parents, Luis Alberto and Luz Marina for helping me to become what I am. Gracias por enseñarme que los sacrificios valen la pena y que cada paso es enorme en esta vida. A ustedes, les debo todo.

Also, to my wife Yaramileth, my "little bunny". These years would be really tough without your presence. My life would not be the same and I'm glad to still walking through the life, taking your hand and following our dreams.

Thanks to all, John Sandoval.
Grenoble, France, February, 2015.

Contents

List of Acronyms **xv**

1 INTRODUCTION GÉNÉRALE **1**

1.1 Contexte général de la thèse 1

1.2 Définition des problématiques et motivations 2

1.2.1 Contextes historiques et technologiques 2

1.2.2 Contexte scientifique 6

1.3 Structure de la thèse 7

1.4 Contributions Principales 9

1.5 Liste de Publications 9

2 MAIN INTRODUCTION **11**

2.1 General Context of the Thesis 11

2.2 Problems definitions and motivations 12

2.2.1 Historical and technological contexts 12

2.2.2 Scientific context 16

2.3 Structure of the thesis 17

2.4 Main contributions 18

2.5 Publications list 19

3 STATE-OF-THE-ART ON LARGE SCALE SYSTEMS AND RENEWABLE POWER GENERATION TECHNOLOGIES **21**

3.1 Control configurations for large scale systems 22

3.1.1 Centralized control structure 23

3.1.2 Decentralized control structure 24

3.1.3 Distributed control structure 25

3.1.4 Distributed-coordinated control structure 26

3.1.5 Discussion and additional remarks 28

3.2 Operative principles of some alternative electric power generation technologies . . . 29
3.2.1 Hydroelectric Power Generation Systems . . . 30
3.2.1.1 Energy conversion principles . . . 30
3.2.1.2 Typical control objectives in hydroelectric power generators . . . 31
3.2.1.3 Advantages and disadvantages of the hydroelectric power generator 32
3.2.2 Wind Turbines Power Generation Systems . . . 33
3.2.2.1 Energy conversion principles . . . 33
3.2.2.2 Typical control objectives in wind power generators . . . 34
3.2.2.3 Advantage and disadvantage of wind power generator . . . 36
3.2.3 Photovoltaic Power Generation Systems . . . 37
3.2.3.1 Energy conversion principles . . . 37
3.2.3.2 Typical control objectives in photovoltaic power generators . . . 38
3.2.3.3 Advantages and disadvantages of the photovoltaic power generator 40
3.2.4 Fuel Cells Power Generation Systems . . . 40
3.2.4.1 Energy conversion principles . . . 40
3.2.4.2 Typical control objectives in fuel cell power generators . . . 42
3.2.4.3 Advantages and disadvantages of the fuel cell power generator . . 43
3.2.5 Comparison of the alternative power generation technologies . . . 44
3.3 Conclusions . . . 44

4 THEORETICAL BACKGROUND ON MODEL PREDICTIVE CONTROL AND INVARIANT SETS 47

4.1 Recalls on Model Predictive Control . . . 48
4.1.1 Unconstrained MPC Formulation . . . 48
4.1.2 Description of constraints for MPC solution . . . 50
4.1.3 Solution of the constrained MPC problem . . . 53
4.1.4 Adaptation of the geometric characteristic . . . 56
4.1.5 Final remarks for the explicit solution algorithm . . . 58
4.1.6 Conclusions . . . 59
4.2 Recalls on Invariant Sets Construction . . . 60

4.2.1 Robust invariant sets based on the bounded-real lemma 61
4.2.2 Computation of polyhedral RPI sets from ellipsoidal ones 62
4.2.3 Computation of invariant sets by expansion of polyhedral sets 64
4.2.4 Illustrative example 65
4.2.5 Computation of robust invariant sets for a family of linear systems 67
4.2.6 Illustrative example 69
4.2.7 Concluding remarks 70
4.3 Conclusions 70

5 CONTRIBUTION TO POWER MAXIMIZATION IN WIND TURBINES AND PREDICTIVE CONTROL IN MICROGRIDS 71

5.1 Maximization of power production by wind-based generators without wind speed sensor 72
5.1.1 Principles of the proposed technique 72
5.1.1.1 Mathematical modeling for the optimal power production strategy 73
5.1.1.2 Analysis of the mathematical model for control purposes 75
5.1.2 Extended Kalman Filter for the estimation of the power characteristics . . 75
5.1.3 Power coefficient polynomial approximation and optimal generator speed estimation 76
5.1.4 Control strategies for power production maximization in wind turbines . . . 78
5.1.4.1 Control strategy for the power converter current 78
5.1.4.2 Control strategy for the generator speed 79
5.1.5 Validation of the technique by simulation 79
5.1.5.1 Validation of the z-estimator block 81
5.1.5.2 Validation of the polynomial estimator 81
5.1.5.3 Validation of the full control strategy 82
5.1.6 Experimental small scale prototype 84
5.1.7 Concluding remarks 85
5.2 Power management of a microgrid with explicit MPC-based control 85
5.2.1 Description of the considered microgrid 86
5.2.2 Low-level control strategies and reduced microgrid model 87

5.2.2.1 Inductor current power converter control strategies 87
5.2.2.2 Microgrid power flow modeling 89
5.2.3 Definition of the constrained optimization problem 90
5.2.4 Computer simulation and control strategy evaluation 92
5.2.5 Concluding remarks 93
5.3 Conclusions 94

6 CONTRIBUTION TO MPC DECOMPOSITION AND DISTRIBUTED COORDINATION UNDER CONSTRAINTS 95

6.1 Centralized MPC problem description with interactions considerations 96
6.1.1 Centralized MPC 96
6.1.2 Centralized MPC problem with interactions consideration 97
6.2 Optimization problem decomposition and coordination 100
6.2.1 Problem decomposition and explicit local solutions 100
6.2.2 Global coordination based on local explicit solutions 102
6.3 Analysis of the proposed approach 104
6.3.1 Complexity of the coordination problem 104
6.3.2 Structure of local controllers and coordination vector influence 106
6.3.3 Coordination period and subsystems sampling periods: performance of the subsysems 107
6.3.4 Control structure for subsystems 109
6.4 Illustrative example 110
6.5 Conclusions 113

7 STABILITY AND PERFORMANCE ANALYSIS OF CONSTRAINED CONTROL SYSTEMS 115

7.1 Stability and Performance of Systems under Constrained Model Predictive Control 116
7.1.1 System dynamics, admissible sets and control structure for the MPC case . 117
7.1.2 Stability analysis of the constrained MPC solution 117
7.1.3 Performance analysis of the contrained MPC solution using invariant sets . 118
7.1.3.1 Analysis of the closed-loop system 119

7.1.3.2 Computation of α_{min} for the MPC case 120

7.1.3.3 Computing the ellipsoidal invariant set 121

7.1.3.4 Obtention of the ellipsoidal invariant sets 121

7.1.4 Recursive algorithm for computing the minimal robust invariant set 121

7.1.4.1 Selection of initial polyhedral set 122

7.1.4.2 Adaptation of the constraints polyhedral set at each iteration . . . 122

7.1.4.3 Algorithm for computing the mRPI 125

7.1.5 Illustrative Example 126

7.2 Global Performance Analysis for a Distributed Constrained Control System with Coordination 127

7.2.1 System dynamics, admissible sets and control structure for the distributed coordinated control scheme 127

7.2.2 Stability analysis of the distributed coordinated control scheme 128

7.2.3 Performance analysis of the distributed coordinated control using invariant sets 129

7.2.3.1 Analysis of the closed-loop system 129

7.2.3.2 Computation of $\bar{\alpha}_{min}$ for the distributed coordinated control scheme 130

7.2.3.3 Computing the ellipsoidal invariant set 132

7.2.3.4 Obtention of the ellipsoidal invariant set 132

7.2.4 Recursive algorithm for computing the minimal robust invariant set 133

7.2.4.1 Selection of initial polyhedral set 133

7.2.4.2 Adaptation of the constraints polyhedral set at each iteration . . . 133

7.2.4.3 Algorithm for computing the mRPI 134

7.2.5 Performance analysis for distributed non-coordinated case 135

7.2.6 Illustrative example 136

7.3 Global Performance analysis by distrubuted-computed invariant sets 138

7.3.1 Expressions for the analysis in the distributed coordinated system 138

7.3.2 Recursive algorithm for computing the local minimal robust invariant set . 139

7.3.3 Illustrative example 141

7.4 Conclusions 141

8 APPLICATION TO DISTRIBUTED POWER GENERATION CONTROL VIA SIMULATION CASE-STUDIES 143

8.1 Two-generator microgrid 143

8.1.1 Considered model and numerical values 145

8.1.2 Control objectives 147

8.1.3 Simulation results 148

8.1.4 Concluding remarks 151

8.2 Alternative generation-based microgrid 151

8.2.1 Dynamical model and system parameters 152

8.2.2 Control objectives 154

8.2.3 Simulation results 155

8.2.3.1 Concluding remarks 157

8.3 Conclusions 158

9 CONCLUSIONS AND FUTURE WORKS 159

A Matrix Developments for the MPC and Distributed-Coordinated Strategies 163

A.1 Matrices for the formulation of the centralized MPC problem 163

A.2 Matrices for the formulation of the centralized MPC problem with interactions consideration 166

A.3 Definition of the constraints polyhedron for the coordinator optimization problem 168

B State Space Model Definition for Estimating the Parameter z to Maximize the Power Production in Wind Speed Sensorless Turbines 169

Bibliography 171

List of Figures

1.1 Configuration typique d'une système de génération distribué 5

2.1 Typical configuration of a distributed power system 15

3.1 General scheme of the Centralized Control Structure 23

3.2 General scheme of the Decentralized Control Structure 24

3.3 General scheme of the Distributed Control Structure 26

3.4 Structure of the Interaction-Prediction Distributed Coordinated Control Structure 27

3.5 Structure of the Price-Driven Distributed Coordinated Control Structure 27

3.6 General schemes of hydroelectric plants: Dam-based and water deviation-based hydro plants 30

3.7 Block Diagram of the AGC for a Typical Hydroelectric Unit [1] 31

3.8 Block Diagram representing the AVR with PSS [1] 32

3.9 General scheme of wind power plant, with a simplified power conversion unit . . . 33

3.10 Typical curves of the power coefficient for various pitch angles 34

3.11 Steady-state power curves of a wind turbine with constant pitch angle 34

3.12 Basic Schemes of Power Controllers for Wind Turbines 36

3.13 PV cell equivalent model 37

3.14 Norton equivalent of a PV generator 38

3.15 I-V curve for an MSX60 solar module [2] 39

3.16 PV module and Boost converter 39

3.17 Fuel Cell Power Generator General Schemes 41

3.18 Fuel cell polarization curve 42

3.19 Fuel cell interconnection topologies 44

4.1 Geometric interpretation of the QP problem 54

4.2 Geometric interpretation of the QP problem after the coordenates transformation . 55

4.3 Characteristic regions of the input space 57

4.4 Adaptation of the geometric solution for the Case 1. 57

4.5 Adaptation of the geometric solution for the Case 2. 58

4.6 Invariant Set Representation 62

4.7 Invariant set representation for the illustrative example 66

4.8 Example of shrinkling procedure from an ellipsoidal invariant set for obtaining an approximation of the minimal robust invariant set 66

4.9 Example of expanding procedure from an ellipsoidal invariant set for obtaining an approximation of the minimal robust invariant set 67

4.10 Example for obtaining the mRPI approximation for a family of linear systems . . . 70

5.1 Scheme of the considered wind power generation system. 73

5.2 Detailed armature circuit with the DC/DC power converter 73

5.3 Block diagram of the control algorithm for the proposed power maximization strategy. 79

5.4 Block diagram of the proposed power maximization strategy for wind turbines. . . 80

5.5 Performance of the state estimator for z under noisy wind speed profile 81

5.6 Original and reduced order C_p curves for optimal power production in the 6 kW EWPG 82

5.7 Block diagram for the alternative power maximization strategy using wind speed measurement 83

5.8 Simulation results of the proposed power production strategy for electric wind power generation systems, without - or with, wind speed sensor. 83

5.9 Small scale wind power generation system prototype at Gipsa-Lab 84

5.10 Fuel cell, Wind turbine and Supercapacitor connection for the power system 87

5.11 Step responses for the inductor current in closed loop 89

5.12 Reduced model scheme of the power system 89

5.13 Unconstrained (left) and Constrained (right) MPC control strategies application to the proposed power system 93

6.1 Information Flow for the Coordination Algorithm 103

6.2 Serial fuel cell interconnection topology with Buck and Boost converters 105

6.3 Information Flow for the Coordination Algorithm 106

6.4 Illustration of coordination and sampling periods 108

6.5 Illustration of coordination and sampling periods when local sampling times are different between subsytems, and and from the coordination one. 109

6.6 Performance of the proposed second order system under centralized MPC vs proposed distributed coordinated approach 111

6.7 Perform of the proposed second order system with the coordinated control approach, when subsystem 2 loses the coordination vector 113

7.1 Small gain theorem 118

7.2 Closed-loop system representation with Model Predictive Controller 119

7.3 Scheme for chosing the limit vector when updating the inputs set 123

7.4 Selection of the admissible inputs set for the MPC strategy 125

7.5 Invariant sets for evaluating the performance of a constrained control system . . . 126

7.6 Closed-loop system representation with constrained price-driven coordination . . . 130

7.7 Invariant sets for evaluating the performance of the descentralized coordinated system 137

7.8 Information flow for computing the local mRPI sets under the coordination scheme 140

7.9 Invariant sets for evaluating the performance of the descentralized coordinated system 141

7.10 Invariant sets for evaluating the performance of the descentralized coordinated system 142

8.1 Configuration of the proposed two-source power generation system 144

8.2 Performanace of the proposed system with the coordinated control approach in Test 1 149

8.3 Performanace of the proposed second order system with the coordinated control approach, when subsystem 2 loses the coordination vector (Test 2) 150

8.4 Configuration of the proposed two-area power generation system 151

8.5 Control structure for each local power generation system 152

8.6 Simulation Results of Centralized MPC and Distrubuted-Coordinated Approach (DMPC) for the Multisource application (Bold: Area 1, Light: Area 2) 156

8.7 Approximations of local minimal invariant sets for the proposed microgrid 157

List of Tables

1.1 Consommation d'Énergie Mondiale Totale et Technologies de Génération - 2013 [3] 4

1.2 Consommation d'Énergie Européen Totale et Technologies de Génération - 2013 [4] 4

2.1 Total World Power Consumption and Providing Generation Technologies - 2013 [3] 14

2.2 Total Europan Power Consumption and Providing Generation Technologies - 2013 [4] 14

3.1 Characteristics of some fuel cells technologies [5] 41

3.2 Relevant properties of the analyzed power generation technologies 45

5.1 6-kW Wind Generator Parameters 80

5.2 Power system characteristics 87

5.3 Current loops transfer functions and PI controllers 88

6.1 Performance comparison for the proposed system under centralized MPC vs under proposed distributed coordinated approach 112

8.1 Parameters for the Two-Generator Microgrid Example 147

8.2 Parameters for the Two areas microgrid 154

List of Acronyms

AC	Alternate Current
DC	Direct Current
FC	Fuel Cell
FCV	Fuel Cell Vehicle
HEV	Hybrid Electric Vehicle
MPC	Model Predictive Control
PV	Photovoltaic
RHC	Receding Horizon Control
RPI	Robust Positive Invariant
SoC	State of Charge

Chapter 1

INTRODUCTION GÉNÉRALE

Contents

1.1 Contexte général de la thèse 1
1.2 Définition des problématiques et motivations 2
1.2.1 Contextes historiques et technologiques 2
1.2.2 Contexte scientifique 6
1.3 Structure de la thèse 7
1.4 Contributions Principales 9
1.5 Liste de Publications 9

Dans ce chapitre on présent le contexte général de cette thèse, ainsi que les principaux problèmes qui seront examinés conjointement avec leurs motivations correspondantes. Dans la dernière partie on présente un aperçu des résultats obtenus.

1.1 Contexte général de la thèse

Cette thèse a été partiellement financée par le gouvernement colombien à travers de COLCIENCIAS (Departamento Administrativo de Ciencia, Tecnología e Innovación), par l'intermédiaire d'une bourse "Francisco José de Caldas" pour le développement des études doctorales à l'étranger. L'objectif de telle subvention est de soutenir des chercheurs colombiens de bon rendement académique, pour recevoir de l'enseignement de haut niveau dans des domaines stratégiques pour le développement de la Colombie, en incluant les domaines considérés dans ce travail : **Automatique** et **Systèmes de Production d'Énergie Électrique**.

Cette thèse a été développé entre Octobre 2011 et Octobre 2014, au sein des équipes de recherche SYSCO[1] et SLR [2] du Département d'Automatique du laboratoire GIPSA-Lab [3]. Le laboratoire est affilié à l'École Doctorale EEATS[4] de l'Université de Grenoble.
Les sujets suivants font partie du cadre général de cette thèse:

- L'utilisation de la commande prédictive sous contraintes comme une méthodologie systématique et bien connu pour la commande des systèmes de production d'électricité de petite et grande taille.

[1] Systèmes non Linéaires et Complexité
[2] Systèmes Linéaires et Robustesse
[3] Grenoble Image Parole Signal Automatique
[4] Électronique, Électrotechnique, Automatique et Traitement du Signal

- L'utilisation de la décomposition hiérarchique du modèle dynamique et la coordination à base de la commande prédictive pour commander les systèmes de production d'électricité distribués.
- L'utilisation des principes d'estimation d'état optimale pour maximiser la production d'énergie dans les éoliennes.
- L'utilisation des ensembles invariants robustes pour évaluer la performance des systèmes coordonnés sous contraintes.

Cette thèse représente une extension de la thèse formulée par **Jennifer Zárate-Florez** [6] "Étude de Commande par Décomposition-Coordination pour l'Optimisation de la Conduite de Vallées Hydroélectriques", également réalisée à GIPSA-Lab, qui porte sur l'étude des régimes de coordination (plus précisément, coordination par prédiction d'interactions et coordination par prix) pour la commande des vallées hydroélectriques. Ce travail donne quelques bases pour la gestion des systèmes de production d'électricité distribués par à travers de la coordination des structures de commande prédictive à niveau local, avec une attention particulière au cas des générateurs hydroélectriques qui interagissent entre eux. Dans ce mémoire on présente, des éléments supplémentaires pour analyser la performance du système commandé par ces techniques et on propose leur applicabilité sur d'autres technologies de production d'énergie, sont envisagés.

1.2 Définition des problématiques et motivations

Premièrement, on présente les principaux problèmes considérés dans cette thèse, ainsi que leurs motivations.

1.2.1 Contextes historiques et technologiques

Pendant des siècles, le développement de la société a été lié à l'exploitation des différentes classes de ressources énergétiques. Sans aller trop loin dans le temps, au cours de la révolution industrielle, par exemple, la puissance de la vapeur - obtenu par l'eau bouillante à partir du bois, a contribué au développement des moyens de transport. Lié à ce progrès, l'exploration et l'exploitation du pétrole en tant que source d'énergie a permis de développer des applications plus adaptés aux véhicules, en donnant les premières conceptions d'applications portables. Aujourd'hui, l'utilisation de combustibles fossiles est généralisée dans la société, très largement présente dans le secteur des transports (voitures, avions, navires, entre autres), donnant lieu à des nouveaux problèmes maintenant liés à l'environnement, comme le réchauffement global, l'exploration des nouveaux gisements de pétrole ou de l'obtention des nouvelles sources d'énergie, etc.
Cependant, dans cette même période de la révolution industrielle, les systèmes de production d'énergie électrique (SPEE) en fonction des propriétés thermoélectriques ou hydroélectriques, ont également été mises au point. Depuis ce temps, la demande d'électricité a augmenté année après année, en nécessitant des investissements et de l'innovation en envisagent trois objectifs principaux:

- Assurer la production d'énergie, ainsi que sa distribution aux industries et aux résidences, tout en réduisant l'empreinte environnementale autant que possible.
- Maintenir la stabilité des systèmes de puissance, dans le sens de maintenir l'amplitude de la tension et les variations de fréquence dans les gammes admises, en tenant compte des

caractéristiques du générateur d'électricité, le profil de demande de charge et la topologie du réseau.

- Assurer l'extensibilité des systèmes de puissance, avec l'objectif d'élargir la capacité installée et permettre l'inclusion de différentes types de technologies de production d'électricité.

Aujourd'hui, les efforts sont dirigés à maintenir et à renforcer les capacités de la production d'électricité, tout en réduisant, en même temps, l'empreinte écologique dans tous les aspects possibles. En outre, depuis les années 80s, les développements suivants ont été considérés pour générer l'électricité requise dans différents niveaux sociaux, y compris les industries et les secteurs résidentiels :

- **Développement des SPEE sur la base de sources d'énergie renouvelables:** Par exemple, des grandes progrès ont été réalisés dans les générateurs à base de panneaux photovoltaïques, éoliennes sur terre et en mer, hydroliennes, piles à combustible, générateurs géothermiques, ainsi qu'une meilleure intégrabilité des générateurs hydroélectriques de petite taille.
- **Remplacement progressif des SPEE basé sur des sources chimiques ou non renouvelables:** Sont compris les remplacements des centrales nucléaires, ou des centrales thermoélectriques à base d'huile ou de charbon, ainsi que des grandes centrales hydroélectriques pas nécessaires (comme l'hydroélectrique «Trois Gorges» en Chine), en raison des niveaux élevés de contamination et les dommages potentiels pour l'environnement.
- **Développement en continu des technologies des véhicules électriques et à base d'hydrogène - Véhicules Électriques Hybrides (VEH) et / ou véhicules à pile à combustible (VPC):** La réduction de la combustion de carburants à base de pétrole sera importante dans les prochaines années, tandis que les besoins d'électricité pour la recharge des véhicules augmentera.
- **Développement de micro réseaux isolés:** Ces réseaux sont communément conçus pour fournir un montant de base d'électricité pour les populations ou les applications telles que les transmetteurs de radio, qui ne peuvent pas se connecter au réseau électrique. Les solutions robustes et réalisables ont été de plus en plus étudiées ces dernières années et les nouvelles tendances se concentrent maintenant sur l'intégration avec le réseau de distribution, afin d'échanger de l'énergie en fonction des conditions opératoires.
- **Développement des réseaux de communication:** Cela vient avec le développement des installations informatiques, et a donné naissance à la notion de ce qu'on appelle Smart Grid, dans laquelle la coordination des nombreuses entités (en comprenant les producteurs d'électricité à grande échelle, des compensateurs de réseau, des stockages d'énergie (batteries), les générateurs locaux ou des charges, etc) est souhaitée afin de maintenir la stabilité et l'efficacité du réseau local. L'imbrication des petits réseaux intelligents est l'un des objectifs, ainsi que le développement des algorithmes efficaces de coordination et reconfiguration du réseau.

En considérant le développement des technologies de production d'énergie, chaque année des informations statistiques peuvent être obtenues en ce qui concerne l'aspect des technologies de production d'énergie et son exploitation dans la société. Par exemple, le tableau 1.1 présente des informations comparatives en termes de consommation d'énergie à travers le monde pour l'année 2013. Au même temps, le tableau 1.2 comprend des informations sur la consommation d'énergie européenne pour l'année 2013.

Table 1.1: Consommation d'Énergie Mondiale Totale et Technologies de Génération - 2013 [3]

Technologie de Génération	**Consommation (MToe) - (%)**
Hydroélectrique	855.8(6.58%)
Photovoltaïque	28.2(0.22%)
Éolienne	142.2(1.09%)
Autres Alternatives (Géothermique, Biomasse, H_2...)	388.2(2.98%)
Biocombustible	0.653(0.005%)
Pétrole	4185.1(32.17%)
Charbon	3826.7(29.42%)
Gaz	3020.4(23.21%)
Nuclear	563.2(4.33%)
Total	**13010 (100%)**

Table 1.2: Consommation d'Énergie Européen Totale et Technologies de Génération - 2013 [4]

Technologie de Génération	**Consommation (MToe) - (%)**
Alternatives	209.7(12.58%)
Pétrole	556.6(33.4%)
Charbon	286.5(17.2%)
Gaz	386.8(23.2%)
Nuclear	226.3(13.58%)
Total	**1666.2 (100%)**

On voit comment la production d'électricité à partir de sources renouvelables représente environ 11% de la consommation mondiale d'énergie, et en Europe, cet indice est similaire (environ 12,5%). Cependant, le 89% restante de la consommation d'énergie (87,5% pour l'Europe) est représenté par les technologies traditionnelles de production d'énergie.
La pénétration de la production d'énergie renouvelable est en effet en augmentation chaque année, influencée principalement par le développement scientifique de différentes disciplines. Par exemple, le développement des unités de conversion d'énergie (c'est-à-dire de nouveaux alliages pour les panneaux photovoltaïques, les nouveaux matériaux pour membranes et électrodes dans les piles à combustible) nécessite la connaissance de physique, chimie et science des matériaux pour transformer autant d'énergie que possible. La transmission et le conditionnement de l'énergie entre l'unité de conversion et l'application finale demande des infrastructures et des circuits qui sont conçus par des ingénieurs électriques et électroniques électrique. Dans la même ligne, le suivi et la commande de ces applications de puissance nécessite des évolutions techniques données par les experts en communication, 'informatique, économie et automatique.
En considérant la quantité de nombreuses disciplines incluses dans le développement de la production d'électricité, dans la présente étude seront traités des défis particuliers à la **contrôle automatique** et **générateurs électriques**. Dans les systèmes d'énergie, chaque générateur est commandé localement en assurant la production d'énergie, tout en maintenant la stabilité locale sous contraintes d'opération. Par exemple, dans une installation photovoltaïque, la production

d'électricité est maximisée en présence de la lumière solaire et cette énergie doit être répartie entre le réseau et le système de stockage local, qui pourrait fournir de l'énergie pendant la période nocturne.
Dans les systèmes de puissance, il existe des *systèmes coordinateurs de réseau*, qui communiquent, à toutes les unités de production réparties dans sa zone, la puissance demandée pour les heures suivantes. Un tel système utilise des algorithmes d'optimisation hors-ligne qui considèrent des informations économiques, environnementales et statistiques pour l'évaluation et le calcul de la puissance nécessaire pour être générée par chaque unité. Toutefois, la planification est effectuée dans des conditions «idéales», et des événements tels que des sûr/sous-chargement locales, des défauts des lignes de transmission ou de générateurs, des changements des conditions météorologistes, entre autres, auront une incidence sur le comportement idéalisée du système de puissance. La figure 1.1 montre la configuration typique d'une portion du système de puissance avec générateurs distribués, systèmes de stockage et charges, ainsi que le système de coordination, assigné à cette portion du réseau. Une des solutions est faire la mise à jour des consignes des

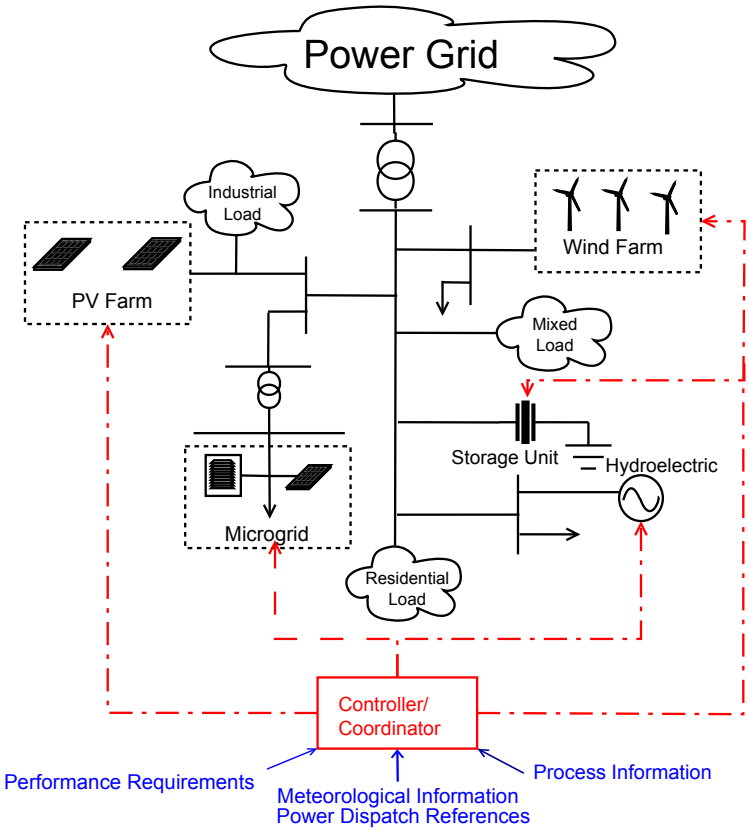

Figure 1.1: Configuration typique d'une système de génération distribué

générateurs, ce qui est une procédure classique et commune dans les centrales hydroélectriques et thermoélectriques. Dans ce cas, les *opérateurs locaux* (ingénieurs et techniciens), en s'appuyant sur des critères empiriques, échangent avec le système de répartition et/ou les stations entourant les nouvelles références pour faire face aux événements actuels. Par ailleurs, cette procédure et les mesures correctives ne sont pas instantanées, et leurs effets peuvent affecter la stabilité du réseau électrique, en dérivant éventuellement vers des pannes locales ou même globales. En fait, cette pratique n'est pas convenable quand les SPEE sont à base d'énergies renouvelables, parce que leurs algorithmes utilisent des techniques de maximisation de la production d'énergie qui sont *a priori* autonomes et adaptatives aux changements des conditions météorologiques en temps réel.

Dans ce contexte, il y a deux défis que nous aimerions examiner plus particulièrement dans cette thèse:

- **Stratégies de coordination.**
  En considérant, en effet, les exigences des générateurs d'électricité à base d'énergies renouvelables, ainsi que la croissante demande d'électricité (en raison du nombre croissant d'installations de services de communication et des stations de recharge des véhicules électriques, par exemple), la conception de stratégies de coordination devrait être révisée, avec l'objectif de maintenir la stabilité du système de puissance, ainsi que le fonctionnement sécurisé de chaque générateur d'énergie, compte tenu l'évolution des paramètres environnementaux ou d'autres contraintes locales. En raison de la tendance générale vers les réseaux intelligents, les algorithmes de commande pour la production d'électricité ne devraient pas seulement être extensibles et reconfigurables, mais aussi doivent agir en temps de décision cours, tout en assurant la stabilité de l'ensemble du système.
- **Optimisation locale.**
  En ce qui concerne la commande des générateurs locaux à base d'énergies renouvelables, chacun devrait fonctionner dans la production de puissance maximale, en exploitant les conditions météorologiques actuelles autant que possible. Par conséquent, l'optimisation locale est nécessaire dans chaque générateur.

1.2.2 Contexte scientifique

Dans le contexte scientifique, le problème de coordination des générateurs distribués a quelques caractéristiques qui devraient être soigneusement analysées au moment de proposer une solution:

- La taille du système et ses caractéristiques distribuées.
- L'indépendance et objectifs particuliers de chaque unité de production d'électricité.
- La complexité du problème d'optimisation, ce qui est liée à la taille du système.
- Les contraintes d'opération pour chaque unité de génération, de même que pour les nœuds du réseau électrique.

Pour ces applications, on peut différentier entre deux enjeux, reliés avec la **coordination** et la **production optimale de puissance** pour les générateurs distribuées. Par rapport à l'aspect *coordination*,les questions techniques suivantes se posent:

- Comment attaquer le problème d'optimisation pour la production d'énergie distribuée, en sachant ses caractéristiques de taille, ainsi que la quantité des contraintes?
- Comment obtenir un algorithme de coordination en temps réel de haute performance, qui prend en compte les interactions dans les réseaux électriques et les contraintes?
- Comment gérer l'évolution des conditions climatologiques et les charges du système, même si une certaine planification précédente a été faite?

Les exigences pour avoir de l'adaptabilité dans la structure du contrôleur, ce qui permettre agir contre les changements des conditions du système, et en même temps assurer une performance

optimale sous contraintes, ont conduit au choix de la *Commande Prédictive sur Modèle* (également connu comme *Commande à Horizon Glissant*) comme stratégie de commande fondamentale de cette thèse, laquelle est introduite dans le chapitre 4. En considérant que les systèmes de génération distribuée ont besoin de certains type d'algorithmes de coordination, quelques basses sur le sujet sont présentées dans le chapitre r 3, lesquelles seront d'utilité pour la compréhension de la structure de coordination choisie pour le développement de l'algorithme de coordination de cette thèse, ce qui est présenté dans le chapitre 6 .

A propos de la *production d'énergie optimale* au niveau des unités de production d'énergie à base d'énergies renouvelables, les questions suivantes peuvent être envisagées:

- Comment est construite et quelles sont les caractéristiques les plus pertinentes de l'unité de conversion de puissance?
- Quel comportement est attendu pour le générateur, selon l'énergie incident?
- Comment l'unité de génération peut être intégrée dans le réseau électrique, avec des garanties de stabilité, même en cas de défaillance de ces instruments?

Dans cette thèse, une attention spéciale est faite aux turbines éoliennes, qui a conduit au développement d'une stratégie de commande qui maximise la production d'énergie. La stratégie est fiable et peut être appliquée sur d'autres unités de génération qui partagent des principes de conversion d'énergie similaires. La proposition pour les éolienne est montrée dans le chapitre 5. Une introduction aux différentes technologies de génération d'énergie considérées dans la thèse est présentée dans le chapitre 3.

1.3 Structure de la thèse

Cette thèse est organisée comme suit:

- **Le chapitre 2** présente l'introduction de la thèse en langue anglaise, laquelle est utilisée dans la totalité du manuscrit.
- **Le chapitre 3** inclut l'état de l'art de différentes stratégies pour la commande de systèmes de grande échelle, avec un accent sur les propositions basées en la commande optimale, qui ont été appliquées dans les systèmes de production d'énergie distribués. Dans ce chapitre, sont également présentés les principes fondamentaux de certaines technologies de production d'électricité, qui seront explorées dans les futures sections de cette thèse (piles à combustible, panneaux photovoltaïques, turbines éoliennes et générateurs hydroélectriques).
- **Le chapitre 4** présente, dans sa première partie, une introduction théorique sur la commande prédictive et une méthodologie particulière de solution explicite qui a été largement appliquée dans le développement de solutions de commandes MPC dans cette thèse. Dans la deuxième partie de ce chapitre, certains principes sur la théorie des ensembles invariants robustes sont introduits. Cette méthodologie est largement utilisée dans le chapitre 7, pour analyser la performance des systèmes dynamiques linéaires avec des stratégies de commande sous contraintes, ainsi que la performance de la méthode de coordination proposée.
- **Le chapitre 5** présente deux contributions faites dans la première partie de la thèse: la commande pour l'obtention maximale de puissance des générateurs renouvelables, et les

méthodes de coordination pour les systèmes de génération multi-énergies.
La première contribution présente une approche pour obtenir la puissance maximale disponible d'une turbine éolienne qui n'a pas la mesure de la vitesse du vent. La méthode proposée est basée sur l'estimation d'une nouvelle variable, qui dépend du coefficient caractéristique de puissance (ci- inconnue) et la vitesse du vent. L'avantage de cette technique proposée est le fait que la stratégie de commande de la puissance de la turbine du système peut prendre en charge des défaillances des capteurs de vitesse du vent.
La deuxième contribution concerne l'utilisation d'une stratégie MPC sous contraintes, en utilisant l'approche de solution explicite présentée au chapitre 4, appliquée à la commande d'un micro-réseau de 1.2 kW qui contient une pile à combustible, une éolienne et une batterie. Dans la procédure de conception de l'algorithme de commande, sont incluses des matrices de pondération appropriées pour pénaliser les actions de décharge de la batterie, ainsi que des contraintes pour limiter le taux de puissance délivrée par la pile à combustible, en fonction de leurs principes opératoires. En outre, l'éolienne n'est pas commandé et il est supposé qu'une stratégie externe garantit la production d'énergie maximale. Par conséquent, cette puissance est considérée comme une perturbation additive qui peut affecter la stabilité du bus de charge. La solution stabilise le bus de charge, sous différentes valeurs de production d'énergie de l'éolienne, en utilisant une action combinée entre la pile à combustible et la batterie.

- **Le chapitre 6** présente les principes, la structure et l'application d'une nouvelle stratégie de coordination pour les systèmes linéaires de grande taille. Le modèle du système est décomposé en sous-systèmes, chacun d'eux avec de l'information explicite de leurs signaux internes et un terme qui dépend des autres sous-systèmes. En considérant cette partition et la définition des interactions, la fonction de coût globale est étendue en incluant ces éléments. Parce que la fonction de coût est également décomposée, chaque bloc de commande des sous-systèmes peut être exprimé en termes d'un retour d'état (*state feedback*) de ses propres signaux, mais aussi un vecteur de coordination externe, qui est calculé par un optimisateur de niveau supérieur, assure la performance globale, en tenant en compte des contraintes locales.
  L'approche est basée sur trois principes: le principe de la coordination par prix des systèmes de commande distribuée à grande échelle, l'utilisation de solutions explicites pour les problèmes locaux (sans-contraintes) et globales (sous-contraintes) de commande MPC, et finalement, la possibilité de décentraliser la structure de commande globale.

- **Le chapitre 7** propose une extension à l'analyse de la performance par le calcul des ensembles invariants, appliqué aux systèmes de commande sous contraintes. Dans ce chapitre, la performance d'un système linéaire avec une commande MPC sous-contraintes est analysée. Puis, quelques extensions sur l'analyse via les ensembles invariants pour la commande distribuée-coordonnée sous contraintes, présentés au chapitre 6, sont considérées. Dans la troisième partie de ce chapitre, une technique alternative pour calculer des ensembles invariants pour les sous-systèmes locaux, obtenue d'une décomposition de modèle, est présentée. L'idée utilise les avantages de l'algorithme de commande distribué et calcule les ensembles invariants locaux pour des conditions de coordination différentes. Les résultats sont suffisants pour analyser la performance locale de chaque sous-système.

- **Le chapitre 8** présente deux cas d'étude dans lesquels la stratégie de commande distribuée-coordonnée est appliquée, ainsi que les outils d'évaluation de performance provenant de la construction des ensembles invariants. Un premier exemple d'un micro-réseau avec deux générateurs et une charge partagée offrent les détails sur la construction des vecteurs d'interactions, tout en maintenant les matrices du système. Dans le deuxième exemple, on a abordé le problème classique des zones de production d'énergie interconnectées, chacun

est composée d'un générateur synchrone et d'un générateur alternatif non contrôlable. La stratégie de commande assure la performance globale dans les conditions de fonctionnement, y compris l'intermittence de la production d'électricité, les contraintes opérationnelles, entre autres.

- **Le chapitre 9** présente les principales conclusions de la thèse, ainsi que les perspectives sur ce travail.

1.4 Contributions Principales

Les contributions de cette thèse peuvent être résumées comme suit:

- Proposition d'une stratégie de coordination pour les systèmes de production d'énergie distribuée, qui permet de coordonner des contrôleurs MPC indépendants, tout en appliquant des contraintes pour tous les sous-systèmes. La stratégie est présentée au chapitre 6.

- Utilisation des ensembles invariants comme un outil d'analyse de la performance des systèmes en boucle fermée sous contraintes, y compris la commande prédictive et l'approche de coordination proposée. Une procédure de mise à jour des ensembles de commande sous contraintes est proposée et révisée. En outre, une méthode de calcul des ensembles invariants pour certaines portions du système est également présentée. Cette contribution est présentée dans le chapitre 7.

- Application de la stratégie de commande distribuée-coordonné sur deux cas d'étude, dont leurs caractéristiques peuvent être trouvées dans certains systèmes de production d'électricité. Ceci est présenté au chapitre 8.

- Contribution à la maximisation de la production d'électricité dans les éoliennes, pour le cas d'absence de capteur de vitesse du vent. Cette contribution, bien que dérivée des premières discussions dans le développement de cette thèse, est directement liée à l'un des problèmes de base dans les systèmes de production d'électricité distribués: la production de puissance maximale pour les générateurs d'énergie à base d'énergies renouvelables. Des détails de la technique proposée sont inclus dans la première partie du chapitre 5.

- Contribution à la coordination de puissance d'un micro réseau, en utilisant la commande à horizon glissant explicite. Le micro réseau considéré est composé d'une pile à combustible, d'une éolienne en opération à puissance maximale, et d'un dispositif de stockage. Les détails de la modélisation du micro réseau et les caractéristiques particulières des signaux de commande et des perturbations sont analyses. Cette contribution est comprise dans la deuxième partie du chapitre 5.

1.5 Liste de Publications

Certains résultats de cette thèse ont déjà été publiés, et autres sont en cours d'édition pour futures soumissions.

Articles dans conférence internationales avec actes

- [7]: *Lagrange Multipliers Based Price Driven Coordination with Constraints Consideration for Multisource Power Generation Systems* (John Sandoval-Moreno, Gildas Besançon and John J. Martinez), in proceedings of the 13^{th} European Control Conference (ECC), Strasbourg, France, 2014.
- [8]: *Model Predictive Control-Based Power Management Strategy for Fuel Cell/Wind Turbine/Supercapacitor Integration for Low Power Generation System* (John Sandoval-Moreno, Gildas Besançon and John J. Martinez), in proceeding of the 15^{th} European Conference on Power Electronics and Applications (EPE), Lille, France, 2013.
- [9]: *Observer-based maximum power tracking in wind turbines with only generator speed measurement* (John Sandoval-Moreno, Gildas Besançon and John J. Martinez), in proceedings of the 12^{th} European Control Conference (ECC), Zurich, Switzerland, 2013.

Chapitres du livre (en cours)

- [10]: *Optimal Distributed-Coordinated Approach for Energy Management in Multisource Electric Power Generation Systems* (John Sandoval-Moreno, John J. Martinez and Gildas Besançon). Topics in optimization based control and estimation, Springer, 2015.

Articles dans des revues internationales (en cours)

- [11]: *Stability Analysis of Distributed-MPC Based in Price Driven Coordination with Invariant Sets* (John Sandoval-Moreno, John J. Martinez and Gildas Besançon).
- [12]: *An observer-based method for maximizing the power production for wind speed sensorless eolian power generators* (John Sandoval-Moreno, Gildas Besançon and John J. Martinez).

Chapter 2

MAIN INTRODUCTION

Contents

2.1 General Context of the Thesis 11
2.2 Problems definitions and motivations 12
2.2.1 Historical and technological contexts 12
2.2.2 Scientific context 16
2.3 Structure of the thesis 17
2.4 Main contributions 18
2.5 Publications list 19

In this chapter are presented the thesis general context, as well as the main problems which will be considered together their motivations and an overview of the obtained results.

2.1 General Context of the Thesis

This thesis was partially supported by the Colombian government through COLCIENCIAS (Departamento Administrativo de Ciencia, Tecnología e Innovación), via a "Francisco José de Caldas" scholarship for developing doctoral studies abroad. The objective of such a grant is to support potential high level Colombian researchers for receiving high level education in different strategic areas for Colombian development, including the two main ones considered in the present work: **Automatic Control** and **Electric Power Generation Systems**.

This thesis was developed between October 2011 and October 2014, within SYSCO [1] and SLR[2] research teams at the Control Systems Department of GIPSA-Lab [3], which is affiliated to the Doctoral School EEATS [4] at the University of Grenoble, France.
The following topics are part of the general framework of this thesis:

- The use of Model Predictive Control under constraints as a systematic and well-known methodology for small and large scale power generation systems.
- The use of hierarchical model decomposition and model predictive-based coordination for controlling distributed power generation systems.

[1] Systèmes non Linéaires et Complexité (Nonlinear Systems and Complexity)
[2] Systèmes Linéaires et Robustesse (Linear Systems and Robustness)
[3] Grenoble Image Parole Signal Automatique (Grenoble Image Speech Signal Control Systems)
[4] Électronique, Électrotechnique, Automatique et Traitement du Signal (Electronics, Electrotechnics, Automatic Control and Signals Treatment)

- The use of principles in optimal state estimation for maximizing the power production in wind turbines.
- The use of Robust Invariant Sets for evaluating the performance of constrained coordinated systems.

This thesis represents an extension of the thesis made by **Jennifer Zárate-Florez** [6] "Étude de Commande par Décomposition-Coordination pour l'Optimisation de la Conduite de Vallées Hydroélectriques", also performed at GIPSA-Lab, that was focused on the study of coordination schemes (more precisely, *interaction-prediction* and *price-driven* coordination methods) for the control of hydro-power valleys. This former work gives some bases for managing distributed power generation systems by means of coordination of locally MPC-based controlled structures, with a special attention to the case of hydro-electrical generators that are interacting with each other. In the present work, additional elements for analyzing the system performance under such techniques, as well as their applicability to other power generation technologies, are considered.

2.2 Problems definitions and motivations

Let us start by presenting the main problems considered in this thesis, alongside the motivations to be treated.

2.2.1 Historical and technological contexts

During centuries, the development of the society has been linked to the exploitation of different classes of energetic resources. Without going too far in time, during the industrial revolution for instance, the steam power - obtained by boiling water with burning wood, was instrumental in developing transport means. Linked to this progress, the exploration and exploitation of petroleum as an energy source started for the development of more suitable vehicular applications, giving some first concepts of portability. Nowadays, the use of fossil-based fuels is common in the society - still widely present in the vehicular sector (cars, airplanes, ships, among other), giving rise to new problems now linked to the environment, such as global warming, exploration for finding new oil deposits or new sources of energy, etc.
However, in this same period of industrial revolution, *electric power generation systems* (EPGS) - based on thermoelectrical or hydroelectrical properties, have also been developed. Since that time, electric power demand has been increasing year after year, requiring investments and innovation for three main objectives:

- To ensure power production, as well as its distribution to the nearby industries and localities, while reducing the environmental footprint as much as possible,.
- To maintain the power systems stability, in the sense of keeping voltage magnitude and frequency variations in admissible ranges, by considering power generator characteristics, load demand profiles, and the instantaneous grid topology.
- To ensure scalability of power systems, with the objective of expanding the installed capacity and allowing the inclusion of different types of electric power generation technologies.

Nowadays, the efforts are directed to maintain and enhance the electrical power generation capacities and scopes, while reducing, at the same time, the environmental footprint in all possible aspects. Moreover, since the 1980's, the following development trends have been considered, for generating the required electric power in different social levels, including industry and population:

- **Development of EPGS on the basis of renewable power sources:** For instance, great advances have been made in generators based on photovoltaic panels, onshore and offshore wind turbines, tidal turbines, fuel cells, geothermal generators, as well as better integrability of small hydroelectric generators, all of them reducing the investments and environmental impacts.

- **Replacement of EPGS based on chemical or non renewable sources:** Here are included the replacement of nuclear power plants, oil or coal-based thermoelectric plants, or unnecessarily-large hydroelectric plants (such as the 'Three Gorges' one in China), due to the high contamination levels and potential damages to the environment.

- **Development of technologies for electrical and partial Hydrogen-based vehicular applications - typically Hybrid Electric Vehicles (HEV) and/or Fuel Cell Vehicles (FCV):** Here, the reduction of petroleum-based fuel combustion will be important in the next years, while increasing the requirements of electricity for charging vehicles.

- **Development of isolated microgrids:**Such grids are for instance conceived for supplying a basic amount of electricity for populations or applications such as radio transmission facilities, that cannot be connected to the power grid. Here, robust and feasible solutions have been more and more studied the latest years. New trends now focus on the integration with transmission grid, in order to exchange energy according to the operative conditions.

- **Development in industrial and communication networks:** This comes along with the development of computer facilities, and has given rise to the concept of so-called *Smart Grid*, in which the coordination of many entities - including large scale power generators, grid compensators, energy harvesters (batteries), local generators or loads, etc - is desired in order to maintain stability and efficiency of the local grid. The nesting of smaller smart grids is one of the goals, as well as the development of efficient coordination and grid reconfiguration algorithms.

In consideration of the development of power generation technologies, each year some statistical information can be obtained regarding the aspect of the different power production technologies and its exploitation in the society. For instance, Table 2.1 presents comparative information in terms of worldwide power consumption for the year 2013. At the same time, Table 2.2 includes information about the European power consumption for the year 2013.

Table 2.1: Total World Power Consumption and Providing Generation Technologies - 2013 [3]

Generation Technology	**Consumption (MToe) - (%)**
Hydro Power	855.8(6.58%)
Solar Power	28.2(0.22%)
Wind Power	142.2(1.09%)
Other Alternatives (Geothermal, Biomass, H_2...)	388.2(2.98%)
Biofuel Power	0.653(0.005%)
Oil Power	4185.1(32.17%)
Coal Power	3826.7(29.42%)
Gas Power	3020.4(23.21%)
Nuclear Power	563.2(4.33%)
Total	**13010 (100%)**

Table 2.2: Total Europan Power Consumption and Providing Generation Technologies - 2013 [4]

Generation Technology	**Consumption (MToe) - (%)**
Alternatives	209.7(12.58%)
Oil Power	556.6(33.4%)
Coal Power	286.5(17.2%)
Gas Power	386.8(23.2%)
Nuclear Power	226.3(13.58%)
Total	**1666.2 (100%)**

It is seen how power production based in renewable sources represents around 11% of the global power consumption, and in Europe, this index is similar (about 12.5%). However, the other 89% (87.5% for Europe) is represented by traditional generation technologies.
The penetration of renewable-based power generation is indeed increasing every year, influenced principally by the scientific development in different disciplines. For instance, the development of efficient energy conversion units (i.e novel alloys for the photovoltaic panels, new materials for membranes and electrodes in fuel cells) requires the knowledge of physics, chemistry and material science for transforming as much power as possible. The transmission and conditioning of the energy from the conversion unit to the final application requires electrical infrastructure and circuits that are designed by electrical and electronic engineers. In the same line, the monitoring and control of such power applications requires technical developments from communications, informatics, economics and automatics experts.
Having in consideration the numerous quantity of disciplines that are included in the development of power generation, in the present study particular challenges in **automatic control** and **electric power generators** motivated the present study.

In the power systems, every generator is locally controlled in such a way that power production is ensured, while maintaining the local stability under operative restrictions. For example, in a photovoltaic facility the power production is maximized with daylight and the

produced energy should be distributed between the grid and the local storage system, that will possibly provide energy in night time.
In power systems there exist *grid coordinator systems* (also known as *dispatch systems*) that communicate, to all the dispatchable generation units within its area, the demanded power for the following hours. Such a system uses off-line optimization algorithms that consider economical, environmental and statistical information for evaluating and computing the required power to be generated by each unit. However, the scheduling is performed under "ideal" conditions, and events such as local over/under-loading, faults in transmission lines or generators, environmental changes, among others, will affect the idealized behavior of the power system. In Fig. 2.1 is shown a typical configuration of a portion of the power system with distributed generators, storage system and loads, as well as the coordination system, assigned to this sector of the grid. One

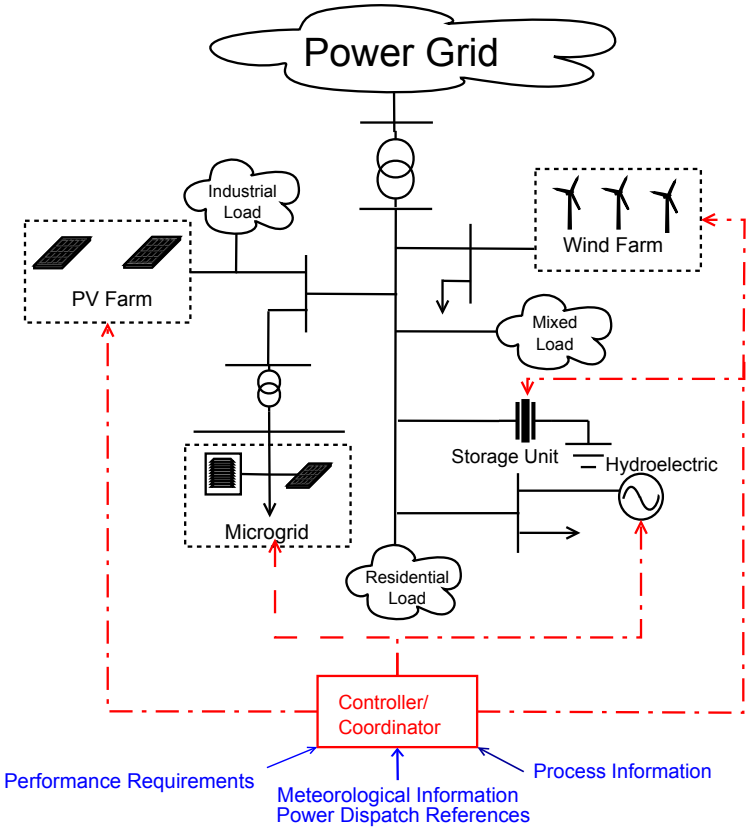

Figure 2.1: Typical configuration of a distributed power system

of the solutions consists in updating generator references, which is a classical and common use in hydro- and thermo-electric facilities. In this case, the *local operators* (engineers and technical staff), relying on empirical criteria, exchange with the dispatch system and/or surrounding substations new references for dealing with the current events. However, this procedure and the corrective actions are not instantaneous, and their effects can affect the power grid stability, possibly deriving towards local or even global blackouts for example. In fact, this practice is not suitable when using renewable-based EPGS, because their algorithms use maximum power generation techniques that are *a priori* autonomous and adaptive to changes in real-time climate conditions.

In this context, there are two elements that we would like to consider more particularly in the present thesis:

- **Coordination strategies.**
  Considering indeed the requirements from the renewable-based electric power generators, as well as the increasing demand of electricity (due to the increasing number of networking service facilities and electrical vehicles charging unities, for instance), the conception of coordination strategies should be revised, with the objective of assuring full power system stability, as well as secure operation of each power generator, considering changes in environmental parameters or other local constraints. Because of the general trend towards smart grids, the control algorithms for power generation not only should be scalable and reconfigurable, but also must act in small decision times, while ensuring stability of the whole system.

- **Local optimization.**
  With respect to the control of local power generators based on renewable energy, each one should operate in maximum power production, exploiting the current environmental conditions as much as possible. Therefore, local optimization is required at each generator.

2.2.2 Scientific context

In the scientific context, the coordination problem of distributed generators has some characteristics that should be carefully analyzed when proposing a solution:

- System size and distributed aspect.
- Independence and particular objectives of each power generation unit.
- Complexity of optimization problem (related to system size).
- Operative constraints for each generation unit, as well as for the power grid nodes.

In this applications, one can differentiate two class of issues, related with the **coordination** and **optimal power production** for the distributed generators. With respect to the *coordination* aspect, the following technical questions arise:

- How to tackle an optimization problem for distributed power production, knowing its large scale characteristics, as well as the quantity of constraints?
- How to obtain a high performance real-time coordination algorithm that takes into account power grid interactions and constraints?
- How to handle the evolution of climatological conditions and the system loads, even when some previous forecasting has been done?

The requirements for having some kind of adaptability in the controller structure, that allows to deal with against the system changing conditions, and at the same time ensuring optimal performance under constraints, led to the choice of *Model Predictive Control* (also known as *Receding Horizon Control*) as the fundamental control strategy for the thesis, which is introduced in Chapter 4. Taking into account that distributed power systems require some class of coordination algorithms, some basis of this subject are presented in chapter 3 that will be useful for understanding the selected coordination structure for the development of the coordination algorithm of this these. which is presented in the chapter 6.

With respect to the *optimal power production*, at the level of renewable-based generation units, the following questions can be considered:

- How is built and what are the most relevant characteristics of the power conversion unit?
- What kind of behavior is expected for the generator, according to the incident environmental energy source?
- How can the unit be integrated into the power grid, with stability guarantees, even in case of failures in the instruments?

In this thesis, an special attention is made to wind turbines, that conducted to develop a control strategy that maximizes its power production. The strategy is suitable to be applied in other generation units that share similar energy conversion principles. The proposal for the turbine is shown in Chapter 5, but an introduction to the different power generation technologies that are considered in the thesis is presented in Chapter 3 .

2.3 Structure of the thesis

According to the above discussion, this thesis is organized as follows:

- **Chapter 3** includes the State-of-the-art of the different strategies for the control of large scale systems, with an emphasis on optimal control-based proposals, that have been applied in distributed power generation systems. In this chapter are also presented the fundamentals of some power generation technologies that will be explored in some sections of this thesis (fuel cells, photovoltaic panels, wind turbines, hydroelectric generators).
- **Chapter 4** presents, in its first part, a theoretical background in Model Predictive Control and a particular explicit solution methodology that has been widely applied in the development of MPC-based solutions of the present thesis. In the second part of this chapter, some fundamentals in Robust Invariant Sets theory are introduced. The methodology is widely used in Chapters 7, for analyzing the performance of linear dynamic systems with constrained control strategies as well as the performance of the proposed coordination method.
- **Chapter 5** focuses on two contributions done in the first stage of the thesis: control for power maximization in renewable-based generators, and coordination methodologies for multi-source power generation.
  The first contribution presents an approach for obtaining the maximizing available power of a wind turbine that has no measurement of the wind speed. The proposed method is based on the estimation of a new variable, which depends of the unknown power characteristic coefficient and the wind speed. The advantage of the proposed technique is that the system's control strategy can support wind speed sensor failures.
  The second contribution concerns the use of a constrained MPC strategy, using the explicit solution approach presented in Chapter 4, applied to the control of a $1.2kW$ microgrid that contains a fuel cell, a wind turbine and a battery. In the control design procedure are included suitable weighting matrices for penalizing the battery discharge actions, as well as constraints for limiting the power rate delivered by the fuel cell, according to their well known operative principles. In addition, the wind turbine is not controlled and it is assumed that an external strategy guarantees the maximum power production. Therefore, this power is considered as an additive disturbance that can affect the load bus stability. The solution

asserts to stabilize the load bus, under different power production values of the wind turbine, using the combined action of the fuel cell and the battery.

- **Chapter 6** presents the principles, the structure and the application of a novel coordination strategy for large scale linear systems. The system model is decomposed into subsystems, each of them with explicit information of its internal signals and some term that depends on the other subsystems. Giving this partition and the definition of *interactions* terms, the global cost function is extended including these elements. Because the cost function is also decomposed, every subsystem control block can be written in terms of a state feedback of its own signals, but also an external coordination vector, computed by an high-level optimizer, which ensures the global performance, while taking into account the local constraints.
  The approach is based on three principles: the principle of the price-driven coordination of large-scale distributed control systems, the use of explicit solutions for the (unconstrained) local and (constrained) global MPC problems, and finally, the availability for decentralizing the global control structure.

- **Chapter 7** proposes an extension to the performance analysis via invariant sets computation, applied to systems with constrained control strategies. In this chapter, the performance of a linear system under constrained MPC is analyzed. Then, some extensions to the analysis via invariant sets for the distributed coordinated control approach in presence of constraints, presented in Chapter 6, are considered. In the third part of this chapter, an alternative technique for computing invariant sets for local subsystems, derived from a model decomposition procedure, is presented. The idea takes advantage from the distributed control algorithm and computes local invariant sets under different coordination conditions. The results are good enough for analyzing the subsystems performance, when using the distributed-coordinated control strategy.

- **Chapter 8** proposes two case studies in which the distributed coordinated control strategy is applied, as well as the performance evaluation tools derived from the invariant set construction. A first example of a microgrid with two generators and a shared load offers details of the construction of interaction vectors, while maintaining the system matrices. In the second example, it is tackled the classical problem of linked power generation areas, each of them composed by a synchronous generator and an undispatchable alternative generator. The control strategy ensures the global performance under the operation conditions, including power generation intermittence, operative constraints, and so on.

- **Chapter 9** presents the main conclusions of the thesis and presents the perspectives of this work.

2.4 Main contributions

The contributions of this thesis can be summarized as follows:

- Proposal of a coordination strategy for distributed power generation systems, that allows coordinating independent Model Predictive Controllers, while enforcing constraints for all subsystems. This is presented in Chapter 6.

- Use of invariant sets as a tool for analyzing the performance of systems under constrained feedback strategies, including MPC and the proposed distributed coordinated approach. A procedure for updating the constrained control sets is proposed and revised. In addition, a

methodology for computing invariant sets for some portions of the system is also presented. This contribution is presented in Chapter 7.

- Application of the distributed coordinated control strategy in two case studies, whose properties can be found in some power generation systems. This is presented in Chapter 8.
- Contribution to the maximization of power production in wind turbines, for the wind speed sensorless case. This contribution, although derived from earlier discussions in the development of this thesis, is directly related to one of the basic problems in distributed power generation systems: the maximum power production for renewable-based power generators. Details of the proposed technique are included in the first part of Chapter 5.
- Contribution to the power coordination of a microgrid using explicit receding horizon control. The considered microgrid includes a fuel cell, a wind turbine at maximum power operation, and a storage device. Details of the microgrid modeling and particular characteristics of control signals and disturbance are presented. This is included in the second part of Chapter 5.

2.5 Publications list

Some results of the present thesis have already been published, and other ones are in edition process for future submissions.

International conference papers with proceedings

- [7]: *Lagrange Multipliers Based Price Driven Coordination with Constraints Consideration for Multisource Power Generation Systems* (John Sandoval-Moreno, Gildas Besançon and John J. Martinez), in proceedings of the 13^{th} European Control Conference (ECC), Strasbourg, France, 2014.
- [8]: *Model Predictive Control-Based Power Management Strategy for Fuel Cell/Wind Turbine/Supercapacitor Integration for Low Power Generation System* (John Sandoval-Moreno, Gildas Besançon and John J. Martinez), in proceeding of the 15^{th} European Conference on Power Electronics and Applications (EPE), Lille, France, 2013.
- [9]: *Observer-based maximum power tracking in wind turbines with only generator speed measurement* (John Sandoval-Moreno, Gildas Besançon and John J. Martinez), in proceedings of the 12^{th} European Control Conference (ECC), Zurich, Switzerland, 2013.

Book Chapter (in progress)

- [10]: *Optimal Distributed-Coordinated Approach for Energy Management in Multisource Electric Power Generation Systems* (John Sandoval-Moreno, John J. Martinez and Gildas Besançon). Topics in optimization based control and estimation, Springer, 2015.

International journal papers (in progress)

- [11]: *Stability Analysis of Distributed-MPC Based in Price Driven Coordination with Invariant Sets* (John Sandoval-Moreno, John J. Martinez and Gildas Besançon).

- [12]: *An observer-based method for maximizing the power production for wind speed sensorless eolian power generators* (John Sandoval-Moreno, Gildas Besançon and John J. Martinez).

Chapter 3

STATE-OF-THE-ART ON LARGE SCALE SYSTEMS AND RENEWABLE POWER GENERATION TECHNOLOGIES

Contents

3.1 Control configurations for large scale systems 22
3.1.1 Centralized control structure 23
3.1.2 Decentralized control structure 24
3.1.3 Distributed control structure 25
3.1.4 Distributed-coordinated control structure 26
3.1.5 Discussion and additional remarks 28
3.2 Operative principles of some alternative electric power generation technologies 29
3.2.1 Hydroelectric Power Generation Systems 30
3.2.2 Wind Turbines Power Generation Systems 33
3.2.3 Photovoltaic Power Generation Systems 37
3.2.4 Fuel Cells Power Generation Systems 40
3.2.5 Comparison of the alternative power generation technologies 44
3.3 Conclusions 44

In this chapter, a discussion is presented after a bibliographical analysis for the context of the present thesis. It covers the following elements:

- Control strategies for large scale systems.
- Operative principles of renewable power generation technologies, highlighting their advantages and disadvantages when explored.
- Control strategies applied to multisource power generation systems.

For a better illustration of this state-of-the-art, some examples of application of the reviewed techniques are included, taken in the field of electric power systems - from small power grids (residential, industrial or communication facilities applications, for example) to facility grid applications.

3.1 Control configurations for large scale systems

In this section, some introductory discussion related to the control of large scale systems is presented.
First, Large Scale Systems have some degrees of complexity according to different elements:

- Complexity due to mathematical modeling: for instance when the system dynamics are written in terms of linear and nonlinear expressions, that may even be time-varying.
- Complexity due to spatial distribution: typically when the system has a big size and includes many variables (as in distillation columns or refineries for example) or the process is distributed in different geographic areas, such as in power systems.
- Complexity due some hierarchical structure: when the system is composed by different control or communication levels, as in industrial control networks for instance.

The complexity in dynamical systems is also linked to their performance and, of course, their control algorithms and procedures. For example, some states may have particular demands in terms of robustness or temporal response, while other parts of the system may be more concerned with optimal performance. Moreover, some states may not be directly measurable, making the use of observation structures necessary. All these aspects, for a single given global system [1], require quite different computation structures for controlling or estimating some variables or parameters, that may also have to be executed in a specified amount of time [13, 14, 15].
According to the control objectives, requirements, complexity and scale of the system, one can find in the literature three well defined structures that are suitable for their exploitation in large scale systems:

- **Centralized Control Structure:** In this control strategy, all the decisions are taken by only one structure that processes the system information and reference from some user (human or other machine) and then, sends the appropriate control values to the plant. Typically multivariable control strategies can be used, including optimal or robust features, or as classical as PID ones [16, 17].
- **Decentralized Control Structure:** In this approach, the global model is decomposed into smaller ones and the control algorithm is also separated into smaller parts, associated with each subsystem. In this case, each subsystem acts by itself and does not process any information from its neighbours.
- **Distributed Control Structure:** Here, the global model is also decomposed, as well as the control structure. However, there are some classes of information exchanges or co-operation between the controllers in order to achieve some particular objective [18, 19, 20, 21, 22], a principle used in *consensus control*. On the other hand, the use of *Coordination* entities for cooperation between controllers can also be found. In that case, some transmission of current state information is required, and a hierarchical structure is typically considered [23, 24].

In fact, the present revision of state-of-the-art is more directed to analyze some contributions of large scale and physically distributed systems. This is justified by the decentralized characteristics of the electric power production systems. Notice that some references are cited for each control configuration, with more emphasis on electric power systems applications, even if some additional ones are also included in a complementary fashion.

[1] From here, an entity that contains smallest parts for some specific objective. For example, an electric power system has distributed generators (smaller parts), but the objective is power generation for a particular region.

3.1.1 Centralized control structure

The *centralized control structure* is the most common one, not only for large scale systems, but also for all basic control theory applications. In short, the controller is an entity that gathers all the required system signals and delivers a suitable control signal, under some conditions. The general structure of this strategy is shown in Fig. 3.1.

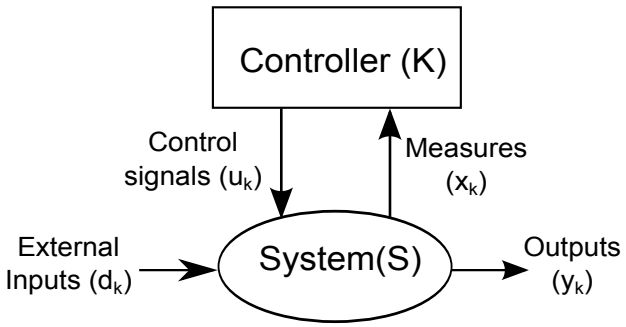

Figure 3.1: General scheme of the Centralized Control Structure

With this strategy, the controller has the following characteristics [16, 25]:

- The controller is unique (here, only one processor).
- The controller has the capability to know most of the system states, by using direct sensors information or state observers.
- The controller has exact or approximated (with their respective tolerance) knowledge of all system parameters, tracking errors, binary signals, and other signals/parameters of interest.
- Thanks to the model knowledge, the controller can predict future states, as well as store past state values.

However, centralised control entities have some disadvantages, in terms of functionality:

- The controller may require high performance computational structures, including high speed processors and good memory stack.
- If the controller includes fixed parts (for example, PID or robust non-adaptive structures), their tuning can be complicated and require suitable plant models and tolerance.
- The choice of controller structure is a challenge, considering the requirements, control objectives and computational resources.
- A centralized control structure may lack of flexibility in case of particular changes. Here, adaptive control could be an option.

In the context of large scale systems, using a centralized control is not a practical option, due to the quantity of communication links between controller and process, the treatment of these signals and their storage, and not less important, the robustness of the computational structure that should not fail in maintaining the good functionality of system, to cite a few drawbacks.

On the contrary, applying centralized controllers in small applications has been the primary choice when applying control strategies in a vast number of cases. The simplicity that can be obtained in a centralized controller is in fact one of its most interesting characteristics [25, 16].
In the context of power systems, a centralized control structure typically results in a suitable configuration when the system is spatially confined. For instance, such a control structure has been used for particular power generation technologies [26, 27, 28, 29, 30] to ensure stability and some performance characteristics. Here, one can find robust, optimal or classical control strategies, each one with its particular characteristics and limitations.
Centralized control blocks are also widely used for energy management proposes. For example, in low power multisource systems [31, 32, 33, 34, 35] , a centralized structure is good enough to impose control requirements and is suitable to be easily modified. Nevertheless, those strategies have interesting performances even with limited computational requirements, while this latest type of constraints may become a problem for large scale systems.

Before closing this part of the discussion, it is worth mentioning that some control and modeling methodologies may allow to obtain different control structures for large scale systems. For example, *model reduction methods* [16] allow to reduce the equivalent model of the system, thus simplifying the control structure, that can still be centralized.
However, other methodologies based in the decomposition of the dynamic system, that can be done by detecting cascade subsystems connection, for instance [14, 18, 36], or using decoupling terms in the controller structure [16], allow to decentralize the control structure, giving rise to other classes of controllers: *Decentralized and Distributed*. These structures will be better refereed in subsequent sections.

3.1.2 Decentralized control structure

The so-called *decentralized control structure*, along with the *distributed* one, considers that the control block is separated into smaller portions that act in particular sections of the system. More precisely, parts of the control signals only act over some specific states [19, 21]. In Fig. 3.2 a typical structure of decentralized control scheme is presented, assuming full state feedback for each local controller.

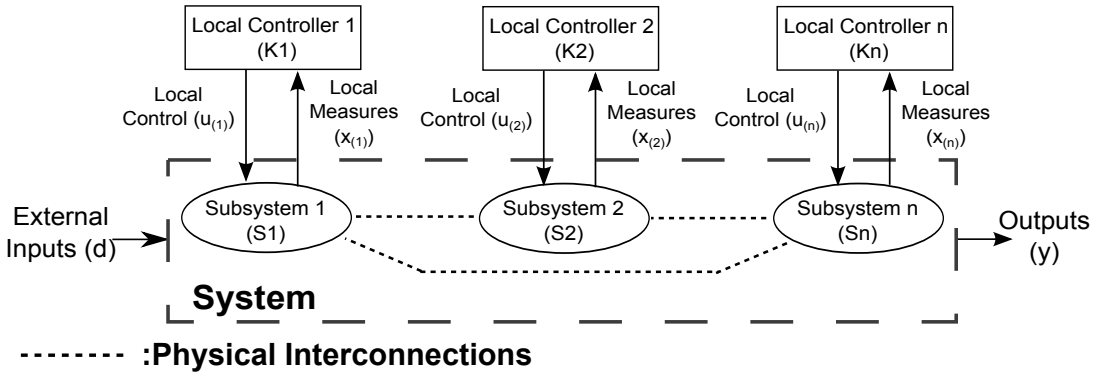

Figure 3.2: General scheme of the Decentralized Control Structure

As previously introduced, model decomposition is a required task before proposing a decentralized control strategy. This procedure can be done:

- Using well known methods such as Singular Value Decomposition or model reduction methods [16]. Then, dominant states can be selected and diagonal system matrices can be adopted, that, in practice, characterize independent subsystems with weak or strong interactions with the other ones. Other techniques based in graphs such as in [37] can also be used, in which interactive systems are obtained in a logical fashion.
- Using the physical disposition of the process. From this, one can define local dynamics with interactions. This can be directly done in power systems, chemical or mechanical processes, to cite some applications [24, 36, 38, 39, 40].

One interesting characteristic of decentralized control strategies is indeed the reduced size of the controller configuration. However, such strategies should be robust enough because each of them act separately, and does not receive any information from other controllers. In some sense, the controllers (sub controllers or local controllers) are considered independent in terms of interactions, although their systems yet interact with each other [16, 19, 41]. This represents a great disadvantage of such an approach: the global system performance can be degraded compared with a centralized control scheme. When a system does not "interpret" what its neighbours have done, its control actions may be inappropriate in terms of some global cost function or performance index, for example. Even worse, the actions taken by one subsystem can affect the states of the other ones, provoking instability in the whole system, due to its interconnections [16, 19].
Thus, this scheme is convenient after defining all the possible operative conditions of the system, as well as after establishing the desired performance. If a solution is not robust or suitable enough in terms of global or local system, some adaptation strategy in the controller might be applied.
However, in large scale systems, a controller reconfiguration may not be so simple. Instead, some modifications can be done to the controller structure, either allowing information exchange between subsystems to enhance the subsystem performance now considering knowledge of the neighbours, or using some class of entity(ies) that gathers the system information and then, computes some complement to the control signal so as to ensure the global performance.
Both solutions to enhance the decentralized control scheme, derives into other schemes that are widely used in large scale systems: *distributed control* and *distributed-coordinated control*, or also called *decomposed-coordinated control*. In [40] for instance, an analysis of decentralized control strategies applied to a multi-tank system is presented. Those structures are analyzed in the following section.

3.1.3 Distributed control structure

As mentioned above, a decentralized control strategy that includes requirements to ensure global stability, either by using communication links between controllers and/or subsystems, or using a coordination element, is refereed to as a *distributed control structure*. Further information about the coordination approach is given in Section 3.1.4.
Before going further, some terminology related to distributed control schemes needs to be specified: any small part of the system is called a *subsystem*, and has an associated control block, commonly call *agent*, that is some class of intelligent element. The agents can communicate between them or with a *coordinator*.
In general, distributed control is an excellent option for developing controllers in large-scale systems due to the possibility of dividing the control strategy into smaller parts, by exploiting the intercommunication capacities of the agents. Some papers such as [18, 42] present generalities in terms of model structure, control disposition and strategies that are typically used. In [22], some elements are more particularly explored for stability with a distributed solution. Game theory has also been used in this context, and contributions such as [43, 44] show how cooperative actions

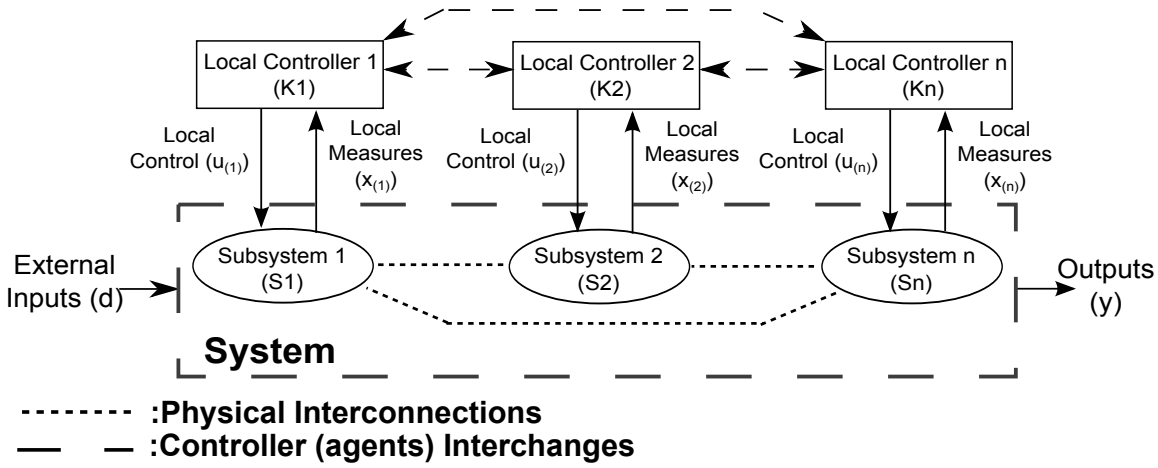

Figure 3.3: General scheme of the Distributed Control Structure

can be translated into other contexts. A general structure of distributed control scheme without coordination level is given in Fig. 3.3.

In the field of power systems, contribution [39] solves the problem of line-power stability of three power generators connected in ring configuration, that exchange information between them. Other strategies of this type, also in power systems, use Lyapunov theory or even principles of Kalman filtering for the coordination task (see [36, 45, 46, 47] for instance). In this context of systems coordinated under Lyapunov-based controllers for power applications, reference [48] proposes an "almost decentralized" scheme, while [49] includes a priority mechanism for weighing the participation of agents to the control.

Considering other fields of application, [20] applies local control signals in a chemical process, obtained when agents solve the same optimization problem, considering full states knowledge, but only concentrating on its local control vector, [50] presents an extension of game theory to tracking purposes in the classical four-tank process, [38] along [51] propose examples for serial connected subsystems for heating applications and [52] shows the benefits of this method for irrigation canals.

Finally, [53] and [54] use Lyapunov stability in various fashions, in order to analyze the stability limits of the systems: the first one is a contribution on decoupled systems and the latter one considers neighbour-to-neighbour communication and uses invariant sets for performance analysis.

3.1.4 Distributed-coordinated control structure

Differently from the aforementioned distributed control scheme, in the distributed-coordinated control the inclusion of a coordinator - or various coordinators - is considered to ensure the control objectives. In this strategy, the so-called *interactions* signal, that is typically obtained from the system by using the mathematical model or some estimation algorithm, becomes an important element for the control structure.

Two configurations can be achieved [21]: the so-called *interactions-prediction* one, and the *price-driven* one. In the first approach, the coordination entity gathers system information (states, disturbances) and then, computes an optimal reference value for the interactions vector that must be tracked by the subsystems. Local controllers then use this information to compute the control signals, generally obtained after solving local optimization problems, whose cost functions are

parts of the formerly decomposed global cost function. A possible drawback with this technique is the necessity of computing precise values of the interactions signals, which demands a good model knowledge, as well as many communication exchanges between subsystems and coordinator. A schematic view of such an approach is proposed in Fig. 3.4.

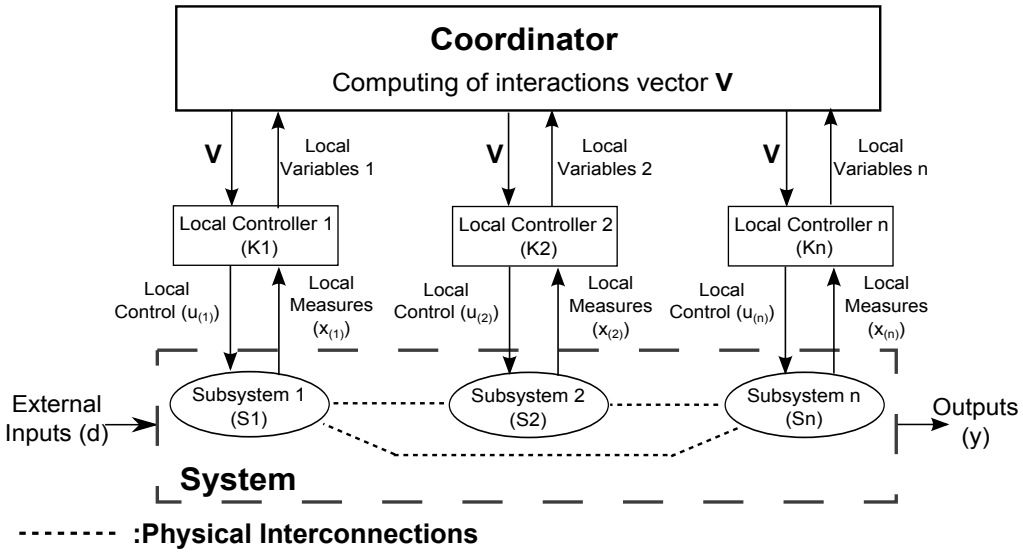

Figure 3.4: Structure of the Interaction-Prediction Distributed Coordinated Control Structure

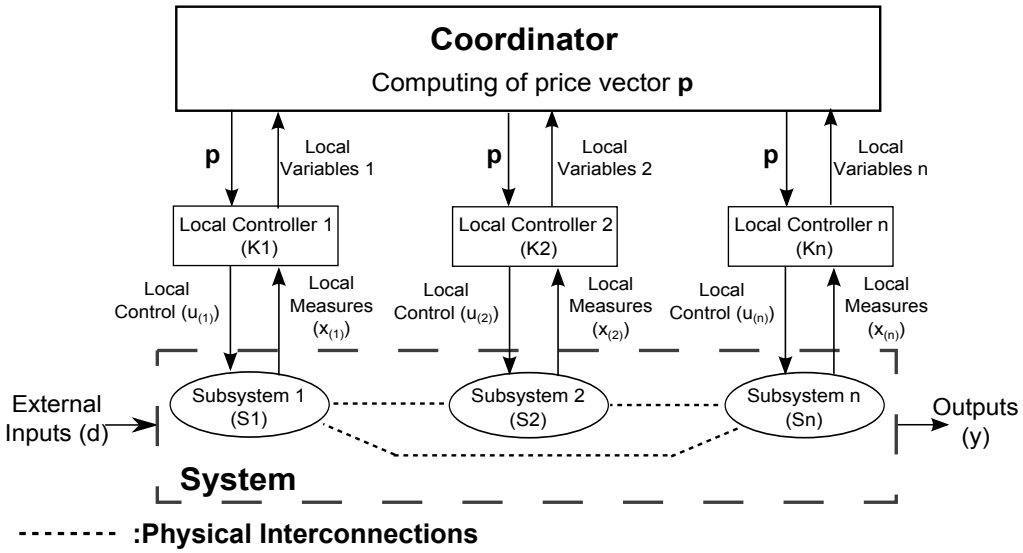

Figure 3.5: Structure of the Price-Driven Distributed Coordinated Control Structure

On the other hand, the *price-driven* coordination method is also used to coordinate different agents in one system. Here the methodology does not require a perfect knowledge of interactions. The coordinator gathers the system information (states and disturbances) and then, computes a cost vector that is used entirely by all local controllers. This cost vector is in fact a Lagrange

multiplier that is used in a global cost function, so as to include interactions as constraints in it [55]. Such a coordination structure is shown in Fig. 3.5.
Notice that in both approaches, the same basic principle is used: decomposition of the global cost function in such way that each agent has to minimize a portion of it. Therefore, optimal local controllers delivers local minimal solutions, that represent a minimization of the global cost function.
Both schemes are interesting, because of their additional control level. The challenge is evaluate which strategy is more suitable for the system: the *interaction-prediction* one requires a good dynamical model for the interaction vector, while the *price-driven* one can perform an optimization that would include the interactions vector, but is not necessary.
Some applications of such methods, more particularly in the field of power systems, can finally be mentioned as follows:

Examples of interaction-prediction coordination.

This coordination method is less found in the literature than the price-driven one. The main reason is the need of intensive information exchange as well as that of precise models for the prediction computations. Nevertheless, contributions such as [56], in which a new gradient-based optimization method is proposed with this approach, demonstrate some interest for this technique. Other contributions in power systems include [57], that presents an application of this method to the load-frequency problem for a couple of power generation units, [58], that uses the interactions to control the temperature of a closed environment, or [6], that proposes the application of this technique to the power production in a hydroelectric valley.

Examples of price-driven coordination.

This approach, when analyzed in details, is an extension of the Lagrangian Duality [55]. The coordinator solves an optimization problem in order to find an optimal value for a Lagrange Multiplier, that is associated with some variable corresponding in most cases to the interaction terms [21, 23]. For instance, [59] presents an analysis considering the Lagragian Dual function and its possible solutions with simple examples, and the implications in the optimization problem, or [60] uses a third-level optimization structure in order to improve performances.
With respect to power systems, one can cite [61], which uses this method for the coordination problem in a small grid with different power generation technologies, while [62] uses the methodology for a hydroelectric valley coordination, but without handling constraints.

3.1.5 Discussion and additional remarks

In the above sections, some characteristics and problems related to the control of large-scale systems have been recalled, in particular thinking of power generation systems.
First, centralized control methods were analyzed and it was reaffirmed that this classical methodology may not be suitable for large scale systems due to aspects such as communication and controller capacities to manage the amount of information. This method will yet be widely used in this thesis in order to get a reference in terms of performances, for evaluation of some proposed control and analysis methods that are detailed in subsequent chapters.
Secondly, decentralized control methods were presented as a well known solution for multivariable systems. Such methodologies do not easily offer guarantees for the system performance, because local controllers do not receive any information from other entities, and their separate actions may result into in instability. However, it opens the door to the distributed control scheme.
Such a distributed scheme includes actions to enhance local controllers, but always considering the

global system performance. In fact, a global objective is split among various subsystems, each of them solving a small portion of the problem. In addition, the use of intercommunication between the agents is vital to know what happens with the other systems, which allows a local agent to modify its control signals accordingly. Such a structure is widely used, and eliminates the needs for having central elements. However, a failure in any agent may affect the performance of the whole system (poor cost-related performance or stability), something that is not desired in power generation applications.
Now, still in the context of distributed control, a coordination element can be added to ensure some performance in the global system. Schemes such as *interaction-prediction* or *price-driven* coordination methods were recalled. In the first one, the coordinator computes an optimal reference for interactions, while the second one computes a weight that ensures the interactivity between subsystems in an optimal fashion. Both proposals consider the global objective function (cost function), which is divided and distributed among the subsystems. Then, local controllers optimize parts of this function, ensuring at the end the desired global performance.
In the remainder of this thesis, only the *price-driven* coordination scheme will be considered (see for instance developments of Chapter 6) for two reasons: the first one is that the amount of data transmissions between the coordinator and agents is reduced to a generic data vector (Lagrange multiplier) that corrects the control signal in such a way that the global cost is minimized and constraints are respected, and the second reason is that the optimization problem structure in the coordinator is suitable to be solved with explicit-fast methods that are desired in power systems, in case of failures or sudden load profiles activation for instance.

3.2 Operative principles of some alternative electric power generation technologies

In the last decades, electric power generation based on new (typically renewable) power sources has become a promising area of development in our society, with the goal of reducing CO_2 emissions, to prevent contamination and climate change for instance, and preserving natural resources, when thinking of oil exploitation for example [63, 64]. In this context, generation technologies based on hydro power, wind, tides, sunlight, geothermal heat, biological decomposition, chemical reactions among other ones, have been included in the integration process of the current power grids facing an increasing electric power demand and consumption, not only due to the increase of population, but also to technology changes and needs.
As introduced in section 2.2.1, most of electric power production in the world and Europe is dominated by non renewable power sources, that include oil, solid fuels and nuclear. However, when such energies are let outside of the analysis, the generation due to alternative power sources reaches about 11% in worldwide [3] and 12.5% in Europe [4], almost in the same levels that Nuclear power.Considering the increasing amount of alternatives, in some years this participation can be more extensive and some sources such as nuclear power may be completely replaced.
Another advantage of the alternative power sources is the possibility of reducing, in long-term, the equivalent environmental impact of their installation. Although the impact can be substantial at the beginning, good maintenance becomes primordial in their development. In recent years, concepts such as *distributed power generation* and *grid integration* have been revised and helped to consolidate these technologies in the society [64]. For example, enormous construction of hydroelectric facilities that alter the nature and society, can be replaced by smaller hydroelectric plants along with photovoltaic and wind farms of small capacities, to produce enough power for the regions that would have been powered by this central otherwise.
Also, some regions with special natural resources choose to replace high-CO_2-emission technologies

by - or just integrate - cleaner and newer ones. For example, Denmark, although pretty small, decided to cover about half of its electric power consumption with alternative power sources by 2030, and close to 100% by 2050 [65], or England, to ensure 15% of its production via alternative sources by 2020 [66].

One of the main purpose of the present work is then to propose tools, from the point of view of automatic control, for the management of distributed power sources, considering the precepts here analyzed. The idea is to consider, in the first place, the characteristics of the most representative alternative power generation technologies: *hydroelectric plant, photovoltaic panel, wind turbine and fuel cell.* Each of them has its own characteristics, in terms of power production and general control objectives. In the present section, an introductory vision is given for each of them, leading at the end to a comparative chart for control perspectives.

3.2.1 Hydroelectric Power Generation Systems

In this first subsection, a general introduction to power production in hydroelectric plants is presented, as well as some fundamentals in related power control.

3.2.1.1 Energy conversion principles

Hydroelectric power production has become the main alternative power generation source in the world. Basically, the hydroelectric power is produced by the action of falling or flowing water through an hydraulic turbine, that is connected to an electrical generator [67]. The first technology is used for high power generation (hundreds of MW), while the second one has been expanded in rural areas for microgeneration, providing also a less invasive generation facilities. In Fig. 3.6 are depicted the general schemes of these plants. Dam-based plants are based on a great amount of water and through an intake, the water is delivered to the penstock that is connected to the turbine. The water then goes to the river. In the water deviation-based case, a deviation of the river (upstream) is made, and a channel network is built in order to deliver the water to the turbine. In both schemes, water is passing from a higher place to a lower place.

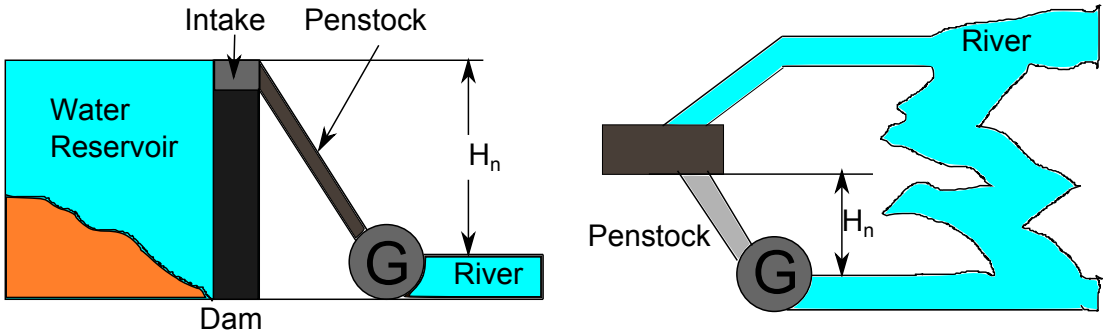

Figure 3.6: General schemes of hydroelectric plants: Dam-based and water deviation-based hydro plants

For such schemes, the following static expressions describe the ideal turbine behavior [68]:

$$\begin{aligned} T_m &= \eta_T \rho g H_n Q / w_R \\ Q &= C_t G_t \sqrt{H_n} \end{aligned} \tag{3.1}$$

Where T_m is the mechanical torque in $kg.m/s$, η_T is the turbine efficiency at flow rate Q in m^3/s, ρ is the water density, g is the gravitational acceleration, H_n is the head in m, w_R is the turbine rotational speed that is equal to the generator speed, C_t is the valve coefficient and G_t is the gate position (between 0 and 1). At the end, one can write the plant capacity as follows [67]:

$$P_{hy} = gQH_n\eta_{ht} \tag{3.2}$$

where η_{ht} is the total efficiency of the plant, that includes the power losses in the turbine (η_T) , the generator and the output transformer. Thus, electric power can be controlled by fixing the flow rate in the turbine.

3.2.1.2 Typical control objectives in hydroelectric power generators

In hydro power generation, two types of controller are traditionally used [1]:

- Frequency control, which is directly associated to the variation of active power generation.
- Voltage control, which is directly related to the variation of reactive power.

Therefore, two well defined control schemes are indeed recognized [1, 69]: Automatic Generation Control (AGC), that is related to the transmission of power from turbine to generator according to the frequency, and Automatic Voltage Regulator (AVR), that is related to the generator side and is focused on the output voltage regulation of the generation system.
The AGC regulates the frequency of the AC power supplied to the grid (50/60 Hz). Its main action consists in controlling the flow rate by opening/closing a valve ($0 - 100\%$), that modifies the mechanical power transmitted to the (typically) synchronous generator. Thus, any variation in the electric load is reflected in a frequency variation. In Fig. 3.7, the basic blocks of the diagram unit are represented, together with the frequency control. Here, ΔP_m is the mechanical power transmitted by the turbine, ΔP_e is the electric power, ΔP_e^* is a reference load value (input signal) Δw_r is the rotor electric frequency. Typical values for the parameters in the figure are:

$$\begin{array}{lll} R_p = 0.05 & T_G = 0.2\ s & M = 6.0\ s \quad D = 1.0 \\ T_W = 1.0\ s & R_T = 0.38 & T_R = 5.0\ s \end{array}$$

It can be seen that the control block is basically a simple Lead Compensator [70]. Any additional mechanism to provide ΔP_e^* can be used for enhancing the system performance.

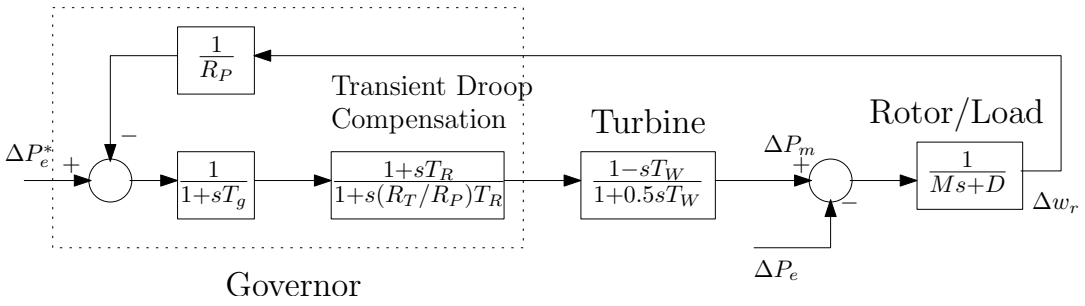

Figure 3.7: Block Diagram of the AGC for a Typical Hydroelectric Unit [1]

When multiple units are interconnected, additional high-level control objectives are required, due to load sharing as well as interconnections, and the so-called Load-Frequency Control (LFC)

is required [1, 39].
About the AVR strategy, it directly acts on the excitation (rotor) circuit. The objective is the regulation of the output voltage around some reference V_{ref} by modifying the generator electric torque through the field circuit. The block diagram of this control is shown in Fig. 3.8. In this case, angle deviations are considered instead of frequency deviations, due to the direct power factor relation with the delivered power. In fact, without this strategy, any increment in generated reactive power results in over-excitation of the synchronous generator, while it is under-excited when the machine absorbs reactive power. It is also possible to add a so-called Power System Stabilizer to the AVR, that feedbacks the generator speed. In this way, frequency variations are compensated and the voltage can be regulated [1, 69].

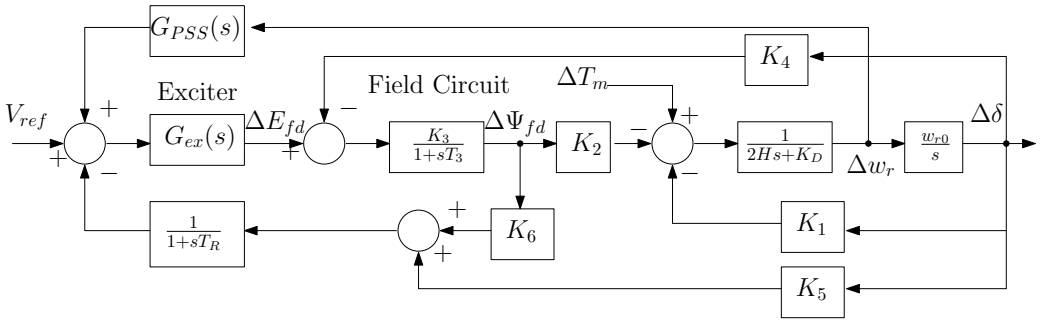

Figure 3.8: Block Diagram representing the AVR with PSS [1]

However, when controlling power factor from a generator unit, the output voltage regulation is lost. Thus, in such generators, output voltage and active power are desirable to be regulated, and reactive compensation is done out of the unit by using any type technology (shunt capacitors or reactors, synchronous condensers, Static Var Compensators (SVC), line compensators, regulating transformers, etc) [1, 71], that can be conveniently added to the power system.
For further information, the reader can refer to [1], where alternative schemes and analysis tools are provided.

3.2.1.3 Advantages and disadvantages of the hydroelectric power generator

The most important element of this technology for power generation is the versatility and scalability that can be gained in its application. Connecting different units in some area, along with control strategies, guarantees the interaction between generators, as it has occurred during decades. Another advantage is the know-how for implementing the different strategies in the technology and the simplicity of the control loops. Thus, changing some control elements is not a problem, considering the dynamical performance and behaviour of electrical and mechanical circuits.
The disadvantages of the technology are related to the environmental impact that is generated when high power facilities are required. The need to build dams, to completely modify river directions, or to displace populations in order to cover only a part of the demanded power, can be considered to significantly affect the benefits of this technology. Besides, the natural water cycle [67] impacts the production of electricity in relation with the capacity of reservoirs that can affect the performance of the plant. Evidently, in a dry period, yet in microgeneration utilities than in gigawatt-size plants. In this context, distributed generation can be a solution, and diversification of the generator technologies an even additional option interesting to be explored in the following decades.

3.2.2 Wind Turbines Power Generation Systems

As done with hydroelectric generators, a small introduction on power conversion principles in wind turbines is here first proposed, together with some discussion on functional characteristics and advantages/disadvantage of this technology.

3.2.2.1 Energy conversion principles

Wind-based generation systems have a mechanism to convert wind power into electrical power, via a wind turbine connected to an electrical generator. The electric load is connected to the excitation (armature) circuit with some power electronics module that allows its connection to the power grid [72, 73]. Contributions such as [74] give interesting details about power conversion topologies applied to wind turbines. A general scheme of such a wind power conversion system is shown in Fig. 3.9.

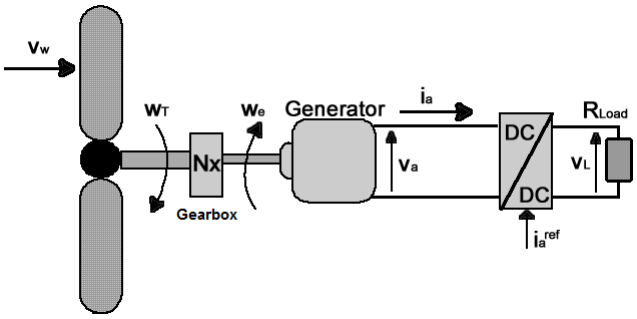

Figure 3.9: General scheme of wind power plant, with a simplified power conversion unit

In this case, the power transmitted from wind turbine to the generator shaft is given by the following relation:

$$P_T = \frac{1}{2}\rho\pi R^2 C_P(\lambda,\beta)v_w^3 \tag{3.3}$$

Where ρ is the air density, R is the wind turbine radius, v_w is the wind speed and C_p is an efficiency parameter that represents the amount of power which can be obtained from the wind. More precisely, C_p is function of the turbine pitch angle β and the so-called Tip-Speed Ratio λ, typically as follows [72, 75]:

$$C_P(\lambda,\beta) = c_1\left(\frac{c_2}{\lambda} - c_3\beta - c_4\right)e^{-c_5/\lambda} \tag{3.4}$$

where $c_1, \cdots c_5$ are constant values and are given by particular characteristics of the turbine[75]. The parameter λ is a relationship between the wind speed w_T and the rotational speed of the wind turbine w_T:

$$\lambda = \frac{w_T}{v_w}R \tag{3.5}$$

About the pitch angle β, it is fixed for the production of some power with respect to some expected mean wind speed value, that can be predicted from environmental forecasts, as well as some amount of required power from the generator [73]. Assuming that β is constant ($\dot{\beta} \simeq 0$), the $C_P(\lambda)$ function can be rewritten as an n-order polynomial of the form:

$$C_P(\lambda) = \sum_{i=0}^{n}\alpha_i(\beta)\lambda^i \tag{3.6}$$

From this, different values of β will result in different values of the $\alpha_i's$, meaning various possible functions of $C_p(\lambda)$ for the same turbine. A representation of such functions is given in Fig 3.10, for a 3-blade turbine [72, 75].

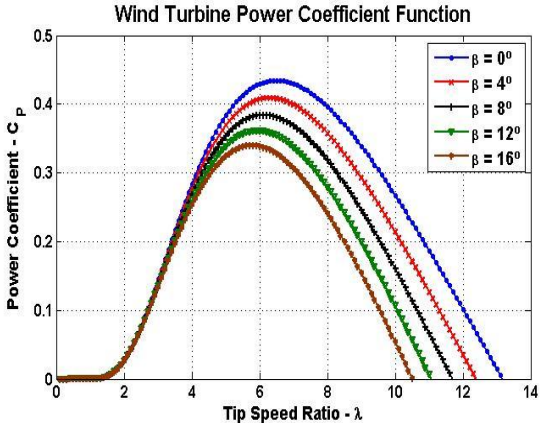

Figure 3.10: Typical curves of the power coefficient for various pitch angles

3.2.2.2 Typical control objectives in wind power generators

Because wind power generators entirely depend on the wind speed, the control is directed to obtain the maximum power from the turbine, while ensuring additional objectives for instance related to the amount of active and/or reactive power that should be delivered to the load.
First of all, a wind turbine has four characteristic power regions, that depend on the wind speed and C_p coefficient at some time [76], and that are illustrated in Fig 3.11, for a small power wind turbine:

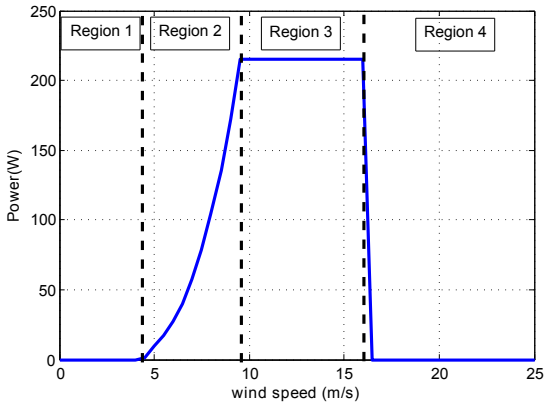

Figure 3.11: Steady-state power curves of a wind turbine with constant pitch angle

- Region 1: In this region of low wind speed, the power production is null due to the high inertia of the equivalent mechanical system. Thus, some mechanism for disconnection of the electrical charge should be taken.

- Region 2: In this region, the power generated by the turbine is proportional to the cube of the wind speed, as seen in the expression (3.3). Here, control strategies for maximizing the power production can be applied.

- Region 3: In this region, the power is limited in order to respect the mechanical and electrical safe operation limits of the system.

- Region 4: In this region, no power production must be generated by the system, because wind speed is too high and mechanical components can be damaged. In fact, winds close to 22 m/s are equivalent to about $80km/h$, that are typical wind speeds for storms and heavy rains.

To start up the machine, for instance, the pitch angle can be increased, in order to accelerate the machine while producing small electrical power. Then, the pitch angle can be decreased until some desired value, according to the expected steady-state efficiency.
Considering the turbine operating in Region 2, power production and its regulation can be done in this region. For example, one can talk of *fixed-speed* or *variable-speed* turbines control schemes [73, 74].
For the *fixed-speed* turbines, the induction generator is connected to the grid through a transformer, while a reactive compensator based on capacitors is added to the system for reduction of the reactive power demand from the generator to the grid. This scheme, although cheap and suitable for fast reparations, is not good for reactive power control.
An alternative solution is the so-called *semi-variable speed* configuration. Here, the generator stator is connected to the grid through a transformer, and the rotor is also connected to the grid throw a power conversion unit. Thus, a rotor-side controller ensures the power production from the wind turbine, while the grid-side controller ensures the quality of the delivered power. Typically, a unitary power factor production ($Q = 0$) is aimed at.
Finally, the *variable-speed* case uses any available generator technology and manipulates accordingly the generator torque and/or flux in order to optimize the power production, and a grid-side converter is used to ensure the power quality.
The schemes corresponding to those three configurations are shown in Fig. 3.12, inspired from [73, 74], where further information can be obtained. In fact, some control techniques are based on the double power conversion scheme offered by the *variable-speed* solution. For example, control strategies based on the measurement or estimation of electrical torque or power coefficient of the wind turbine, in real time, consider the electrical torque as control variable [9, 30, 73, 77]. In this sense, the maximum available power is injected to the grid, either directly - storing some power in an inner battery of the generation system, or changing the blade angle in order to modify the machine efficiency and apply the adequate amount of power to the load. Any control strategy that uses the torque as control objective is based on the mechanical equation of the generator of the form [78]:

$$J\dot{w}_t = T_T - T_e + f(w_t) \tag{3.7}$$

where w_T is the generator speed, J the equivalent inertia, T_T the mechanical torque, T_e the electrical torque (controllable through the power electronics block) and $f(w_T)$ a nonlinear term depending on the current speed.
In the present thesis a contribution to the power maximization of wind turbines in the case of a wind speed sensorless scenario is proposed in chapter 5, based on a variable-speed scheme for a small wind generator using a DC-generator for power conversion [9].

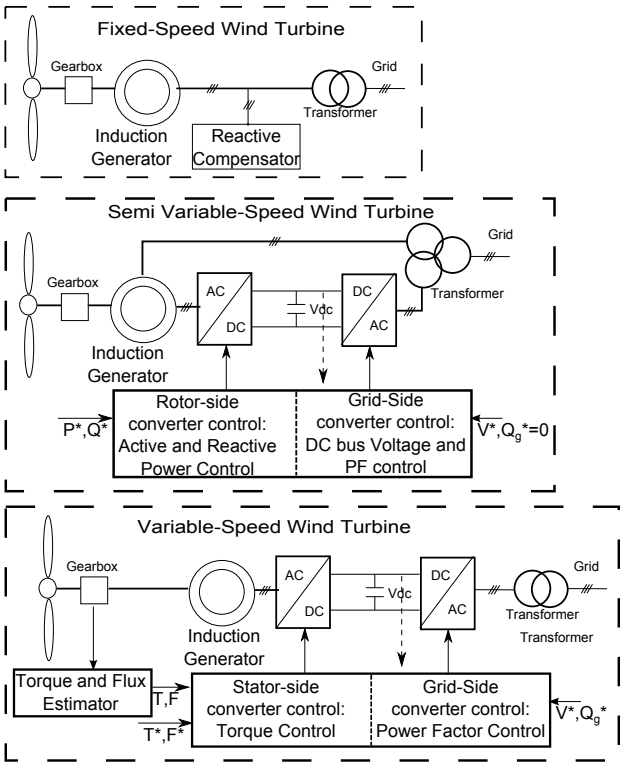

Figure 3.12: Basic Schemes of Power Controllers for Wind Turbines

3.2.2.3 Advantage and disadvantage of wind power generator

Wind turbines have become one of the most developed technologies among the alternative power generation systems [79]. In fact, the purpose of nations such as Denmark to have all its power demand covered by alternative sources by 2050 is largely based on wind power, considering two versions: on-shore and off-shore [65, 72].
Wind turbines can be distributed in some fields, therefore defining wind farms, that include different control strategies for the power injection to the grid. Here, different strategies can be applied, such as prediction of generated power after meteorological data, maximum power production, power quality, etc.
However, this great advantage of modularity and distributivity also becomes its main cause of disadvantages: for example, some inhabited regions have become wind farms, disturbing the local fauna (birds or bats are affected by the new wind patron, that confuse them and provoke their collision with the structure). In a similar way, the augmentation of noise due to the aerodynamical effects provoked by turbines affects all the species, including humans, causing in the long-term, stress and disorientation. Details of such disadvantages and other ones can be revised in [80].
From the point of view of power production, the power generation intermission is one of the most important aspects to be considered. The idea is to capture as much power from the wind as possible. However, in calm or strong wind conditions, power production is cancelled due to the low amount of available energy or to the needs to protect the aerodynamic structure [73]. Therefore, some storage mechanism should be added to the wind power plant, or other types of power coordination must be used when operating with wind turbines. This particular aspect will be further treated in the present work.

3.2.3 Photovoltaic Power Generation Systems

This section is devoted to the electric power generation based on photovoltaic conversion. Its operative principles are recalled, and a short summary of its control objectives as well as its advantage/disadvantages are given.

3.2.3.1 Energy conversion principles

Photovoltaic panels are composed by serial and parallel arrangements of photovoltaic cells (PV cells), that are made of classical semiconductor p-n junctions. When photons reach them, an electrical current is generated and thus delivered to a load [81]. A classical electrical model for the PV cell is shown in Fig. 3.13 [82].

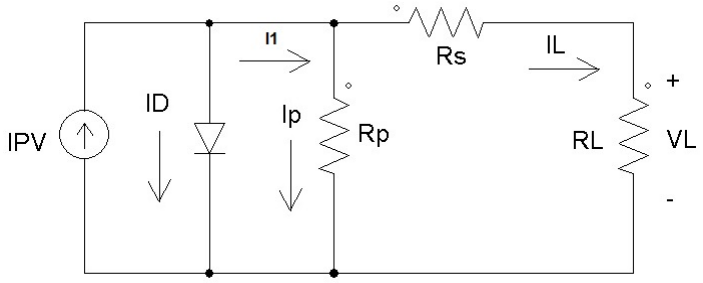

Figure 3.13: PV cell equivalent model

In this model, resistor R_p is related to the leakage current I_p, and R_s to the PV cell losses, while R_L, V_L represent the load. In practice, typical values are $R_s = 0.05 - 0.1\Omega$ and $R_p = 200 - 300\Omega$ [83], but one can deduce these values for any cell by using some measurements as described in [82]. For this PV cell model, and considering an open-circuit operation ($R_L = \infty$), the following expression describes the produced current I_L:

$$I_L = I_{PV} - \underbrace{I_{0,cell}\left[exp\left(\frac{qV}{akT}\right) - 1\right]}_{I_d} - I_p \tag{3.8}$$

where I_{PV} is the current generated by the sunlight, and I_d is the Shockley diode current, with $I_{0,cell}$ the reverse saturation current, V the voltage across the diode ($V = V_L + R_s I_L$), q the electron charge ($1.602x10^{-19}C$), k the Boltzmann constant ($1.3806x10^{-23}J/K$), T the temperature, and a the diode ideality constant (in the range $1.0 - 2.5$, depending on the PV device type) [82].
As for current I_{PV}, it is proportional to the sun irradiation G and temperature T as:

$$I_{PV}(G,T) = [I_{sc,r} + k_I(T - T_r)]\frac{G}{G_r} \tag{3.9}$$

with G_r, T_r the irradiance and temperature at *Standard Test Conditions* (STC) respectively, $I_{sc,r}$ the short-circuit current at STC, and k_I the short-circuit temperature coefficient, that can be found in the datasheet provided by the manufacturer [82].
Considering that PV cell voltage can go up to $0.7V$ as the p-n junction, commercial photovoltaic modules are formed by combination of N_s serial and N_p parallel modules. Then, a Norton equivalent for the PV generator can be obtained, as seen in Fig. 3.14, that is suitable to be adapted in simulation environments [82].

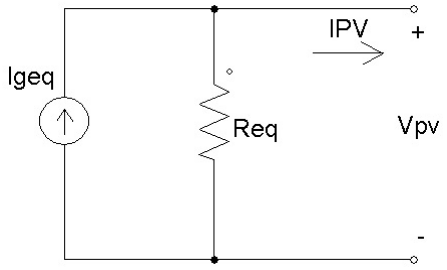

Figure 3.14: Norton equivalent of a PV generator

For obtaining this equivalent model, note that from Fig. 3.13, one can obtain:

$$I_1 = I_{PV} - I_{0,cell}\left[exp\left(\frac{q(V_L + R_s I_1)}{akT}\frac{R_p}{R_s + R_p}\right) - 1\right] \tag{3.10}$$

and from Fig. 3.14, along (3.10) the following equivalent current I_{eq} and resistance R_{eq} can be defined:

$$I_{eq} = I_1 \frac{R_p}{R_p + R_s} \quad R_{eq} = R_s + R_p \tag{3.11}$$

Finally, the equivalent model for the PV generator is written in terms of a current source I_{geq} and a shunt resistor R_{geq}, defined as follows:

$$\begin{aligned} I_{qeg} &= N_p I_{eq} = N_p I_1 \frac{R_p}{R_p + R_s} \\ R_{geq} &= \frac{N_s}{N_p} R_{eq} = \frac{N_s}{N_p}(R_s + R_p) \end{aligned} \tag{3.12}$$

In simulation studies such [81, 82], I_1 should be computed at each step after (3.10). The output voltage V_{pv} depends on the load the PV generator.
For example, for a PV generator connected to a load R_L, the supplied power is finally obtained as:

$$P_{pv} = V_{pv} I_{pv} = R_L I_{pv}^2; I_{pv} = I_{geq} \frac{R_{eq}}{R_{eq} + R_L} \tag{3.13}$$

3.2.3.2 Typical control objectives in photovoltaic power generators

From the elements presented in the previous section, the power production in a photovoltaic generation system is proportional to the environmental temperature (T) and radiation (G), as well as to the quantity of interconnected modules in the generator. In addition, PV modules have some particular characteristics due to the current of the pn junction. In Fig. 3.15 the Current-Voltage (I-V) curve for an MSX60 solar module [2] is presented, also showing the maximum power curves obtained for various radiance measurements G, here in $Suns$ - where 1 $Suns = 1000W/m^2$, for a temperature $T = 50^oC$. With the same principle as in the case of wind turbines, the maximum power production in photovoltaic panels must be ensured. For this purpose, as well as for coupling power levels between the power generator and the load, DC/DC power converters are usually installed in the terminals of PV modules so as to change the equivalent load impedance [26]. In Fig. 3.16, a PV panel is connected through a boost converter [84] to a load resistor R_L. The idea is to transmit the maximum possible power from the PV panel to the load, by controlling the inductor current I_L that is absorbed by the converter, or the voltage at the coupling capacitor C_{in}. Notice that due to controllability properties of the converter, only one action can be made at one time in order to match the maximum available power in the panel with the current characteristics.

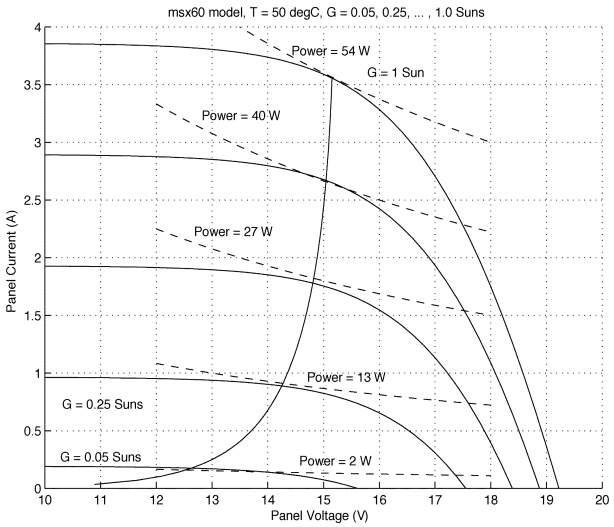

Figure 3.15: I-V curve for an MSX60 solar module [2]

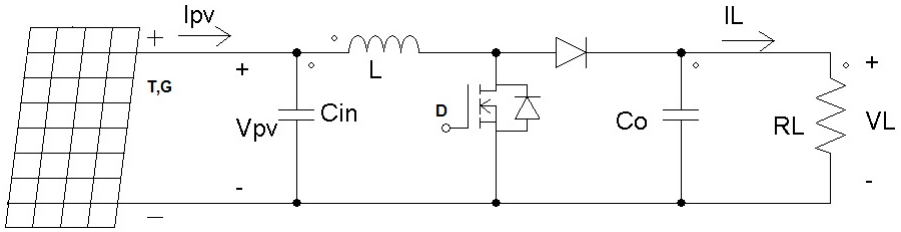

Figure 3.16: PV module and Boost converter

This principle is used in the well-known and widely studied *Maximum Power Point Tracking* strategies. Algorithms such as *Perturb and Observe* (P&O) or *Incremental Conductance* (IC) can be used to achieve the power production [26, 82, 85]. Although these techniques have different operative principles, the idea is always to change the reference voltage V_{pv} in such a way that power is maximized according to some real-time gradient measurements. For example, P&O method tries to maintain the power around the maximum point, even provoking some oscillations when the generated power is close to the optimal. In the IC method, the idea is maintain the system working at each optimal point in the $I-V$ curve (see Fig. 3.15) and the Maximum Power Point is close to those points. In [82] a good synthesis of these methods is presented.
However, there are some conditions in which these algorithms require some special attention. For example, when radiation changes in a fast way, the mentioned algorithms can deliver false maximum power point values, due to bad computation of the gradient. Thus, the updated voltage reference can be erroneous and, in extreme conditions, even result in more power losses. In addition, when some section of the panels are shadowed, the IV characteristic completely changes. Here, more than one *inflexion point* can appear in the $I-V$ curve, and the apparent optimal value cannot be confirmed when the module model is not robust in this sense [86]. The modeling of PV modules in total or partial shadowing events is still currently under investigation, for the purpose of adapting the required reference to the power converter control block [87, 88].

3.2.3.3 Advantages and disadvantages of the photovoltaic power generator

This power generation technology has been adapted in places where obviously the sunlight is permanent all along the year. The use of power electronic modules for the integration to the grid and/or the storage of this energy in batteries for night-time supply increases the possibilities of expansion of this technology as one of the most flexible alternative power generation systems. In particular, the modularity that can be obtained with PV panels makes them of particular interest in places where accessibility to the power grid is limited or impossible.
The main disadvantage of this technology however, is the impossibility to generate power during the night time, or even under cloudy environments. The PV generators require auxiliary energy systems to gather the excess of energy that is not transmitted to the load, evidently to re-provide it in periods when the power demand surpasses the generated one, or during the nights. Another disadvantage is related to the (present) prices of the panels, and the high number of modules required for generating some power in the scale of MW, as required in cities or industries. Fortunately, the technology is being developed interestingly fast, and the implementation and maintenance costs should drop accordingly in the near future.

3.2.4 Fuel Cells Power Generation Systems

In this final subsection for this part, the operative principles of the fuel cells are recalled, and again the related basic control strategies are discussed, together with their main advantages and disadvantages as an alternative power generation system.

3.2.4.1 Energy conversion principles

Power conversion in Fuel Cells (FC) is based in chemical reactions that require Hydrogen and Oxygen for their development [5]. The reactor section of a fuel cell system includes a membrane of ionic interchange that is located between an anode and a cathode. Through the anode, pressurized Hydrogen enters to the fuel cell, that is dissociated into electrons and H+ ions. Here, the electrons flow through the electrical load, while the H+ ions go to the cathode, where they react with Oxygen, producing water and heat. This operation can be summarized by the following reactions:

$$\begin{array}{ll} \text{Anode reaction:} & H_2 \rightarrow 2H^+ + 2e^- \\ \text{Cathode reaction:} & 2H^+ + 2e^- + 0.5O_2 \rightarrow H_2O + heat \\ \textbf{Equivalent FC reaction:} & H_2 + 0.5O_2 \rightarrow H_2O + heat + electricity \end{array} \tag{3.14}$$

For a better illustration of the exact places of these reactions, Fig. 3.17 presents two schemes: a first one for the fuel cell stack, and a second for the main auxiliary systems that allow this generation technology to work: air compressors, humidifiers, valves, cooling units, among other ones.
Considering the different technological advances in the development of auxiliary subsystems, fuel cells are not only applied in stationary generation systems [32, 89, 90], but also in embedded applications, including automobiles, trains and other ones [91, 92, 93, 94]. Within the fuel cell technologies, the most developed one in the latest years is the so-called *PEMFC* (Proton Exchange Membrane Fuel Cell). This class of fuel cell is characterized by a high power density, low corrosion and low working temperature, making it suitable for fast start-up applications [29]. Other fuel cells, such as PAFC (Phosforic Acid Fuel cells), MCFC (Molten Carbonate Fuel Cells) or SOFC(Solid Oxide Fuel cells), are more common for fixed power generation facilities. Table 3.1 summarizes some fuel cells technologies with their main characteristics.

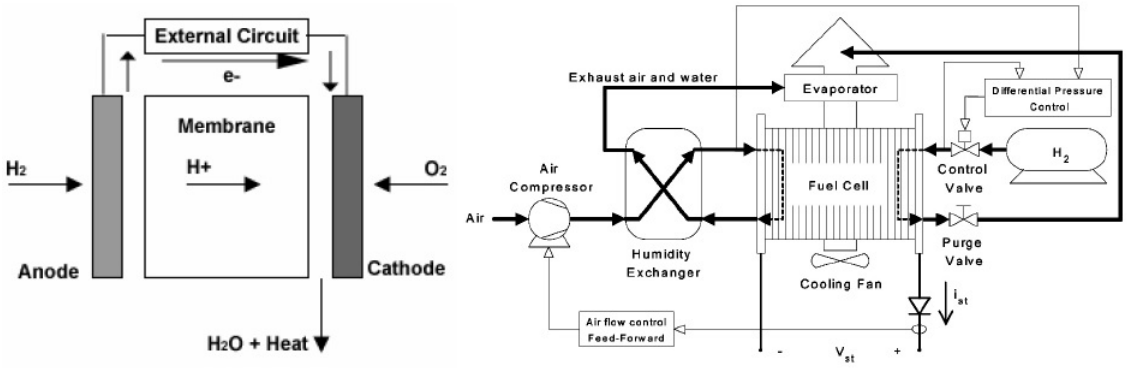

(a) Functional Scheme (b) Fuel cell stack and its auxiliary elements

Figure 3.17: Fuel Cell Power Generator General Schemes

Table 3.1: Characteristics of some fuel cells technologies [5]

Fuel cell Type	**Fuel Type**	**Membrane Material**	**Temperature**	**Applications**
AFC	H_2	KOH	$50-200^oC$	Transport, Portable Generators, Spatial vehicles
PEMFC	H_2	Solid Polymer	$50-100^oC$	Portable and Distributed Generation
DMFC	CH_4	Methanol	$20-90^oC$	Low Power and Large Period Operation Systems
PAFC	H_2	Phosphoric Acid	$\simeq 220^oC$	Isolated/Distributed Generation: Hundreds of kW
MCFC	H_2CO, CH_4	Li, K_2CO_3	$\simeq 650^oC$	Isolated/Distributed Generation: Up to tens of MW
SOFC	H_2CO, CH_4	Solid Oxide	$500-1000^oC$	Isolated/Distributed Generation: Up to hundreds of MW

In terms of power production in fuel cells, it is necessary to recall that a single cell only gives up to $1.2V$. Therefore, fuel cell stacks must be considered, formed by a multiple serial-parallel connection of many individual cells[5, 29].
For a current demand I_{ST} in the external circuit, the following general expression is obtained for the fuel cell voltage:

$$V_{ST}(I_{ST}) = N_c \left[E_0 + \frac{RT_{ST}}{2F} ln\left(\frac{p_{H2}\sqrt{p_{O2}}}{p_{H2O}} \right) \right] - \alpha I_{ST} - \beta ln(I_{ST}) - \eta e^{\theta I_{ST}} \tag{3.15}$$

where E_0 is the activation voltage (about $1.2V$), N_c is the the quantity of cells connected in series, R is the universal gas constant, T_{ST} is the internal fuel cell temperature, F is the Faraday constant, p_{H2}, p_{O2}, p_{H20} are the partial pressures of Hydrogen, Oxygen and water respectively, and $\alpha, \beta, \eta, \theta$ are constant parameters obtained from the polarization curve of the fuel cell [5], shown in Fig. 3.18.

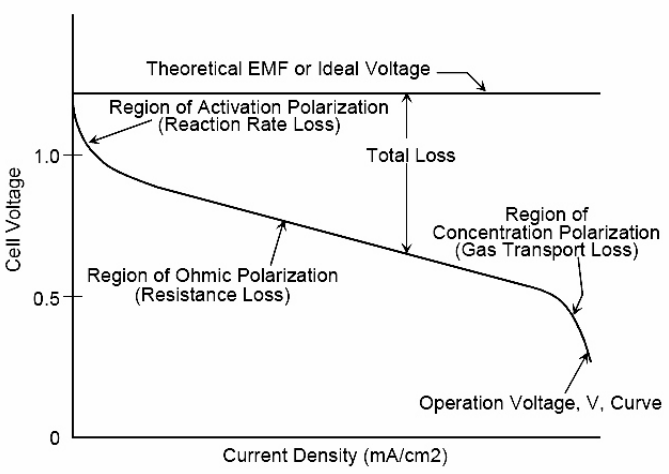

Figure 3.18: Fuel cell polarization curve

Finally, the electric power generated by a fuel cell can be expressed as:

$$P_{fc} = V_{ST} I_{ST} \tag{3.16}$$

3.2.4.2 Typical control objectives in fuel cell power generators

As previously mentioned, the power generated by the fuel cell depends on the reaction of some Hydrogen-based full supplied in the anode and some Oxygen captured in the air at the cathode. Thus, for a demanded current I_{ST}, the following reactive (H_2, O_2) and products (vaporized water) are required/obtained:

$$W_{O2,reac} = M_{O2} \frac{N_c I_{ST}}{4F} \quad W_{H2,reac} = M_{H2} \frac{N_c I_{ST}}{2F} \quad W_{vap,gen} = M_{vap} \frac{N_c I_{ST}}{2F} \tag{3.17}$$

where M_x is the molar mass of each element and W_x is the flow of the reactive/product in the fuel cell. Evidently, and considering the mechanical components that are part of the fuel cell power system, it is possible to write a dynamical model regarding pressures and mass variations, as it can be seen in [27, 29]. However, the interest of this introductory part is only concerned with the analysis of the mechanism of power production and some performance conditions that are ensured by control strategies.
In this context, there is a variable that should be monitored in the fuel cell, known as the *oxygen excess ratio*, λ_{O2}, defined as:

$$\lambda_{O2} = \frac{W_{O2,in}}{W_{O2,reac}} \tag{3.18}$$

where $W_{O2,in}$ is the oxygen injected by the air compressor to the cathode. This ratio can be written in terms of the demanded current as (3.17):

$$\lambda_{O2} = \frac{4F}{N_c M_{O2}} \frac{W_{O2,in}}{I_{ST}} = K_{\lambda,O2} \frac{W_{O2,in}}{I_{ST}} \tag{3.19}$$

Therefore, an increasing current demand - considering a constant air flow, reduces the oxygen ratio. If $\lambda_{O2} < 1$, which implies a lower oxygen concentration required for the reaction, the power system enters into *Oxygen Starvation* that can be destructive for the fuel cell if maintained for a

too long time [29]. In fact, the compressor dynamical response can be described by a model of the form [27]:

$$W_{O2,in}(s) \simeq \frac{a_2 s^2 + a_1 s + a_0}{s^3 + b_2 s^2 + b_1 s + b_0}.u_{comp}(s) \simeq \frac{K_{comp}}{\tau_{com} s + 1}.u_{comp}(s) \tag{3.20}$$

where u_{comp} is the signal from the λ_{O2} controller. The time constant τ_{comp} is of order of seconds and depends on the fuel cell model (size, power range, compressor technology, etc).
One solution consists in monitoring the fuel cell current and applying some filtering action [29, 32, 35], and then, using the control profile along some high level optimization strategy to reduce the power losses in order to fix the control signal in the compressor. However, in practice if the demanded current from the fuel cell is controlled with a bandwidth lower than τ_{comp}, then the Oxigen Starvation (OST) can be prevented and this can be used in simulation studies as made in the present thesis in [8].
Along with this strategy, the need of monitoring the Hydrogen mass is also an important one when using stored Hydrogen. Evidently, as much current is generated, much hydrogen is required, and long-term current demands can be determinant in the future power generation. Thus, this variable should be at least monitored. In fact, the use of an electrolyzer to get Hydrogen from the resulting water is an interesting solution to aim at auto-sufficiency of this power generation unit [95, 96]. In conclusion, two main strategies are required: the control of Oxygen excess ratio, that is linked with the closed-loop bandwidth of the fuel cell, and the control of Hydrogen, to ensure the long-term functionality of the system. Evidently, other control strategies are used for pressures, temperatures, humidity, for instance, but are commonly omitted when dealing with power control objectives.

3.2.4.3 Advantages and disadvantages of the fuel cell power generator

The fuel cells have become an interesting solution for clean power production. For example, the PEMFC only needs Hydrogen and Oxygen for producing electricity, and requires small start time due to its low operation temperature. Its integration to vehicles and small distributed power generation have thus been increasing in the last decade, supported by well-known control strategies and developments.
Considering also the limitations of power bandwidth due to mechanical elements, the use of interconnection topologies that include a fast power unit (battery, supercapacitor or their combination) [97], has made fuel cells more integrable and safer for fixed power generation facilities. In Fig. 3.19 *Serial* ans *Parallel* fuel cell interconnection topologies are shown, where *AESS* means *Auxiliary Energy Storage System*. In this way, an autonomous fuel cell plant can ensure power reliability and autonomy with appropriate control strategies and power storage units.
However, the integration of fuel cells as an economic reliable solution is affected by one important element: the obtention of Hydrogen-based fuel. Even the PEMFC requires highly pure Hydrogen in order to perform good reactions [29], and the other types of fuel cells require acids or gases that are highly contaminant [5]. The production of such reactants can be difficult by itself, reducing the reliability of the power plant project. In this case, fuel cell plants receive some residual chemicals from other processes that can be used for obtaining Hydrogen. On the other hand, the dynamical performance of the stack is not suitable for a direct integration into the grid, as this can be done with some wind turbines for instance, requiring therefore more equipments than other generation technologies. Nevertheless, during the last decades these points have been studied and fuel cells are getting the status of good backup generation units. For instance, in periods of no productivity in wind or solar plants, fuel cells can supply the lack of power, and then be disconnected if required.

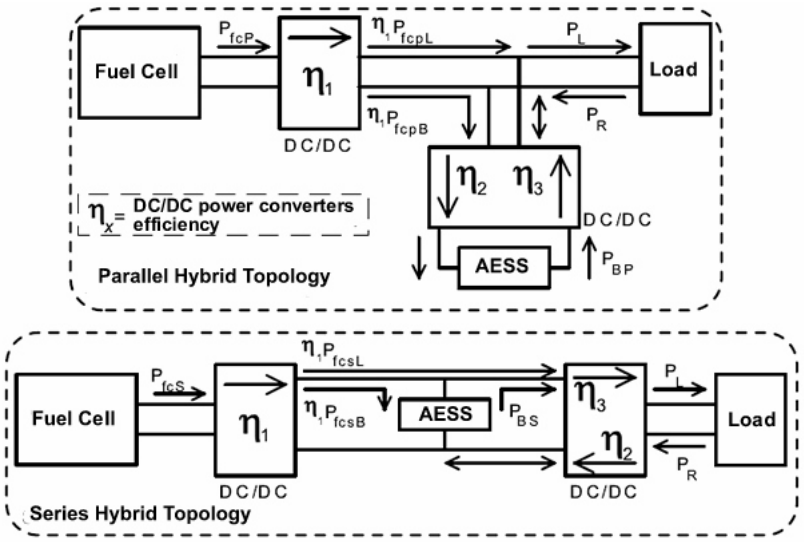

Figure 3.19: Fuel cell interconnection topologies

3.2.5 Comparison of the alternative power generation technologies

As a conclusion of this discussion about alternative generation technologies that will be considered in the thesis, a comparative summary is proposed in Table 3.2: it gathers the most important properties that can help or affect the integration of each of those technologies in the distributed electricity generation context. This information is obtained after analyzing the presented technologies and do not pretend to be exhaustive.

3.3 Conclusions

In this chapter, basic ingredients for the thesis were recalled. In a first part, an overview on the most common concepts in the context of large scale control systems was given: the different strategies that can be used were listed (centralized, decentralized and distributed approaches), their most relevant properties were discussed, and some applications in the context of distributed power generation systems were given. In particular, it has been seen how distributed control methods, along with optimization policies, have become relevant in the development of power coordination solutions for distributed power systems. In this context, the use of price-driven coordination was selected for our contributions.
In the second part of this chapter, the operative principles, control requirements and characteristics of hydroelectric, wind-based, photovoltaic and fuel cell power generation systems were introduced. The purpose was to give some short introduction to those technologies, highlighting their control requirements and expected performance, as well as their drawbacks. Finally, a summary of their characteristics was given in Table 3.2, as a reference for the subsequent developments and analysis. When reading the characteristics of hydroelectric plants, some of the cited characteristics are indeed shared with any large power plant.

Table 3.2: Relevant properties of the analyzed power generation technologies

Generator Technology	Advantages	Disadvantages
Hydroelectric	• Traditional power generation technology • Possibility of implementing high power generation plants (GW) in same facility • Typical control strategies (power,frequency) have good reliability and strong background. • Microgenerators can be adapted directly in natural affluents with minimal impact. • Direct grid integration of generated power. • Power generation at any time.	• Regulation after load change requires tenths of seconds (Governor+Turbine+ Generator dynamics). •Massive power generation facilities demands great environment changes, affecting the surrounding natural areas and populations. • Faulty control strategies can turn into failures in the whole power grid. Security strategies are required.
Wind Turbine	• Operative principles similar to those of hydroelectric generators(induction machines). • Electric generators technologies allows massification of this technology in isolated areas or even cities/towns. • Typical control strategies (power,frequency) have good reliability and strong background. • With power electronics modules, complete integrability with the power grid, ensuring power demand and quality. • Multiple control algorithm proposals to ensure maximum power point tracking. •Current interest for reducing shadowing events for better MPPT strategies.	•Unproductive power generation solution for calm or strong winds. •Massive power generation requires large land extensions for building wind farms. •Wind farms can affect the species that lives near to it.
Photovoltaic	• Scalable technology, well integrated in cities and industries. • Minor maintenance required. • Using power electronic modules, direct grid integration is possible. • Excessive power can be stored for darktime operation.	• Direct power production is constrained to daylight time. • Massive power production demands large solar farms. • Still expensive technology. Profitability in the long-term. • Lifespan of the modules: about 20 years
Fuel Cell	• It can be the cleanest generation technology if PEMFC is used. • Technology highly adaptable to embarked applications. • Generates power if Hydrogen-based fuel is available. Use of electrolyzer as current Hydrogen generator. • High power facilities can be built with some high power fuel cells modules.	• Slow dynamical response due to mechanical elements (air compressor, valves). • Grid integration or even application requires interaction with fast storage device. • Hydrogen-based fuel is sometimes obtained from contaminant chemical process. • strict power demand limitation for avoiding fuel cell damage due to OST.

Chapter 4

THEORETICAL BACKGROUND ON MODEL PREDICTIVE CONTROL AND INVARIANT SETS

Contents

4.1 Recalls on Model Predictive Control 48
4.1.1 Unconstrained MPC Formulation 48
4.1.2 Description of constraints for MPC solution 50
4.1.3 Solution of the constrained MPC problem 53
4.1.4 Adaptation of the geometric characteristic 56
4.1.5 Final remarks for the explicit solution algorithm 58
4.1.6 Conclusions 59
4.2 Recalls on Invariant Sets Construction 60
4.2.1 Robust invariant sets based on the bounded-real lemma 61
4.2.2 Computation of polyhedral RPI sets from ellipsoidal ones 62
4.2.3 Computation of invariant sets by expansion of polyhedral sets 64
4.2.4 Illustrative example 65
4.2.5 Computation of robust invariant sets for a family of linear systems 67
4.2.6 Illustrative example 69
4.2.7 Concluding remarks 70
4.3 Conclusions 70

In the present chapter, a theoretical background is presented, in the following topics:

- The principles, mathematical expressions and details of the explicit solution method for the Model Predictive Control strategy, that is considered fundamental in the present thesis. Many textbooks discuss this strategy [17, 41, 98] and it is convenient to highlight part of them for better understanding of this contribution by the reader. In particular, details of the explicit solution method proposed in [41], based in the geometrical characteristic are recalled.
- The principles of Invariant Sets computation for dynamical systems. In the present thesis, this Lyapunov-based theory is used for performing stability test for constrained control schemes. This theory is exploited in Chapter 6 where stability tests are performed for some particular cases of constrained control applications.

4.1 Recalls on Model Predictive Control

Basically, the technique of *Model Predictive Control* (MPC), also called *explicit receding horizon control* or *predictive model-based control* was developed at the end of the 70's, as commented in [17, 41, 98]. The MPC has been used in a wide amount of applications that includes chemical processes [17], power generation systems [33], vehicular applications [91], for instance.
The operation of MPC can be summarized as follows: the system states should reach some reference values that can be predefined by an upper level entity, taking into account that some perturbations would act on the system. At each time k the control algorithm selects the best control actions according to a decision criterion that assures the system performance under a well defined period $k+N$, where N is known as *prediction horizon*. The information is obtained by using the *predicted* variables by using the dynamical model. Then, at time $k+1$ the control algorithm recomputes the control vector values, by assuring the system performance up to $k+N+1$, considering that perturbations could change between sampling events.
MPC is not referred to a particular control strategy but instead, is in fact a set of control strategies that use a process model for computing a control signal sequence that will *minimize* some cost function. Therefore, the principles of *optimal control* theory are well adapted when working with MPC, requiring that some tasks should be carried out for each problem:

- To select an adequate cost function that will penalize the system dynamics, control actions and their possible interactions.
- To specify the admissible set for solving the optimization problem, based on the defined constraints.
- To choose an appropriate prediction horizon N for solving the problem.

These elements are in fact related and affect the optimization problem. For instance, the prediction horizon is the time window that is used for optimizing the cost function, from the current instant $t = k$ until the prediction horizon time $t = k + N$. However, the *predicted states vector*, obtained directly from the dynamical model, will have a greater dimension when N increases.
On the other hand, the selection of the admissible optimization relies on the system limitations, as well as operative conditions that can change at each sampling time. This is in fact an advantage for the MPC-based applications, because the control signals are calculated at each sampling time according to the current constraints set definition.
Considering these characteristics, the MPC is typically suitable for controlling complex systems subject to saturations that must be avoided.

4.1.1 Unconstrained MPC Formulation

In this first part, the principle of decomposition and the definition of matrices, vectors and cost functions will be shown. Let consider the following linear discrete time system:

$$\begin{aligned} x_{k+1} &= Ax_k + Bu_k + Ed_k \\ y_k &= Cx_k \end{aligned} \tag{4.1}$$

with k denoting the current time, x_k, u_k, d_k, y_k the states, inputs, disturbances and outputs vectors of order n, m, q and o respectively, and the state, input, disturbance and output matrices respectively as $A \in \Re^{n\times n}$, $B \in \Re^{n\times m}$, $E \in \Re^{n\times q}$ and $C \in \Re^{o\times n}$.
Define reference values for states and inputs vectors x_s and u_s for some expected steady state

disturbance d_s. If the matrix A has some eigenvalues equals to 1, the references values would be set according to the initial operative condition. Otherwise, one can compute the reference values vectors from desired output values y_s and known disturbance vector steady state values d_s, by using methods such the proposed in [41] for fixing these reference values:

$$\begin{aligned} x_s &= C^{-1} y_s \\ u_s &= B^{-1}[(I - A)x_s - E d_s] \end{aligned} \tag{4.2}$$

where it is assumed that B and C are non-singular matrices.
In the context of MPC, the optimization problem will minimize the control and state tracking errors, $\tilde{u}_k = u_k - u_s$ and $\tilde{x}_k = x_k - x_s$ under the effect of disturbances variation around an expected steady state disturbance value $\tilde{d}_k = d_k - d_s$, in a time window equivalent to the prediction horizon N, with a final state tracking error $\tilde{x}_N = x_N - x_s$.
The cost function J_g (subindex g stands for "general") to be minimized by selecting an appropriate control vector sequence sequence $\boldsymbol{u} = [u_0 ... u_{N-1}]^T$ and the weighting matrices $P = P^T \geq 0, Q = Q^T$ such that $Q - S_u R_u^{-1} S_u^T \geq 0$ is:

$$J_g = \frac{1}{2}\left(\tilde{x}_N^T P \tilde{x}_N + \sum_{k=0}^{N-1} \tilde{x}_k^T Q \tilde{x}_k + \sum_{k=0}^{N-1} \tilde{u}_k^T R_u \tilde{u}_k + 2 \sum_{k=0}^{N-1} \tilde{u}_k^T S_u \tilde{x}_k \right) \tag{4.3}$$

with the constraints imposed by the system dynamics in (4.1). In practice, only the first term of the control sequence (i.e the first m elements of the solution) are applied and the problem is resolved for the next sampling time. According to the system dynamics (4.1) one can obtain an optimization problem in a *Quadratic Programming* (QP) context [55], by defining the following predicted system vectors of states, inputs and disturbances:

$$\begin{aligned} \boldsymbol{x} &= \begin{bmatrix} x_1 & \cdots & x_N \end{bmatrix}^T & \boldsymbol{x_s} &= \begin{bmatrix} x_s & \cdots & x_s \end{bmatrix}^T \\ \boldsymbol{u} &= \begin{bmatrix} u_0 & \cdots & u_{N-1} \end{bmatrix}^T & \boldsymbol{u_s} &= \begin{bmatrix} u_{s0} & \cdots & u_{sN-1} \end{bmatrix}^T \\ \boldsymbol{d} &= \begin{bmatrix} d_0 & \cdots & d_{N-1} \end{bmatrix}^T & \boldsymbol{d_s} &= \begin{bmatrix} d_{s0} & \cdots & d_{sN-1} \end{bmatrix}^T \end{aligned} \tag{4.4}$$

Remark: It is considered that the disturbance reference value d_s is known and will be considered the same during the prediction horizon N. However, if there are available values for future disturbance references, they can be included in the computing.

Considering the control sequence $\boldsymbol{u}$ as decision variable, one can write the *predicted* states and states error vectors as function of the current states vector x_0 as follows:

$$\begin{aligned} \boldsymbol{x} &= \Omega x_0 + \Gamma \boldsymbol{u} + \Theta \boldsymbol{d} \\ \tilde{\boldsymbol{x}} &= \Omega(x_0 - x_s) + \Gamma(\boldsymbol{u} - \boldsymbol{u_s}) + \Theta(\boldsymbol{d} - \boldsymbol{d_s}) \end{aligned} \tag{4.5}$$

where matrices Ω, Γ and Θ are defined as (see Appendix A for more details):

$$\Omega = \begin{bmatrix} A \\ A^2 \\ \vdots \\ A^N \end{bmatrix} \quad \Gamma = \begin{bmatrix} B & 0 & \cdots & 0 \\ AB & B & \cdots & 0 \\ \vdots & \vdots & \ddots & \vdots \\ A^{(N-1)}B & A^{(N-2)}B & \cdots & B \end{bmatrix} \quad \Theta = \begin{bmatrix} E & 0 & \cdots & 0 \\ AE & E & \cdots & 0 \\ \vdots & \vdots & \ddots & \vdots \\ A^{(N-1)}E & A^{(N-2)}E & \cdots & E \end{bmatrix} \tag{4.6}$$

Before giving the QP problem, let define the following extended weighting matrices for the system, where Q, R_u and S_u are chosen according to the required system performance, while P, the same one introduced at (4.3), is obtained after solving the Discrete-time Ricatti Algebraic Equation [16] for the system dynamics (4.1) and the preselected weight matrices.

$$\boldsymbol{Q} = diag\{Q \ \cdots Q \ P\}, \boldsymbol{R_u} = diag\{R_u \cdots R_u\}, \boldsymbol{S_u} = diag\{S_u \cdots S_u\} \tag{4.7}$$

Thus, the cost function (4.3) can be initially expressed, as function of $\tilde{\boldsymbol{x}}$ and $\tilde{\boldsymbol{u}}$ as:

$$J_g = \frac{1}{2}\left(\tilde{x}_0^T Q \tilde{x}_0 + \tilde{\boldsymbol{x}}^{\boldsymbol{T}}\boldsymbol{Q}\tilde{\boldsymbol{x}} + \tilde{\boldsymbol{u}}^{\boldsymbol{T}}\boldsymbol{R_u}\tilde{\boldsymbol{u}} + 2\tilde{\boldsymbol{u}}^{\boldsymbol{T}}\boldsymbol{S_u}\tilde{\boldsymbol{x}}\right) \tag{4.8}$$

After replacing (4.5) into (4.8) is obtained the following expression for the cost function:

$$J_g = \bar{V} + \frac{1}{2}\boldsymbol{u}^{\boldsymbol{T}}\boldsymbol{H}\boldsymbol{u} + \boldsymbol{u}^{\boldsymbol{T}}[\boldsymbol{K_1}(x_0 - x_s) + \boldsymbol{K_2}(\boldsymbol{d} - \boldsymbol{d_s}) - \boldsymbol{H}\boldsymbol{u_s}] \tag{4.9}$$

Where $\bar{V}$ includes all the terms independent of $\mathbf{u}$, and the other matrices are defined as:

$$\boldsymbol{H} = \Gamma^T\boldsymbol{Q}\Gamma + \boldsymbol{R_u} + 2\boldsymbol{S_u}\Gamma;\ \boldsymbol{K_1} = \Gamma^T\boldsymbol{Q}\Omega + \boldsymbol{S_u}\Omega;\ \boldsymbol{K_2} = \Gamma^T\boldsymbol{Q}\Theta + \boldsymbol{S_u}\Theta. \tag{4.10}$$

As a consequence, the minimization of the cost function (4.9) has an explicit solution in terms of the input sequence vector, denoted as $\boldsymbol{u}^*_{uc}$ as:

$$\boldsymbol{u}^*_{uc} = -\boldsymbol{H}^{-\mathbf{1}}[\boldsymbol{K_1}(x_0 - x_s) + \boldsymbol{K_2}(\boldsymbol{d} - \boldsymbol{d_s}) - \boldsymbol{H}\boldsymbol{u_s}] \tag{4.11}$$

This solution is in fact the *unconstrained solution*, denoted by the subindex *uc* for the aforementioned cost function, i.e. the solution without ANY constraint. This solution has three properties:

1. One can obtain a solution for the optimization problem for any condition of the states vector x_0.
2. The steady state system behaviour by using $\boldsymbol{u}^*_{uc}$ is similar to the one provided by a Linear Quadratic Regulator (LQR) [41]. One can therefore conclude that LQR is an special case of MPC when $N = \infty$.
3. The computed control sequence is indeed optimal, but is commonly not feasibility, due to saturation in states and/or actuators when applied.

Therefore, it is necessary to include some constraints in terms of the admissible system conditions.

4.1.2 Description of constraints for MPC solution

In practice, one can define an admissible domain for finding a solution for the problem described in (4.9), with direct dependence on the admissible domains of states, inputs, outputs and disturbance in any required configuration according to the problem ([17, 41, 98]). In the context of this thesis, the following sets represents the admissible domains for the states, inputs, inputs change and disturbance respectively:

$$\begin{array}{ll} x_k \in \mathcal{X} & \text{where } \mathcal{X} = \{x_k \in \Re^n : x_{min} \leq x_k \leq x_{max}\} \\ u_k \in \mathcal{U} & \text{where } \mathcal{U} = \{u_k \in \Re^m : u_{min} \leq u_k \leq u_{max}\} \\ \delta u_k \in \delta\mathcal{U} & \text{where } \delta\mathcal{U} = \{u_k, u_{k-1} \in \Re^m : \delta u_{min} \leq u_k - u_{k-1} \leq \delta u_{max}\} \\ d_k \in \mathcal{D} & \text{where } \mathcal{D} = \{d_k \in \Re^q : d_{min} \leq d_k \leq d_{max}\} \end{array} \tag{4.12}$$

Each inequality in (4.12) must be respected component by component. Here, one can distinguish hard and soft constraints, according to the admissible solutions and system configuration [41].
For example, the input constraints u_k and δu_k should be always assured, because they are related to actuators capacities. In the case of states and disturbance constraints, the first ones may be violated in transient conditions and should be fixed in terms of tolerance values. In the same way, the disturbance can be out of its admissible set in case of faults or unbounded disturbances. Here,

one can talk of soft constraints, that can be violated in some ways, but should be *a priori* respected. The type of constraints fixes some parameters that can be treated when finding an optimal solution for the optimization problem in terms of admissibility, directly related with possible computational issues.
At the end, all the constraints can be written in terms of the control sequence vector $\mathbf{u}$, after using the system dynamics and the predicted state values. More details for each constraints construction are given in Appendix A. Before describing each expression for the predicted constraints, let define the following extended vectors of admissible values for each quantity:

$$\begin{aligned}
\boldsymbol{x_{max}} &= \begin{bmatrix} x_{max_1} & \cdots & x_{max_{(N)}} \end{bmatrix}^T & \boldsymbol{x_{min}} &= \begin{bmatrix} x_{min_1} & \cdots & x_{min_{(N)}} \end{bmatrix}^T \\
\boldsymbol{u_{max}} &= \begin{bmatrix} u_{max_0} & \cdots & u_{max_{(N-1)}} \end{bmatrix}^T & \boldsymbol{u_{min}} &= \begin{bmatrix} u_{min_0} & \cdots & u_{min_{(N-1)}} \end{bmatrix}^T \\
\boldsymbol{d_{max}} &= \begin{bmatrix} d_{max_0} & \cdots & d_{max_{(N-1)}} \end{bmatrix}^T & \boldsymbol{d_{min}} &= \begin{bmatrix} d_{min_0} & \cdots & d_{min_{(N-1)}} \end{bmatrix}^T \\
\boldsymbol{\delta u_{max}} &= \begin{bmatrix} \delta u_{max_0} & \cdots & \delta u_{max_{(N-1)}} \end{bmatrix}^T & \boldsymbol{\delta u_{min}} &= \begin{bmatrix} \delta u_{min_0} & \cdots & \delta u_{min_{(N-1)}} \end{bmatrix}^T
\end{aligned} \tag{4.13}$$

States constraints

The states constraints can be written as follows:

$$x_{min} \leq x_k \leq x_{max} \tag{4.14}$$

This expression can be separated into two inequalities as follows:

$$\begin{aligned} x_k &\leq x_{max} \\ -x_k &\leq -x_{min} \end{aligned} \tag{4.15}$$

Using the dynamical equation (4.1) and the predicted states values (4.5), by considering that $\mathbf{d}$ will be saturated for each case, and considering the matrices Γ, Ω and Θ defined in (4.6), one can write the states constraints as:

$$\begin{aligned} \Gamma \boldsymbol{u} &\leq \quad \boldsymbol{x_{max}} - \Omega x_0 - \Theta \boldsymbol{d_{max}} \\ -\Gamma \boldsymbol{u} &\leq -\boldsymbol{x_{minx}} + \Omega x_0 + \Theta \boldsymbol{d_{min}} \end{aligned} \tag{4.16}$$

Inputs constraints

The inputs constraints can be written as follows:

$$u_{min} \leq u_k \leq u_{max} \tag{4.17}$$

That can be separated into the following inequalities:

$$\begin{aligned} u_k &\leq u_{max} \\ -u_k &\leq -u_{min} \end{aligned} \tag{4.18}$$

One can express the inputs constraints with the inputs extreme vectors of (4.13) and the identity matrix $I_{N \times m}$, with N as the prediction horizon and m the size of the input vector, as follows:

$$\begin{aligned} I_{N \times m} \boldsymbol{u} &\leq \quad \boldsymbol{u_{max}} \\ -I_{N \times m} \boldsymbol{u} &\leq -\boldsymbol{u_{min}} \end{aligned} \tag{4.19}$$

Input's slew rate constraints

Similarly to the other constraints description, the slew rate of inputs can be specified as follows:

$$\delta u_{min} \leq u_k - u_{k-1} \leq \delta u_{max} \tag{4.20}$$

Again, the expression can be separated into two inequalities as:

$$\begin{aligned} u_k - u_{k-1} &\leq \delta u_{max} \\ -u_k + u_{k-1} &\leq -\delta u_{min} \end{aligned} \tag{4.21}$$

One can write the constraints for input's slew rate as a function of the previously applied input u_{-1} and the limit vectors in (4.5) as follows:

$$\begin{aligned} E_\delta \boldsymbol{u} &\leq \quad \delta \boldsymbol{u_{max}} + E_{-1} u_{-1} \\ -E_\delta \boldsymbol{u} &\leq -\delta \boldsymbol{u_{min}} - E_{-1} u_{-1} \end{aligned} \tag{4.22}$$

with E_δ and E_{-1} defined as follows:

$$E_\delta = \begin{bmatrix} I_m & 0 & \cdots & 0 \\ -I_m & I_m & \cdots & 0 \\ \vdots & \ddots & \ddots & \vdots \\ 0 & \cdots & -I_m & I_m \end{bmatrix} \quad E_{-1} = \begin{bmatrix} I_m \\ 0 \\ \vdots \\ 0 \end{bmatrix} \tag{4.23}$$

Definition of the Constraints Polyhedral

Taking the expressions for the constraints obtained in (4.16), (4.19) and (4.22), one can write the constraints, for the prediction horizon N in terms of the control sequence $\mathbf{u}$ as the following polyhedral set:

$$L\boldsymbol{u} \leq W(x_0, u_{-1}) \tag{4.24}$$

where L and $W(x_0, u_{-1})$ are matrices, and inequalities should be verified line by line. Notice that W depends of x_0 and, when slew rate should be limited, also of u_{-1}, giving rise to a polyhedral that changes with the evolution of states and inputs. More precisely:

$$\begin{aligned} & W = \Delta + \bar{\xi} x_0 + \bar{\xi}_u u_{-1} \\ \text{With, } L = \begin{bmatrix} \phi \\ -\phi \end{bmatrix} \quad & W = \begin{bmatrix} \bar{\Delta} \\ -\underline{\Delta} \end{bmatrix} + \begin{bmatrix} -\xi \\ \xi \end{bmatrix} x_0 + \begin{bmatrix} -\xi_u \\ \xi_u \end{bmatrix} u_{-1} \end{aligned} \tag{4.25}$$

$$\begin{aligned} \phi &= \begin{bmatrix} \Gamma \\ I_{N\times m} \\ E_\delta \end{bmatrix} \quad \bar{\Delta} = \begin{bmatrix} \boldsymbol{x_{max} - \Theta d_{max}} \\ \boldsymbol{u_{max}} \\ \boldsymbol{\delta u_{max}} \end{bmatrix} \quad \underline{\Delta} = \begin{bmatrix} \boldsymbol{x_{min} - \Theta d_{min}} \\ \boldsymbol{u_{min}} \\ \boldsymbol{\delta d_{min}} \end{bmatrix} \\ \xi &= \begin{bmatrix} \Omega \\ 0_{N\times m} \\ 0_{N\times m} \end{bmatrix} \qquad \xi_{-1} = \begin{bmatrix} 0_{N\times m} \\ 0_{N\times m} \\ E_{-1} \end{bmatrix} \end{aligned} \tag{4.26}$$

Considering this result, the polyhedral previously defined defines the admissible set for the following optimization problem:

$$\begin{aligned} \min_{\boldsymbol{u}} \quad & \tfrac{1}{2}\boldsymbol{u^T H u} + \boldsymbol{u^T}[\boldsymbol{K_1}(x_0 - x_s) + \boldsymbol{K_2}(\boldsymbol{d} - \boldsymbol{d_s}) - \boldsymbol{H u_s}] \\ \text{subject to} \quad & L\boldsymbol{u} \leq W \end{aligned} \tag{4.27}$$

Where the objective function gains are defined in (4.10) and the polyhedral matrices of the constraints polyhedral defined in (4.25). By using appropriate computational tools, one can solve the problem (4.27) that will give an optimal constrained control sequence $\boldsymbol{u}_c^* = [u_0^* \cdots u_{N-1}^*]^T$, whose components will respect the following property:

$$\boldsymbol{u}_c^* \in \mathcal{U}_c \qquad \text{where } \mathcal{U}_c = \{\boldsymbol{u} \in \Re^{N\times m} : L\boldsymbol{u} \leq W\} \tag{4.28}$$

4.1.3 Solution of the constrained MPC problem

The purpose of this thesis is not to propose new algorithms for the solution of constrained MPC problems as (4.27). However, it is needed an algorithm that delivers a reliable solution in small computational time, and also that allows any class of manipulation at every step, typically signals and polyhedral manipulation at each sampling time.
Some methods are based on classical and well-known tools such as interior-point (barrier, logarithmic barrier), active set or other gradient(Newton)-based methods [41, 55] that are still used when the cost function or the constraints are difficult to manipulate, or the system has non-linear dynamics that does not allow other class of treatment, and iteractive methods result effective. Some recent works using such methodologies are shown in [38, 99].
However, in the last years, explicit solution methods have been developed with the objective of solving constrained MPC problems while using low computational and high speed algorithms. The most explored characteristic in these solutions is in fact the geometry of the problem, based on the admissible states and/or input domains, as well as the expected critical conditions at the system, typically given by the disturbances norm and the current states values. For example, contributions such as [100, 101] use the geometry of the QP problem for detecting solutions according to the current state region for some bounded disturbances and then, some feedback gain is computed and used as control signal. However, the pre-computation of these regions is a vital element for the success of the algorithm, as well as the possibility to merge consecutive regions into more complex polytopes for reducing the complexity. In [41] a similar procedure is followed, in which the admissible states set is divided accordingly to the admissible values of the inputs. Again, the input vector selection relies on the region in which the states are located. The regions policies are stored in a look-up table that verifies the violated constraints and then, the selection of the control vector is made. Nevertheless, the need of storing data would not be a reliable solution for large scale systems.
Additionally, in [41] a methodology for computing explicit solutions for the constrained MPC is also presented, and used accordingly in [24, 62]. This methodology will be used all along the document and has been used in the contributions [7, 8]. Here, the method is developed under the following hypothesis: the model is linear and discrete time, with a quadratic cost function and linear constraints.
Considering the solution of the QP problem (4.27), with the solutions contained in $\mathcal{U}_c$, one have:

$$\begin{aligned} \boldsymbol{u}_c^* &= \min_{\boldsymbol{u}\in\mathcal{U}_c} \tfrac{1}{2}\boldsymbol{u}^{\boldsymbol{T}}\boldsymbol{H}\boldsymbol{u} + \boldsymbol{u}^{\boldsymbol{T}}[\boldsymbol{K_1}(x_0 - x_s) + \boldsymbol{K_2}(\boldsymbol{d} - \boldsymbol{d_s}) - \boldsymbol{H}\boldsymbol{u_s}] \\ \boldsymbol{u}_c^* &= \min_{\boldsymbol{u}\in\mathcal{U}_c} \tfrac{1}{2}\boldsymbol{u}^{\boldsymbol{T}}\boldsymbol{H}\boldsymbol{u} + \boldsymbol{u}^{\boldsymbol{T}}[\boldsymbol{K_1}x_0 + f_s] \end{aligned} \tag{4.29}$$

where the term f_s gathers the reference values and the disturbance extended vector as:

$$f_s = \boldsymbol{K_1}x_s + \boldsymbol{K_2}(\boldsymbol{d} - \boldsymbol{d_s}) - \boldsymbol{H}\boldsymbol{u_s} \tag{4.30}$$

The QP problem in (4.29) has a geometric interpretation in the domain of $\mathbf{u}$, as seen using the following equation, with c as a constant:

$$\frac{1}{2}\boldsymbol{u}^{\boldsymbol{T}}\boldsymbol{H}\boldsymbol{u} + \boldsymbol{u}^{\boldsymbol{T}}[\boldsymbol{K_1}x_0 + f_s] = c \tag{4.31}$$

(4.31) represents an ellipsoid in $\Re^2$ with center in:

$$\boldsymbol{u}_{uc}^* = -\boldsymbol{H}^{-1}[\boldsymbol{K_1}x_0 + f_s] \tag{4.32}$$

That is in fact, the unconstrained solution of the problem. Finally, the QP problem can be seen as follows: find the smaller ellipsoid that intercepts the constraints region $\mathcal{U}_c$. Then, the vector $\boldsymbol{u}_{uc}^*$ is the point in which the ellipsoid intercepts $\mathcal{U}_c$ and is the optimal control sequence that will

be applied. This is illustrated in Fig. 4.1.

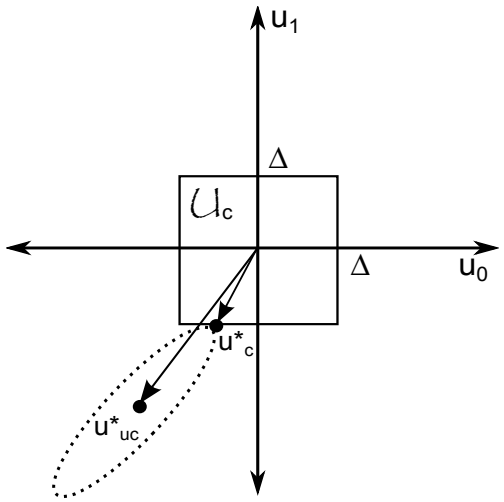

Figure 4.1: Geometric interpretation of the QP problem

The problem can be modified by using the following transformation, via the square root of the Hessian matrix, which is definite positive due to the properties of the cost function.

$$\tilde{\boldsymbol{u}} = \boldsymbol{H}^{1/2}\boldsymbol{u} \tag{4.33}$$

This transformation makes that the ellipsoid and the constraints polyhedral will change into the domain $\tilde{\boldsymbol{u}}$. Therefore, the QP problem is rewritten as:

$$\begin{aligned} \tilde{\boldsymbol{u}}_c^* &= \min_{\tilde{\boldsymbol{u}}\in\tilde{\mathcal{U}}_c} \ \tfrac{1}{2}\tilde{\boldsymbol{u}}^{\boldsymbol{T}}\tilde{\boldsymbol{u}} + \tilde{\boldsymbol{u}}^{\boldsymbol{T}}[\boldsymbol{H^{-1/2}K_1}x_0 + \boldsymbol{H^{-1/2}}f_s] \\ \tilde{\mathcal{U}}_c &= \{\tilde{\boldsymbol{u}} \in \Re^{N\times m} : \tilde{L}\tilde{\boldsymbol{u}} \leq W\} \end{aligned} \tag{4.34}$$

With the constraints polyhedron $\tilde{\mathcal{U}}_c$ defined as follows (Notice that the right side of the constraints polyhedron does not change with the transformation (4.33)) :

$$\tilde{\phi}\tilde{\boldsymbol{u}} \leq \ \bar{\Delta} - \xi x_0 - \xi_u u_{-1} \tag{4.35a}$$

$$-\tilde{\phi}\tilde{\boldsymbol{u}} \leq -\underline{\Delta} + \xi x_0 + \xi_u u_{-1} \tag{4.35b}$$

With this transformation, the geometric topology of the problem is modified. The problem now is to find the smallest sphere centred in $\tilde{\boldsymbol{u}} = -\boldsymbol{H}^{-1/2}[\boldsymbol{K_1}x_0 + f_s]$ that intercepts the set $\tilde{\mathcal{U}}_c$. Here, the solution is expressed as $\tilde{\boldsymbol{u}}_c^*$ that can be taken to the domain of $\boldsymbol{u}$ with the inverse transformation (4.33).
Therefore, the solution of the constrained optimization problem is in fact the projection of $\tilde{\boldsymbol{u}}_{uc}^*$ (the unconstrained solution) into the set $\tilde{\mathcal{U}}_c$ (the constraints polyhedral). The projection is made using the normal vector from the polyhedral to the unconstrained solution, for assuring the minimal Euclidian distance vector $\tilde{\boldsymbol{u}}_c^*$. An illustration of the technique for a system with $\tilde{\boldsymbol{u}} \in \Re^2$ is given in Fig. 4.2.

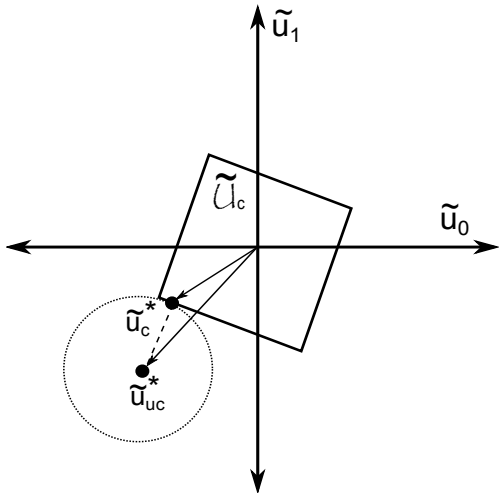

Figure 4.2: Geometric interpretation of the QP problem after the coordenates transformation

Because this projection should be done for each time step, the algorithm must be well defined and with the least quantity of steps. First, define the following notation:

Notation 4.1. *Considering a matrix M and $l \in \mathbb{N}$, as large as the quantity of lines of the constraints polyhedral (4.35). Therefore, M_l denotes the submatrix of M formed by the corresponding lines indicated at l with all their columns. For example, if $l = \{2, 8\}$, $M_l = \{M_2, M_8\}$ the submatrix is formed by the second and eight lines of M.*

The idea is to use this notation, after finding which lines of the constraint polyhedron $\tilde{L}\tilde{\boldsymbol{u}} \leq W$ of (4.34) are violated by the the unconstrained solution $\tilde{\boldsymbol{u}}^*_{uc}$. Consider the rank of the polyhedron $q_L = \text{rank}\ (\phi)$ (see 4.25 for the definition of ϕ) as the length of the set l at Notation 4.1. Now, define the following elements:

- The *active set* l, defines the indices of the constraints that are *active* in the polyhedron (4.35). Here, it is seen which lines violate the constraints.
- The *active set vector* Δ, identifies whether the terms in l correspond to a violated inequality at (4.35a) or at (4.35b), as follows:

$$\begin{array}{lll} \Delta = \bar{\Delta}_l & if & \tilde{\phi}_l\tilde{\boldsymbol{u}} = \bar{\Delta}_l - \xi_l x_0 - \xi_{ul} u_{-1} \\ \Delta = -\underline{\Delta}_l & if & \tilde{\phi}_l\tilde{\boldsymbol{u}} = \underline{\Delta}_l + \xi_l x_0 - \xi_{ul} u_{-1} \end{array} \tag{4.36}$$

- Finally, the *inactive set* s, identifies the index of the constraints that are not active (respected).

The following concept can be defined based in the aforementioned definitions of active set and active set vector:

Definition 4.1. *[41] Considering that a **face** of the constraint polyhedron is the interception, with the constraint polyhedron, of the hyperplane defined by some active constraints at (4.35a), (4.35b). This active constraint can be described as the **active pair** (l, Δ) with the following characteristic (hyperplane of violated inequalities):*

$$\tilde{\phi}_l\tilde{\boldsymbol{u}} = \Delta - \xi_l x_0 - \xi_{ul} u_{-1} \tag{4.37}$$

At the end, each active face will be associated with an ***active region****, in which the constrained solution* $\tilde{\boldsymbol{u}}_c^*$ *is given by the nearest point (minimal euclidean distance) with respect to the unconstrained solution* $\tilde{\boldsymbol{u}}_{uc}^*$

Finally, one can define properly the active region as follows:

Lemma 4.1. *[41]The active region associated with the active face represented by (4.37) is given by:*

$$S\{[\tilde{\phi}_l\tilde{\phi}_l^T]^{-1}[\tilde{\phi}_l\tilde{\boldsymbol{u}} - \Delta + \xi_l x_0 + \xi_{ul}u_{-1}]\} \leq 0 \tag{4.38a}$$

$$-\underline{\Delta}_s \leq \tilde{\phi}_s\tilde{\boldsymbol{u}} + \xi_s x_0 - \tilde{\phi}_s\tilde{\phi}_l^T[\tilde{\phi}_l\tilde{\phi}_l^T]^{-1}[\tilde{\phi}_l\tilde{\boldsymbol{u}} - \Delta + \xi_l x_0 + \xi_{ul}u_{-1}] \leq \bar{\Delta}_s \tag{4.38b}$$

Where S *is a sign diagonal matrix such that its* $(k,k) - th$ *entry is* $S_{kk} = 1$ *if* $\Delta_k = -\underline{\Delta}_{lk}$ *and* $S_{kk} = -1$ *if* $\Delta_k = \bar{\Delta}_{lk}$.

Theorem 4.1. *Under the conditions of Lemma 4.1, the projection* X_l *at the state space of the active region defined by (4.38) is given by:*

$$\begin{aligned} S\{[\tilde{\phi}_l\tilde{\phi}_l^T]^{-1}G(x_0,u_{-1},f_s)\} &\leq 0 \\ -\tilde{\phi}_s\boldsymbol{H}^{-1/2}(\boldsymbol{K_1}x_0 + f_s) + \xi_s x_0 + \xi_{ul}u_{-1} - \tilde{\phi}_s\tilde{\phi}_l^T[\tilde{\phi}_l\tilde{\phi}_l^T]^{-1}G(x_0,u_{-1},f_s) &\leq \bar{\Delta}_s \\ \tilde{\phi}_s\boldsymbol{H}^{-1/2}(\boldsymbol{K_1}x_0 + f_s) - \xi_s x_0 - \xi_{ul}u_{-1} + \tilde{\phi}_s\tilde{\phi}_l^T[\tilde{\phi}_l\tilde{\phi}_l^T]^{-1}G(x_0,u_{-1},f_s) &\leq \underline{\Delta}_s \end{aligned} \tag{4.39}$$

$$\text{where } G(x_0,u_{-1},f_s) = -\tilde{\phi}_l\boldsymbol{H}^{-1/2}(\boldsymbol{K_1}x_0 + f_s) - \Delta + \xi_l x_0 + \xi_{ul}u_{-1}$$

As a consequence, if $x_0 \in X_l$, *the constrained optimal control* $\boldsymbol{u}_c^*$ *sequence will have the following explicit expression:*

$$\boldsymbol{u}_c^* = \boldsymbol{H}^{-1/2}\tilde{\phi}_l^T[\tilde{\phi}_l\tilde{\phi}_l^T]^{-1}(\Delta - \xi_l x_0 - \xi_{ul}u_{-1}) - \boldsymbol{H}^{-1/2}[I - \tilde{\phi}_l^T[\tilde{\phi}_l\tilde{\phi}_l^T]^{-1}\tilde{\phi}_l]\boldsymbol{H}^{-1/2}(\boldsymbol{K_1}x_0 + f_s) \tag{4.40}$$

where $\tilde{\phi}_l$, ξ_l, ξ_u *and* Δ *defined at (4.35) and (4.36), and* f_s, $\boldsymbol{K_1}$ *defined at (4.30).*

Finally, equation (4.40) is in fact the projection of the unconstrained solution $\boldsymbol{u}_{wc}^*$ to the activated constraints at the polyhedron $\tilde{\mathcal{U}}_c$. However, the projection must be done with respect to the active face of any particular active region, obtained by verifying each inequality (4.35). Evidently, the analysis must be done at each time step, due to the information of the current state x_0, past control signal u_{-1} if required, the current $N - step$ disturbance vector $\boldsymbol{d}$ and the desired reference values x_s, $\boldsymbol{u}_s$ and $\boldsymbol{d}_s$.

4.1.4 Adaptation of the geometric characteristic

The mentioned solution method gives a solution to the optimization problem under constraints, based on the geometric characteristics of the problem. However, some projections to the constraints set $\tilde{\mathcal{U}}_c$ are not included in it, making the solution unsuitable. Here, some concepts used in [6] for fixing the solution method, with the details for the explicit solutions from [41] are taken and explored.
Let consider the space formed by a control sequence $\tilde{\boldsymbol{u}} \in \Re^2$, but also consider the regions $R1$ to $R8$ that are outside of the set $\tilde{\mathcal{U}}_c$, as seen in Fig. 4.3, where are defined the active set indexes for the constraints $l = l_1, l_2, l_3, l_4$ The division in regions helps to establish which constraints are violated for a solution $\tilde{\boldsymbol{u}}_{uc}^*$, and where should be the projection to the constraints space. For example, if the unconstrained solution is located in R_1, that means that inequality l_3 is violated, and the projection will be done in this plane. But if the solution is in R_4, then constraints l_1 and l_4 are

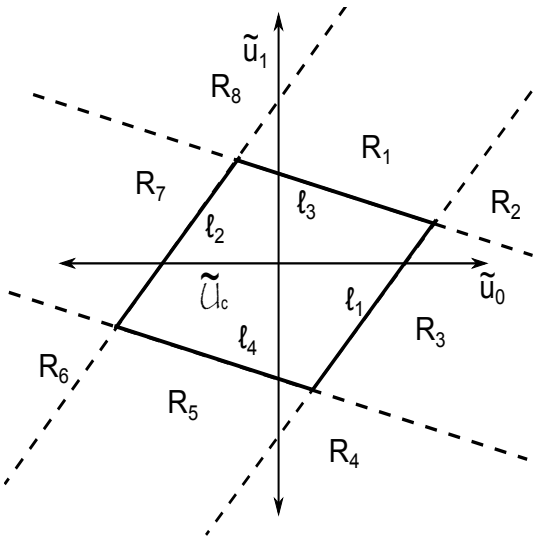

Figure 4.3: Characteristic regions of the input space

violated and the solution is the edge made by the interception of these lines.
However, when the unconstrained solution is near to the interception of a couple of regions, the projection to the polyhedron can remain outside of $\tilde{\mathcal{U}}_c$, and the choice of the optimal solution must be revised. For making this, let define the following temporally constrained solution $\tilde{\boldsymbol{u}}\prime$, obtained after using (4.40) with the current states, disturbances and references values. The solution is obtained after verifying the following cases (see [6] for further information):

- **Case 1:** In the case where ALL the projections of the unconstrained solution over the hyperplanes of the constraints polyhedron $\tilde{\boldsymbol{u}}\prime$ are out of the set $\tilde{\mathcal{U}}_c$, it is selected the CLOSEST vertex with respect to the unconstrained solution $\tilde{\boldsymbol{u}}^*_{uc}$. In Fig. 4.4 an example for this case is given. Here, the solution is close to the line l_3 that divides R_2 and R_3. However, the projection $\tilde{\boldsymbol{u}}\prime$ touches the line l_1, staying outside the constraints set. Therefore, the edge a is selected as solution, $\tilde{\boldsymbol{u}}^*_c$

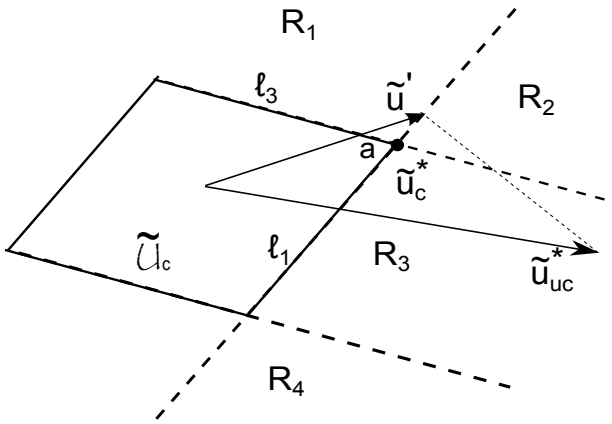

Figure 4.4: Adaptation of the geometric solution for the Case 1.

- **Case 2:** In the case where $\tilde{\boldsymbol{u}}\prime$ includes various active constraints, the constrained solution will be the one included in $\tilde{\mathcal{U}}_c$ and that has the minimal Euclidean distance. Otherwise, if

all the projections $\tilde{\boldsymbol{u}}\prime$ finish out of the constraints set, it is assumed to be brought to Case 1. In Figure 4.5 an example for this situation is presented. Here, the unconstrained solution is located in region R_4, close to R_5. The vector $\tilde{\boldsymbol{u}}^*_{uc}$ can be projected against two different constraints at l_1 or l_4. The projection with l_1 is marked as the well known $\tilde{\boldsymbol{u}}\prime$, and for this potential solution, the vertex b is suitable. However, the projection at l_4 is closest to the center of $\tilde{\mathcal{U}}_c$, that is different from b (smaller Euclidean distance) and will be selected as the unconstrained solution $\tilde{\boldsymbol{u}}^*_c$.

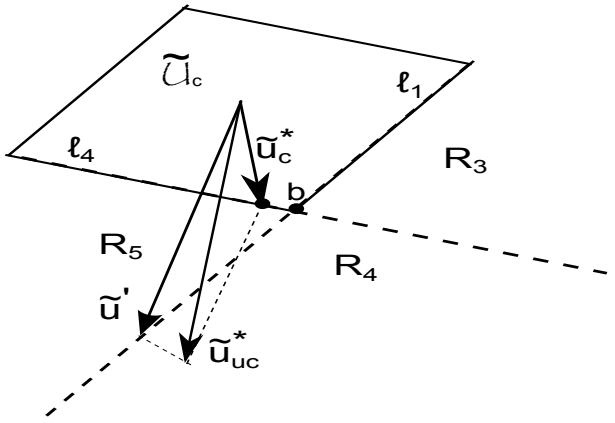

Figure 4.5: Adaptation of the geometric solution for the Case 2.

4.1.5 Final remarks for the explicit solution algorithm

For closing this section, some remarks are added for finding admissible solutions of the constrained QP problem for the receding horizon control.
The first remark is related to the topology of the constraints polyhedron and the cost function for the QP problem here rewritten for easier reading:

$$\begin{array}{ll} \min\limits_{\boldsymbol{u}} & \frac{1}{2}\boldsymbol{u^T H u} + \boldsymbol{u^T}[\boldsymbol{K_1}(x_0 - x_s) + \boldsymbol{K_2}(\boldsymbol{d} - \boldsymbol{d_s}) - \boldsymbol{H u_s}] \\ \text{subject to} & \boldsymbol{L u} \leq W \end{array} \tag{4.41}$$

The explicit unconstrained solution for this problem, $\boldsymbol{u}^*_{uc} = -\boldsymbol{H}^{-1}[\boldsymbol{K_1}x_0 + f_s]$, is optimal if the matrix $\mathbf{H}$ is definite positive, which provokes the cost function to be *twice differentiable*, where its second derivative is positive and therefore, is a minimal solution. In fact, it is said that the cost function is *convex* and a minimal is assured if it satisfies this condition [41, 55].
The second remark is an extension of the former one. The constraints polyhedron should be a *convex set*, which is defined as follows:

Definition 4.2. *[41] A set $S \in \Re^n$ is convex if the line segment joining any two points of the set also belongs to the set. In other words, if x_1, $x_2 \in S$ then $\lambda x_1 + (1-\lambda)x_2$ must belong to $S \; \forall \; \lambda \in [0,1]$.*

This property should be assured for the constraints polyhedron, due to the requirement of numeric-based solution methods (interior points, barrier [41, 55]), and the gradients must be continuous and also convex for obtaining an admissible solution. Therefore, at each time step the vector W of the polyhedron changes according to the current states and past inputs (see (4.25)), making necessary to verify the convexity of the constraints polyhedron.
It is common that $\mathcal{U}_c$ is not always feasible, due to current signals and the selected limit values

included as constant part at W. When is not possible to build a convex constraints polyhedron, it is considered the *constraints relaxation* for, at least, assuring a control signal that can be injected in the system. Here, the idea is to conserve the lines at L and W that are only related with the input signal constraints. This should be done for real time applications, because in practice the system is evolving and typically, the polyhedron turns infeasible when states or disturbance are out of the admissible values, aspect that should be carefully analyzed when selecting these limits. The algorithm for computing the explicit solution for the MPC problem with constraints is shown next.

Algorithm 1 Algorithm for computing the explicit constrained solution for the MPC problem

Require: Off-line computation of QP matrices: $\Gamma, \Omega, \Theta, \boldsymbol{H}, \boldsymbol{K_1}, \boldsymbol{K_2}$, according to (4.6) and (4.10)
Require: Off-line computation of the constraints matrices: $\phi, \bar{\Delta}, \underline{\Delta}, \xi_x, \xi_u$ according to (4.26). If required, these matrices must be adjusted in the online computation.
START
S1: At the instant $t = k$, calculate the explicit solution without constraints $\tilde{\boldsymbol{u}}^*_{uc}$ as (4.32), and then, apply the transformation (4.33).
S2: Verify $\tilde{\boldsymbol{u}}^*_{uc} \in \tilde{\mathcal{U}}_c$.
if $\tilde{\boldsymbol{u}}^*_{uc} \in \tilde{\mathcal{U}}_c$ **then**
Go to **S3.**
else
a) Find the active constraints l by verifying line by line (4.35), and then obtain the matrices $\tilde{\phi}_l$, ξ_l and Δ in (4.36)
b) Compute the vertex of the constraint polyhedron, v.
c) Compute the orthogonal projections $\tilde{\boldsymbol{u}}\prime$ of the unconstrained solution over the active constraints by using (4.40).
d) Build the set of admissible solutions $\tilde{\mathcal{U}}_{Rc} = \{\tilde{\boldsymbol{u}}\prime \in (\tilde{\mathcal{U}}_c \cup v)\}$
e) Compute the euclidean distances $\bar{d}$ for all the admissible solutions at $\tilde{\mathcal{U}}_{rc}$.
f) The constrained solution is the element of the set $\tilde{\mathcal{U}}_{Rc}$ with the minimal Euclidean distance $\tilde{\boldsymbol{u}}^*_c = \min_{\bar{d}} \tilde{\mathcal{U}}_{rc}$
end if
S3: Use the inverse transformation (4.33), and then, select the first m elements from $\boldsymbol{u}^*_c$ as control value, $u_0 = u^*_c$. If required, set $u_{-1} = u_0$ for the next step constraints management.
S4: Wait for the following time sampling and go back to **S1**.

4.1.6 Conclusions

In this section it was presented, in first place, the formulation of the MPC problem, where it was shown how to obtain the Quadratic Problem formulation for the optimization problem, including the construction of the constraints polyhedron. Then, it was analysed the explicit solution method that will be used along this thesis, which is based in the geometric characteristic [6, 41] of the optimization problem. Here, it is obtained an admissible solution of the problem that respects the system constraints, based in the projection of the unconstrained solution to the constraints polyhedron, according to some computational conditions. In the same way, some elements were analyzed, with respect to the polyhedron computation for always obtaining a convex one, according to the current conditions of the system. Finally, the MPC formulation and the solution algorithm was exploited in some contributions that will be further analyzed.

4.2 Recalls on Invariant Sets Construction

In dynamical system analysis, positively invariant sets are used to characterize the trajectories of stable systems. The concept of positively invariant set could be directly related with the surfaces described by a Lyapunov function of a dynamical system [102]. In fact, it is said that when the trajectories of a particular system belongs to the so-called invariant set, they will evolve into that set and will not leave it [103], until reaching some equilibrium steady state condition. This analysis turns more important for evaluating the control performances if the system is subject to exogenous and bounded disturbances. In this case, it is more suitable to compute *minimum Robust Positively Invariant Sets* (mRPI) (see [104, 105, 106]), which describes the smallest possible invariant set for a given perturbed system.

In this section, it will be presented the computation procedure of robust invariant sets and mRPI sets for linear dynamical systems and for polytopic linear systems. These results will be used in Chapter 6 for analysis of closed-loop control systems in presence of control constraints and bounded disturbances. These results were initially presented and discussed in [106].

Preliminaries

Considering the following stable linear system in discrete time:

$$x_{k+1} = Ax_k + Bu_k + Ed_k; \quad y_k = Cx_k \tag{4.42}$$

with k denoting the current time, x_k, u_k, d_k, y_k are the states, inputs, disturbances and outputs vectors of order n, m, q and o respectively, and the state, input, disturbance and output matrices represented, in this order, as $A \in \Re^{n\times n}$, $B \in \Re^{n\times m}$, $E \in \Re^{n\times q}$ and $C \in \Re^{o\times n}$. Here it is assumed a control law in the form of a simple state feedback control of the form $u_k = -Kx_k$. The system turns into:

$$\begin{aligned} x_{k+1} &= (A - BK)x_k + Ed_k \\ x_{k+1} &= \bar{A}x_k + Ed_k \end{aligned} \tag{4.43}$$

The feedback gain K could be computed by any suitable control design method. The gain K has to assure that the eigenvalues of the new dynamic matrix $\bar{A}$ are inside the unitary circle. Here we assume that the maximum bound for the disturbances d_k will be $\bar{d} = \sup d_k$. In addition, it is assumed that the following conditions holds for d_k:

$$d_k \in \mathcal{D} \qquad \text{where } \mathcal{D} = \{d_k \in \Re^q : d_{min} \leq d_k \leq d_{max},\ \forall k \geq 0\} \tag{4.44}$$

The following theorem can be applied for defining any candidate *Lyapunov functions* for discrete time systems.

Theorem 4.2. ***(Lyapunov Functions)***
Let $V(x_k) : \Re^n \to \Re$ be a quadratic Lyapunov function, that is $V(x_k) = x_k^T P x_k$ with a matrix $P > 0$. Considering the discrete time system dynamics $x_{k+1} = Ax_k$. If the evolution of the Lyapunov function $\Delta V(x) := V(x_{k+1}) - V(x_k)$ can be bounded as follows:

$$\begin{aligned} \Delta V(x) = V(x_{k+1}) - V(x_k) &\leq -\phi(\|x_k\|) \\ x_k^T(A^T P A - P)x_k &\leq -\phi(\|x_k\|) \end{aligned} \tag{4.45}$$

where ϕ is a κ-function, then asymptotic stability is ensured, and the matrix P verifies the following inequality:

$$A^T P A - P < 0 \tag{4.46}$$

The following definitions appears as an extension of the concept of Lyapunov stability for stable perturbed systems (4.43).

Definition 4.3. ***Robust Positive Invariance***
The set $\Pi \in \Re^n$ is a robust positively invariant (RPI) set for the discrete time system (4.43) with disturbances d_k if for any $x_k \in \Pi,\ \forall k > \mathbb{N}^+$ and any $d_k \in \mathcal{D}$, it holds that $x_{k+1} \in \Pi$.

Definition 4.4. ***Ultimate Boundness***
It is said that a system is ultimately bounded (UB) to the set Π, if for each $x_0 \in \Re^n$, there exist a $k^* > 0$ such that any trajectory of (4.43) with initial condition x_0 and any arbitrary disturbance $d_k \in \mathcal{D}$, satisfies $x_k \in \Pi,\ \forall k > k^*$.

Robust positively invariant (RPI) sets for perturbed linear systems can be computed by using the Bounded-real Lemma (see [107] for further details). This lemma allows to obtain ellipsoidal RPI sets (equivalent to Lyapunov-based level curves). The obtained ellipsoidal sets are used to computed a polyhedral invariant set, where the complexity depends of the number of vertices of the polyhedron [108]. This polyhedral set is refined using an iterative method (see [105, 106]) for obtaining an outer approximation of the *minimal Robust Invariant Set* (mRPI) for system trajectories.

4.2.1 Robust invariant sets based on the bounded-real lemma

Considering the dynamical equation for the perturbed linear system:

$$x_{k+1} = Ax_k + Ed_k \tag{4.47}$$

where $A \in \Re^{n\times n}$ and $E \in \Re^{n\times q}$, a candidate Lyapunov function could be $V(x_k) = x_k^T P x_k$ with $P > 0$. Now assume that, for a given constant $\gamma > 0$, the evolution of the Lyapunov function could be described by the following dissipation inequality:

$$\Delta V(x) = V(x_{k+1}) - V(x_k) \leq \gamma^2 d_k^T d_k - x_k^T x_k \tag{4.48}$$

Replacing the candidate Lyapunov function and the dynamical equation (4.47) in (4.48), one can obtain the following inequality:

$$x_k^T(A^TPA - P + I_n)x_k + x_k^T(A^TPE)d_k + d_k^T(E^TPA)x_k + d_k^T(E^TPE - \gamma^2 I_q)d_k \leq 0 \tag{4.49}$$

This inequality is equivalent to the following LMI, that is used in the *Bounded-real Lemma* [109]:

$$\begin{bmatrix} x \\ d \end{bmatrix}^T \begin{bmatrix} A^TPA - P + I_n & A^TPE \\ E^TPA & E^TPE - \gamma^2 I_q \end{bmatrix} \begin{bmatrix} x \\ d \end{bmatrix} \leq 0 \tag{4.50}$$

Taking the Shur complement, one can write the expression (4.50) as the following Ricatti-like quadratic matrix inequality, where I_n and I_q are identity matrices of dimensions n and q, respectively:

$$A^TPA - P + I_n - A^TPE(E^TPE - \gamma^2 I_q)^{-1}E^TPA \leq 0 \tag{4.51}$$

Considering that one can establish a bound of the disturbances as follows $d^Td \leq \bar{d}^T\bar{d}$, the evolution of the Lyapunov function turns into:

$$\Delta V(x) \leq \gamma^2 d_k^T d_k - x_k^T x_k \leq \gamma^2 \bar{d}_k^T \bar{d}_k - x_k^T x_k < 0 \tag{4.52}$$

Analyzing more deeply (4.52), it can be said that $\Delta V(x)$ will be negative if the states are outside of the ball B_w, defined as:

$$B_w = \{x_k \in \Re^n : x_k^T x_k \leq \gamma^2 \bar{d}^T \bar{d}\} \tag{4.53}$$

This implies that, for a constant value c, any level set of the Lyapunov function $\Pi_c = \{x_k \in \Re^n : x_k^T P x_k \leq c\}$, that contains the ball B_w is an **attractive invariant set**. The figure 4.6 illustrates the inclusion condition for invariant sets. Here, the set Π_c represents the level set of the Lyapunov function containing the ball B_w of radius $\gamma\bar{d}$. If the states are included in this set and due to the invariant set properties, it will tend, at steady state (represented by x_{k+n} in the figure), to the minimum Robust invariant set Π_∞, represented by the shaded area. The computation of this set will be analyzed more ahead.
Now, considering that $x^T x \leq r^2$, implies that $x^T P x \leq \lambda_{max}(P) r^2$ with $r^2 = \gamma^2 \bar{d}^T \bar{d}$, one can compute the (ellipsoidal) invariant set $\Pi_c = \bar{\Pi}$ as follows:

$$\bar{\Pi} = \{x \in \Re^n : x^T P x \leq \lambda_{max}(P)\gamma^2 \bar{d}^T \bar{d}\} \tag{4.54}$$

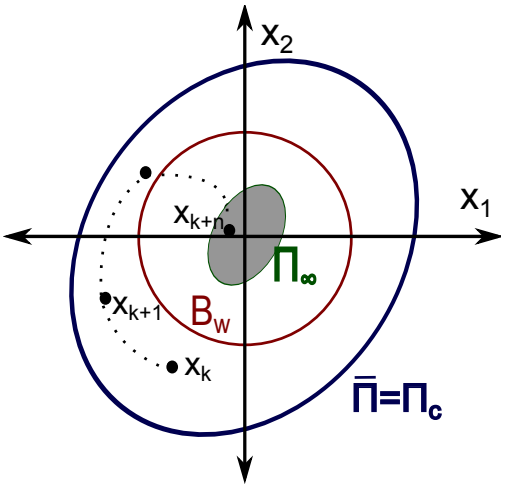

Figure 4.6: Invariant Set Representation

4.2.2 Computation of polyhedral RPI sets from ellipsoidal ones

In this section we will compute a polyhedral invariant set from ellipsoidal ones. Even if the polyhedral sets are more complex than ellipsoidal ones, the goal here is to obtain a tractable set intended for reducing the conservatism of the ellipsoidal minimal invariant sets, which is in general bigger. The size of the invariant polyhedral set could be reduced by using a shrinking procedure that will be presented in the next section. Suppose that a polyhedral set P_v satisfies the following condition:

$$\bar{\Pi}(k+1) \subseteq P_v \subseteq \bar{\Pi}(k) \tag{4.55}$$

then, the polyhedral set P_v is an invariant set since $\bar{\Pi}(k)$ is invariant and $\bar{\Pi}(k+1)$ characterizes the one-step ahead system trajectories starting into $\bar{\Pi}(k)$. Remark that all the points into the set P_v are included into the invariant set $\bar{\Pi}(k)$, and the fact that all trajectories in that set converges into the set $\bar{\Pi}(k+1)$ at the instant $k+1$, then the set P_v will be also included into $\bar{\Pi}(k+1)$ at the instant $k+1$. As a consequence, any polyhedral set between $\bar{\Pi}(k)$ and $\bar{\Pi}(k+1)$ will be a polyhedral invariant set.
Consider the following invariant set:

$$\bar{\Pi}(k) = \{x \in \Re^n : x^T P x \leq \lambda_{max}(P)\mu\gamma^2 \bar{d}^T \bar{d}\} \tag{4.56}$$

with a constant $\mu > 1$. From [106] one can compute the evolution of this ellipsoidal invariant set using the following expression:

$$\bar{\Pi}(k+1) = \{x \in \Re^n : x^T P x \leq [(\lambda_{max}(P) - 1)\mu + 1]\gamma^2 \bar{d}^T \bar{d}\} \tag{4.57}$$

Therefore, the polyhedral set P_v could be any *inner approximation* of the invariant set $\bar{\Pi}(k)$ which includes $\bar{\Pi}(k+1)$. An interesting method to compute a polyhedral set which verifies (4.55) is proposed in [110].

Minimum invariant set computation

For obtaining a polyhedral minimum invariant set, one can use a recursive procedure, using the system dynamics. Consider the system dynamics (4.47), as well as the polyhedral sets $S(k)$ and $\mathcal{D}$ that descrive the system states and disturbances trajectories, respectively. The algorithm computes the evolution of $S(k)$ by mapping it with the dynamical matrix A, obtaining a polyhedral set in $\Re^n$ and adding the set $E\mathcal{D} \in \Re^n$, as follows:

$$\mathcal{S}(k+1) = A\mathcal{S}(k) \oplus E\mathcal{D}, \quad \mathcal{S}(0) = P_v \tag{4.58}$$

where the symbol $\oplus$ denotes the Minkowski sum of sets [108]. Remark that the recursive algorithm (4.58) can be written into a more explicit form:

$$\mathcal{S}(k) = A^k \mathcal{S}(0) \oplus \left(\bigoplus_{i=1}^{k} A^{i-1} E\mathcal{D} \right) \tag{4.59}$$

Remark also that the term $A^k S(0)$ converges to zero when k converges to infinity. Therefore, it is possible to establish the following statement:

$$\mathcal{S}(\infty) \subseteq \cdots \subseteq \mathcal{S}(1) \subseteq \mathcal{S}(0) \tag{4.60}$$

where it is shown that states starting at $\mathcal{S}(0)$ evolve into $\mathcal{S}(1)$, which is contained in $\mathcal{S}(0)$. More generally the property $\mathcal{S}(k+1) \subseteq \mathcal{S}(k)$ holds and therefore the successive evolution of the original set is indeed invariant. The set $\mathcal{S}(\infty)$ is then the minimal invariant set (mRPI set).

Stopping criterion and precision of the algorithm

Considering the work [104], one can establish an stopping criterion for the shrinking recursive algorithm. The idea is to consider that the approximation error belongs to an $n-$dimensional ball of radius ϵ with respect to the $p-$norm (typically the norm-2), $\mathcal{B}_\epsilon^p$, that will represent the effect of the states mapping the term $A^k\mathcal{S}(0)$. The algorithm will stop at the iteration h^*, which provides an *outer*-ϵ approximation of the minimal invariant set.
For performing this analysis, consider (4.59) as follows:

$$\mathcal{S}(k) = A^k \mathcal{S}(0) \oplus \left(\bigoplus_{i=1}^{k} A^{i-1} E\mathcal{D} \right) = A^k \mathcal{S}(0) \oplus \Xi(k) \tag{4.61}$$

Now, define the set Ξ_∞ as follows:

$$\Xi_\infty = \lim_{k \to \infty} \Xi(k) = \bigoplus_{i=i}^{\infty} A^{i-1} E\mathcal{D} \tag{4.62}$$

This set is in fact a lower bound for the following sequence:

$$\Xi_\infty \subseteq \mathcal{S}(k+1) \subseteq \mathcal{S}(k) \cdots \subseteq \mathcal{S}(0) \tag{4.63}$$

More deeply, one can write Ξ_∞, according to (4.61) and (4.64), and using k^* as the final iteration for finding the approximation, in the following way:

$$\Xi_\infty = \Xi(k^*) \oplus \left(\bigoplus_{i=k^*+1}^{\infty} A^{i-1} E\mathcal{D} \right) \tag{4.64}$$

It is then possible to establish from (4.64) the following relations:

$$\Xi_\infty \subseteq \Xi(k^*) \cdots \subseteq \mathcal{S}(0) \tag{4.65a}$$

$$\Xi_\infty \subseteq A^{k*}\mathcal{S}(0) \oplus \Xi(k^*) \subseteq \mathcal{S}(0) \tag{4.65b}$$

$$\Xi_\infty \subseteq A^{k*}\mathcal{S}(0) \oplus \Xi_\infty \subseteq \mathcal{S}(0) \tag{4.65c}$$

That is, the recursive algorithm can be stopped when the following property is satisfied:

$$A^{k*}\mathcal{S}(0) \subseteq \mathcal{B}_\epsilon^p \tag{4.66}$$

and the outer approximation of the minimal invariant set will be $\Xi(k^*)$. Remark that the approximation error explicitly depends on the initial set $\mathcal{S}(0)$, the matrix A and the "finite" number of iterations $k*$.

4.2.3 Computation of invariant sets by expansion of polyhedral sets

An alternative way to compute the minimal invariant set is to consider the recursive algorithm (4.58) but starting with an initial and arbitrary polyhedral $\mathcal{S}(0) \simeq 0$. The sequence will also provide a set:

$$\mathcal{S}(k) = A^k\mathcal{S}(0) \oplus \left(\bigoplus_{i=1}^{k} A^{i-1} E\mathcal{D} \right) \tag{4.67}$$

which, strictly speaking, is a non-invariant set for system trajectories but an inner approximation of the theoretical minimal invariant set. This method could provide a good approximation of the minimal invariant set after a certain number of k^* iterations. Using (4.67) we can estimate the error of the invariant set approximation that has to be included into a predetermined ball (characterizing the desired precision), as follows:

$$\left(\bigoplus_{i=k^*+1}^{\infty} A^{i-1} E\mathcal{D} \right) \subseteq \mathcal{B}_\epsilon^p \tag{4.68}$$

Remark that the approximation error explicitly depends on a "infinity" number of non-performed iterations $\infty - k^*$. This error also depends on the matrices A, E and the size of the disturbance set $\mathcal{D}$. In practice it is enough to check the size of the set $A^{k*}E\mathcal{D}$ to stop the sequence (4.67).
This method is considered an *expansion* method for computing an approximation of the invariant set, because is considered that the initial set $\mathcal{S}(0)$ is a polyhedral set really small, differently from the *shrinking* method, in which $\mathcal{S}(0)$ is a polyhedral approximation of the invariant set, as introduced in 4.2.2. The convenience of choosing one method from the other is related with the complexity for expressing the set $\mathcal{S}(0)$, related with the system's order. In further examples and applications, it will be seen how both methods can be profited in particular circumstances.

4.2.4 Illustrative example

A simple example is here presented to illustrate the methodology for computing invariant sets. Once an ellipsoidal invariant set is obtained, we compute a polyhedral approximation that will be an outer ϵ-approximation of the minimal invariant set. This approach could present high computational cost for high dimensional systems. However, the links with invariant sets computed using the Bounded-real lemma could provide a metric of how small the minimal invariant set could be.

Consider the following open-loop stable system ($\lambda_{1,2} = -4.50 \pm 1.33j$):

$$\dot{x}(t) = \begin{bmatrix} -5 & 2 \\ -1 & -4 \end{bmatrix} x(t) + \begin{bmatrix} -5 & 0.5 \\ 5 & 2.5 \end{bmatrix} u(t) + \begin{bmatrix} -1 & 0.5 \\ 0.2 & 1 \end{bmatrix} d(t)$$

Using a sampling period $T_s = 1/150s$, the discrete-time model is:

$$x_{k+1} = \begin{bmatrix} 0.9667 & 0.0133 \\ -0.0067 & 0.9733 \end{bmatrix} x_k + \begin{bmatrix} -0.0333 & 0.0033 \\ 0.0333 & 0.0167 \end{bmatrix} u_k + \begin{bmatrix} -0.0067 & 0.0033 \\ 0.0013 & 0.0067 \end{bmatrix} d_k$$

The eigenvalues of the discrete matrix A are inside the unitary circle ($\lambda_{1,2} = 0.97 \pm 0.0088j$). Now, a state feedback of the form $u_k = -Kx_k$ will be used to control the system. The state-feedback gain matrix K is computed by using an LQR control design with weighting matrices $Q = 10I$ and $R = 0.1I$, being I an identity matrix of order 2. We obtain:

$$K = \begin{bmatrix} -5.6860 & 4.4642 \\ 4.4783 & 6.3164 \end{bmatrix}$$

The closed-loop dynamical model, with eigenvalues $\lambda_1 = 0.8662,\ \lambda_2 = 0.6153$) is:

$$x_{k+1} = \begin{bmatrix} 0.7622 & 0.1411 \\ 0.1082 & 0.7183 \end{bmatrix} x_k + \begin{bmatrix} -0.0067 & 0.0033 \\ 0.0013 & 0.0067 \end{bmatrix} d_k$$

Now we will compute an invariant set for this closed-loop system.

Consider the following disturbance vector bound $\bar{d} = 3$. Then, using the expression (4.50) one can compute the parameter γ and the Lyapunov matrix P, obtaining:

$$\gamma = 0.0603; \quad P = \begin{bmatrix} 13.2487 & -8.1524 \\ -8.1524 & 18.9447 \end{bmatrix}$$

Now, using the expression (4.54) with $\mu = 1$, and the data problem: $\bar{d}, \gamma$ and P, an ellipsoidal set is obtained. The figure 4.7 depicts the obtained invariant set.

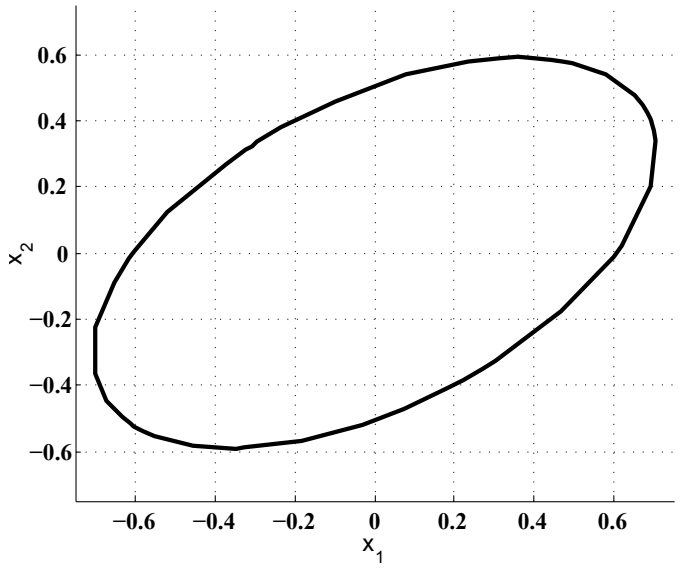

Figure 4.7: Invariant set representation for the illustrative example

The obtained set could be refined by using the previously presented shrinking technique. Considere now a ball $\mathcal{B}_\epsilon^p = 1e^{-3}$ as a criterion for stopping the recursive algorithm. Then, it is used the expressions (4.55)-(4.57) for computing an inner approximation of the invariant set.

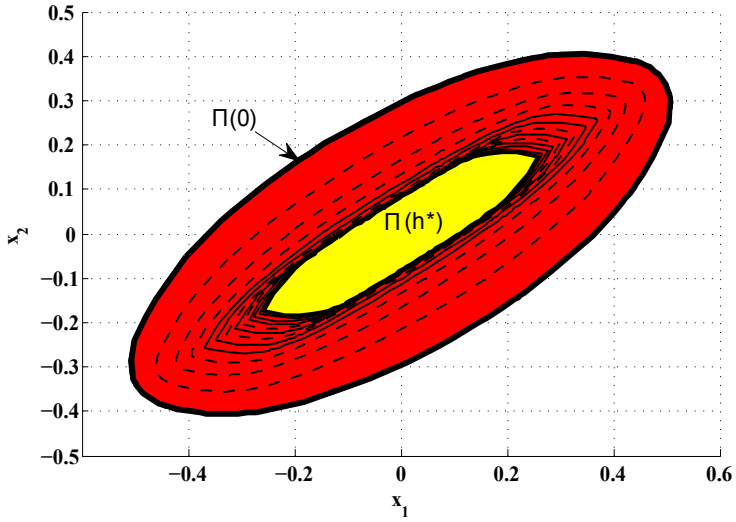

Figure 4.8: Example of shrinkling procedure from an ellipsoidal invariant set for obtaining an approximation of the minimal robust invariant set

Figure 4.8 illustrates the obtained ellipsoidal invariant set and the approximated minimum invariant set, as well as the partially obtained polyhedral sets. The final iteration is equal to $k^* = 13$. Now, we will computed the same minimal invariant set by using the expanding method. In this case, the idea is to start with a polyhedral $\mathcal{S}(0)$ defined by a very small hypercube (with a 2-norm smaller than $1e^{-4}$). Here, it was used a similar stopping criterion, obtaining $k^* = 17$. In figure 4.9 the mRPI set approximation with this method is compared with respect to the mRPI approximation using the shrinking procedure. The initial set is kind small for being represented

along the obtained sets.

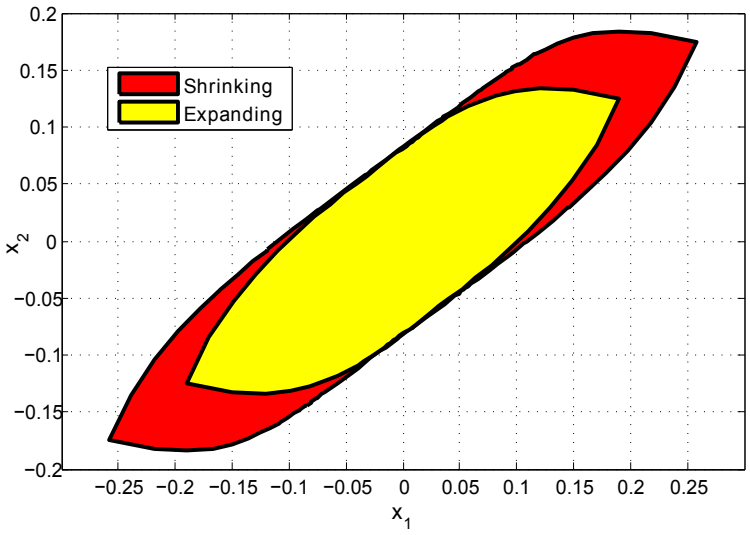

Figure 4.9: Example of expanding procedure from an ellipsoidal invariant set for obtaining an approximation of the minimal robust invariant set

After observation, it can be inferred that mRPI has a topology that directly depends of the perturbations polyhedral set topology, affected evidently by the dynamical and disturbances matrices from the model. In case of unknowing any initial ellipsoidal invariant set for obtaining an approximation of a mRPI, an expanding computation could be useful, but the procedure probably demands more iterations before to obtain an admissible approximation to the minimal invariant set.

4.2.5 Computation of robust invariant sets for a family of linear systems

The computation of invariant sets for a family of N linear systems is indeed an extension of the linear systems approach. First, consider the following dynamical equation:

$$x_{k+1} = A_i x_k + E_i d_k \tag{4.69}$$

with $i = 1 \cdots N$, $A_i \in \Re^{n \times n}$ and $E_i \in \Re^{n \times q}$. It is considered that every A_i has eigenvalues strictly inside of the unitary circle. Therefore, the idea is to find a **common Lyapunov function** such that $V(x) = x^T P x$ and a scalar $\gamma > 0$ satisfy the following LMI:

$$\begin{bmatrix} x \\ d \end{bmatrix}^T \begin{bmatrix} A_i^T P A_i - P + I_n & A_i^T P E_i \\ E_i^T P A_i & E_i^T P E_i - \gamma^2 I_q \end{bmatrix} \begin{bmatrix} x \\ d \end{bmatrix} \leq 0 \tag{4.70}$$

for $i = 1 \cdots N$. Therefore, when a matrix $P > 0$ and $\gamma > 0$, and considering that $d^T d \leq \bar{d}^T \bar{d}$, an invariant set for the family of the linear systems can be written as:

$$\bar{\Pi}_N = \{x \in \Re^n : x^T P x \leq \lambda_{max}(P) \gamma^2 \bar{d}^T \bar{d}\} \tag{4.71}$$

Remark that this method could be used for invariance analysis of polytopic linear parametric varying system.

Minimum invariant set computation for a family of linear systems

Considering the system dynamics (4.69), one can obtain the following states evolution $\bar{\mathcal{S}}_i(h)$ for a particular states set $\mathcal{S}_i(h)$:

$$\bar{\mathcal{S}}_i(k) = A_i\mathcal{S}(k) \oplus E_i\mathcal{D}, \quad \mathcal{S}(0) = P_v \tag{4.72}$$

where P_v is the polyhedral approximation of $\bar{\Pi}_N$, the invariant set computed using (4.71). Now, one can compute the following set:

$$\mathcal{S}(k+1) = hull\{\bar{\mathcal{S}}_i(k), i = 1 \cdots N\} \tag{4.73}$$

Considering that $\bar{\mathcal{S}}_i$ is the image of a states set $\mathcal{S}(k)$ for a given system i. It is clear that the convex hull of such images corresponds to an invariant set that is included in the original one $\bar{\Pi}_N$, that is indeed an invariant set for the family of N-systems.
Moreover, for all time instances $k > 0$, if $x(k) \in \mathcal{S}(k+1)$, then $x(k+1) \in \mathcal{S}(k+1)$ due to the invariant set properties. Therefore, there will be an iteration k^* in which the following relation is true:

$$\Xi_\infty \subseteq \mathcal{S}(k^*+1) \subseteq \mathcal{S}(k^*) \cdots \subseteq \mathcal{S}(0) = \bar{\Pi}_N \tag{4.74}$$

where Ξ_∞ is the minimum Robust Invariant Set for the family of systems (4.69).

Stopping criterion and precision of the algorithm

First, consider the following recursion equation:

$$\mathcal{S}(k+1) = hull\{A_i\mathcal{S}(k) \oplus E_i\mathcal{D}, i = i \cdots N\}, \mathcal{S}(0) = \bar{\Pi}_N \tag{4.75}$$

Considering that states and disturbances sets $\mathcal{S}(k)$ and $\mathcal{D}$ are compact and convex sets, the following relationships, based in (4.75) are true:

$$\mathcal{S}(k+1) = hull\{A_i\mathcal{S}(k)\} \oplus hull\{E_i\mathcal{D}\}, i = 1 \cdots N \tag{4.76a}$$

$$\mathcal{S}(k+1) = \left(\sum_{i=1}^{N} \alpha_i A_i\right) \mathcal{S}(k) \oplus \left(\sum_{i=1}^{N} \alpha_i E_i\right) \mathcal{D} \tag{4.76b}$$

Making the following considerations: $\alpha_i \geq 0$ and $\sum_{i=1}^{N} \alpha_i = 1$, one can write the following convex combinations:

$$\bar{A} = \sum_{i=1}^{N} \alpha_i A_i \ , \ \bar{E} = \sum_{i=1}^{N} \alpha_i E_i \tag{4.77}$$

Therefore, the recursive expression (4.76b) can be written as:

$$\mathcal{S}(k+1) = \bar{A}\mathcal{S}(k) + \bar{E}\mathcal{D} \tag{4.78}$$

which can be written in a more explicit way as follows:

$$\mathcal{S}(k) = \bar{A}^k\mathcal{S}(0) \oplus \sum_{i=1}^{k} \bar{A}^{i-1}\bar{E}\mathcal{D} \tag{4.79}$$

Defining the set $\Xi(k) = \sum_{i=1}^{k} \bar{A}^{i-1}\bar{E}\mathcal{D}$. Now, considering $k \to \infty$, and due to the shared Lyapunov function of the convex combination $\bar{A}$, it is concluded that Ξ_∞ is the smallest Robust invariant set for the family of systems (4.69).

With the same order of ideas, the iterative algorithm can be stopped when the image of the states set for time k^* is contained in a ball $\mathcal{B}_\epsilon^p$ of radius ϵ:

$$\mathcal{S}(k^*) = \bar{A}^{k^*}\mathcal{S}(0) \subseteq \mathcal{B}_\epsilon^p \tag{4.80}$$

However, this condition cannot be evaluated in real time, because the matrix $\bar{A}^{k^*}$ is *a priori* unknown. But, one can use a bound in the following form:

$$\bar{A}^{k^*}\mathcal{S}(0) \subseteq \rho(k^*)\mathcal{S}(0) \subseteq \mathcal{B}_\epsilon^p \tag{4.81}$$

where $\rho(k) = \left(\frac{\lambda_{max}(P)}{\lambda_{min}(P)}\beta^k\right)^{1/2}$, with $\beta > 0$ satisfying:

$$A_i^T P A_i - \beta P < 0; i = 1 \cdots N \tag{4.82}$$

Finally, using (4.74) is concluded that the set $\Xi(k^*)$ is a Robust Invariant Set and an ϵ-outer approximation of the Minimum Robust Invariant Set Ξ_∞, that is:

$$\Xi_\infty \subseteq \mathcal{S}(k^*) \subset \mathcal{B}_\epsilon^p \oplus \Xi_\infty \tag{4.83}$$

In this way one can obtain an ellipsoidal invariant set for a family of N subsystems, as well as the expressions for obtaining by an iterative way their minimum RPI set. This is useful for systems in which the model or the feedback structure includes some class of scheduling or uncertain parameter, in the same way that Linear Parameter Varying systems. This fact will be important in further sections, in which constrained feedback will be considered in dynamic systems.

4.2.6 Illustrative example

Considering the following discrete-time linear switched system (4.69) with matrices:

$$A_1 = \begin{bmatrix} 0.85 & 0 \\ 0.25 & 0.65 \end{bmatrix} \quad A_2 = \begin{bmatrix} 0.05 & 0 \\ -0.3 & 0.65 \end{bmatrix} \quad A_3 = \begin{bmatrix} 0.55 & -1 \\ 0.3 & -0.65 \end{bmatrix}$$
$$E_1 = \begin{bmatrix} 0.5 & 0.1 \end{bmatrix}^T \quad E_2 = \begin{bmatrix} 0.1 & -0.3 \end{bmatrix}^T \quad E_3 = \begin{bmatrix} 0.1 & 0.3 \end{bmatrix}^T$$

the system is affected by disturbances $|d(k)| \leq 1\ \forall k \geq 0$. Using the LMI (4.70), there are obtained the following values for γ and P:

$$\gamma = 4.2687 \quad P = \begin{bmatrix} 23.4709 & -16.2434 \\ -16.2434 & 23.1613 \end{bmatrix}$$

Now, the polyhedral approximation for the invariant set $P_v = \mathcal{S}(0)$, is obtained as the set included between the ellipsoidal sets $\bar{\Pi}(k)$ and $\bar{\Pi}(k+1)$ as seen in the expressions (4.54) and (4.57), respectively, considering $\mu = 3$. In this case, the shrinking process has been stopped for $k^* = 10$, that guarantees that the outer approximation of the mRPI is achieved with an error smaller than a ball of radius $\epsilon < 4e^{-3}$. The results for this example are shown in Fig. 4.10.

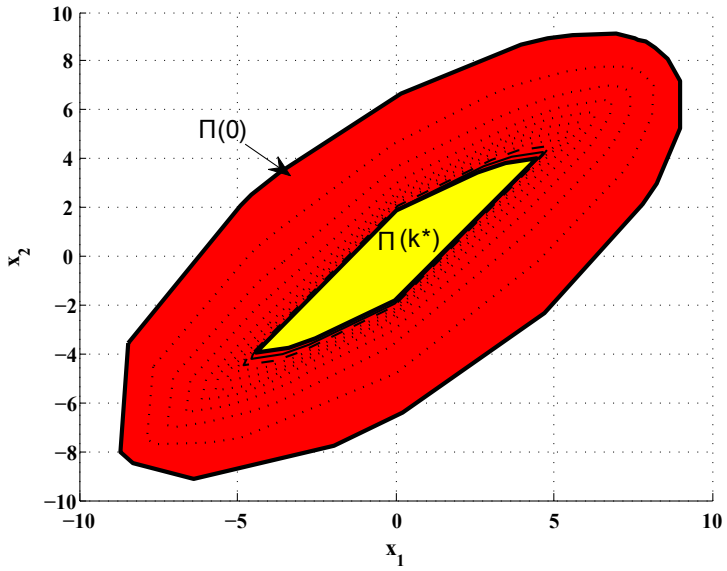

Figure 4.10: Example for obtaining the mRPI approximation for a family of linear systems

4.2.7 Concluding remarks

In this section was presented an introduction to the computation of robust invariant sets for stable linear systems. Here, the use of the concept of invariance in dynamical systems was used, considering the use of a quadratic Lyapunov function, obtained after using the Real Bound Lemma. In the presented material, it was shown the expressions for computing first a polyhedral approximation for an initial ellipsoidal invariant set. Then, using the dynamical equation it was obtained the recursive equation for obtaining the so-called minimal robust invariant set, according to a fixed approximation error. The results for computing the invariant sets for linear systems were extended for a family of N linear systems, in which the Lyapunov function is common for the family and the algorithm for computing the mRPI is adapted accordingly.
One example for each case were presented, showing that the methodology is suitable to be implemented. The concepts here presented will be exploited in Chapter 7, where invariant sets are used for analyzing the stability properties of constrained control and distributed-coordinated control schemes.

4.3 Conclusions

In the first part of this chapter, it was first given a recall of the principles of MPC, strategy widely used in this thesis. Definitions of the strategy objectives, constraints descriptions and adopted solution methods were analyzed.
In the second part, the construction of invariant sets for linear systems were introduced. The construction principles of invariant sets, for an individual system and a family of linear ones, were given with some examples for their understanding.
Those basic tools, both the MPC and invariant sets, will be instrumental in the contributions presented next.

Chapter 5

CONTRIBUTION TO POWER MAXIMIZATION IN WIND TURBINES AND PREDICTIVE CONTROL IN MICROGRIDS

Contents

5.1 Maximization of power production by wind-based generators without wind speed sensor 72
5.1.1 Principles of the proposed technique 72
5.1.2 Extended Kalman Filter for the estimation of the power characteristics . . 75
5.1.3 Power coefficient polynomial approximation and optimal generator speed estimation 76
5.1.4 Control strategies for power production maximization in wind turbines . . . 78
5.1.5 Validation of the technique by simulation 79
5.1.6 Experimental small scale prototype 84
5.1.7 Concluding remarks 85
5.2 Power management of a microgrid with explicit MPC-based control . 85
5.2.1 Description of the considered microgrid 86
5.2.2 Low-level control strategies and reduced microgrid model 87
5.2.3 Definition of the constrained optimization problem 90
5.2.4 Computer simulation and control strategy evaluation 92
5.2.5 Concluding remarks 93
5.3 Conclusions 94

In this chapter a couple of initial contributions are presented, that were firstly developed while discussing and working around the coordination of distributed power generation systems. They provide a good concrete introduction into the two aspects considered in the thesis: control issues for renewable power sources, and MPC-based control of sets of such sources.
The first contribution indeed is about optimal power production of Electric Wind Power Generators (EWPG) without wind speed sensor, where the use of an original *observer approach* is part of the contribution. Some of this work was presented in the conference paper [9].
The second contribution is dedicated to the use of MPC for the power flow control in a microgrid composed by a fuel cell, an optimized wind turbine, and a battery as a storage device. Here, one original aspect is the use of an *explicit solution*, as presented in Section 4.1, that is fast enough for an embedded implementation. These results were presented in the conference paper [8].

5.1 Maximization of power production by wind-based generators without wind speed sensor

For the proposed maximization of the power production in EWPG without wind speed measurement, we first analyze the mechanical power generator model, as well as the characteristics of the wind speed admissible variations for possible energy transfer between the wind and the mechanical system. Then, the conception of an Extended Kalman Filter (EKF) observer is proposed for the estimation of the product between the power coefficient and the cube of the wind speed. This product is related to the power efficiency of the whole system and should be maximized by fixing an optimal electrical generator speed. The latter is obtained by using a Recursive Least Square (RLS) Algorithm to obtain a polynomial estimation of the generator speed. At the end, the on-line observer and efficiency curve estimation will allow to act against variations of the wind speed and other operative conditions in the wind turbine.

5.1.1 Principles of the proposed technique

Let us first recalled, as previously presented in Section 3.2.3, that the *mechanical power* produced by a wind turbine, P_T, can be written as function of the wind speed v_w and the power coefficient C_p as follows:

$$P_T = \frac{1}{2}\rho\pi R^2 C_P(\lambda,\beta)v_w^3 \tag{5.1}$$

where ρ is the air density and R is the wind turbine radius. In fact, ρ is time variant, but in this study is assumed constant ($\dot{\rho}=0$).
The power coefficient C_p is in fact a parameter that reflects the efficiency obtained by transforming the wind energy into mechanical energy, therefore meaning that $0 < C_p < 1$ for any blade configuration. It typically depends on the turbine pitch angle β and the Tip Speed Ratio λ, as follows [72, 75]:

$$C_P(\lambda,\beta) = c_1\left(\frac{c_2}{\lambda} - c_3\beta - c_4\right)e^{-c_5/\lambda} \tag{5.2}$$

where $c_1 \cdots c_5$ are constant values depending on the turbine characteristics, and λ is given by:

$$\lambda = \frac{w_T}{v_w}R \tag{5.3}$$

with v_w the wind speed, and w_T the rotational speed of the wind turbine. In practice, the pitch angle β is fixed according to the wind speed values, environmental conditions and requirements of power production in the generator [73]. However, for control purposes, one can assume that β is constant, or in other words, $\dot{\beta} \simeq 0$. Therefore, the $C_p(\lambda)$ function can be rewritten in an n-polynomial way as:

$$C_P(\lambda) = \sum_{i=0}^{n}\alpha_i(\beta)\lambda^i \tag{5.4}$$

Typical curves of C_P have been presented in figure 3.10 of section 3.2.3. From such typical curves, if one searches the maximum power transfer from wind to mechanical power in a wind turbine with constant pitch angle, it is necessary to fix an optimal Tip Speed Ratio (λ^{opt}), that maximizes the power coefficient (C_p^{opt}). For instance, for $0^o < \beta < 16^o$ value, the range of the optimal λ is around $5.5 < \lambda^{opt} < 7.8$.
Therefore, for real time applications, λ^{opt} should be fixed to obtain the maximum value C_p^{opt} of the particular C_p function under consideration. Then, the optimal value of w_T is related to the wind speed value v_w according to(5.3).

In the considered scenario, it is assumed that wind speed measurement is not available or is not feasible to obtain a good value for w_T. In addition, the profiles of C_p are assumed to be not accurate, requiring a real time adaptation strategy for maximizing the power production.
In the remainder of this part, we propose a solution for the power production maximization with a wind turbine, assuming constant pitch angle β, no wind speed measurement, partial knowledge of C_p curve coefficients, and operation in the so-called *Partial Load Region* of the turbine (see [73, 76, 111, 112]).

5.1.1.1 Mathematical modeling for the optimal power production strategy

In order to develop our strategy for the maximization of power production in wind turbines, the most simple structure of such turbines is considered: the one that includes a DC separately excited electrical generator, as shown in Fig 5.1. The armature circuit, including the DC/DC Boost power converter and the electrical load, is better exposed in Fig 5.2.

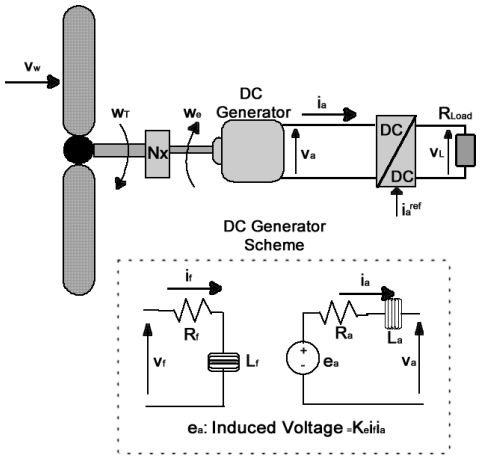

Figure 5.1: Scheme of the considered wind power generation system.

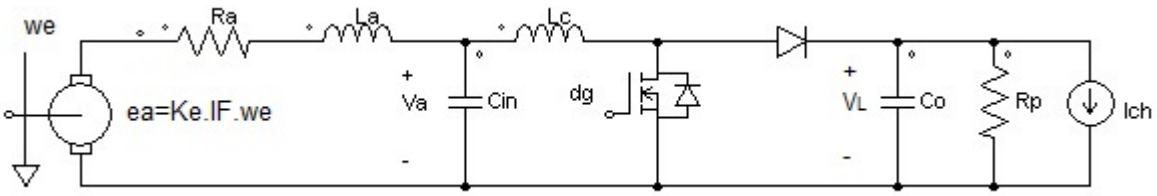

Figure 5.2: Detailed armature circuit with the DC/DC power converter

According to Fig 5.1, the system is composed by the mechanical part, in fact the wind turbine, that is coupled via a gearbox to the electrical generator shaft. The armature winding is coupled to a DC/DC power converter - in the present case a Boost converter [84], that regulates the power produced by the electrical generator, and also serves as a power conditioner within the DC generator and the load - which is typically a DC/AC conversion system for the interaction with the grid [74] or for its use in microgrids [113].

The selected technology of electrical generator and power converter can be modified into more complex ones if needed to operate at higher powers or to interact with the power grid in a more direct way. In wind turbines, Permanent Magnet Synchronous Generators (PMSG) are the most common ones for the control of the power delivered by the turbine, with a double conversion driver (AC/DC/AC) in order to handle the interaction the AC load [73, 74].
The criterion of selection for the electrical generator and its driver entirely depends on the application. For the present contribution, the construction at Gipsa-Lab of a micro turbine with a DC driver, gave the motivation for conceiving the control strategy for this class of generators, due to their simplicity and higher penetration for low power applications.

Returning to the discussion, the dynamical model for the EWPG based on a DC generator, first restricted to the field and armature circuits, without DC/DC converter for the latter, can be:

$$\dot{i_f} = \frac{U_f}{L_f} - \frac{R_f}{L_f} i_f \tag{5.5}$$

$$\dot{i_a} = \frac{K_e i_f}{L_a} w_e - \frac{R_a}{L_a} i_a - \frac{U_a}{L_a} \tag{5.6}$$

where U, i, L, R respectively denote voltage, current, inductance and resistance variables, with index f or a respectively for field and armature, and K_e is the induced EFM constant. The units of the variables are Volts (V) for the voltages, Amperes (I) for the currents, Henries (H) for the inductances and Ohms (Ω) for the resistances.
Now, considering the boost power converter, an extended description of the armature circuit can be obtained via the *average modeling* of power converters [84], as follows:

$$L_a \dot{i}_a = e_a - R_a i_a - v_a \tag{5.7a}$$
$$C_{in} \dot{v}_a = i_a - i_{Lc} \tag{5.7b}$$
$$L_c \dot{i}_{Lc} = v_a - v_L(1 - d_g) \tag{5.7c}$$
$$C_o \dot{v}_L = i_{Lc}(1 - d_g) - v_L/R_p - i_{ch} \tag{5.7d}$$

where C_{in} and C_o are the capacitances at the converter input and output ports, L_c is the converter inductance with i_{Lc} being its current, v_L is the load voltage, R_p is a pre-charge resistor that is used for the start-up (representing about 5% of the maximum load), i_{ch} represents the load current, or in other words, the current transmitted to other possible stages, and d_g is the duty cycle of the power converter. From(5.7), it is possible to obtain the steady state conditions of the armature circuit, from which can some parameters be obtained in order to linearise it around some operation regime. One thus obtains:

$$E_a = R_a I_a + V_a \tag{5.8a}$$
$$I_a = I_{Lc} \tag{5.8b}$$
$$V_a = V_L(1 - D_g) \tag{5.8c}$$
$$I_{Lc} = (V_L/R_p + I_{ch})/(1 - D_g) \tag{5.8d}$$

where capital letters refer to steady state values of the variables previously defined.
After those electrical equations, let us move to the mechanical one. In fact, the equation obeys the Newton's law for rotational elements:

$$\dot{w_e} = \frac{K_T C_p {v_w}^3}{J_{eq} w_e} - \frac{B_e}{J_{eq}} w_e - \frac{K_e i_f}{J_{eq}} i_a \tag{5.9}$$

where J_{eq} is the equivalent inertia (referred to the generator shaft), B_e is the friction constant of the generator and w_e its angular speed. In addition C_p is the power coefficient, and $K_T = 0.5\pi\rho N_x R^2$,

with ρ the air density (in kg/m^3), R the wind turbine radius (in m), and N_x the speed ratio, fixed by the gearbox.
Equation (5.9) also includes the wind speed v_w, that is assumed to vary around a mean value V_{w0} with a bandwidth represented by α_v and stochastic fluctuations described by η_v (zero mean white noise). Therefore, a valid model for the wind speed variations can be:

$$v_w = V_{w0} + \widetilde{v_w} \tag{5.10}$$

$$\dot{\widetilde{v_w}} = -\alpha_v \widetilde{v}_w + \eta_v \tag{5.11}$$

It should be noticed that α_v actually represents the frequency range of wind speed components that allows the electrical generation of a significant amount of energy. In practice, the turbine usually generates rotational energy for low frequency wind speed components, due to its mechanical characteristics. This parameter α_v is then defined from the turbine model (response vs wind variations) or even from the wind speed spectral response. In [73], one can find some characterization of wind energy behaviors and its effective bandwidth - which depends on the wind speed mean value, but can be fairly considered to lie between 0.05 and 0.8 rad/s to give an idea.

5.1.1.2 Analysis of the mathematical model for control purposes

Looking more deeply at mechanical equation (5.9), two main components can be seen: the mechanical torque and the electrical torque. Taking into consideration the objective of the proposed technique, previously explained in Section 5.1.1, one needs to fix an electrical generator speed w_e, that translates into w_T via mechanical transmission, modifying therefore the Tip Speed Ratio, λ. Assuming that field voltage is constant (see eq. (5.5)), the term i_f becomes constant in (5.6) and (5.9), letting then the armature current i_a as the control signal, which is modified in the DC converter through the duty cycle d_g (see (5.7)).
However, in the mechanical equation (5.9), the mechanical torque is a nonlinear function of the instantaneous generator speed w_e, the power coefficient C_p, and the wind speed v_w. Assuming that i_a is the control variable, and considering slow variations in the power coefficient compared to the wind speed variations (5.11), ie $C_P \simeq C_{P0}$, $\dot{C}_{P0} = 0$, one can set $z := C_p v_w^3$ as a new variable, and $K_1 := K_T/J_{eq}$, $K_2 := B_e/J_{eq}$, $K_3 := K_e i_f/J_{eq}$ as new (known) constants, so that the mechanical equation and the dynamics of z (see Appendix B for more details), can be re-written as:

$$\dot{w_e} = \frac{K_1 z}{w_e} - K_2 w_e - K_3 u \tag{5.12}$$

$$\dot{z} = -3\alpha_v z + 3\alpha_v C_{P0} V_{w0} v_w^2 + \eta_z \tag{5.13}$$

where V_{w0} is the mean wind speed value that can be obtained by, for example, some meteorological prediction or by other class of measurement, C_{p0} is an initial power coefficient value that can be selected close to the optimal one according to the pitch angle β. In addition, η_z derives from definition of z and η_v in equation (5.11), α_v is established according to the effective wind bandwidth that affects the turbine (if nothing is known about it, it could be used as a tuning parameter).
From this new representation, one can estimate z in order to control the power generator: an observer is proposed to that end in next subsection.

5.1.2 Extended Kalman Filter for the estimation of the power characteristics

As seen in the previous section, z is in fact an image of the turbine power characteristic, multiplied by the cube of v_w. Therefore, the new power characteristic is a scaled version of

the curves shown in Fig. 3.10, allowing to maintain the maximization principles for the power production.
Based on mechanical equation (5.12) and on z dynamics (5.13), and assuming $u = i_a$ and $y = w_e$ as control input and measured output for these dynamics, the model can be transformed in order to design a Kalman observer, following a similar procedure as in [114]. Let define the following variables for an extended system from (5.12) and (5.13):
$x_1 = w_e$, $x_2 = z$, $x_3 = 3\alpha_v C_{P0} V_{w0} v_w^2$, $x_4 = 6{\alpha_v}^2 C_{P0} V_{w0}^2 v_w$ and $x_5 = 6{\alpha_v}^3 C_{P0} V_{w0}^3$. Then the model becomes:

$$\begin{aligned}
\dot{x}(t) = &\quad A(y(t))x(t) + Bu(t) + \eta_{z_{obs}} \\
\dot{x}(t) = &\begin{bmatrix} -K_2 & \frac{K_1}{y} & 0 & 0 & 0 \\ 0 & -3\alpha_v & 1 & 0 & 0 \\ 0 & 0 & -2\alpha_v & 1 & 0 \\ 0 & 0 & 0 & -\alpha_v & 1 \\ 0 & 0 & 0 & 0 & 0 \end{bmatrix} x(t) + \begin{bmatrix} -K_3 \\ 0 \\ 0 \\ 0 \\ 0 \end{bmatrix} u(t) + \begin{bmatrix} 0 \\ \eta_z \\ \eta_{z_3} \\ \eta_{z_4} \\ 0 \end{bmatrix} \\
y(t) = &\quad Cx(t) = \begin{bmatrix} 1 & 0 & 0 & 0 & 0 \end{bmatrix} x(t)
\end{aligned} \tag{5.14}$$

with the η_{z_i}'s are noise terms resulting from η_z and the transformation.
In (5.14), it can be seen that $y = x_1$ can be injected directly in the dynamic matrix, so that the system takes the form of a time-varying linear one, for which a Kalman-like observer can be designed [115]. In addition, it can be noticed that this model requires that $y > 0$, which means that the observer will actually work normally if the machine is moving. Otherwise, this algorithm will not be working.
Assuming discrete-time measurements, a discretized version of the above model can be considered, for which a classical Kalman observer can be designed as follows (see eg [116]):

$$\begin{aligned}
P_{k|k} &= A_k P_{k|k-1} A_k^T + Q \\
K_k &= P_{k|k} C^T \left(C P_{k|k} C^T + R\right)^{-1} \\
\hat{x}_{k+1|k} &= A_k \hat{x}_{k|k} + B_k u_k + K_k \left(y_k - C\hat{x}_{k|k}\right) \\
P_{k|k+1} &= (I - K_k C) P_{k|k}
\end{aligned} \tag{5.15}$$

where $A_k = I + T_s A(x(kT_s))$, $B_k = T_s B$ with A, B and C taken from (5.14) and T_s is the sampling period for the observer, P_k is the state error covariance matrix (P_0 should be high), Q and R are the input and output noise covariance matrices, both related to the noise levels at each stage, $\hat{x}_k$ is the predicted state vector and K_k is the adaptive Kalman gain. It is noticed that lower values of R increases the Kalman gain, increasing also the convergence speed. However, the elements of Q and R should be carefully selected according to the expected noise levels in the system.
In section 5.1.5 some simulation results showing the efficiency of the observer for a small power turbine model will be shown. Therefore, one can get an estimation for z, denoted as $\hat{z} = \hat{x}_2$, from the observer. With this information, and its relationship with the power coefficient C_P, one can then obtain the optimal reference for the generator speed. This information will also be useful for the subsequent control strategy.

5.1.3 Power coefficient polynomial approximation and optimal generator speed estimation

In order to obtain the optimal generator speed that maximizes the power generation, let us first consider a polynomial approximation for the power coefficient C_P curve. Here, a third order polynomial is considered of the form:

$$C_p(\lambda) = \alpha_0 + \alpha_1 \lambda + \alpha_2 \lambda^2 + \alpha_3 \lambda^3 \tag{5.16}$$

where coefficients α_i, $i = 0, 1, 2, 3$ are uncertainly known. In general, they are initially obtained from bench tests at each pitch angle as seen in Fig. 3.10, but may not be trusted for optimal control purposes.
Because the objective is the maximization of z with respect to w_e, one can use expression (5.16), along with the definitions of λ and $z = C_p v_w^3$, and its real-time estimation $\hat{z}$, in order to obtain real-time estimates for power coefficient polynomial expression. Then, the polynomial for the estimation of z is expressed as:

$$\begin{array}{rcl} \hat{z} & = & C_p(\lambda) v_w^3 \\ \hat{z} & = & \left(\alpha_0 + \alpha_1\lambda + \alpha_2\lambda^2 + \alpha_3\lambda^3\right) v_w^3 \\ \hat{z} & = & \bar{\alpha}_0(t) + \bar{\alpha}_1(t)\omega_e + \bar{\alpha}_2(t)\omega_e^2 + \bar{\alpha}_3(t)\omega_e^3 \end{array} \tag{5.17}$$

where coefficients $\bar{\alpha}_i$ are obtained after replacing $\lambda = \frac{Rw_e}{N_x v_w}$ in (5.17), finally giving:

$$\bar{\alpha}_0(t) = \alpha_0 v_w^3,\ \bar{\alpha}_1(t) = \frac{\alpha_1 R}{N_x} v_w^2,\ \bar{\alpha}_2(t) = \frac{\alpha_2 R^2}{N_x^2} v_w,\ \bar{\alpha}_3(t) = \frac{\alpha_3 R^3}{N_x^3} \tag{5.18}$$

Coefficients $\bar{\alpha}_i$'s are clearly time-varying parameters due to the wind speed dependence, as well as the α_i's that come from the $C_p - \lambda$ curve for constant pitch angle. Therefore, when initializing the algorithm, some initial wind speed value can be used from some external source such as meteorological or statistical information, according to the current weather conditions.
One can re-write the final expression of (5.17) in the following form:

$$\hat{z} = \theta^T \phi \tag{5.19}$$

with $\theta^T = [\bar{\alpha}_0(t)\ \ \bar{\alpha}_1(t)\ \ \bar{\alpha}_2(t)\ \ \bar{\alpha}_3(t)]$ and $\phi = [1\ \ \omega_e\ \ \omega_e^2\ \ \omega_e^3]^T$, and assuming slow variations of θ, a *Recursive Least Square algorithm - RLSA*, as given by (5.20) below, can be used for the on-line adjustment of the time-varying parameter vector θ with measurement w_e and estimation $\hat{z}$ from the observer. The RLSA includes a forgetting factor ζ in the range $0 < \zeta < 1$, that priories the recent information against the older one [116], modifying the convergence speed of the parameter estimator.
Before showing the algorithm, let us define $\bar{z}$ as the z estimation given by the RLSA. The idea is basically to reduce the error $e_k = \bar{z} - \hat{z}$, or in other words, reduce the gap between the (assumed) real $\hat{z}$, that comes from the Kalman observer, and the one estimated by the regression algorithm $\bar{z}$, by adapting the coefficient vector θ_k. The algorithm is shown next:

$$\begin{array}{rcl} \bar{z} & = & \hat{\theta}_{k-1}^T \phi_k \\ e_k & = & \bar{z}_k - \hat{z}_k \\ R_k & = & \zeta + \phi_k P_k \phi_k^T \\ P_{k+1} & = & \zeta^{-1}\left(P_k - P_k^{-1}\phi_k^T \phi_k P_k\right) \\ \hat{\theta}_k^T & = & \hat{\theta}_k^T - R_k^{-1} P_k e_k \phi_k \end{array} \tag{5.20}$$

where $\hat{\theta}_k^T = [\hat{\alpha}_0\ \ \hat{\alpha}_1\ \ \hat{\alpha}_2\ \ \hat{\alpha}_3]_k$ is the estimated coefficient vector for the z curve, P_k is the error covariance matrix that should be initialized high enough, R_k is the measurement covariance matrix that works as additional tuning and filtering element for the information $\hat{z}$. The initial values for the vector $\hat{\theta}$ can be obtained by theoretical information on the C_p curve and some mean wind speed value.
Notice that to obtain convergence of this algorithm, some pseudo-random binary signal (PRBS) is added to the control signal, in order to achieve enough information richness.

The algorithm may be stopped when the error $e_k = \bar{z}_k - \hat{z}_k$ is considered to have become close enough to zero.

Now coming back to (5.17), one can obtain the optimal value of w_e by looking for the one maximizing the polynomial, which can be obtained among the the values cancelling the derivative of z with respect to w_e, or in other words, among the roots of the gradient of z:

$$\frac{\partial \bar{z}}{\partial w_e} = \hat{\alpha}_1(k) + 2\hat{\alpha}_2(k)\omega_e + 3\hat{\alpha}_3(k)\omega_e^2 = 0 \tag{5.21}$$

In fact, among those roots, the one corresponding to the maximum should satisfy:

$$\frac{\partial^2 \bar{z}}{\partial w_e^2} = 2\hat{\alpha}_2(k) + 6\hat{\alpha}_3(k)\omega_e^* < 0 \tag{5.22}$$

with w_e^* solution of (5.21).
Even more precisely, w_e should be an admissible value for the electrical generator, i.e should be found within some *a priori* expected range. Obviously, negative or really small/big values are forbidden due to the characteristic of the C_p curve. In fact, with the chosen third order polynomial approximation, one has only to decide between two values, with usually one being close to $\lambda = 0$, and the maximum one near the middle range of λ.

Remark: For the RLSA and the root finding algorithm, the computational time should be lower than the sampling time used by the Kalman-like observer to obtain $\hat{z}$.

5.1.4 Control strategies for power production maximization in wind turbines

Let us now discuss the control strategies proposed as the subsequent step of our approach, both in terms of Boost converter and generator speed control.

5.1.4.1 Control strategy for the power converter current

As discussed before, the idea is to use the inductance current i_a as the control variable for the generator speed, and thus that it is itself appropriately controlled in the converter by the duty cycle d_g. Various studies have been made about this converter control problem, such as [117, 118, 119]. A simple idea can be to use the average model obtained in (5.7) with state vector $x = [i_a\ v_a\ i_{Lc}\ v_L]^T$, input vector $u = [d_g]$, and disturbance vector $d = [e_a\ i_{ch}]^T$, and obtain from it a linearised model around some operation point given by state, input and disturbance values (respectively) as $X = [I_a\ V_a\ I_{Lc}\ V_L]^T$, $U = [D_g]$, $D = [E_a\ I_{ch}]^T$ (respectively). Then, the following linear model in terms of signals variations ($\tilde{x}$, $\tilde{u}$ and $\tilde{d}$) can be written:

$$\begin{aligned}
\dot{\tilde{x}}(t) = &\ A\tilde{x}(t) + B\tilde{u}(t) + E\tilde{d}(t) \\
\dot{\tilde{x}}(t) = &\begin{bmatrix} -R_a/L_a & -1/L_a & 0 & 0 \\ 1/C_{in} & 0 & 1/C_{in} & 0 \\ 0 & 1/L_c & 0 & -(1-D_g)/L_c \\ 0 & 0 & (1-D_g)/C_o & -1/R_pC_o \end{bmatrix} \tilde{x}(t) + \begin{bmatrix} 0 \\ 0 \\ V_L/L_c \\ -I_{Lc}/C_o \end{bmatrix} \tilde{u}(t) + \\
&\begin{bmatrix} 1/L_a & 0 \\ 0 & 0 \\ 0 & 0 \\ 0 & -1/C_o \end{bmatrix} \tilde{d}(t)
\end{aligned} \tag{5.23}$$

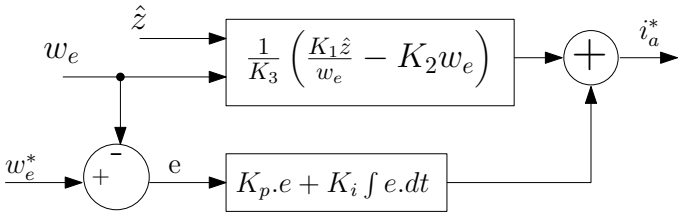

Figure 5.3: Block diagram of the control algorithm for the proposed power maximization strategy.

On this basis, classical controllers such as PID or H_∞ can be used [118], allowing to obtain a response fast enough so that this stage becomes transparent. For the proposed technique, a simple PI controller with anti wind-up function was used for the current control of the generator driver. Nevertheless, in further works a MPC will be used to ensure the operation of the machine, while maintaining admissible input and state values for the system. For instance, i_a should be positive, and saturations should be avoided in the machine operation. The results will be shown in Section 5.1.5.

5.1.4.2 Control strategy for the generator speed

Let us now come to the control strategy for the generator speed. Assuming the power converter well controlled, we are left with the control by $u = i_a$ of the following dynamical system:

$$\dot{w_e} = \frac{K_1 z}{w_e} - K_2 w_e - K_3 i_a \tag{5.24}$$

with a reference value w_e^* for w_e resulting from the maximization of $\bar{z}$. The control signal is here simply chosen as a "linearizing part" (as in standard feedback linearization [120] added to a stabilizing linear controller u_L, as follows:

$$u = i_a^* = \frac{1}{K_3}(K_1\hat{z}/w_e - K_2 w_e - u_L) \tag{5.25}$$

This turns the system into:

$$\dot{w_e} = u_L \tag{5.26}$$

where u_L is to be chosen so as to control the generator speed w_e according to its reference value w_e^* obtained at (5.21).
In practice, a simple linear PI controller can be used, tuned for example by using some optimal LQ design for reference tracking purposes [16]. The full structure of the controller block is depicted in Fig. 5.3. There, one can find the measurements $\hat{z}$ from the Kalman-like estimator, w_e that is the generator speed, and its optimal reference value w_e^*, obtained when finding the maximum value for the z curve. In the output side, the reference armature current i_a^* is obtained, that is delivered to the power converter current control strategy.

5.1.5 Validation of the technique by simulation

Let us here first summarize the whole algorithm to be implemented, in Fig 5.4.

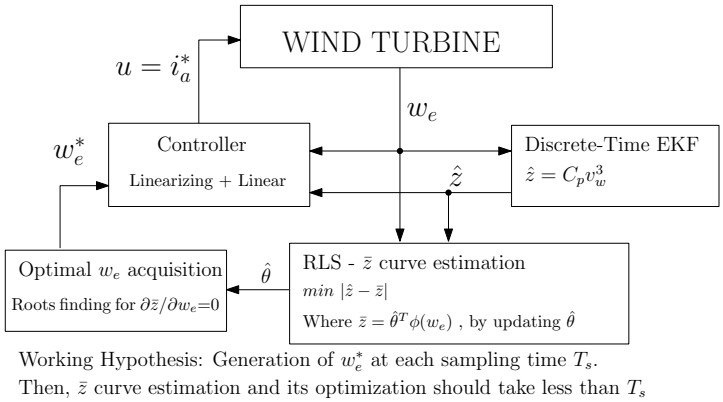

Figure 5.4: Block diagram of the proposed power maximization strategy for wind turbines.

On this basis, a validation of the proposed methodology is considered in a simulation context, with a model of a 6 kW-turbine and a DC generator. The corresponding mechanical and electrical characteristics, along with the coefficients of an eight-order polynomial representation of the C_P coefficient, are given in Table 5.1.

Table 5.1: 6-kW Wind Generator Parameters

PARAMETER	**VALUE**
Mechanical Parameters	
Turbine Radio, R	4.0 m
Turbine inertia, J_T	1.5 kgm^2
Wind speed range	$2 - 12\ ms^{-1}$
Transmission ratio, N_x	10
Wind density, ρ	1.25 kgm^{-3}
DC generator inertia, J_e	0.3 kgm^2
Electrical Parameters	
Maximum DC generator output power, P_{gen}	7.6 kW
Nominal case DC generator output power	3.0 kW
Rated field voltage, V_f	120 V
Rated armature voltage, V_a	240 V
Rated field flow, ϕ_f	0.12 Wb
Rated field current flow, I_F	2 A
Field inductance, L_f	60 mH
Field resistance, R_f	60 Ω
Armature inductance, L_a	10 mH
Armature resistance, R_a	2.0Ω
Friction constant, B_e	0.6
Induced EFM constant, K_e	0.5
Other Parameters	
Wind speed time constant, α_v	0.2
Theoretical $\alpha_{i=0\ldots8}$'s for the C_p polynomial $C_P(\lambda) = \sum_{i=0}^{8} \alpha_i \lambda^i$ [0.002897 0.001346 $-$ 0.03324 0.03313 -0.008475 0.00101 $-\ 6.345x10^{-5}$ $2.031x10^{-6}$ $-\ 2.621x10^{-8}$]	

5.1.5.1 Validation of the z-estimator block

The first step for the validation is that of the Kalman-like observer for the estimation of z. In the simulation, a constant current $u = i_a$ is set to the turbine, which implies a constant w_e for some initial wind speed value, subject to some high frequency additive noise. Then, a small step variation in the wind speed is introduced, and after some time, the wind speed is brought back to its initial mean value.
The main goal here is the comparison of the estimated $\hat{z}$ with the simulated z, obtained when using the polynomial expression for constant pitch angle β - introduced in (5.4), with the coefficients of Table 5.1, and the measurements of w_e, instantaneous wind speed value v_w, and assumed wind speed bandwidth α_v - also given in the table.
For this test, a mean wind speed equal to $5.3m/s$ was considered as an initial value, and $7.2m/s$ after the step, while assuming a wind speed high frequency noise amplitude of about $0.3m/s$, and an effective wind variation bandwidth α_v of 0.2 (see again Table 5.1). For the generator speed, it was initially fixed at about $160rad/s$, and raised up to $175rad/s$ after the increase of wind speed.
For the Kalman-based observer, the weight matrices were selected for the presented results as: $P = 1000I$, $Q = 0.5I$ and $R = 5$, with I representing an identity matrix of dimension 5, and the sampling time was chosen $T_s = 10ms$.
The performance of the estimator in those conditions is presented in Fig 5.5, where it can be seen that with an initialization of $\hat{z}(0) = 0$, the observer, converges quickly to the simulated value (less than $5s$). It is also clear that the observer tracks well the z variations after the wind speed step, showing the effectiveness of the proposed scheme, suitable for the control actions included in the strategy.

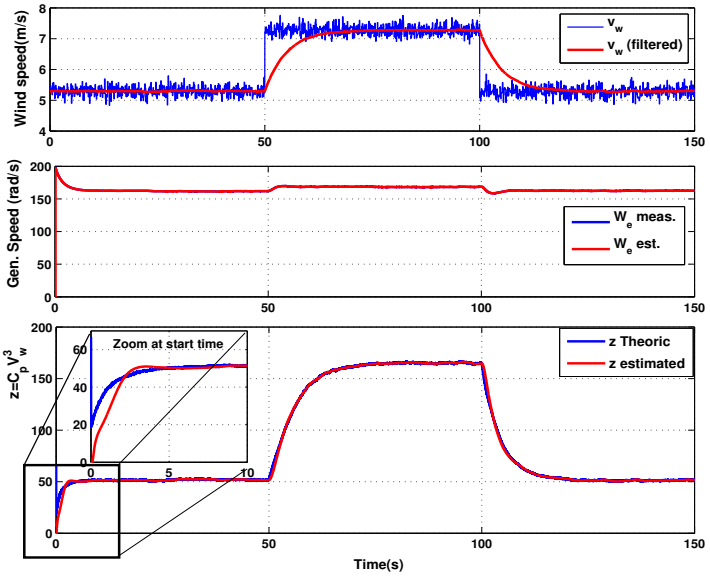

Figure 5.5: Performance of the state estimator for z under noisy wind speed profile

5.1.5.2 Validation of the polynomial estimator

For the RLSA estimation of the coefficients for the z polynomial representation (as in 5.17), it can be checked that the considered 3rd-order approximation indeed approaches well a more

accurate model (here described by an 8-order polynomial): First, notice that the optimal couple $(\lambda^{opt}, C_p^{opt})$ obtained from the 8-order polynomial is (7.6, 0.4521), corresponding to the point in which the wind turbine should operate. Then, after some curve fitting operation, one can obtain for the 3rd-order approximation coefficients as:

$$\alpha_0 = -0.405,\ \alpha_1 = 0.25, \alpha_2 - 0.0213,\ \alpha_3 = 4.3x10^{-4} \tag{5.27}$$

for which the optimal couple (λ^*, C_{pt}^*) is $(7.6, 0.4535)$, that is indeed close to our reference one. Fig. 5.8 shows the high and low order C_p curves, confirming equivalent values around the optimal point, as well as the regions of λ in which no power production is expected.
Therefore, the RLSA-based approach can indeed provide a good estimate for the optimal operation conditions, when initializing parameter vector θ (made of $\bar{\alpha}_i$'s) from initial guesses on α_i's (ideally close to the above values) and some apparent mean value of the wind speed (according to (5.18)). In the presented results, this algorithm was initialized with $\zeta = 0.975$, and $P = 2x10^5 I$ with I an identity matrix of order 4.

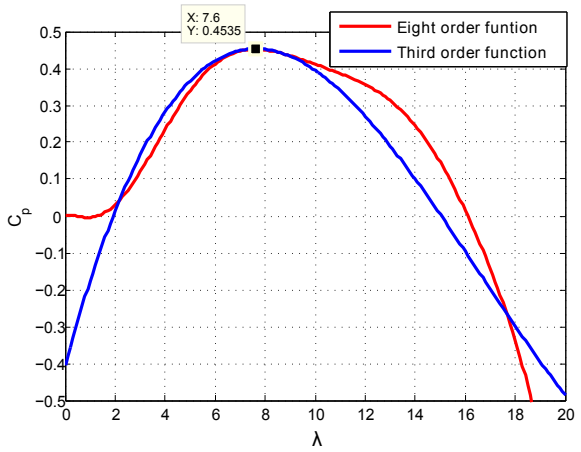

Figure 5.6: Original and reduced order C_p curves for optimal power production in the 6 kW EWPG

5.1.5.3 Validation of the full control strategy

In this example, the control signal is computed according to (5.25), with term u_L coming from an optimal PI controller, tuned proportional gain $K_p = 1.1892$ and integral gain $K_i = -0.7071$, after using the equivalent model represented at (5.26) with $Q = diag\{0, 1\}$ and $R = 2$.

The idea then is to validate the full control approach by illustrating its behaviour under a wind profile scenario, but also by comparing it to the case of a similar control strategy when some wind speed measurement is available.
This means that the approach used for comparison will still consider imperfect knowledge of the C_p curve, and include an RLSA method to get a polynomial approximation for it. This approximation will also use the estimated z coming from the Kalman observer. However, in the case of measured wind speed, λ can be obtained directly from w_e and v_w, and the polynomial approximation of $\hat{C}_p$ becomes:

$$\begin{aligned} \hat{C}_p(\lambda) &= \hat{\alpha}_0 + \hat{\alpha}_1\lambda + \hat{\alpha}_2\lambda^2 + \hat{\alpha}_3\lambda^3 \\ \hat{C}_p(\lambda) &= [\hat{\alpha}_0\ \hat{\alpha}_1\ \hat{\alpha}_2\ \hat{\alpha}_3][1\ \lambda\ \lambda^2\ \lambda^3]^T \\ \hat{C}_p(\lambda) &= \hat{\theta}^T\phi(\lambda) \end{aligned} \tag{5.28}$$

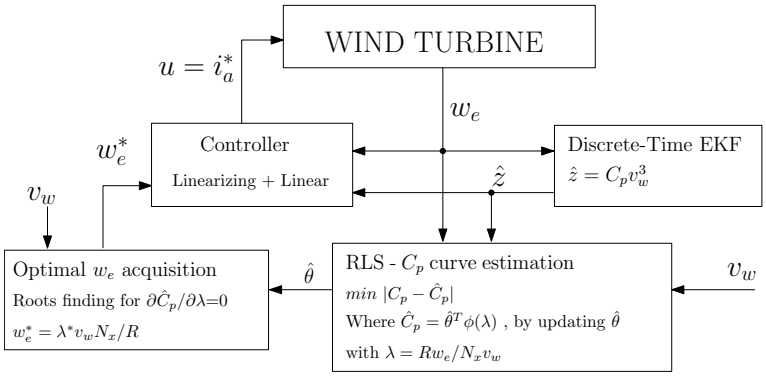

Figure 5.7: Block diagram for the alternative power maximization strategy using wind speed measurement

The RLSA can thus directly estimate coefficients $\hat{\alpha}_i$'s in this case, and the corresponding C_p can be optimized with respect to λ so as to finally give the optimal generator speed w_e^*.
This 'comparison algorithm' is summarized by the block diagram of Fig. 5.7.

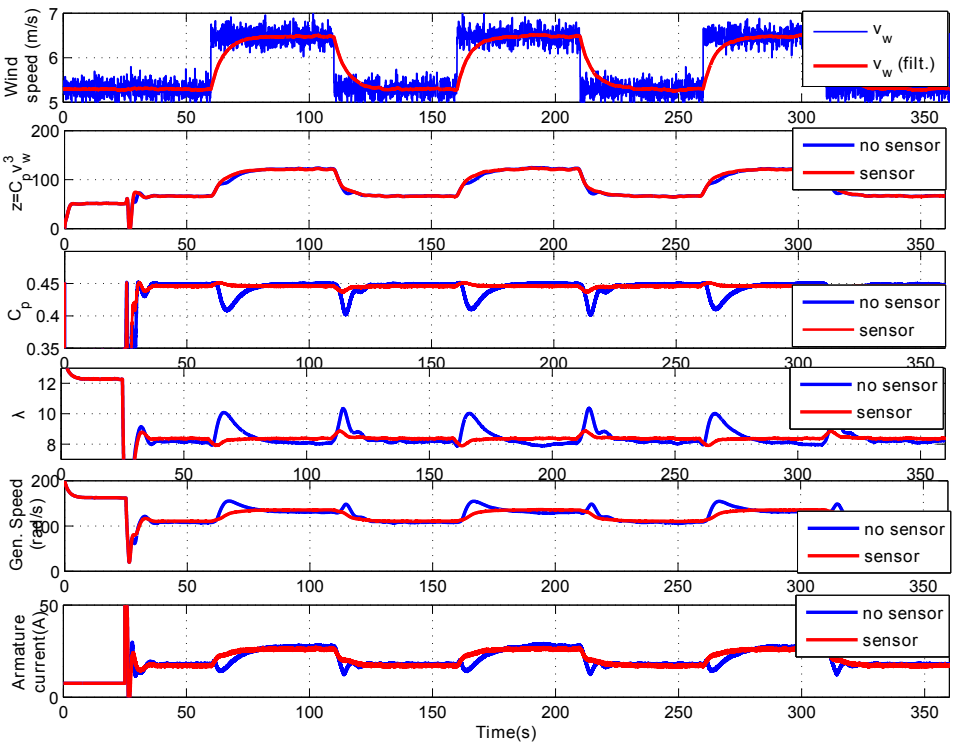

Figure 5.8: Simulation results of the proposed power production strategy for electric wind power generation systems, without - or with, wind speed sensor.

The results of the proposed maximum power production approach without wind speed measurement are shown in Fig. 5.8, where results of the proposed 'comparison algorithm' (with wind speed measurement) are also included. In Fig. 5.8, the proposed sensorless approach results are

marked as *no sensor*, while the 'comparison algorithm' results are marked as *sensor*. The first chart shows the wind speed profile, in which some zero mean high frequency noise, as well as step mean wind speed variation, are considered. In the second chart one can see that the estimated z from the observer is correctly obtained in both cases.

The other curves, which show the measured C_p, λ, w_e and i_a, reflect that, evidently the knowledge of wind speed enhances the performance of the system. For example, the C_p and λ evolutions are continuous around the optimal values. In the case of the sensorless technique, there is a stronger transient response when mean wind speed changes, but the final value of C_p and λ are close to the optimal ones. In addition, the transient response is fast and the machine produces its optimal energy in small time when strong wind speed variations are present.

According to those results, some conclusions can be obtained with the method. The first one is that the proposed methodology for optimizing the power production in wind turbines shows good performance when poor or no measurement of wind speed is available. The proposed approach is also applicable for sudden wind speed sensor failure, ensuring near optimal power production as well as stable operation of the wind generator.
The second remark is to emphasize the adaptive aspect of the technique. The procedure to obtain power curve coefficients (z for the proposed case, C_p for the traditional one), provides real-time knowledge of the power coefficient, and therefore, allows a better power maximization via a better estimation of optimal generator speed reference.

Remark: This method could also be used for real time optimal control of wind turbines when the wind speed measurement is available.

5.1.6 Experimental small scale prototype

Considering the potential use of the proposed methodology for optimal power production in wind turbines, some experimental essays are currently in progress on a small wind turbine prototype at Gipsa-Lab [1].

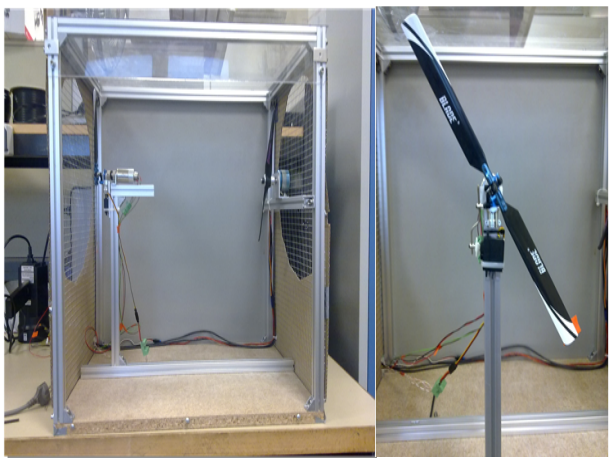

Figure 5.9: Small scale wind power generation system prototype at Gipsa-Lab

[1] Laboratory of Images, Speech, Signal and Control Systems of Grenoble

In the prototype, an industrial fan produces the desired wind speed, and its value is monitored with an anemometer. In addition, the turbine has the possibility of changing the pitch angle, allowing the manipulation of this parameter for further essays in power generation control with this structure. The power conversion system is also represented by a DC generator with a simple current sink, allowing a total capacity of 1 W in electrical power. The system is controlled in real-time with an acquisition card in the Matlab/simulink environment, allowing fast and feasible experiments when desired.
The small turbine is in a robust cage that eliminates adverse aerodynamical effects that can affect the air flow in the turbine. Experimental validation of the previously proposed control technique is obviously an interesting perspective to this work.

5.1.7 Concluding remarks

In this section, an approach for maximizing the power production in wind power generation systems was presented, when considering a sensorless wind speed situation that can occur when the anemometer or other mechanism fails, or when the measurement is not feasible.
The technique is based on various steps: First, a Kalman-based estimator is built to provide a real time power coefficient characteristic $z = C_p v_w^3$. In fact the shape of z is similar to the well known C_p curve.
The second step is a real time estimation algorithm for the power coefficient of the modified wind speed polynomial. A good knowledge of this polynomial allows its maximization with respect to the generator speed and then, an optimal reference is obtained that ensures maximum power production in the generator.
The third step is the control design, that includes two elements: a linearising term that cancels the nonlinearities in the mechanical equation, and a linear one that ensures the tracking of the generator speed according to the optimal reference, obtained from the last mentioned block.
Finally, it is noticed that the proposed approach, mostly based on the mechanical equation and the power characteristic curve, may be applicable to any class of wind turbine.

5.2 Power management of a microgrid with explicit MPC-based control

In this section, a complete methodology is presented for the control of a microgrid that is suitable to be used in stand alone power applications such as residences, communication equipments or road lighting systems for instance [31, 89, 121].
In such applications, the coordination of different power generation technologies, each one with its own functional characteristics, is fundamental, and a suitable control strategy is needed in the final implementation process [122]. For instance, the fact that fuel cells generate power in a limited way, avoiding the Oxygen Starvation (OST) phenomenon that can damage them permanently, requires the use of battery or supercapacitors for high frequency load components compensation [29, 35].
Another important element in microgrids is the interactivity between the power generators. For instance, power converters that operate at high switching frequencies (typically 1-50 kHz) require dedicated low level control strategies for the inductor current regulation, as a measure of protection for the power circuit. However, the effectiveness of the whole topology - with the controlled converters, will depend on high level power management strategies that will be devoted to objectives such as voltage regulation for each bus, as well as managing the harvested power in

the support units.
In this context, some classical approaches such as PID or LQR have been used [32, 89, 121]. However, the configuration and the system performance may be degraded and constraints may not be satisfied with such schemes. Obviously, the use of constrained MPC represents here a solution [33, 91, 123], but an *explicit solution* for the optimization problem, which means low computational load, is desired for real-time implementation in devices such as micro-controllers or FPGAs.

For all these reasons, our point here is to propose a procedure for MPC-based control of a microgrid, with explicit solution. First, the microgrid itself is presented, along with its generators, power converters and low level control strategies (current loops). Then, the constraints to be considered in the control strategy are introduced, and the MPC solution is given. Finally, some simulation results are presented, and compared with an LQR-based approach. The results of this section were presented in the contribution [8].

5.2.1 Description of the considered microgrid

The proposed power system is shown in Fig. 5.10. The system is composed by the following elements:

- A fuel cell-based generation unit, whose internal control strategies are out of the scope of the present thesis (see [27, 29] for further details). As already mentioned, this power unit has limited bandwidth operation due to its functional constraints to avoid Oxygen Starvation.
- A wind power generator, that has a maximum power production algorithm, in a similar fashion to the one presented in Section 5.1.
- A power storage and high frequency load compensator, composed by a supercapacitor.
- A DC load, that includes a bus capacitor, a preload resistance R_p related to fixed loads (electronic components, sensors, etc. and a current sink that models the consumed power by the load i_L. Such consumed power includes DC or AC loads, that can be connected to the proposed microgrid through standard inverters.

From Fig. 5.10, it can be seen that interactions between power units and supercapacitor with the DC bus are made by means of power converters. For this low power application, Boost (step-up) converters were used for the interconnection of fuel cell (named as DCDC1) and wind turbine (named as DCDC3) with the power bus; for the supercapacitor, a bidirectional Buck-Boost converter was used for its interconnection with the DC bus (named as DCDC2).
In the proposed system, the power coordination algorithm (PCA) will deliver control signals U_1, U_2 to the control blocks of DCDC1 and DCDC2, that will be discussed more ahead. For the DCDC3, it is assumed that control actions will be obtained by a *Maximum Power Point Tracking* strategy (as mentioned in Section 5.1), and meaning that **no control action** will be made over the converter DCDC3: as consequence, there will be some uncontrolled power injected to the DC bus from the wind turbine power system. In fact, this approach is completely valid in the context of maximum exploitation of instantaneous wind energy, in which the electrical generator only injects power to a load, either an inverter or a DC bus as in this case.
About the PCA block, it will in fact get information from all the buses of the system, including voltages and currents. Output current load i_L and wind unit current i_w, which are considered as disturbances, are assumed to be known, via estimators or sensors. The PCA block will compute

optimal references signals for the power converters control blocks, U_1 and U_2, according to some pre-defined cost function that should be optimized, and considering some constraints on the system.

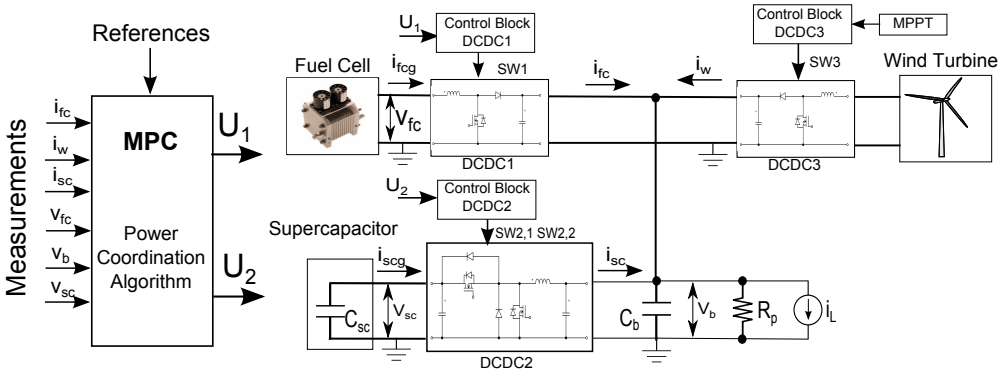

Figure 5.10: Fuel cell, Wind turbine and Supercapacitor connection for the power system

The Table 5.2 provides the considered numerical values for the parameters of the proposed power system, including power and voltage range for the units, as well as some details about the construction of the power converters DCDC1 and DCDC2, whose low level control strategies will be detailed more ahead.

Table 5.2: Power system characteristics

Fuel Cell	**Wind Turbine**	**Supercapacitor**	**DC Bus Characteristic**
Generated voltage ($\bar{V}_{g1}$): 35 VDC Maximum Power: 1.5 kW Power Slew Rate: 300 W/s	Maximum Power: 1 kW	Operative Range: 330-450 VDC Nominal Voltage($\bar{V}_{g2}$): 400 VDC Capacitance(C_{sc}): 10 mF	Bus Voltages ($\bar{V}_{c1}$, $\bar{V}_{c2}$): 300 VDC Capacitance (C_b): 400 uF Maximum Power: 5kW Nominal Power: 100W (preload) + 300W (Load)
Converter DCDC1		**Converter DCDC2**	
Inductance (L_1): 0.6 mH Capacitance (C_1): 1 mF Rated Duty Cycle ($\bar{D}_{c1}$) : 0.883		Inductance (L_2): 10.5mH Capacitance (C_2) : 4 mF Duty Cycle for both modes ($\bar{D}_{c2,1}$, $\bar{D}_{c2,2}$): 0.25	

5.2.2 Low-level control strategies and reduced microgrid model

In this section the microgrid model as well as its low level controls strategies (used in the current control for the power converters) are presented. In the sequel, all variables are expressed as: $x = \bar{X} + \tilde{x}$, where $\bar{X}$ stands for its equilibrium value and $\tilde{x}$ for its variations around it.

5.2.2.1 Inductor current power converter control strategies

In practice, a hierarchical structure is assumed for these power systems with power electronics as coupling elements. For instance, the power converters include an inductor current control

strategy that enhances its stability against perturbations, either at their input (source) or at the output (load) nodes. Typical control strategies are based on PID, robust, or even nonlinear control laws [84, 117, 118].
For the DCDC1 and DCDC2 converters, PID-based strategies were used for current control for the sake of their simplicity Well-known transfer functions between the duty cycle variation $\tilde{d}_c$ and the inductor current variation $\tilde{i}_l$, denoted by $G_{i_l d_c}(s)$, can be considered for the converters (obtained from averaged-state space modeling - see [84]), reading for the Buck converter as:

$$G_{i_l d_c}(s) = \frac{\tilde{i}_l(s)}{\tilde{d}_c(s)} = \frac{\bar{V}_g/L(s+1/RC_{eq})}{s^2 + s/RC_{eq} + 1/(LC_{eq})} \text{ with } d_c = \frac{v_c}{v_g} \tag{5.29}$$

and for the Boost converter as:

$$G_{i_l d_c}(s) = \frac{\tilde{i}_l(s)}{\tilde{d}_c(s)} = \frac{\bar{V}_c/L(s+2/RC_{eq})}{s^2 + s/RC_{eq} + \bar{D}_{cp}^2/(LC_{eq})} \text{ with } d_c = 1 - \frac{v_c}{v_g}, d_{cp} = 1 - d_c \tag{5.30}$$

where R, L, C_{eq} are the nominal load resistor, inductance and equivalent capacitance for each converter, $\bar{V}_g, \bar{V}_c$ are the equilibrium values of the input and output voltages, v_g, v_c. Notice that for the Boost converter, the transfer function depends on some equilibrium duty cycle value: $\bar{D}_{cp} = 1 - \bar{V}_c/\bar{V}_g$.
Numerical values for (5.29)-(5.30) can be obtained from Table 5.2. Equivalent capacitances C_{eq} for the converters are $C_{eq1} = C_b + C_1 + C_2$ for DCDC1 and DCDC2 in discharge (Buck) mode, and $C_{eq2,2} \approx C_{sc}$ for DCDC2 in charge (Boost) mode. These modes are called like this because they inform on the power flow from the supercapacitor: discharging when injecting power to the DC bus, and charging when absorbing power from it. Another aspect is that for DCDC2 the duty cycle value $d_{c2,1}$ is related to the discharge (Buck) mode, whereas $d_{c2,1}$ is related to the charge (Boost) mode.
For the inductor current control strategies, the following closed-loop performance was considered: The minimum gain and phase margins are 6dB and 45^o, respectively, and closed loop bandwidth up to 1/5 of the converter switching frequency (20kHz), hence 4kHz. This value is chosen because the transfer function is valid up to half of the switching frequency, and also because under this selected bandwidth, any switching effect will be canceled on the inductor current value [84, 124]. The inductor currents and controller transfer functions, $G_{i_l d_c}(s)$ and $G_c(s)$, are shown in Table 5.3, while step responses (step at $t = 0s$) for the closed loop current controllers are shown in Fig 2. From those results, it can be seen that the equivalent behaviour for the current converters can be modeled as a first order transfer function with a time constant of $0.5ms$. Therefore, this suggests that the current control loop can be considered as a static component for the upper-level control strategies, and only reference values would be provided to control the system, while each power converter is seen as a current source for the system. In addition, it can be seen that dynamical performances of the DCDC2 for charge and discharge modes are quite similar.

Table 5.3: Current loops transfer functions and PI controllers

$G_{i_1 d_c}$ **DCDC1**	$G_{i_1 d_c}$ **DCDC2-Discharge**	$G_{i_1 d_c}$ **DCDC2-Charge**
$\frac{5e^5(s+9.01)}{s^2+4.505s+3.083e^4}$	$\frac{4e^5(s+4.505)}{s^2+4.505s+1.351e^6}$	$\frac{4e^5(s+0.938)}{s^2+4.505s+1.406e^6}$
G_c **for DCDC1**	G_c **for DCDC2 - Discharge**	G_c **for DCDC2 - Charge**
$\frac{0.0562(0.008s+1)}{0.008s}$	$\frac{0.008s+1}{0.008s}$	$\frac{0.008s+1}{0.008s}$

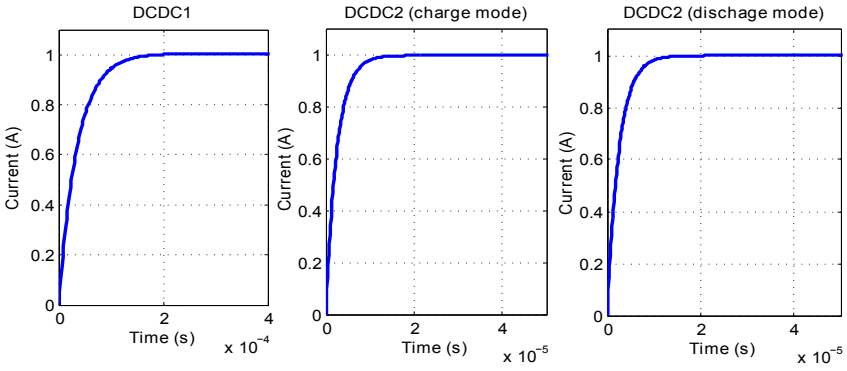

Figure 5.11: Step responses for the inductor current in closed loop

5.2.2.2 Microgrid power flow modeling

After considering that DCDC1 and DCDC2 have inner current control strategies, these converters can be transformed into controlled current source elements, as shown in Fig. 5.12. In the reduced model of the microgrid, current references i_{fc} and i_{sc} respectively correspond to signals U_1, U_2 from the PCA. In addition, the interaction between the supercapacitor and the load bus, made by the converter DCDC2, has an equivalent model in which the current given from the supercapacitor to the bus is denoted as i_{sc}, while the current generated from the supercapacitor can be expressed as $R_v i_{sc}$, where R_v is the voltage relation between the supercapacitor and the DC bus, which is equivalent to $\bar{D}_{c2,1}$.

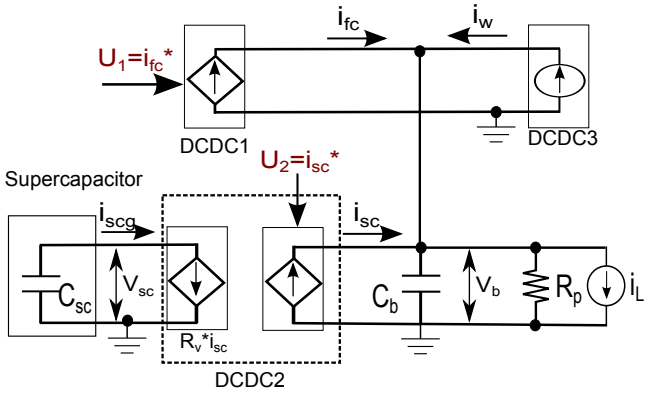

Figure 5.12: Reduced model scheme of the power system

From this reduction strategy, it is possible to establish a dynamical model for the capacitor voltages (C_b, C_{sc}) in terms of inputs $(U_1 = i^*_{fc}, U_2 = i^*_{sc})$ (where symbol $*$ stands for reference values) and disturbances, i_w, i_L. Here, equations for the absolute energy variation in each capacitor are written as follows,

$$\begin{aligned} \dot{E}_b &= P_{fc} + P_{sc} + P_w - P_{pre} - P_L \\ \dot{E}_{sc} &= -P_{scg} \end{aligned} \tag{5.31}$$

where E_b, E_{sc} are the energies in each capacitor, P_{fc}, P_{sc}, P_w are the powers given from the fuel cell, supercapacitor, wind turbine to the DC bus, P_{scg} is the power entering from the supercapacitor to

DCDC2, and P_{pre}, P_L are the demanded preload and load to the DC bus. Therefore, considering that the energy for each capacitor satisfies $E = 0.5CV^2$, with C its capacitance and V its voltage, and the fact that powers are the product of currents and voltages, a state space model for the system can be represented by:

$$\dot{x} = \begin{bmatrix} K_{b2} & 0 \\ 0 & -R_v\bar{I}_{sc} \end{bmatrix} x + \begin{bmatrix} \bar{V}_b & \bar{V}_b \\ 0 & -R_v\bar{V}_{sc} \end{bmatrix} u + \begin{bmatrix} \bar{V}_b & -\bar{V}_b \\ 0 & 0 \end{bmatrix} d \tag{5.32}$$

where $x = [\tilde{v}_b \ \tilde{v}_{sc}]^T$ is the state vector, $u = [\tilde{i}_{fc} \ \tilde{i}_{sc}]^T$ is the input vector and $d = [\tilde{i}_w \ \tilde{i}_L]^T$ is the disturbance vector. In addition, let us define: $R_v = \bar{D}_{c2,1} = 0.5$ (considered fixed due to the controller actions), $K_b = C_b\bar{V}_b$,$K_{b2} = \bar{I}_{fc} + \bar{I}_{sc} + \bar{I}_w - \bar{I}_L - (2/R_{pre})\bar{V}_b$ and $K_{sc} = C_{sc}\bar{V}_{sc}$. From now, a discrete-time model will be considered, by applying the well-known forward Euler discretization method to system (5.32) with a sampling time T_s.

5.2.3 Definition of the constrained optimization problem

After having defined the reduced model of the microgrid that is suitable for the coordination (high level) strategy, this section introduces the optimization problem to be considered, and more precisely the cost function, its weighting matrices and the constraints according to the microgrid operative conditions.
The selected cost function for the power management algorithm is as follows:

$$J = \frac{1}{2}\left(\tilde{x}_N^T P \tilde{x}_N + \sum_{k=0}^{N-1} \tilde{x}_k^T Q \tilde{x}_k + \sum_{k=0}^{N-1} \tilde{u}_k^T R \tilde{u}_k + \sum_{k=0}^{N-1} \tilde{x}_k^T S \tilde{u}_k\right) \tag{5.33}$$

where N is the prediction horizon, P, Q, R and S are weighting matrices with $P \geq 0, Q \geq 0, S \geq 0, R > 0$, $\tilde{x}_k$ is the state vector error to be reduced (defined as $\tilde{x}_k = x_k - x_{ref}$) and $\tilde{u}_k$ is the control signal variations with respect to a reference control value u_{ref} ($\tilde{u}_k = u_k - u_{ref}$). The methodology for transforming the cost function into a quadratic function in the control sequence to be chosen has already been discussed in Section 4.1.1.
In addition, the weighting matrices Q, R, S can here be selected under the following conditions:

- Regulation of the DC bus voltage is more important than regulation of the supercapacitor voltage. Therefore, more weight is imposed in Q for the DC bus voltage state.
- For the fuel cell, which is a chemical-based power source, the fuel consumption should be particularly reduced. However, in steady state the fuel cell must provide the main part of the power demanded by the load. This is reflected in the selection of matrix R.
- Considering the former condition, the supercapacitor must not discharge in steady state, penalizing therefore the power flow that can be generated by supercapacitor through the selection of S.

Considering the microgrid parameters of Table 5.2, weighting matrices can be numerically chosen as:

$$Q = \begin{bmatrix} 100 & 0 \\ 0 & 10 \end{bmatrix}, R = \begin{bmatrix} 10 & 0 \\ 0 & 1 \end{bmatrix}, S = \begin{bmatrix} 0 & 0 \\ 0 & 0.25 \end{bmatrix} \tag{5.34}$$

With respect to the definition of constraints, the idea is to establish each of them according to the microgrid ranges defined in Table 5.2. Evidently, their selection also impacts the system performance.
The following elements can finally be considered in order to define the optimization strategy constraints:

- The bus voltage V_b must be regulated around some reference value. With this objective, the load stability is ensured, which is indeed important when using some inverter to connect an AC load to the system.

- The supercapacitor voltage V_{sc} must be maintained in an admissible range. This is related to its state-of-charge (SoC) and support units should not be full charged or discharged for compensating any load transitions that cannot be supplied by the main energy sources. In addition, some minimal voltage must be guaranteed in the supercapacitor for the correct operation of the bidirectional converter DCDC2 [84, 91].

- Current references for converters DCDC1 and DCDC2, represented by control signasl U_1 and U_2 respectively, must be also limited. For instance, the fuel cell generator cannot absorb any power from the load bus, but can generate up to 1.5 kW of power, and both actions are considered when computing the signal U_1.
  In the case of the bidirectional converter, that allows the supercapacitor-load bus interaction, it can inject and absorb power from the load bus, and its power range depends on the maximum power delivered by the fuel cell (2.5 kW) and the wind turbine (1.0 kW). Therefore, the control signal U_2 will be limited for generating/absorbing up to 2.5 kW at the supercapacitor.

- Due to the operational constraints of fuel cell and supercapacitors, some restrictions are applied to their reference signals so as to maintain admissible slew rate in both units. In the case of the fuel cell, and considering a commercial prototype such the BALLARD Nexa fuel cell, the slew rate is limited to 300 W/s [27]. For the supercapacitor, a slew rate of 300 A/s is assumed for charging and discharging processes, for the protection of internal capacitor structure.

- Considering that power generated from the wind turbine and current sink are disturbances for the model, some additional constrains can be needed: the maximum power delivered from wind turbine is limited to 1 kW, and the maximum power absorbed by the load is 5 kW.

Considering the nominal bus voltage of 400 VDC, included in Table 5.2, the following constraints can be written for states, inputs and input slew rates:

$$\begin{array}{cc} 295V \leq x_1 \leq 305V & 0 \leq u_1 \leq 5A \\ 450V \leq x_2 \leq 330V & -8.3A \leq u_2 \leq 8.3A \\ -1A/s \leq \delta u_1 \leq 1A/s & 0 \leq d_1 \leq 3.3A \\ -300A/s \leq \delta u_2 \leq 300A/s & 0 \leq d_2 \leq 16.6A \end{array} \tag{5.35}$$

Remember from Section 4.1.1 that one can write the optimization problem under constraints in QP form, only in terms of the control sequence vector $\boldsymbol{u} = [u_0 \cdots u_{N-1}]^T$, where N is the prediction horizon. Therefore, considering the microgrid reduced order dynamics (5.32), along with the cost function (5.33), weight matrices (5.34) and constraints (5.35), one can write the optimization problem in the following form:

$$\begin{array}{ll} \min\limits_{\boldsymbol{u}} & \frac{1}{2}\boldsymbol{u^T H u} + \boldsymbol{u^T}[\boldsymbol{K_1}(x_0 - x_s) + \boldsymbol{K_2}(\boldsymbol{d} - \boldsymbol{d_s}) - \boldsymbol{H u_s}] \\ \text{subject to} & \boldsymbol{L u} \leq W \end{array} \tag{5.36}$$

for matrices H, K_1, K_2, L, W resulting from the previous modeling.
The solution is computed in the PCA unit, which then delivers signals U_1 and U_2, as references for the low level current control strategies for each power converter.

5.2.4 Computer simulation and control strategy evaluation

In this section simulation results for the proposed power system and its control can be presented.
The MPC-based approach resulting from the solution of (5.36) will be compared to some standard feedback law - here based on LQR design, with weighting matrices (5.34), and operative constraints added as limiters and filters for the reference inputs $U_1 = i^*_{fc}, U_2 = i^*_{sc}$ according to (5.35).
Remember that the microgrid includes a wind power generator assumed to have noisy energy production, and that MPPT strategies are used to produce maximum power, but the wind energy is time-varying and the control algorithm will have to face those fast wind speed changes. Another element in the simulation is that at some time, the load - although defined as a DC one, will admit an AC component up to grid frequency (50 Hz): this will allow to show that the control strategy can be reliable not only for DC loads, but also for AC or fast time-varying load profiles. For the system, the model presented in (5.32) was considered, with the following initial values for all the states, controls and disturbances:

$$\bar{V}_b = 300V,\ \bar{V}_{sc} = 400V,\ \bar{I}_{fc} = 0.667A,\ \bar{I}_w = 0.33A,\ \bar{I}_{sc} = 0.0A,\ \bar{I}_L = 0.667A,\ R_p = 900\Omega. \tag{5.37}$$

Finally, the system was discretized with a sampling time of $5ms$ (considering its relative small dimension) and the prediction horizon was fixed as $N = 3$. Therefore, a fast solution to the optimization problem is required and the explicit solution fits perfectly this target.
The power profiles used in the tests can be described as follows:

- For the load profile: over time period $t = 0 - 2s$, the demanded current (power) is $0.667A\,(200W)$. Then, it is incremented up to $2.5A(750W)$ over $t = 2 - 10s$, and augmented again to $5A(1.5kW)$ over $t = 10 - 25s$. In the interval $t = 25 - 50s$, the load has a DC component and an AC component as follows: over $t = 25 - 40s$, the DC load is $6A(1.8kW)$ and the AC load has an amplitude of $1A(300W)$ and frequency of 5Hz. Over $t = 40 - 50s$, the DC load is $4A(1.2kW)$ and the AC load has an amplitude of $1A(300W)$ and frequency of 50Hz (line frequency). Finally, over $t = 50 - 60s$, the DC load is $3.5A(1.05kW)$ and the AC load has an amplitude of $1.5A(450W)$ and frequency again of 5Hz. After $t = 60$, the load is returned to its initial value $0.667A(200W)$.

- For the wind turbine: it generates its current (power) with some noise of zero mean. However, the injected current (power) basic values are: $0.333A(100W)$ over $t = 0 - 10s$, then incremented up to $1.333A(400W)$ and again incremented to $2.33A(700W)$ for the intervals $t = 10 - 25s$ and $t = 25 - 40s$, respectively. After $t = 40s$, the basic value returns to $0.333A(100W)$.

This power profile was used to evaluate the LQR and contrained MPC control strategies for power coordination of the system, and the respective results are shown in Fig. 5.13. For both cases, and deliberately, the selection of the supercapacitor was lower than the recommended one for a support power unit, whose dimensions are selected according to the peak power and required autonomous time [122]. Without this assumption, the state constraint for the supercapacitor would be useless due to its stored energy, and the variation of this state with the selected power profile would not be clear.

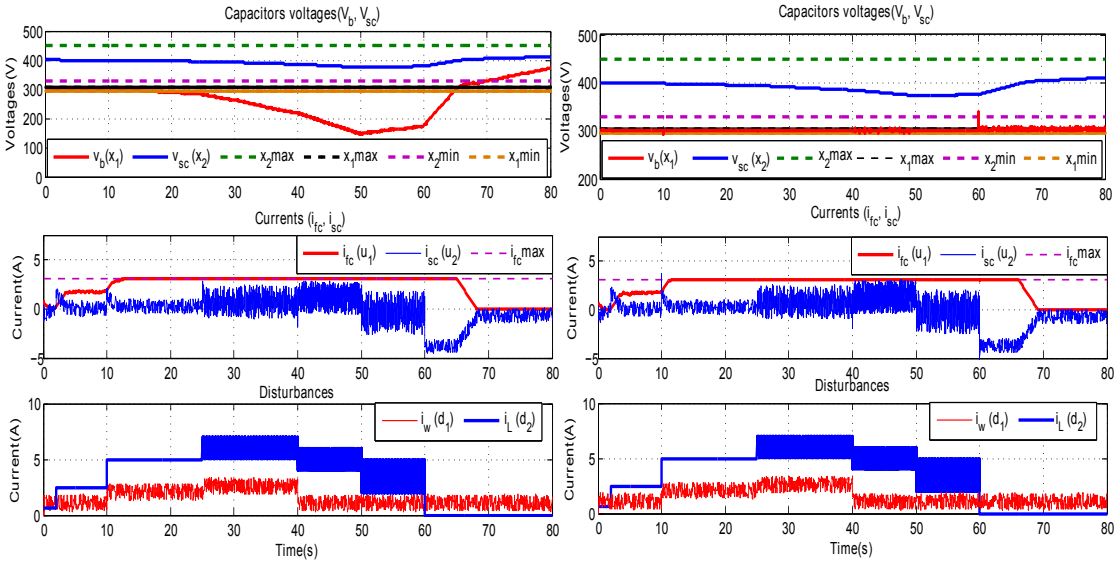

Figure 5.13: Unconstrained (left) and Constrained (right) MPC control strategies application to the proposed power system

With those results, common characteristics can be noted. One of them is that the power injected by the supercapacitor to the DC bus will have high frequency components, not only to compensate the ripple provided by the wind turbine, but also by the load, when some AC component is superposed to the DC value. In addition, for both cases, the best decision, regarding the fuel cell generated current, consists in its saturation, which is kindly positive because this generator is, in fact, the main one at the system.
However, the constrained MPC solution offers better stability and reliable conditions when compared to the LQR solution. In particular, the DC bus voltage, for the unconstrained case, has a deep reduction, even below the minimum admissible value of $295V$, as well as bigger control effort provided by the supercapacitor. In addition, and after returning to the initial power demand, it can be seen that the bus voltage is raising over its upper limit, showing a stability issue for this solution. On the contrary, the constrained MPC shows better performance, by achieving the control objectives and system restrictions, which are directly considered in the controller design.

5.2.5 Concluding remarks

In this section, a coordination method was presented for a small power microgrid, composed by a fuel cell, a wind turbine that always delivers the maximum amount of power, and a supercapacitor. The strategy, based on a Model Predictive Control solution, ensures all the considered objectives such as voltage regulation in the DC bus and voltage range in the supercapacitor, while respecting constraints such as the admissible maximum power delivered by all the sources, the voltage ranges and slew rate for the fuel cell. The proposed controller was compared with an LQR coordination strategy with constraints in the actuators, showing better results and constraints enforcement, specially in the state variables. One fact that can be emphasized is the importance of weighting matrices, which directly affect the performance of the optimization algorithm, and therefore, the system behavior.
According to this, it is seen that for low complexity systems, a centralized solution can be suitable

for coordinating the power flows. However, when the power system is more complex, including more storage devices, voltage buses and loads for instance, the centralized solution would not be so efficient. For this reason, in the following chapter a coordination approach is considered for distributed systems that have their own internal control strategies, and where a coordination algorithm can deliver some signal to ensure the overall system performance, considering a global cost function and constraints.

5.3 Conclusions

In this chapter, two contributions of the thesis were presented.
The first one is an approach for power maximization of wind power generation systems, that considers a wind speed sensorless scheme, and that can be adapted to any class of electrical generator of the turbine. The approach thus allows to handle cases when wind speed measurements are not always reliable, due to instrument noise and/or its placement with respect to the turbine blades, or when the wind speed sensor is damaged. The solution allows that the turbine to work close to its optimal operation point, for a fixed blade pitch angle. Future works will be devoted to improve the algorithm in start-up conditions, or even when the pitch angle varies according to the wind speed profile.
In the second part, an algorithm for the power management in a microgrid power system was proposed, when considering a grid made of a fuel cell, an optimized wind generator, and a supercapacitor as an auxiliary device. Here, a model predictive control solution that helps to maintain the voltage regulation in the buses was evaluated, considering a reduced model for the power flows in the system, after approximating the DC/DC converters by fast dynamics units. The solution, that includes constraints and considers the fuel cell as the main source, was compared with a classical LQR approach with actuator constraints. In future works, a deeper evaluation can be made, and some related experimental works would be of course profitable.

Chapter 6

CONTRIBUTION TO MPC DECOMPOSITION AND DISTRIBUTED COORDINATION UNDER CONSTRAINTS

Contents

6.1 Centralized MPC problem description with interactions considerations 96
6.1.1 Centralized MPC . . . 96
6.1.2 Centralized MPC problem with interactions consideration . . . 97
6.2 Optimization problem decomposition and coordination . . . 100
6.2.1 Problem decomposition and explicit local solutions . . . 100
6.2.2 Global coordination based on local explicit solutions . . . 102
6.3 Analysis of the proposed approach . . . 104
6.3.1 Complexity of the coordination problem . . . 104
6.3.2 Structure of local controllers and coordination vector influence . . . 106
6.3.3 Coordination period and subsystems sampling periods: performance of the subsysems . . . 107
6.3.4 Control structure for subsystems . . . 109
6.4 Illustrative example . . . 110
6.5 Conclusions . . . 113

In previous chapters, explicit solutions for constrained MPC were recalled, and illustrated, on the basis of [6, 41] typically. The problem could also be solved with other available numerical methods, as commented in [55], or other geometrical-like approaches as in [100, 101]. But in all cases, one can verify that the complexity of solutions increases with the selected prediction horizon, as well as with the size of the system.
Now in the case of systems of large scale or physical disposition, one can consider either *centralized* or *distributed* model-based algorithms to adequately solve the problem. Here, one can assume to have one entity that gathers information and delivers input signals to the whole system, respecting some constraints. Those input signals should be the solution of the *centralized control problem*, that can be really complex and time demanding for the system. However, if the system can be dynamically separated into smaller ones by using simple inspection methods or tools for multivariable control systems - such as Singular Value Decomposition (SVD), Relative Gain Arrays (RGA) or Order Reduction [16], one can divide the control entity into smaller ones accordingly. In such a scheme, an entity, the *coordinator*, will receive information from the *subsystems*, and in turn, deliver some information to coordinate their actions, according to some

policy. The subsystems are then driven by local controllers, and local stability can be ensured, which is an important aspect in general, and more particularly for power generation applications. With such an approach, one can talk of a *distributed control problem*, which can be solved via hierarchical-based strategies, as seen in [21], related with solutions such as those of [7, 23, 24, 39] to cite a few.

In the present chapter, it is shown how explicit solutions for MPC can be extended to a case of decomposed-coordinated implementation, in the presence of constraints. In this way, this contribution extends the former study of [6], where the problem of constraints was not fully solved.
More precisely, it is first shown how a centralized MPC problem can be re-written in terms of a control problem for interconnected subsystems. Then, from the corresponding MPC problem decomposition, a coordination strategy is proposed on the basis of local explicit unconstrained solutions, in such a way that it can be itself reformulated as a QP optimization problem, under linear inequality constraints representing the global constraints on the system, and finally allowing for a global explicit solution (for instance as discussed in Section 4.1).
This coordination approach is also discussed in our conference paper [7], with an extended version dealing with its stability in [11].

6.1 Centralized MPC problem description with interactions considerations

Here a summary of the QP formulation for the constrained MPC in the centralized case is first recalled. Then, a reformulation of the problem in an distributed way is presented, in which the global system is divided into subsystems, that interact with each other.

6.1.1 Centralized MPC

Consider the following discrete-time dynamical system:

$$\begin{aligned} x_{k+1} &= Ax_k + Bu_k + Ed_k \\ y_k &= Cx_k \end{aligned} \tag{6.1}$$

with k denoting the current time, x_k, u_k, d_k, y_k the state, input, disturbance and output vectors of orders n, m, q and o respectively, and $A \in \Re^{n\times n}$, $B \in \Re^{n\times m}$, $E \in \Re^{n\times q}$, $C \in \Re^{o\times n}$ the state, input, disturbance and output matrices respectively.
The cost function J_g to be minimized by a control vector sequence $\boldsymbol{u} = [u_0 ... u_{N-1}]^T$ over a prediction horizon N, and with weighting matrices $P \geq 0, R_u \geq 0, Q, S_u$ such that $Q \geq S_u R_u^{-1} S_u^T$, is:

$$J_g = \frac{1}{2}\left(\tilde{x}_N^T P \tilde{x}_N + \sum_{k=0}^{N-1} \tilde{x}_k^T Q \tilde{x}_k + \sum_{k=0}^{N-1} \tilde{u}_k^T R_u \tilde{u}_k + 2\sum_{k=0}^{N-1} \tilde{u}_k^T S_u \tilde{x}_k\right) \tag{6.2}$$

The predicted states vector, expressed in terms of the current state x_0, the control sequence $\boldsymbol{u}$ and the disturbance sequence $\boldsymbol{d}$ is:

$$\begin{aligned} \boldsymbol{x} &= \Omega x_0 + \Gamma \boldsymbol{u} + \Theta \boldsymbol{d} \\ \tilde{\boldsymbol{x}} &= \Omega(x_0 - x_s) + \Gamma(\boldsymbol{u} - \boldsymbol{u_s}) + \Theta(\boldsymbol{d} - \boldsymbol{d_s}) \end{aligned} \tag{6.3}$$

where x_s, u_s and d_s are the state, input and expected disturbance values. while details on matrices Ω, Γ and Θ can be found in Appendix A. The cost function (6.2) can be transformed into a

quadratic form with decision variable $\boldsymbol{u}$ as:

$$J_g = \bar{V} + \frac{1}{2}\boldsymbol{u^T H u} + \boldsymbol{u^T}[\boldsymbol{K_1}(x_0 - x_s) + \boldsymbol{K_2}(\boldsymbol{d} - \boldsymbol{d_s}) - \boldsymbol{H u_s}] \tag{6.4}$$

with $\bar{V}$ gathering elements independent of $\boldsymbol{u}$, and matrices $\boldsymbol{H}, \boldsymbol{K_1}$, $\boldsymbol{K_2}$ defined in (4.10).The *explicit unconstrained solution* for this cost function is:

$$\boldsymbol{u}^*_{uc} = -\boldsymbol{H^{-1}}[\boldsymbol{K_1}(x_0 - x_s) + \boldsymbol{K_2}(\boldsymbol{d} - \boldsymbol{d_s}) - \boldsymbol{H u_s}] \tag{6.5}$$

The optimization of the cost function (6.4) can also include inequality constraints, that gathers limit values for states, inputs, disturbances and input derivatives, finally reading as:

$$\begin{array}{ll} \min\limits_{\boldsymbol{u}} & \frac{1}{2}\boldsymbol{u^T H u} + \boldsymbol{u^T}[\boldsymbol{K_1}(x_0 - x_s) + \boldsymbol{K_2}(\boldsymbol{d} - \boldsymbol{d_s}) - \boldsymbol{H u_s}] \\ \text{subject to} & L\boldsymbol{u} \leq W \end{array} \tag{6.6}$$

where the constraint polyhedron matrices $\boldsymbol{L}, \boldsymbol{W}$ are defined in (4.25) and (4.26). For the solution, an explicit methodology based on the geometric characteristic of the QP problem was already recalled in Section 4.1, allowing to obtain low computation time, adaptability, and problem relaxation with other potential constraints.

6.1.2 Centralized MPC problem with interactions consideration

In this part, the *interactions* are explicitly considered in the system model. Remember that a complex system can be divided into smaller ones, each one with local states, inputs and disturbances, and additionally, they have a local interaction term, that depends on the signals coming from the other subsystems.
Let us first consider the case of a *fully interactive* system, namely a system where all the states are affected by the actions of other states, inputs and perturbations. The global representation of the form (6.1) considering the *global signal vectors*, can be re-written as the union of some *local signal vectors*, denoted with the sub index $i = 1 \cdots z$, with $x_{(i)} \in \Re^{n(i)}$, $u_{(i)} \in \Re^{m(i)}$, $d_{(i)} \in \Re^{q(i)}$, as follows:

$$\begin{bmatrix} x_{(1)} \\ \vdots \\ x_{(z)} \end{bmatrix}_{k+1} = A \begin{bmatrix} x_{(1)} \\ \vdots \\ x_{(z)} \end{bmatrix}_k + B \begin{bmatrix} u_{(1)} \\ \vdots \\ u_{(z)} \end{bmatrix}_k + E \begin{bmatrix} d_{(1)} \\ \vdots \\ d_{(z)} \end{bmatrix}_k \tag{6.7}$$

Therefore, one can write each subsystem dynamics in terms of its own signals, and the interaction vector $v_{(i)} \in \Re^{r(i)}$ as in (6.9) below:

$$x_{(i)k+1} = A_{ii}x_{(i)k} + B_{ii}u_{(i)k} + E_{ii}d_{(i)k} + v_{(i)k} \tag{6.8}$$

$$v_{(i)k} = \sum_{\substack{j=1 \\ j \neq i}}^{z} (A_{ij}x_{(j)k} + B_{ij}u_{(j)k} + E_{ij}d_{(j)k}) \tag{6.9}$$

The full system *interaction vector* v_k, based on (6.9), satisfies:

$$\begin{bmatrix} v_{(1)} \\ \vdots \\ v_{(z)} \end{bmatrix}_k = v_A \begin{bmatrix} x_{(1)} \\ \vdots \\ x_{(z)} \end{bmatrix}_k + v_B \begin{bmatrix} u_{(1)} \\ \vdots \\ u_{(z)} \end{bmatrix}_k + v_E \begin{bmatrix} d_{(1)} \\ \vdots \\ d_{(z)} \end{bmatrix}_k \tag{6.10a}$$

$$v_k = v_A x_k + v_B u_k + v_E d_k \tag{6.10b}$$

where v_A, v_B and v_E are the matrices A, B and E, but with zero matrices in their main diagonal. Notice that v_k is of order r for some $r \leq n$. This expression is thus an *equality constraint* (along with the system dynamics) that is added in the optimization algorithm in the following way: first, define the matrices for the *diagonal system*:

$$A_d = A - v_A \quad B_d = B - v_B \quad E_d = E - v_E \tag{6.11}$$

and then add the interaction vector to re-obtain system (6.1), as follows:

$$x_{k+1} = A_d x_k + B_d u_k + E_d d_k + v_k \tag{6.12}$$

On this basis, and in the frame of MPC, the cost function for this new representation should have additional terms for the interactions, and related weighting matrices $R_v \geq 0$, and S_v such that $Q \geq S_v R_v^{-1} S_v^T$, as follows:

$$J_{gv} = \tfrac{1}{2}\left[\tilde{x}_N^T P \tilde{x}_N + \sum_{k=0}^{N-1}\left(\tilde{x}_k^T Q \tilde{x}_k + \tilde{u}_k^T R_u \tilde{u}_k + 2\tilde{u}_k^T S_u \tilde{x}_k\right)\right] + \tfrac{1}{2}\sum_{k=0}^{N-1}\left(\tilde{v}_k^T R_v \tilde{v}_k + 2\tilde{v}_k^T S_v \tilde{x}_k\right) \tag{6.13}$$

At this stage, the idea is to solve an optimization problem for the cost function (6.13), but considering the system dynamics (6.12). More precisely, because the interaction variable v_k is dependent on u_k, the idea is to rewrite the optimization problem for the new decision variable $\boldsymbol{u_{ext}} = [\boldsymbol{u}^T\ \boldsymbol{v}^T]^T$, where $\boldsymbol{v} = [v_0 \cdots v_{N-1}]^T$. This last one is the $N-step$ predicted interaction vector. The problem is therefore made of a cost function J_{gv} with decision variable $\boldsymbol{u_{ext}}$, equality constraints given by dynamics(6.12) and interactions (6.10), as well as inequality constraints also in terms of $\boldsymbol{u_{ext}}$ built in the same way as presented in (6.6). The new problem, in general terms has the following structure:

$$\begin{array}{ll} \min\limits_{\boldsymbol{u_{ext}}} & J_{gv}(\boldsymbol{u_{ext}}) \\ \text{subject to} & L_{ext}\boldsymbol{u_{ext}} \leq W_{ext} \\ & x_{k+1} = A_d x_k + B_d u_k + E_d d_k + v_k,\ 0 \leq k \leq N-1 \\ & v_k = v_A x_k + v_B u_k + v_E d_k,\ 0 \leq k \leq N-1 \end{array} \tag{6.14}$$

In order to re-write the cost function $J_{gv}(\boldsymbol{u_{ext}})$ in QP form, first consider the following predicted vectors, including the interactions:

$$\begin{array}{ll} \boldsymbol{x} = \begin{bmatrix} x_1 & \cdots & x_N \end{bmatrix}^T & \boldsymbol{x_s} = \begin{bmatrix} x_s & \cdots & x_s \end{bmatrix}^T \\ \boldsymbol{u} = \begin{bmatrix} u_0 & \cdots & u_{N-1} \end{bmatrix}^T & \boldsymbol{u_s} = \begin{bmatrix} u_{s0} & \cdots & u_{sN-1} \end{bmatrix}^T \\ \boldsymbol{v} = \begin{bmatrix} v_0 & \cdots & v_{N-1} \end{bmatrix}^T & \boldsymbol{v_s} = \begin{bmatrix} v_{s0} & \cdots & v_{sN-1} \end{bmatrix}^T \\ \boldsymbol{d} = \begin{bmatrix} d_0 & \cdots & d_{N-1} \end{bmatrix}^T & \boldsymbol{d_s} = \begin{bmatrix} d_{s0} & \cdots & d_{sN-1} \end{bmatrix}^T \end{array} \tag{6.15}$$

and then the $N-$ step (predicted) states and state error vectors with $\boldsymbol{u_{ext}} = [\boldsymbol{u}^T\ \boldsymbol{v}^T]^T$ and $\boldsymbol{u_{ext-s}} = [\boldsymbol{u_s}^T\ \boldsymbol{v_s}^T]^T$ are:

$$\begin{array}{c} \boldsymbol{x} = \Omega_d\ x_0 + \Psi_d\ \boldsymbol{u_{ext}} + \Theta_d\ \boldsymbol{d} \\ \tilde{\boldsymbol{x}} = \Omega_d\ (x_0 - x_s) + \Psi_d\ (\boldsymbol{u_{ext}} - \boldsymbol{u_{ext-s}}) + \Theta_d\ (\boldsymbol{d} - \boldsymbol{d_s}) \end{array} \tag{6.16}$$

where matrices Ω_d, Γ_d, Θ_d and Ψ_d are obtained after using (6.12) and vectors of (4.4). For further details, please consult Appendix A:

$$\begin{array}{l} \Omega_d = \begin{bmatrix} A_d \\ A_d^2 \\ \vdots \\ A_d^N \end{bmatrix} \quad \Gamma_d = \begin{bmatrix} B_d & 0 & \cdots & 0 \\ A_d B_d & B_d & \cdots & 0 \\ \vdots & \vdots & \ddots & \vdots \\ A_d^{N-1} B_d & A_d^{N-2} B_d & \cdots & B_d \end{bmatrix} \\ \Theta_d = \begin{bmatrix} E_d & 0 & \cdots & 0 \\ A_d E_d & E_d & \cdots & 0 \\ \vdots & \vdots & \ddots & \vdots \\ A_d^{N-1} E_d & A_d^{N-2} E_d & \cdots & E_d \end{bmatrix} \quad \Lambda_d = \begin{bmatrix} I & 0 & \cdots & 0 \\ A_d & I & \cdots & 0 \\ \vdots & \vdots & \ddots & \vdots \\ A_d^{N-1} & A_d^{N-2} & \cdots & I \end{bmatrix} \quad \Psi_d = [\Gamma_d \ \ \Lambda_d] \end{array} \tag{6.17}$$

With the same philosophy, the $N-step$ predicted interaction vector can be expressed in terms of the dynamics and interactions equations, using again $\boldsymbol{u_{ext}} = [\boldsymbol{u}^T \quad \boldsymbol{v}^T]^T$, obtaining:

$$\begin{array}{rl} \overline{\Lambda}\boldsymbol{v} = & \overline{\Gamma}\boldsymbol{u} + \overline{\Omega}\ x_0 + \overline{\Theta}\ \boldsymbol{d} \\ 0 = & \overline{\Psi}\boldsymbol{u_{ext}} + \overline{\Omega}\ x_0 + \overline{\Theta}\ \boldsymbol{d} \end{array} \tag{6.18}$$

where matrices $\overline{\Omega}$, $\overline{\Gamma}$, $\overline{\Theta}$ and $\overline{\Psi}$ are defined by using (6.10) and (6.12) (with more details in Appendix 1):

$$\begin{array}{l} \overline{\Omega} = \begin{bmatrix} v_A \\ v_A A_d \\ \vdots \\ v_A A_d^{N-1} \end{bmatrix} \overline{\Gamma} = \begin{bmatrix} v_B & 0 & \cdots & 0 \\ v_A B_d & v_B & \cdots & 0 \\ \vdots & \vdots & \ddots & \vdots \\ v_A A_d^{(N-2)} B_d & A_d^{(N-3)} B_d & \cdots & v_B \end{bmatrix} \\ \overline{\Theta} = \begin{bmatrix} v_E & 0 & \cdots & 0 \\ v_A E_d & v_E & \cdots & 0 \\ \vdots & \vdots & \ddots & \vdots \\ v_A A_d^{(N-2)} E_d & v_A A_d^{(N-3)} E_d & \cdots & v_E \end{bmatrix} \overline{\Lambda} = \begin{bmatrix} I & 0 & \cdots & 0 \\ -v_A & I & \cdots & 0 \\ \vdots & \vdots & \ddots & \vdots \\ -v_A A_d^{(N-2)} & -v_A A_d^{(N-3)} & \cdots & I \end{bmatrix} \overline{\Psi} = [\overline{\Gamma} \quad -\overline{\Lambda}] \end{array} \tag{6.19}$$

With equation (6.16), one can absorb the equality constraints derived by the dynamical equation, by replacing $\tilde{\boldsymbol{x}}$ in the cost function. With respect to the interactions equality, one can use an Augmented Lagragian expression [39], by using the Lagrange multiplier $\boldsymbol{p} = [p_0 \cdots p_{N-1}]^T$ for relaxing the problem in terms of quantity of constraints [55].
But before, define the following cost function matrices, where R_v is to be chosen large enough to guarantee convexity of the problem [24, 39] and S_v is typically zero:

$$\begin{array}{c} \boldsymbol{Q} = diag\{Q \ \cdots Q \ P\} \\ \boldsymbol{R_u} = diag\{R_u \cdots R_u\}, \boldsymbol{R_v} = diag\{R_v \cdots R_v\}, \boldsymbol{R_{ext}} = diag\{\boldsymbol{R_u} \ \boldsymbol{R_v}\}, \\ \boldsymbol{S_u} = diag\{S_u \cdots S_u\}, \boldsymbol{S_v} = diag\{S_v \cdots S_v\}, \boldsymbol{S_{ext}} = diag\{\boldsymbol{S_u} \ \boldsymbol{S_v}\} \end{array} \tag{6.20}$$

Matrix P is obtained by solving the discrete time Ricatti Algebraic Equation for the system. With these new variables, the cost function J_{gv} can be transformed into a quadratic form one now called J_{ext} with the variable $\boldsymbol{u_{ext}}$ as follows, and $\bar{V}_{ext}$ gathering all terms independent of variables $\boldsymbol{u_{ext}}$ and $\boldsymbol{p}$:

$$\begin{array}{c} J_{ext}(\boldsymbol{u_{ext}}, \boldsymbol{p}) = \bar{V}_{ext} + \frac{1}{2}\boldsymbol{u_{ext}^T H_c u_{ext}} + \boldsymbol{u_{ext}^T}[\boldsymbol{K_{1c}}(x_0 - x_s) + \boldsymbol{K_{2c}}(\boldsymbol{d} - \boldsymbol{d_s}) + \boldsymbol{K_{3c}p} - \boldsymbol{H_c u_{ext_s}}] + \\ \boldsymbol{p^T}(\overline{\Omega}x_0 + \overline{\Theta}\boldsymbol{d}) \end{array} \tag{6.21}$$

where matrices $\boldsymbol{H_c}, \boldsymbol{K_{1c}}, \boldsymbol{K_{2c}}$ and $\boldsymbol{K_{3c}}$ are defined as:

$$\boldsymbol{H_c} = \Psi_d^T \boldsymbol{Q} \Psi_d + \boldsymbol{R_{ext}} + 2\boldsymbol{S_{ext}}\Psi_d; \ \boldsymbol{K_{3c}} = \overline{\Psi}^T; \ \boldsymbol{K_{1c}} = \Psi_d^T \boldsymbol{Q} \Omega_d + \boldsymbol{S_{ext}}\Omega_d; \ \boldsymbol{K_{2c}} = \Psi_d^T \boldsymbol{Q} \Theta_d + \boldsymbol{S_{ext}}\Theta_d \tag{6.22}$$

As consequence, the *augmented centralized optimization problem* is written as:

$$\begin{array}{c} \max\limits_{\boldsymbol{p}} \min\limits_{\boldsymbol{u_{ext}}} J_{ext}(\boldsymbol{u_{ext}}, \boldsymbol{p}) \\ \text{subject to } L_{ext}\boldsymbol{u_{ext}} \leq W_{ext} \end{array} \tag{6.23}$$

The constraints polyhedron matrices L_{ext}, W_{ext} have a structure equivalent to that of (4.24), using again the the limit value vectors for states, inputs and disturbances:

$$\begin{array}{ll} \boldsymbol{x_{max}} = \begin{bmatrix} x_{max_1} & \cdots & x_{max_{(N)}} \end{bmatrix}^T & \boldsymbol{x_{min}} = \begin{bmatrix} x_{min_1} & \cdots & x_{min_{(N)}} \end{bmatrix}^T \\ \boldsymbol{u_{max}} = \begin{bmatrix} u_{max_0} & \cdots & u_{max_{(N-1)}} \end{bmatrix}^T & \boldsymbol{u_{min}} = \begin{bmatrix} u_{min_0} & \cdots & u_{min_{(N-1)}} \end{bmatrix}^T \\ \boldsymbol{v_{max}} = \begin{bmatrix} v_{max_0} & \cdots & v_{max_{(N-1)}} \end{bmatrix}^T & \boldsymbol{v_{min}} = \begin{bmatrix} v_{min_0} & \cdots & v_{min_{(N-1)}} \end{bmatrix}^T \\ \boldsymbol{d_{max}} = \begin{bmatrix} d_{max_0} & \cdots & d_{max_{(N-1)}} \end{bmatrix}^T & \boldsymbol{d_{min}} = \begin{bmatrix} d_{min_0} & \cdots & d_{min_{(N-1)}} \end{bmatrix}^T \\ \boldsymbol{\delta u_{max}} = \begin{bmatrix} \delta u_{max_0} & \cdots & \delta u_{max_{(N-1)}} \end{bmatrix}^T & \boldsymbol{\delta u_{min}} = \begin{bmatrix} \delta u_{min_0} & \cdots & \delta u_{min_{(N-1)}} \end{bmatrix}^T \end{array} \tag{6.24}$$

For the interactions, the definition of terms v_{maxk} and v_{mink} are obtained as follows:

$$\begin{aligned} v_{maxk} &= v_A x_{maxk} + v_B u_{maxk} + v_E d_{maxk} \\ v_{mink} &= v_A x_{mink} + v_B u_{mink} + v_E d_{mink} \end{aligned} \tag{6.25}$$

In (6.26), we present the structure of the constraints polyhedron, again function of current states x_0, past input value u_{e-1} and expected disturbance vector $\boldsymbol{d}$, and (6.27) shows each component of the matrices, better detailed in Appendix 1.

$$\begin{aligned} L_{ext}\boldsymbol{u_{ext}} &\leq \bar{W} + W_x x_0 + W_u u_{e-1} \\ \begin{bmatrix} \phi_{ext} \\ -\phi_{ext} \end{bmatrix} \boldsymbol{u_{ext}} &\leq \begin{bmatrix} \bar{\Delta}_{ext} \\ -\underline{\Delta}_{ext} \end{bmatrix} + \begin{bmatrix} -\xi_{ext} \\ \xi_{ext} \end{bmatrix} x_0 + \begin{bmatrix} -\xi_{u-ext} \\ \xi_{u-ext} \end{bmatrix} u_{e-1} \end{aligned} \tag{6.26}$$

$$\phi_{ext} = \begin{bmatrix} \Psi_d \\ I_{N\times m} \quad 0_{N\times r} \\ 0_{N\times m} \quad I_{N\times r} \\ E_{\delta,ext} \quad 0_{N\times r} \end{bmatrix} \quad \bar{\Delta}_{ext} = \begin{bmatrix} \boldsymbol{x_{max} - \Theta d_{max}} \\ \boldsymbol{u_{max}} \\ \boldsymbol{v_{max}} \\ \boldsymbol{\delta u_{max}} \end{bmatrix} \quad \underline{\Delta}_{ext} = \begin{bmatrix} \boldsymbol{x_{min} - \Theta d_{min}} \\ \boldsymbol{u_{min}} \\ \boldsymbol{v_{min}} \\ \boldsymbol{\delta u_{min}} \end{bmatrix}$$

$$\xi_{ext} = \begin{bmatrix} \Omega_d \\ 0_{N\times m} \\ 0_{N\times r} \\ 0_{N\times m} \end{bmatrix} \quad \xi_{u-ext} = \begin{bmatrix} 0_{N(m+r)\times(m+r)} \\ 0_{Nm\times(m+r)} \\ 0_{Nr\times(m+r)} \\ E_{-1,ext} \end{bmatrix} \quad E_{\delta,ext} = \begin{bmatrix} I_m & 0_m & \cdots & 0_m \\ -I_m & I_m & \cdots & 0_m \\ \vdots & \vdots & \ddots & \vdots \\ 0_m & \cdots & -I_m & I_m \end{bmatrix}$$

$$E_{-1,ext} = \begin{bmatrix} I_m \\ 0_{(N-1)\times m} \end{bmatrix} \tag{6.27}$$

In conclusion, it has been obtained an expression for the centralized constrained optimization problem in terms of the vector $\boldsymbol{u_{ext}}$ that includes inputs and interaction signals sequences, as well as a Lagrange multiplier vector $\mathbf{p}$ for adding the interactions to the cost function. In this way, one can find a solution for the problem, that optimizes the interactions between the subsystems of an application in a centralized manner. However, the decomposition of the cost function into as many parts as the number of considered subsystems will above all be advantageous for a distributed control strategy.

6.2 Optimization problem decomposition and coordination

As mentioned, the idea is to decompose the optimization problem, by dividing the cost function among all the z subsystems that compose the global system. First, the decomposition strategy is presented along with the subsystem explicit solutions, and secondly, the *Price Driven*-like coordination strategy is shown [23, 24, 99].

6.2.1 Problem decomposition and explicit local solutions

The extended cost function (6.13) in its original form, and (6.21) in quadratic form, can now be divided into the z subsystems that are considered. Remember that each $i-th$ subsystem has its own states, inputs, disturbances and interactions $x_{(i)k}, u_{(i)k}, d_{(i)k}$ and $v_{(i)k}$, respectively, as well as its own dynamical model (6.8). The split extended cost function is shown in (6.28), where local extended input-interaction vector $\bar{u}_{ext(i)} = [u_{(i)}^T \;\; v_{(i)}^T]^T$ and matrices $R_{ext(i)} = diag\{R_{u(i)} \; R_{v(i)}\}$,

$S_{ext(i)} = [S_{u(i)}\ S_{v(i)}]^T$ are used:

$$\begin{aligned} J_{ext} &= \sum_{i=1}^{h} J_{ext(i)} = \sum_{i=1}^{h} J_{gv(i)} + \sum_{i=1}^{h} J_{eq(i)}, \text{where:} \\ J_{gv(i)} &= \tfrac{1}{2}\left(\tilde{x}_{(i)N}^T P_{(i)} \tilde{x}_{(i)N} + \sum_{k=0}^{N-1} \tilde{x}_{(i)k}^T Q_{(i)} \tilde{x}_{(i)k}\right) + \\ &\tfrac{1}{2}\left(\sum_{k=0}^{N-1} \tilde{\bar{u}}_{ext(i)k}^T R_{ext(i)} \tilde{\bar{u}}_{ext(i)k} + 2\sum_{k=0}^{N-1} \tilde{\bar{u}}_{ext(i)k}^T S_{ext(i)} \tilde{x}_{(i)k}\right) \\ J_{eq(i)} &= \boldsymbol{p}^T \sum_{k=0}^{N-1} \left(M_{(i)} \bar{u}_{ext(i)} + \delta_{(i)k}\right) \end{aligned} \tag{6.28}$$

In (6.28) a matrix $M_{(i)}$ appears that represents the *effect of inputs at subsystem i over the full system interactions vector*. Therefore, computing optimal values for $\boldsymbol{\bar{u}_{ext(i)}}$ will optimize the interactions among the subsystems. Matrix $M_{(i)}$ is obtained by taking the left size of (6.10) and working to form the vectors $\bar{u}_{ext(i)k}$. For instance, for a system divided into two subsystems, matrices M_i have the following structure:

$$\begin{aligned} \begin{bmatrix} v_{(1)} \\ v_{(2)} \end{bmatrix}_k &= \begin{bmatrix} 0 & A_{12} \\ A_{21} & 0 \end{bmatrix} \begin{bmatrix} x_{(1)} \\ x_{(2)} \end{bmatrix}_k + \begin{bmatrix} 0 & E_{12} \\ E_{21} & 0 \end{bmatrix} \begin{bmatrix} d_{(1)} \\ d_{(2)} \end{bmatrix}_k + \begin{bmatrix} 0 & B_{12} \\ B_{21} & 0 \end{bmatrix} \begin{bmatrix} u_{(1)} \\ u_{(2)} \end{bmatrix}_k \\ 0 &= \sum_{i=1}^{z} \delta_{(i)k} + \begin{bmatrix} 0 & -I \\ B_{21} & 0 \end{bmatrix} \begin{bmatrix} u_{(1)} \\ v_{(1)} \end{bmatrix}_k + \begin{bmatrix} B_{12} & 0 \\ 0 & -I \end{bmatrix} \begin{bmatrix} u_{(2)} \\ v_{(2)} \end{bmatrix}_k \\ 0 &= \sum_{i=1}^{z} \delta_{(i)k} + M_1 \bar{u}_{ext(1)k} + M_2 \bar{u}_{ext(2)k} \end{aligned} \tag{6.29}$$

where $\delta_{(i)}$ are submatrices that gather the effects of local states and disturbances on the interactions that, in our case, will be considered independent of $\boldsymbol{\bar{u}_{ext(i)}}$.
As previously made, one can then obtain the $N-step$ forward prediction(6.30) for each subsystem, with dynamical equation in terms of $\bar{u}_{ext(i)k}$, and using matrix $\overline{B}_{(i)} = [B_{ii}\ \ I_{v(i)}]$:

$$\begin{aligned} x_{(i)k+1} &= A_{ii} x_{(i)k} + \bar{B}_i \bar{u}_{ext(i)k} + E_{ii} d_{(i)k} \\ \boldsymbol{x_{(i)}} &= \Omega_{(i)} x_{0(i)} + \Gamma_{(i)} \boldsymbol{\bar{u}_{ext(i)}} + \Theta_{(i)}\ \boldsymbol{\bar{d}_{(i)}} \end{aligned} \tag{6.30}$$

where matrices $\Omega_{(i)}$, $\Gamma_{(i)}$ and $\Theta_{(i)}$ are defined as follows, with $\boldsymbol{\bar{d}_{(i)}} = [d_{(i)0} ... d_{(i)N-1}]^T$ defined as the local predicted disturbance vector (see Appendix A for further details):

$$\Omega_{(i)} = \begin{bmatrix} A_{ii} \\ A_{ii}^2 \\ \vdots \\ A_{ii}^N \end{bmatrix} \quad \Gamma_{(i)} = \begin{bmatrix} \bar{B}_i & 0 & \cdots & 0 \\ A_{ii}\bar{B}_i & \bar{B}_i & \cdots & 0 \\ \vdots & \vdots & \ddots & \vdots \\ A_{ii}^{(N-1)}\bar{B}_i & A_{ii}^{(N-2)}\bar{B}_i & \cdots & \bar{B}_i \end{bmatrix} \quad \Theta_i = \begin{bmatrix} E_{ii} & 0 & \cdots & 0 \\ A_{ii}E_{(i)} & E_{ii} & \cdots & 0 \\ \vdots & \vdots & \ddots & \vdots \\ A_{ii}^{(N-1)}E_{ii} & A_{ii}^{(N-2)}E_{ii} & \cdots & E_{ii} \end{bmatrix} \tag{6.31}$$

With these arrangements, the cost function for each subsystem, originally shown in (6.28), can be rewritten in terms of $\boldsymbol{\bar{u}_{ext(i)}}$ and $\mathbf{p}$ as follows, with the respective matrices defined in (6.33):

$$J_{ext(i)} = \tfrac{1}{2}\boldsymbol{\bar{u}_{ext(i)}}^T \boldsymbol{H_{(i)}} \boldsymbol{\bar{u}_{ext(i)}} + \boldsymbol{\bar{u}_{ext(i)}^T}[\boldsymbol{K_{1(i)}}(x_{0(i)} - x_{(i)s}) + \boldsymbol{K_{2(i)}}(\boldsymbol{\bar{d}_{(i)}} - \boldsymbol{\bar{d}_{(i)s}}) + \boldsymbol{K_{3(i)}p} - \boldsymbol{H_{(i)}}\boldsymbol{\bar{u}_{ext(i)s}}] + \bar{V}_{ext(i)} \tag{6.32}$$

$$\begin{gathered} \boldsymbol{Q_{(i)}} = diag\{Q_{(i)} \cdots P_{(i)}\}, \boldsymbol{R_{u(i)}} = diag\{R_{u(i)} \cdots R_{u(i)}\}, \boldsymbol{R_{v(i)}} = diag\{R_{v(i)} \cdots R_{v(i)}\} \\ \boldsymbol{R_{ext(i)}} = diag\{\boldsymbol{R_{u(i)}}\ \boldsymbol{R_{v(i)}}\} \boldsymbol{S_{u(i)}} = diag\{S_{u(i)} \cdots S_{u(i)}\}, \boldsymbol{S_{v(i)}} = diag\{S_{v(i)} \cdots S_{v(i)}\} \\ \boldsymbol{S_{ext(i)}} = diag\{\boldsymbol{S_{u(i)}}\ \boldsymbol{S_{v(i)}}\} \end{gathered} \tag{6.33}$$

$$\begin{gathered} \boldsymbol{H_{(i)}} = \Gamma_{(i)}^T \boldsymbol{Q_{(i)}} \Gamma_{(i)} + \boldsymbol{R_{ext(i)}} + 2\boldsymbol{S_{(i)}}\Gamma_{(i)},\ \boldsymbol{K_{1(i)}} = \Gamma_{(i)}^T \boldsymbol{Q_{(i)}} \Omega_{(i)} + \boldsymbol{S_{ext(i)}} \Omega_{(i)} \\ \boldsymbol{K_{2(i)}} = \Gamma_{(i)}^T \boldsymbol{Q_{(i)}} \Theta_{(i)} + \boldsymbol{S_{ext(i)}} \Theta_{(i)},\ \boldsymbol{K_{3(i)}} = [\text{diag}\{M_{(i)} \cdots M_{(i)}\}]^T \end{gathered}$$

Finally, from each subsystem cost function (6.32), the *explicit optimal solution* with respect to $\bar{\boldsymbol{u}}_{\boldsymbol{ext(i)}}$ is:

$$\bar{\boldsymbol{u}}^{\boldsymbol{opt}}_{\boldsymbol{ext(i)}} = -\boldsymbol{H_{(i)}}^{-1}\left[\boldsymbol{K_{1(i)}}\tilde{x}_{0(i)} + \boldsymbol{K_{2(i)}}\tilde{\bar{\boldsymbol{d}}}_{(i)} + \boldsymbol{K_{3(i)}p} - \boldsymbol{H_{(i)}}\bar{u}_{ext(i)_s}\right] \tag{6.34}$$

This expression shows that the explicit local unconstrained control sequence for each subsystem i, not only depends on its own states and disturbances, but also on the information of the Lagrange Multiplier vector $\boldsymbol{p}$, sent by the coordinator. Evidently, in case of loss of coordination information for any subsystem, it could switch to a local control and some constraints could be added, for which the problem can be solved as exposed in section 4.1.3.

6.2.2 Global coordination based on local explicit solutions

Knowing that each subsystem $i = 1 \cdots z$ computes a control sequence vector influenced by vector $\boldsymbol{p}$, an *unconstrained global explicit solution* is obtained for the global extended control vector:

$$\bar{\boldsymbol{u}}^{\boldsymbol{opt}}_{\boldsymbol{ext}} = [(\bar{\boldsymbol{u}}^{\boldsymbol{opt}}_{\boldsymbol{ext(1)}})^T \cdots (\bar{\boldsymbol{u}}^{\boldsymbol{opt}}_{\boldsymbol{ext(z)}})^T]^T \tag{6.35}$$

by merging all the local explicit local solutions as follows:

$$\bar{\boldsymbol{u}}^{\boldsymbol{opt}}_{\boldsymbol{ext}} = -\widetilde{\boldsymbol{K}}_{\boldsymbol{1}}\tilde{x}_0 - \widetilde{\boldsymbol{K}}_{\boldsymbol{2}}\tilde{\bar{\boldsymbol{d}}} - \widetilde{\boldsymbol{K}}_{\boldsymbol{3}}\boldsymbol{p} + \bar{\boldsymbol{u}}_{ext-s} \tag{6.36}$$

Where the matrices and vectors are defined as follows:

$$\begin{gathered}\widetilde{\boldsymbol{K}}_{\boldsymbol{1}} = diag\{\boldsymbol{H}^{-\boldsymbol{1}}_{\boldsymbol{(1)}}\boldsymbol{K_{1(1)}} \cdots \boldsymbol{H}^{-\boldsymbol{1}}_{\boldsymbol{(z)}}\boldsymbol{K_{1(z)}}\},\ \widetilde{\boldsymbol{K}}_{\boldsymbol{2}} = diag\{\boldsymbol{H}^{-\boldsymbol{1}}_{\boldsymbol{(1)}}\boldsymbol{K_{2(1)}} \cdots \boldsymbol{H}^{-\boldsymbol{1}}_{\boldsymbol{(z)}}\boldsymbol{K_{2(z)}}\} \\ \widetilde{\boldsymbol{K}}_{\boldsymbol{3}} = [\boldsymbol{H}^{-\boldsymbol{1}}_{\boldsymbol{(1)}}\boldsymbol{K_{3(1)}} \cdots \boldsymbol{H}^{-\boldsymbol{1}}_{\boldsymbol{(z)}}\boldsymbol{K_{3(z)}}]^T\end{gathered} \tag{6.37}$$

$$\tilde{x}_0 = \begin{bmatrix} x_{0(1)} - x_{s(1)} \\ \vdots \\ x_{0(z)} - x_{s(z)} \end{bmatrix} \quad \tilde{\bar{\boldsymbol{d}}} = \begin{bmatrix} \bar{\boldsymbol{d}}_{\boldsymbol{(1)}} - \bar{\boldsymbol{d}}_{\boldsymbol{(1)s}} \\ \vdots \\ \bar{\boldsymbol{d}}_{\boldsymbol{(z)}} - \bar{\boldsymbol{d}}_{\boldsymbol{(z)s}} \end{bmatrix} \quad \bar{\boldsymbol{u}}_{\boldsymbol{ext-s}} = \begin{bmatrix} \bar{\boldsymbol{u}}_{\boldsymbol{(1)ext-s}} \\ \vdots \\ \bar{\boldsymbol{u}}_{\boldsymbol{(z)ext-s}} \end{bmatrix} \tag{6.38}$$

Next, a transformation should be applied to the vectors $\bar{\boldsymbol{u}}_{\boldsymbol{ext}}$ and $\bar{\boldsymbol{d}}$, for passing them into the global extended control vector $\boldsymbol{u_{ext}}$ and the global extended disturbance vector $\boldsymbol{d}$, respectively, both required for solving the problem (6.23). Let consider the transformation $\boldsymbol{d} = Y_d\bar{\boldsymbol{d}}$ and $\boldsymbol{u_{ext}} = Y_u\bar{\boldsymbol{u}}_{\boldsymbol{ext}}$ with Y_d and Y_u non singular matrices, built by inspection, so as to match the vectors of the optimization problem with the sum of explicit solutions. This allows to express the *global optimal unconstrained solution* as:

$$\begin{gathered}\boldsymbol{u}^{\boldsymbol{opt}}_{\boldsymbol{ext}} = -\boldsymbol{\varphi_1}(x_0 - x_s) - \boldsymbol{\varphi_2}(\boldsymbol{d} - \boldsymbol{d_s}) - \boldsymbol{\varphi_3 p} + \boldsymbol{u_{ext-s}} \\ \boldsymbol{\varphi_1} = Y_u\widetilde{\boldsymbol{K}}_{\boldsymbol{1}}, \boldsymbol{\varphi_2} = Y_u\widetilde{\boldsymbol{K}}_{\boldsymbol{2}}Y_d^{-1}, \boldsymbol{\varphi_3} = Y_u\widetilde{\boldsymbol{K}}_{\boldsymbol{3}}\end{gathered} \tag{6.39}$$

This expression allows substituting (6.39) in the global optimization problem (6.23), as part of its solution (see Lagrange Dual Theory in [55] for more details). It can be seen that $\boldsymbol{\varphi_1}, \boldsymbol{\varphi_2}, \boldsymbol{\varphi_3}$ are time invariant matrices and vector $\boldsymbol{p}$ can be used to adjust local control signal values according to the coordinator policy, that will be directed to optimize the performance of the global system while respecting the constraints.
Therefore, replacing (6.39) in the cost function (6.21) for the problem (6.23), including the constraints, one can obtain an expression for the cost function (6.40) with only the decision variable $\boldsymbol{p}$:

$$\begin{gathered}J_{ext} = \bar{V}_p + \tfrac{1}{2}\boldsymbol{p}^T\boldsymbol{H_p p} + \boldsymbol{p}^T[\boldsymbol{K_{1p}}\tilde{x}_0 + \boldsymbol{K_{2p}}\tilde{\boldsymbol{d}} + \boldsymbol{K_{3p}u_{ext_s}}] + \boldsymbol{p}^T(\bar{\Omega}x_0 + \bar{\Theta}\boldsymbol{d}) \\ \text{where: } \boldsymbol{K_{3p}} = \boldsymbol{K^T_{3c}},\ \boldsymbol{H_p} = \boldsymbol{\varphi^T_3 H_c \varphi_3} - 2\boldsymbol{\varphi^T_3 K_{3p}}, \\ \boldsymbol{K_{1p}} = \boldsymbol{\varphi^T_3(H_c\varphi_1 + K_{1c})} - \boldsymbol{K_{3p}\varphi_1},\ \boldsymbol{K_{2p}} = \boldsymbol{\varphi^T_3(H_c\varphi_2 + K_{2c})} - \boldsymbol{K_{3p}\varphi_2}\end{gathered} \tag{6.40}$$

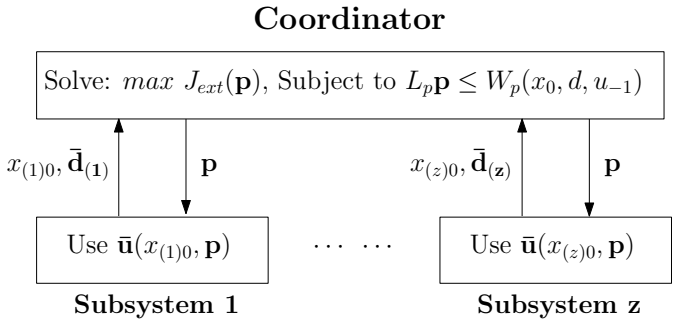

Figure 6.1: Information Flow for the Coordination Algorithm

In the same way, one can write the constraints polyhedral in terms of $\mathbf{p}$, as in (6.41) below, where it is clear that it is also affected by the current state x_0 and projected disturbance $\boldsymbol{d}$ vectors.

$$\begin{aligned} L_p\boldsymbol{p} \leq\ & \overline{W}_p + W_{xp}x_0 + W_{dp}\boldsymbol{d} + W_{up}u_{ext-1} \\ \begin{bmatrix} \phi_p \\ -\phi_p \end{bmatrix}\boldsymbol{p} \leq\ & \begin{bmatrix} \bar{\Delta}_p - \delta_{sp} \\ -\underline{\Delta}_p + \delta_{sp} \end{bmatrix} + \begin{bmatrix} -\xi_{xp} \\ \xi_{xp} \end{bmatrix} x_0 + \begin{bmatrix} -\xi_{dp} \\ \xi_{dp} \end{bmatrix}\boldsymbol{d} + \begin{bmatrix} -\xi_{u-ext} \\ \xi_{u-ext} \end{bmatrix} u_{ext-1} \end{aligned} \tag{6.41}$$

The matrices included in the constraints definition for $\boldsymbol{p}$, obtained using the variables defined in (6.26)-(6.27) are (see again Appendix A for details) :

$$\begin{array}{ccc} \phi_p = -\phi_{ext}\varphi_3 & \bar{\Delta}_p = \bar{\Delta}_{ext} & \underline{\Delta}_p = \underline{\Delta}_{ext} \\ \delta_{sp} = \phi_{ext}(\boldsymbol{\varphi_1}x_s + \boldsymbol{\varphi_2 d_s} + \boldsymbol{u_{exts}}) & \xi_{xp} = \xi_{ext} - \phi_{ext}\boldsymbol{\varphi_1} & \xi_{dp} = -\phi_{ext}\boldsymbol{\varphi_2} \end{array} \tag{6.42}$$

Thus, the admissible solutions for $\boldsymbol{p}$ are in the domain $\mathcal{P}$, defined as follows:

$$\mathcal{P} = \{\mathbf{p} \in \Re^{N.r} \ :\ L_p\mathbf{p} \leq \overline{W}_p + W_{xp}x_0 + W_{dp}\boldsymbol{d} + W_{up}u_{ext-1},\ x_0 \in \Re^n, \mathbf{d} \in \Re^{N.q}, u_{ext-1} \in \Re^{m+r}\} \tag{6.43}$$

It can be noticed from (6.41) that term $\overline{W}_p$ is made of two parts: one fixed part that depends on the extreme values for the signals, and a second part from term δ_{sp} that is related to the desired set point values for the signals, as seen in (6.42). In fact, the reference values can be turned into 0 for stability analysis purposes, or can be updated in the application. However, it is important again, to consider that the constraints polyhedron should be feasible and convex for using the geometric solution method for constrained optimization, presented in the Chapter 4.1.
After all this mathematical treatment, the problem that will be solved by the coordinator is done under the consideration of merging all the local explicit unconstrained MPC problem solutions. Then, the coordinator computes the coordination vector $\mathbf{p}$ that ensures the global constraints and performance . Therefore, the signal $\mathbf{p}$ received at each subsystem will tune them accordingly, without compromising the local stability *a priori* ensured by the structure of the local dynamical matrix A_{ii}. Therefore, the new *global optimization problem* to be solved by the coordinator is:

$$\begin{array}{ll} \max\limits_{\boldsymbol{p}} & J_{ext}(\boldsymbol{p}) \\ \text{subject to} & L_p\boldsymbol{p} \leq W_p \end{array} \tag{6.44}$$

Solving this problem guarantees coordination and global constraint enforcement for all the subsystems. Thanks to the quadratic form in $\boldsymbol{p}$ of the cost function (6.40), the problem is convex and any method to solve it can be applied, including the explicit one analyzed in Chapter 3.
The proposed coordination algorithm can be graphically summarized as shown in Fig. 6.1, as well as summarized as in **Algorithm 2** shown next.

Algorithm 2 Proposed Coordination Algorithm for local receding horizon-based controllers

Require: Off-line computation of matrices for the local QP problems: $\Gamma_{(i)}, \Omega_{(i)}, \Theta_{(i)}, \boldsymbol{H}_{(i)}, \boldsymbol{K_1}_{(i)}, \boldsymbol{K_2}_{(i)}$, according to (6.33).

Require: Off-line computation of matrices for the original coordination QP problem (6.23): $\Gamma_d, \Omega_d, \Theta_d, \Psi_d, \boldsymbol{H}_c, \boldsymbol{K_{1c}}, \boldsymbol{K_{2c}}, \overline{\Gamma}, \overline{\Omega}, \overline{\Theta}, \overline{\Psi}$ as consigned in (6.31),(6.19), (6.22).

Require: Off-line computation of matrices for the original coordination QP problem constraints polyhedral: $L_{ext}, \overline{W}, W_x, W_u$ as indicated in (6.26)-(6.27). In case of not using control derivative penalizations, set $W_u = 0$

Require: Off-line computation of matrices for the modified coordination QP problem (6.44): $\boldsymbol{\varphi_1}, \boldsymbol{\varphi_2}, \boldsymbol{\varphi_3}, \boldsymbol{K_{1p}}, \boldsymbol{K_{2p}}, \boldsymbol{K_{3p}}$ according to (6.39), (6.40).

Require: Off-line computation of the constraints polyhedron for the modified QP problem (6.44): $L_p, \overline{W}_p, W_{xp}, W_{dp}, W_{up}$, according to (7.8). In case of not using control derivative penalizations, set $W_{up} = 0$.

START

S1: At time $t = k$, The coordinator receives the state, disturbance and reference vectors from each subsystem: $\tilde{x}_{o(i)}$, $\tilde{\tilde{\boldsymbol{d}}}_{\boldsymbol{i}}$ and $\boldsymbol{u_{ext(i)}}$, where $i = 1 \cdots z$. Then, it merges the vectors accordingly to obtain $x_k, \boldsymbol{d}$ and $\boldsymbol{u_{ext}}(k-1)$

S2: The coordinator solves the optimization problem (6.44), obtaining $\mathbf{p}$.

S3: The coordinator sends vector $\mathbf{p}$ to each subsystem. Locally, it is solved an unconstrained MPC problem obtaining the local extended control sequence $\boldsymbol{u_{ext(i)}}$, at time $t = k$, as seen in (6.34)

S4: Each subsystem applies the first $m(i)$ control elements of $\boldsymbol{u}^{\boldsymbol{opt}}_{\boldsymbol{ext(i)}}$ as the local control. Go back to **S1** at the next sampling time $(t = k + 1)$.

6.3 Analysis of the proposed approach

Before showing the effectiveness of the proposed technique through an illustrative example, there are some elements that should be underlined and considered when using this approach.

6.3.1 Complexity of the coordination problem

This remark is referred to the size of the problem to be solved by the coordinator entity (6.44) as compared to the original global optimization problem with interactions as equality constrains (6.23). The original problem admits $\boldsymbol{u_{ext}}$ and $\boldsymbol{p}$ as decision variables, with constraints only in $\boldsymbol{u_{ext}}$. Then, providing some admissible solution for $\boldsymbol{u_{ext}}$, by gathering all the unconstrained solutions of the local MPCs, this global problem turns into another one in terms of $\boldsymbol{p}$ as the only decision variable, that when solved, coordinates all the subsystems while respecting the constraints.
Therefore, the new optimization problem finds some $\boldsymbol{p} \in \Re^{N.r}$, where typically $r \leq n$, instead of $\boldsymbol{u} \in \Re^{N.m}$, that is the solution for a centralized approach without interaction constraints, or even $\boldsymbol{u_{ext}} \in \Re^{N.(m+r)}$ in the case of a centralized approach that includes interactions as equality constraints and one decides to solve a multi parametric optimization problem [55]. This means that for large scale systems, with a low number of interactions for instance, the dimension of the optimization problem would be substantially reduced.
Typically, process with serial-like interactivity are quite common with the mentioned configuration. For example, the solar heating/cooling system shown in [38] has this serial interactivity. Here, the state of one subsystem is linked with the actions of the previous one. To get even more easy evidence of this, one can consider the following example:

Example 6.1. *The serial interconnection topology for fuel cell power systems, shown in Fig. 6.2, is composed by two DC/DC power converters connected in series [97, 35].*

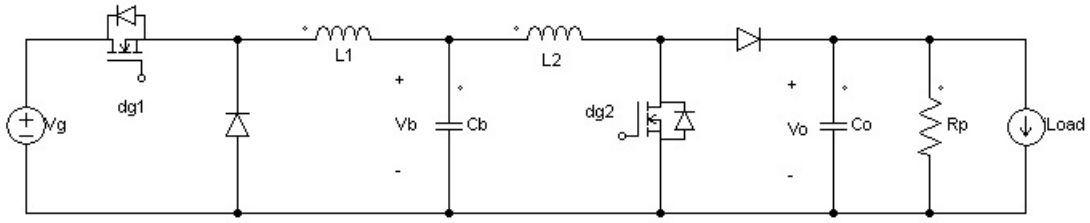

Figure 6.2: Serial fuel cell interconnection topology with Buck and Boost converters

The topology works as follows: the fuel cell generates a voltage V_g and delivers power to the first converter (here, a Buck converter), whose nodes are connected to the second converter (here a Boost converter) through a supercapacitor C_b. At the end of the second converter, a pre-load resistor R_p and the system load i_{Load}, are included. Each converter has a switch that is controlled according to some duty cycle, referenced as d_{g1} and d_{g2}, respectively, as well as inductances L_1 and L_2 for the first and second converter, respectively. The control objectives of this topology are the regulation of the output voltage V_o and the regulation of the supercapacitor voltage V_b, directly linked with its state-of-charge.
Now, taking as states, inputs and disturbances the following variables: $x = [i_{L1}\ v_b\ i_{L2}\ v_o]^T$, $u = [d_{g1}\ d_{g2}]^T$, $d = [v_g\ i_{Load}]^T$, a state-averaged continuous time model [84] can be obtained as:

$$\dot{x} = Ax + Bu + Ed$$

$$\dot{x} = \begin{bmatrix} 0 & -1/L_1 & 0 & 0 \\ 1/C_b & 0 & -1/C_b & 0 \\ 0 & 1/L_2 & 0 & D_{g2}/L_2 \\ 0 & 0 & (1-D_{g2})/C_o & -1/(R_p.C_o) \end{bmatrix} x + \begin{bmatrix} V_g/L_1 & 0 \\ 0 & 0 \\ 0 & V_o/L_2 \\ 0 & -I_{L2}/C_o \end{bmatrix} u + \begin{bmatrix} D_{g1}/L_1 & 0 \\ 0 & 0 \\ 0 & 0 \\ 0 & -1/C_o \end{bmatrix} d \tag{6.45}$$

Now, following the methodology previously exposed for the decomposition of the global system into subsystems, one can form two well differenced subsystems as follows: the first one with state vector $x_{(1)} = [x_1\ x_2]^T$, input $u_{(1)} = u_1$ and disturbance $d_{(1)} = d_1$, while the second subsystem is formed with state vector $x_{(2)} = [x_3\ x_4]^T$, input $u_{(2)} = u_2$ and disturbance $d_{(2)} = d_2$.
According to the proposed methodology and given the system configuration, the interaction vector v for the proposed subsystems, as it can be seen in the non-diagonal submatrices of (6.45), are only dependent on states. In fact, the continuous model with the interaction vector (last term at right) is:

$$\dot{x} = A_d x + B_d u + E_d d + v$$

$$\dot{x} = \begin{bmatrix} 0 & -1/L_1 & 0 & 0 \\ 1/C_b & 0 & 0 & 0 \\ 0 & 0 & 0 & D_{g2}/L_2 \\ 0 & 0 & (1-D_{g2})/C_o & -1/(R_p.C_o) \end{bmatrix} x + \begin{bmatrix} V_g/L_1 & 0 \\ 0 & 0 \\ 0 & V_o/L_2 \\ 0 & -I_{L2}/C_o \end{bmatrix} u + \begin{bmatrix} D_{g1}/L_1 & 0 \\ 0 & 0 \\ 0 & 0 \\ 0 & -1/C_o \end{bmatrix} d + \begin{bmatrix} +0 \\ -x_3/C_b \\ x_2/L_2 \\ 0 \end{bmatrix} \tag{6.46}$$

*For this system, the **interactions vector** is defined as $v = [0\ -x_3/C_b\ x_2/L_2\ 0]^T$. However, if only the non-zero elements of this vector are considered, one can write a simplified version of this*

vector, called $\bar{v}$, as follows:

$$\begin{aligned} \bar{v} &= Fv \\ \begin{bmatrix} -x_3/C_b \\ x_2/L_2 \end{bmatrix} &= \begin{bmatrix} 0 & -1/C_b & 0 & 0 \\ 0 & 0 & 1/L_2 & 0 \end{bmatrix} \begin{bmatrix} 0 & x_3 & x_2 & 0 \end{bmatrix}^T \end{aligned} \tag{6.47}$$

Considering this last transformation, one can simply replace the interconnection vector v by $v = F^{\dagger}\bar{v}$ when writing all the matrices for the N-step predicted states (6.16) and interactions (6.18) vectors. For instance, the following expression is the modified continuous time expression:

$$\dot{x} = A_d x + B_d u + E_d d + F^{\dagger}\bar{v} \tag{6.48}$$

In this example, the simplified interaction vector $\bar{v}$ is of dimension $\bar{r} = 2$, while the inputs and interactions vectors are of dimension $m = 2$ and $r = 4$, respectively. Because the coordination vector is of dimension $N.\bar{r}$, it is smaller than that of a centralized solution with constraints consideration, that would have dimension $N.(m + r)$.

6.3.2 Structure of local controllers and coordination vector influence

The second remark, and with high relevance in the context of distributed control schemes, is that the coordinator does not compute the control signals for each subsystem, but instead delivers an external signal for coordinating all subsystems according to the global cost function objectives. First, remember the subsystem control scheme, defined in (6.34) and pictured in Fig 6.3 in a quite general way (no reference is added and the gains are written in general form).

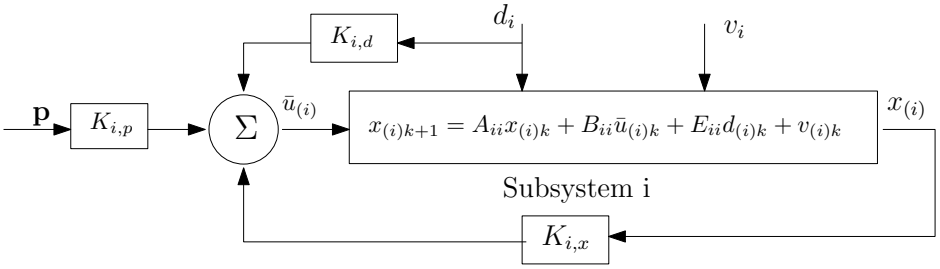

Figure 6.3: Information Flow for the Coordination Algorithm

Remember also that the coordination vector is computed externally by the coordinator after receiving state and disturbance information from each subsystem. This vector $\boldsymbol{p}$ belongs to the domain $\mathcal{P}$, defined in (6.43), for which constraints are satisfied. According to the structure in Fig 6.3, the coordination signal acts as a correction element for the subsystem, ensuring that $x_{(i)}$ tracks its reference value without violating the local input constraints (on $u_{(i)}$) while also avoiding constraints violation in the subsystems that interact with i. In other words, *the coordinator can aid in the global system stabilization, by assuring local constraints.* However, this depends on the system dynamics and disturbance influence.
The properties provided by this configuration keep some similarities with the characteristics of *reference governors* for constrained systems, in which reference values are modified in such a way that constraints are respected, ensuring system stability while probably losing some performance [125, 126]. In the proposed approach, $\boldsymbol{p}$ is reconfigured accordingly, instead of $u_{(i)s}$ or even $x_{(i)s}$.

The independence provided by this coordination scheme permits that in case of communication loss FROM the coordinator for a particular subsystem i, while the other ones yet receive

information from the coordinator, the subsystem can operate in local constrained control.
The control problem that must be locally solved, for such systems without coordination, requires a modified version of the local dynamical expression (6.12):

$$\begin{aligned} x_{(i)k+1} &= A_{ii}x_{(i)k} + B_{ii}u_{(i)k} + E_{ii}d_{(i)k} + v_{(i)k} \\ x_{(i)k+1} &= A_{ii}x_{(i)k} + B_{ii}u_{(i)k} + [E_{ii} \;\; I][d_{(i)k} \;\; v_{(i)k}]^T \\ x_{(i)k+1} &= A_{ii}x_{(i)k} + B_{ii}u_{(i)k} + \bar{E}_{ii}\bar{d}_{(i)k} \end{aligned} \tag{6.49}$$

Where local interactions vector, $v_{(i)}$ extends the local disturbances vector. The cost function that should be optimized, being $P_{(i)} = P_{(i)}^T \geq 0$, $Q_{(i)} = Q_{(i)}^T$, $R_{(i)} = R_{(i)}^T > 0$ and $S_{u(i)} \geq 0$ such that $Q_{(i)} \geq S_{u(i)}R_{(i)}^{-1}S_{(i)}^T$, with $P_{(i)}$ as the solution of the discrete-time algebraic Ricatti equation, is the following:

$$J_{gv,uc(i)} = \frac{1}{2}\left[\tilde{x}_{(i)N}^T P_{(i)}\tilde{x}_{(i)N} + \sum_{k=0}^{N-1}\left(\tilde{x}_{(i)k}^T Q_{(i)}\tilde{x}_{(i)k} + \tilde{u}_{(i)k}^T R_{u(i)}\tilde{u}_{(i)k} + 2\tilde{u}_{(i)k}^T S_{u(i)}\tilde{x}_{(i)k}\right)\right] \tag{6.50}$$

Evidently, the cost function can be converted into a QP form, and the following optimization problem should be solved for obtaining the local control sequence $\boldsymbol{u_{(i)}}$:

$$\begin{aligned} \min_{\boldsymbol{u_{(i)}}} \quad & J_{gv,uc(i)}(\boldsymbol{u_{(i)}}) \\ \text{subject to} \quad & L_{(i)}\boldsymbol{u_{(i)}} \leq W_{(i)} \end{aligned} \tag{6.51}$$

where the local constraint polyhedral set is built with the same principles as that of the global one, but considering that there exist appropriate bounds for the interactions vector $v_{(i)}$, defined indeed by the signals bounds of the neighbours subsystems. At the end, the local controller keeps the system in admissible regimen, only if the remaining subsystems also operates in admissible ranges, either by the coordinator actions of such yet coordinated systems or by action of the local controllers. However, when coordination is lost in some degree, there are no guarantees that global or local constraints are respected.
For example, in the classical Line Frequency Control problem [39, 18], the use of a decentralized or a poor coordinated control structure can affect the frequency regulation, that can deteriorate the mechanical components of the induction generators. In this case, coordination is vital for the system regulation as exposed in such mentioned contributions.

As concluding remark for this situation, the proposed approach allows that each subsystem computes its local control signals. The coordinator not only assures the global performance, but also the constraints respect by all subsystems. When coordination is lost for some subsystem, it passes to local constrained control, considering the neighbour subsystems working in their admissible sets. Thus, global system performance is degraded, while local operation could be kept. Evidently, this depends on the system characteristics and would not be generalized for all the scenarios. In further works, this aspect would be studied.

6.3.3 Coordination period and subsystems sampling periods: performance of the subsysems

The present approach benefits from the fact that explicit solutions for the constrained optimization problem in the QP configuration are faster than traditional methods such as gradient or barrier ones [55].
For this proposal, it is assumed that all subsystems share the same sampling period and prediction horizon, allowing that each local control signal respect the global constraints, defined in the

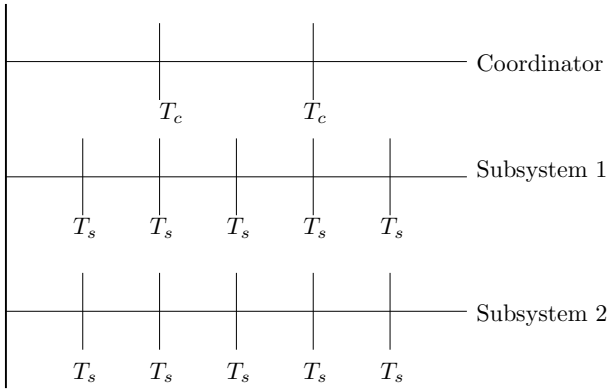

Figure 6.4: Illustration of coordination and sampling periods

coordination algorithm. This consideration is done thanks to the efficiency of the solution algorithm at the coordinator, based on the geometric properties in this problem, presented in Section 4.1.3.

In addition, because the local controller structure, previously analyzed, is so simple and the solution can be obtained so fast, the constrained coordination is ensured within one sampling time. Therefore, it is said that *coordination period* T_c is equal to the *sampling period* T_s.

However, although the coordination problem is solved in small time and only requires the current states, disturbances and reference values from the subsystems, there are some elements that must be analyzed for further improvements of the present technique.

A first question can be: what would happen, in terms of compliance of constraints, when the coordination period is larger than the subsystems sampling period? This case is illustrated in Fig. 6.4 where $T_c = 2T_s$. For answering this question, some prior analysis can be found in the thesis [6], where the coordination of a hydro-power valley is considered. The author there compares the performance,in terms of the final cost values, when using $T_c = T_s$ and $T_c = kT_s, k \in \mathbb{N}^+ > 1$. It is seen that when coordination is less frequent, the system performance is degraded, due to the poor coordination capacities when k grows.

More deeply, in the cited contribution, a price-driven coordination approach is also included based on Uzawa's algorithm for explicit computation of coordination vector $\boldsymbol{p}$. However, the coordination vector is obtained in an algebraic way, after gathering the state and disturbance from the subsystems, and no constraint policy was taken into account when computing the coordination vector. Instead, each subsystem solves an equivalent problem to the one of (6.51), while maintaining the same coordination vector until a new T_c have passed.

On the contrary here, the proposed approach ensures that coordination respects the constraints. However, if coordination period is different from the sampling period, it is possible that subsystems endure some performance - or even stability - degradation, due to the action of the $\boldsymbol{p}$ vector in the local controllers (see Fig. 6.3), and its lack of adaptation with the system evolution.

There are two actions that can be considered as a remedy in this case: One of them is to consider constrained local problems as in(6.51), maintaining the last computed $\boldsymbol{p}$, and then, using the explicit local expression when a new coordination cycle is done. The other possibility is to analyze the subsystems through the so-called *Invariant Set Analysis* that will presented in the following Chapter. In general terms, the idea is to make the analysis for a fixed and admissible $\boldsymbol{p}$, and then study how much deviation from the equilibrium would have the local states while respecting the local constraints. According to the deviation, one can propose a T_c that allows some admissible operative conditions, and then, avoid constant communication between the subsystems and the coordinator.

A second question that can arise is: what would occur with the constraints when the subsystems sampling periods are desynchronized between each other? This case is illustrated in Fig. 6.5.

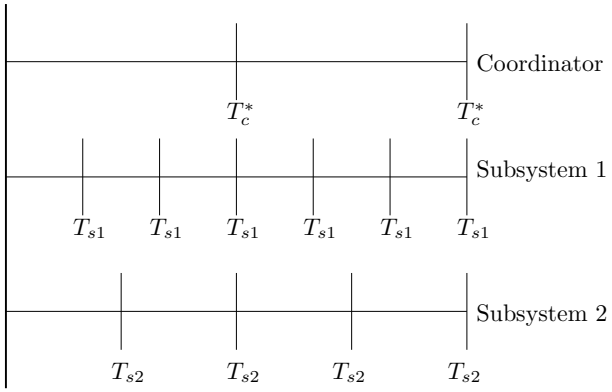

Figure 6.5: Illustration of coordination and sampling periods when local sampling times are different between subsytems, and and from the coordination one.

Consider here a scenario in which subsystem 1 has a sampling period T_{s1}, subsystem 2 a sampling period T_{s2} and the coordinator a sampling time T_c. Let us assume that $T_{s2} = kT_{s1}, k \in \mathbb{N}^+$ and $T_c \geq T_{s2}$.
A possible solution for selecting the times for coordinating this system can start with finding a common time where $b_1 T_{s1} = b_2 T_{s2} = T_c^*$, with b_1, b_2 positive constants. For instance, in Fig 6.5, $3T_{s1} = 2T_{s2} = T_c^*$.
Therefore, one can set the coordination time to T_c^*, ensuring that the subsystems can transmit simultaneously their information to the coordinator, that will perform the well known computations. Then, the coordination vector is used locally and some action such as local constrained control could be directed. Again, some analysis would give some indications of what should be done between two coordination times (switch to constrained control or maintain the unconstrained one) and what would happen if a fixed $\boldsymbol{p}$ is maintained, while performing a constrained or an unconstrained strategy.
To close this remark, the proposed coordination strategy considers $T_s = T_c$, and if this condition is violated, the respect of constraints or even subsystems stability is not guaranteed, due to the lack of instantaneous coordination when computing the control sequence. Some additional mechanism for the real time control or analysis must be done when these periods are different. In addition, different sampling times in each subsystem require a T_c value well chosen, but again, some analysis or control configuration should be done. This point will be analyzed in future works, considering the vast quantity of distributed multi-rate systems with a unique coordination structure.

6.3.4 Control structure for subsystems

It is finally noticed here that constrained coordination is indeed based on the hypothesis that local controllers are MPC-based. This fact helps to obtain a partial solution for the control signal parameter in the global problem. Then, $\boldsymbol{p}$ is computed and sent to the subsystems.
However, it will be analyzed in future works, what should be the procedure to express the coordination problem when using other classes of control strategy in the subsystems, such as Robust or Adaptive control, for example. The controller structures are fixed or only gains will be modified instead of the control signal, requiring therefore some adaptation for real-time coordination. Or, in

other situations, one can reformulate the coordination algorithm, coming back to Uzawa theorem as in [6].
Nevertheless, in case of MPC-based local controllers and explicit coordination solution, the subsystems perform fast control actions, while the coordination mechanism does not take too much time. With other structures, some gain identification methods or something similar would be needed to be added in the coordinator, if the proposed structure would be to be exploited.

6.4 Illustrative example

For a better understanding of the technique, it is here applied to second order example system and compared to a centralized coordination approach. To that end, let us consider again the discrete-time system of section 4.2.4, with $T_s = 1/150s$:

$$x_{k+1} = \begin{bmatrix} 0.9667 & 0.0133 \\ -0.0067 & 0.9733 \end{bmatrix} x_k + \begin{bmatrix} -0.0333 & 0.0033 \\ 0.0333 & 0.0167 \end{bmatrix} u_k + \begin{bmatrix} -0.0067 & 0.0033 \\ 0.0013 & 0.0067 \end{bmatrix} d_k$$

The eigenvalues for this system are equal to ($\lambda_{1,2} = 0.97 \pm 0.0088j$). Because the proposed approach is based on the decomposition of a centralized-MPC solution, the following weight matrices, prediction horizon and constraints vectors are considered for the **centralized MPC problem**:

$$Q = \begin{bmatrix} 100 & 0 \\ 0 & 100 \end{bmatrix};\ R = \begin{bmatrix} 1 & 0 \\ 0 & 1 \end{bmatrix};\ S = \begin{bmatrix} 0 & 0 \\ 0 & 0 \end{bmatrix};\ P = \begin{bmatrix} 452.56 & 195.15 \\ 195.15 & 431.85 \end{bmatrix};\ N = 2;$$

$$x_{min} = \begin{bmatrix} -2 \\ -2 \end{bmatrix};\ x_{max} = \begin{bmatrix} 2 \\ 2 \end{bmatrix}; u_{min} = \begin{bmatrix} -3 \\ -3 \end{bmatrix};\ u_{max} = \begin{bmatrix} 3 \\ 3 \end{bmatrix}; d_{min} = \begin{bmatrix} -1 \\ -1 \end{bmatrix};\ d_{max} = \begin{bmatrix} 1 \\ 1 \end{bmatrix}$$

The matrix P is obtained from the solution of the discrete-time LQR for the dynamical system. The dynamical system is distributed into two subsystems, each one with one state, one input, one disturbance and one interaction variable. The following subsystems are thus proposed:

$$x_{(1)k+1} = 0.9667x_{(1)k} - 0.0333u_{(1)k} - 0.067d_{(1)k} \underbrace{+0.0133x_{(2)k} + 0.0333u_{(2)k} + 0.0033d_{(2)k}}_{v_{(1)k}}$$

$$x_{(2)k+1} = 0.9733x_{(2)k} + 0.0167u_{(2)k} + 0.067d_{(2)k} \underbrace{-0.0067x_{(1)k} + 0.0333u_{(1)k} + 0.0013d_{(1)k}}_{v_{(2)k}}$$

where elements $x_{(i)}, u_{(i)}, d_{(i)}, i = 1, 2$ are indeed the elements from the original system. Considering this decomposition, the following weight matrices, under the same prediction horizon ($N = 2$) are selected for the **decomposition-coordination approach**:

$$Q_{(1)} = Q_{(2)} = 100;\ R_{u(1)} = R_{u(2)} = 1;\ R_{v(1)} = R_{v(2)} = 1e^7;\ S_{u(1)} = S_{u(2)} = 0;$$
$$S_{v(1)} = S_{v(2)} = 0;\ P_{(1)} = 452.55;\ P_{(2)} = 195.15;$$

Now, some tests are proposed: a first one for an evaluation of the system performance when using a centralized control approach and the proposed one based in decomposition, and a second one in which the coordination is lost and the subsystem switches to a local constrained control.

Test Scenario 1: Comparison of the system performance under a centralized MPC vs the proposed distributed MPC

For this illustrative situation, similar reference profiles for states and disturbances (x_s and d_s) are selected, over the same simulation times. Therefore, the following cost integral is evaluated

for both configurations, considering that states and inputs are measured in both subsystems:

$$J = \frac{1}{2}\sum_{k=0}^{k_f}\left(\tilde{x}_k^T Q \tilde{x}_k + \tilde{u}_k^T R \tilde{u}_k + 2\tilde{x}_k^T S \tilde{u}_k\right) \tag{6.52}$$

where k_f is the final step in the discrete time system. Remember that variables with *tilde* are error at step k with respect to some reference value, that could change in the simulation window. The following simulation scenario was considered:

- The initial state vector was set to $x = [1 \quad -1]^T$, with disturbances and inputs at 0. The state references were set to $x_s = [0 \quad 0]^T$ between $t = 0$ and $t = 0.7s$.
- Between $t = 0.7s$ and $t = 1s$, the *a priori* known disturbance vector was set to $d_s = [0.1 \quad 0]^T$ and the state reference vector was modified to $x_s = [0.1 \quad 0]^T$
- Finally, between $t = 1s$ and $t = 2s$, the following disturbance and state references were selected: $d_s = [0.5 \quad -0.5]^T$, $x_s = [1 \quad -0.5]^T$.
- For the system, the real disturbance value is assumed to be equal to d_s. In practice, d_k would be previously known as a "predicted disturbance", but its real value can deviate from it.

The corresponding simulation results are shown for both cases in Fig. 6.6, in which one can see the state evolutions, the applied control signals and the disturbances, both for the centralized MPC and the decomposed MPC solution. It can be seen for example, that centralized MPC solution requires more control signal changes but ensures a fast dynamical response while respecting the system constraints. The proposed solution also offers good tracking performance, with a lower

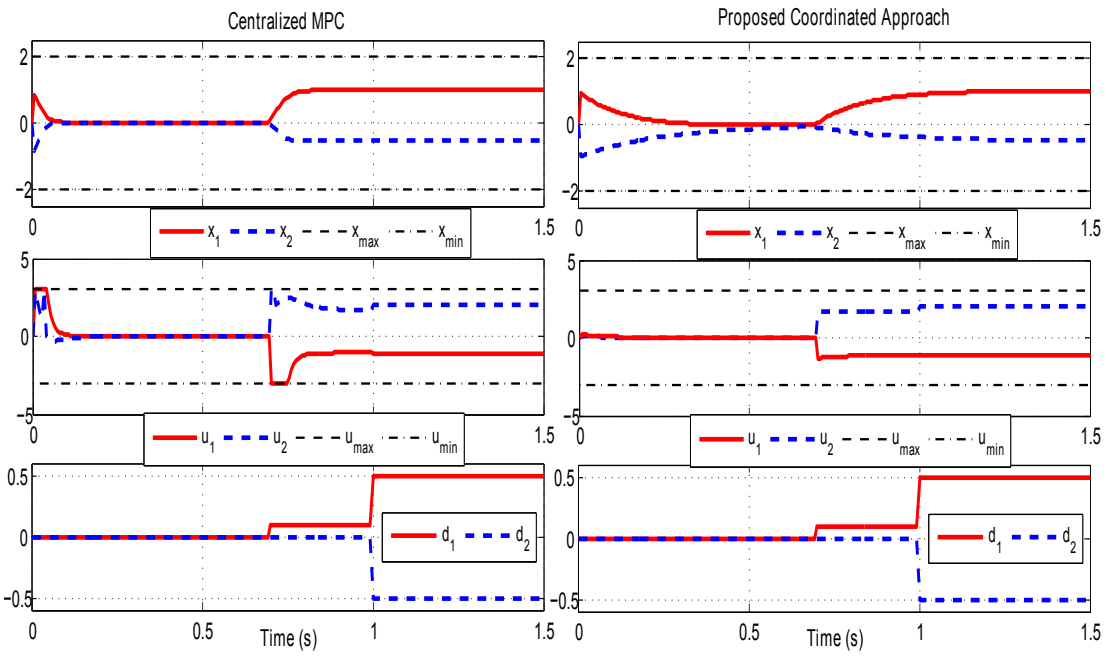

Figure 6.6: Performance of the proposed second order system under centralized MPC vs proposed distributed coordinated approach

bandwidth than with the centralized case yet, but with fewer changes in the control signals,

including less saturation. In fact, the equivalent cost value for both situations are given in Table 6.1.
Table 6.1 also includes the mean cost between three different tests for each controller configuration, in which a zero mean noise of amplitude 0.5 was added for both disturbance channels on the reference vector d_s. Here, the system performance is evaluated when real disturbances act on it: one can know an estimated d_s value by observers or predictors, but in reality, the disturbance may be different from this value. In this case, the proposed control scheme appears to reduce the fast disturbance changes with lower control effort than with the centralized MPC case, that this is interesting for distributed control schemes.

Table 6.1: Performance comparison for the proposed system under centralized MPC vs under proposed distributed coordinated approach

Parameter	**Centralized MPC**	**Propossed Approach**
Total Cost (Eq. 6.52)	$7.816x10^3$	$7.275x10^3$
Time Constant (x_1)	37 ms	130 ms
Time Constant (x_2)	30 ms	175 ms
Mean cost [1]	$7.799x10^3$	$6.799x10^3$

Considering these results and the methodological details, the proposed distributed MPC-based solution offers similar results to those with a centralized MPC strategy, but with the possibility of decentralizing the control algorithm between subsystems. In the second situation, shown next, it will be seen how decentralizing allows to ensure local stability when coordination is lost for one or even both subsystems, even if the global cost may be degraded.

Test Scenario 2: Stability and performance of subsystems under the proposed approach when coordination data is lost

In this case, the system has the distributed and coordinated control approach by default. However, the coordination vector $\boldsymbol{p}$ may not be communicated to one of the subsystems, requiring therefore that its local controller changes to a constrained MPC scheme, in which the new optimization problem to be solved is (6.51). Again, for the no coordinated subsystem, only the first $m_{(i)}$ elements of $\bar{\boldsymbol{u}}_{(\boldsymbol{i})}$ are applied as control signal. The purpose of this test is to illustrate the stability of the local subsystems, when is necessary to change to non coordinated local control policies. In this case, because the second subsystem is still coordinated, then its constraints are assured and the interactions terms are bounded. This scheme is useful in this work, considering that subsystems are local power generators that have some functional constraints that must be ensured, although the coordination unit fails. This aspect will be better explained and analyzed in Chapter 8.
For this simulation, it is considered the same profile as in the previous one, but it was added some noise to the disturbance vector. The system starts with coordination, but at at $t = 0.65s$, subsystem 2 loses the feedback signal (the $\boldsymbol{p}$ vector) from the coordinator due to a communication error, while transmitting its local information normally, allowing therefore that subsystem 1 maintains its operation with the not well tuned coordination information.
Therefore, subsystem 2 switches to local MPC, and as seen in Fig. 6.7, the subsystems will main-

[1] Three essays adding zero mean noise of amplitude 0.5 with $d_k = d_s$

tain stable operation, although some steady state error is present in the states at the end of the test: reference values are $x_s = [1 \quad -0.5]^T$ and the measured ones are $x = [0.961 \quad -0.487]^T$. are presented.

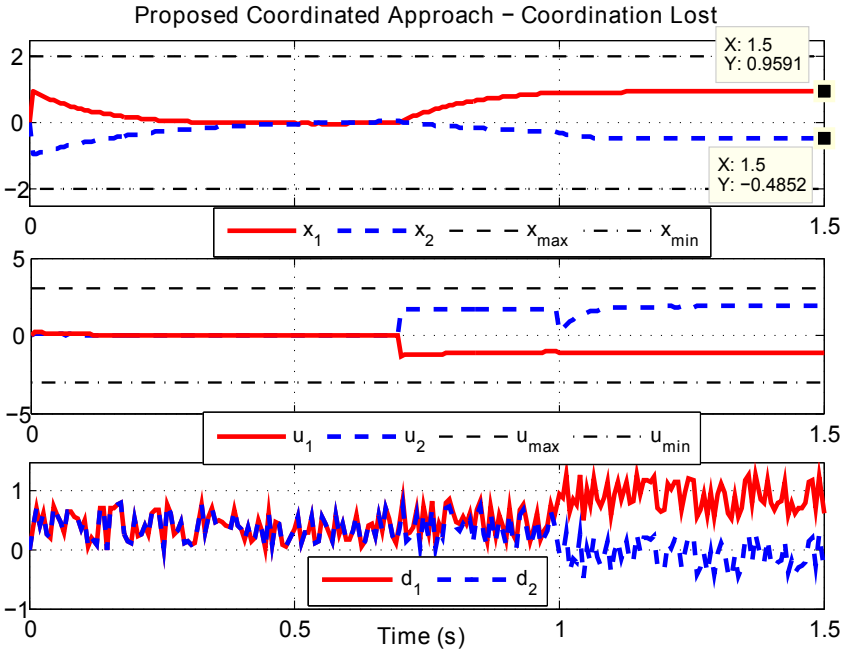

Figure 6.7: Perform of the proposed second order system with the coordinated control approach, when subsystem 2 loses the coordination vector

6.5 Conclusions

In this chapter, we have proposed a price-driven coordination strategy for distributed systems, that respect the global constraints while decentralizing the control computation for each subsystem, in the spirit of explicit solutions. The methodology uses a distributed model of the system, considering that each subsystem has interaction variables with the other ones. With this same philosophy, the objective function of the optimization problem for the Model Predictive Control strategy is separated along the subsystems, and each of them locally solves an unconstrained problem, that will depend on the system signals, but also on a coordination term obtained at each step.

The solutions for all subsystems are merged, and a first part of the global optimization problem is solved with some admissible local solutions. The other part of the global optimization problem is associated to the selection of the coordination vector, which is itself constrained to an admissible domain directly related to the one of the original optimization problem. Finally, each subsystem tunes its local control signal, according to the coordination policy, always respecting the global constraints.

If one particular subsystem loses the communication with the coordinator, it can switch to its local constrained control strategy. In this way, the global performance may be degraded, but the local stability might be kept, only if the neighbours have their signals in admissible sets.

In the following chapter, a stability analysis based on invariant sets will be performed for this strategy, allowing global and local performance analysis, under normal condition or under some coordination loss.

Chapter 7

STABILITY AND PERFORMANCE ANALYSIS OF CONSTRAINED CONTROL SYSTEMS

Contents

7.1 Stability and Performance of Systems under Constrained Model Predictive Control 116
7.1.1 System dynamics, admissible sets and control structure for the MPC case . 117
7.1.2 Stability analysis of the constrained MPC solution 117
7.1.3 Performance analysis of the contrained MPC solution using invariant sets . 118
7.1.4 Recursive algorithm for computing the minimal robust invariant set 121
7.1.5 Illustrative Example 126
7.2 Global Performance Analysis for a Distributed Constrained Control System with Coordination 127
7.2.1 System dynamics, admissible sets and control structure for the distributed coordinated control scheme 127
7.2.2 Stability analysis of the distributed coordinated control scheme 128
7.2.3 Performance analysis of the distributed coordinated control using invariant sets 129
7.2.4 Recursive algorithm for computing the minimal robust invariant set 133
7.2.5 Performance analysis for distributed non-coordinated case 135
7.2.6 Illustrative example 136
7.3 Global Performance analysis by distrubuted-computed invariant sets . 138
7.3.1 Expressions for the analysis in the distributed coordinated system 138
7.3.2 Recursive algorithm for computing the local minimal robust invariant set . 139
7.3.3 Illustrative example 141
7.4 Conclusions 141

This chapter presents an approach for stability and performance analysis of constrained control systems. Since any control, state and outputs constraints can be written in terms of only control constraints, the proposed approach could be used for more general control system analysis. Here, the original model predictive control problem is rewritten as a quadratic program problem only subject to the inequality constraints on the control sequence. In linear systems, the unconstrained optimal control could be written in an explicit form, and then, the constraints can be evaluated and considered just before application of the control signal. In this section, we consider a stable

system in feedback with a constrained control for which the small gain theorem can be used to establish the stability conditions for the system [16] . On the other hand, the performance analysis of such constrained control system is based on the computation of invariant sets. This approach considers that the constrained control system can be written as a polytopic linear system and then the invariant sets can be computed by using the approach presented in Section 4.2.

The advantage of this approach is the fact that the existence of such a bounded set implies that the controlled system remains stable if the states start inside the invariant set (even if the system is open-loop unstable). The latter point is also useful to establish the initial conditions for which the system remains stable in presence of control constraints. The obtained invariant sets have to be contrasted with the admissible sets for control and/or states signals. This is important from a practical point of view since the state trajectories that violate the admissible sets could produce instability of the system. Thus, the "boundeness" of the obtained invariant sets is not sufficient condition to establish the stability property of the constrained control system. For instance in [127] the system invariant set has to belong to the constraints sets to guarantee stability of a model predictive control system.

The proposed approach will be extended to distributed constrained control systems. For instance, in [54], the authors propose a strategy for distributed control with neighbour-to-neighbour communication and evaluate the system performance by using an invariant set approach.

In this order of ideas and considering the analytic tools presented in Section 4.2, the invariant set analysis is here performed for two different systems configurations: the first one, for systems that use centralized MPC control, and the second one for distributed control systems with exogenous coordination similar to that introduced in Chapter 6. At the end of the present chapter, it is proposed an alternative method for performing an invariant sets analysis for distributed controlled systems, considering a particular coordination scheme.

7.1 Stability and Performance of Systems under Constrained Model Predictive Control

In this section are presented the stability and performance analysis for systems controlled with a receding horizon strategy that considers constraints. With respect to stability of MPC solutions for dynamic systems, the contribution [127] presents a deep analysis in this aspect. However, here is used the *small gain theorem* [16] to determinate the system stability when a constrained control is applied.
With respect to the performance, the invariant set analysis is used. Notions of this approach can be found in [128], that includes deeper analysis of reachable and controllable sets for autonomous and controlled systems. It will be shown how to adapt the dynamical model for allowing the invariant sets computation. For instance, it will be shown how to compute a *worst case* scenario invariant set, as well as approximations of the minimal RPI.
The results of this section will be extended for other scenarios, such the coordinated scheme presented in Chapter 6 and the possibility of using a distributed computation strategy of invariant sets, when the problem has size complexity.

7.1.1 System dynamics, admissible sets and control structure for the MPC case

Consider again the following dynamic system:

$$x_{k+1} = Ax_k + Bu_k + Ed_k \tag{7.1}$$

with k denoting the current time, x_k, u_k, d_k, y_k are the states, inputs, disturbances and outputs vectors of order n, m, q and o respectively, and the state, input, disturbance and output matrices represented, in this order, as $A \in \Re^{n\times n}$, $B \in \Re^{n\times m}$, $E \in \Re^{n\times q}$ and $C \in \Re^{o\times n}$, with matrix A eigenvalues in the interior of the unitary circle (open loop stable). Now,let define the following admissible sets for states, inputs and disturbances:

$$\begin{array}{ll} x_k \in \mathcal{X} & \text{where } \mathcal{X} = \{x_k \in \Re^n : x_{min} \leq x_k \leq x_{max}\} \\ u_k \in \mathcal{U} & \text{where } \mathcal{U} = \{u_k \in \Re^m : u_{min} \leq u_k \leq u_{max}\} \\ \delta u_k \in \delta\mathcal{U} & \text{where } \delta\mathcal{U} = \{u_k, u_{k-1} \in \Re^m : \delta u_{min} \leq u_k - u_{k-1} \leq \delta u_{max}\} \\ d_k \in \mathcal{D} & \text{where } \mathcal{D} = \{d_k \in \Re^q : d_{min} \leq d_k \leq d_{max}\} \end{array} \tag{7.2}$$

According to the elements presented in Section 6.1, the following optimization problem is associated for a system under MPC for prediction horizon N. Its solution is in fact the optimal input sequence $\boldsymbol{u} = [u_0 \cdots u_{N-1}]^T$, that should respect the constraints that are rewritten in terms of $\boldsymbol{u}$.

$$\begin{array}{ll} \min\limits_{\boldsymbol{u}} & \frac{1}{2}\boldsymbol{u^T H u} + \boldsymbol{u^T}[\boldsymbol{K_1}(x_0 - x_s) + \boldsymbol{K_2}(\boldsymbol{d - d_s}) - \boldsymbol{H u_s}] \\ \text{subject to} & L\boldsymbol{u} \leq W \end{array} \tag{7.3}$$

where the variables with subindex s are reference values of states (x_s) and inputs (u_s) for expected disturbances (d_s). Details of the construction of all this functions and inequalities are included in Section 4.1.2. Considering that the optimization problem (7.3) has an unconstrained explicit solution in the form:

$$\boldsymbol{u}^*_{uc} = -\boldsymbol{H^{-1}}[\boldsymbol{K_1}(x_0 - x_s) + \boldsymbol{K_2}(\boldsymbol{d - d_s}) - \boldsymbol{H u_s}] \tag{7.4}$$

where $x_0 = x_k$ (current state value), it shows a well-known *state feedback* topology, where the state gain is represented by $\boldsymbol{H^{-1}K_1}$ and disturbance compensation gain $\boldsymbol{H^{-1}K_2}$.
As seen in Chapter 4, the unconstrained solution is fixed to be admissible, giving therefore an input vector contained in $\mathcal{U}$ that is applied to the system. Considering this constrained mechanism, the stability and performance is next analyzed.

7.1.2 Stability analysis of the constrained MPC solution

The applied control signals in the constrained MPC are computed after a state feedback and then, a saturation-like function is applied, obtaining an admissible input vector. As consequence, the closed-loop system stability will depend on the actions of the controller block, considering its saturated behavior. For this motive, it is introduced the *small gain theorem* for evaluating the closed-loop system performance.

Theorem 7.1. ***Small gain theorem [16]***

Consider a stable system $G(s)$ in feedback with a controller $K(s)$. The closed-loop system is stable if the following condition holds:

$$\|K(jw)\|\|G(jw)\| < 1 \ \forall w \tag{7.5}$$

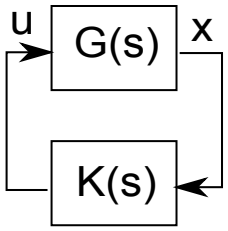

Figure 7.1: Small gain theorem

Theorem 7.1 can be applied by considering the infinite norm of systems $G(s)$ and $K(s)$ for performing the stability analysis, based in the worst case scenario. Then, define the following gains γ_G and γ_K as:

$$\gamma_G := \|G(s)\|_\infty, \quad \gamma_K := \|K(s)\|_\infty \tag{7.6}$$

This gains can be computed as follows:

- For the gain γ_G, concerning the states-to-inputs gain, one can use the discrete time system model (7.1), with $d_k = 0$, and use the Bounded Real Lemma (4.50) for computing P and γ_G, that is

$$\begin{bmatrix} x_k \\ u_k \end{bmatrix}^T \begin{bmatrix} A^TPA - P + I_n & A^TPB \\ B^TPA & B^TPB - \gamma_G^2 I_m \end{bmatrix} \begin{bmatrix} x_k \\ u_k \end{bmatrix} \leq 0 \tag{7.7}$$

- For finding the value γ_K, that is the equivalent gain of the constrained control block, one should analyze the constraints polyhedral term that links the states with the desired input values. Considering the constraints polyhedron structure, presented in (4.24)-(4.26) in Section 4.1.2, one have:

$$\begin{array}{c} L\boldsymbol{u} \leq W(x_k, u_{k-1}) \\ L = \begin{bmatrix} \phi \\ -\phi \end{bmatrix} \quad W = \begin{bmatrix} \bar{\Delta} \\ -\underline{\Delta} \end{bmatrix} + \begin{bmatrix} -\xi \\ \xi \end{bmatrix} x_k + \begin{bmatrix} -\xi_u \\ \xi_u \end{bmatrix} u_{k-1} \end{array} \tag{7.8}$$

  For simplicity take $W := \Delta + \bar{\xi} x_k + \bar{\xi}_u u_{k-1}$.

  Suppose a worst case situation where control saturation appears. Therefore, a bound of $\boldsymbol{u}$ in terms of x_k can be obtained as follows:

$$\boldsymbol{u} = L^\dagger \bar{\xi} x_k = K_{lw} x_k \tag{7.9}$$

  where $L^\dagger$ denotes the pseudoinverse matrix of L. Then, γ_K is obtained as the biggest linewise gain of the matrix K_{lw}. Thus:

$$\gamma_K = \|\bar{\gamma}\|_\infty, \text{ where } \bar{\gamma}_i = \|K_{lw,i}\|_\infty \quad \text{for } i = 1 \cdots rank(K_{lw}) \tag{7.10}$$

Thus, if $\gamma_K \gamma_G < 1$, it means that the dynamical system (7.1), with a constrained control (7.3) is closed-loop stable. If stability is assured, therefore the performance analysis can be performed as it is shown next.

7.1.3 Performance analysis of the contrained MPC solution using invariant sets

Here, it is presented the detailed procedure for computing the invariant set and using the aforementioned recursive algorithm for finding the minimal invariant set representation (mRPI).

7.1.3.1 Analysis of the closed-loop system

Looking back to the explicit solution for the MPC problem (Chapter 4), the unconstrained control sequence is processed and constrained in such way that all constraints are accomplished. However, when performing a numerical procedure for computing invariant sets, it should be verified, at each iteration, that the input vector satisfies its constraints. The methodology is based in the closed loop scheme shown in Fig. 7.2, that represents the constrained control strategy and is explained as follows:

- The dynamic system has a control inputs vector $u_k \in \mathcal{U}$ and is also affected by a perturbations vector $d_k \in \mathcal{D}$.
- The unconstrained control sequence $\boldsymbol{u}^*_{uc}$ is based in a state feedback law. This block includes disturbance compensation and knowledge of set-points for tracking proposes(x_s, u_s, d_s).
- A saturation (non-linear) block that process u^*_{uc} (the first m elements of $\boldsymbol{u}^*_{uc}$, extracted with the matrix $\boldsymbol{K_u}$, and delivers the admissible u_k the computed input of the system.

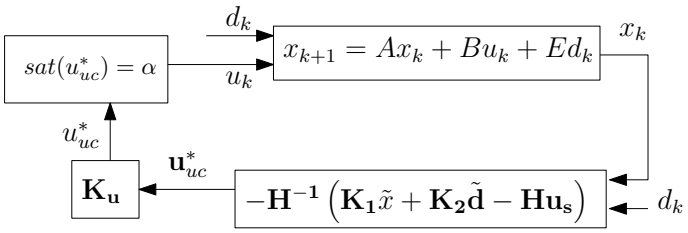

Reference values ignored in the scheme: x_s, u_s, d_s

Figure 7.2: Closed-loop system representation with Model Predictive Controller

Considering the block diagram, one can write the admissible input vector u_k as function of the unconstrained control sequence $\boldsymbol{u}^*_{uc}$ as follows:

$$u_k = \alpha K_u \boldsymbol{u}^*_{uc} \tag{7.11}$$

where $K_u = [I_{m\times 1}\ 0_{(N-1)m\times 1}]$ is a matrix that takes the first m elements from the unconstrained control sequence vector and $\alpha \in \Re^{mxm}$ is a diagonal matrix. The applied input vector u_k, considering that u^*_{uc} is built from the first m elements from the unconstrained control sequence, can be written as:

$$u_k = \alpha u^*_{uc} \tag{7.12}$$

The matrix α has the following property:

$$\alpha_{min} \prec \alpha \preceq I \tag{7.13}$$

and its construction is done under the following points:

- If the first m elements of the control sequence are included in the admissible inputs set, the diagonal elements of α are equal to 1.
- Otherwise, if any of the first m elements of the control sequence violates its constraint, denoted as $i = 1 \cdots m$, the α value associated is $\alpha_i = u_i^{lim}/u^*_{uc,i}$

- α_{min} is computed based in the smallest α_i values, that can be obtained when considering the admissible sets $\mathcal{X}$,$\mathcal{U}$ and $\mathcal{D}$ in the system signals.

In synthesis, the proposed approach for relating the unconstrained and constrained effective control vectors through the matrix α, representates the saturation effect of the control block. Because extreme values are obtained for the matrix α, one can use a polytopic notation for writing the system dynamics in closed loop, as will be seen next.

7.1.3.2 Computation of α_{min} for the MPC case

Before presenting the computation of the invariant set, it is detailed an approach for computing the matrix α_{min}. This procedure can be also made for other class of systems with constrained feedback.
For computing this matrix, it is necessary to evaluate every possible extreme value of $\boldsymbol{u}^*_{uc}$. This is obtained when applying (7.4) with the sets $\mathcal{X}$ and $\mathcal{U}$, considering the set point at the origin, $x_s = u_s = d_s = 0$ with their corresponding dimensions. Therefore, one can obtain the following set $\boldsymbol{U}_{uc} \in \Re^{N.m}$:

$$\boldsymbol{U}_{uc} = (-\boldsymbol{H^{-1}K_1})\mathcal{X} \oplus (-\boldsymbol{H^{-1}K_2}K_d)\mathcal{D} \tag{7.14}$$

In second instance, consider now the following subspace of $\boldsymbol{U}_{uc}$ after using the condition of first m elements in the control sequence:

$$\mathcal{U}_{uc} = K_u \boldsymbol{U}_{uc} \tag{7.15}$$

That is a subset in $\Re^m$, whose bounds are given by the possible solutions. $V_u = 2^m$ refers the maximum quantity of vertexes that describes the set $\mathcal{U}_{uc}$.

Considering that $\mathcal{U}_{uc}$ can be written in matrix form, whose dimension is $m \times V_u$, after applying the following operation:

$$U_{uc} = vertex\{\mathcal{U}_{uc}\}$$

, one can create the matrix of constrained controls $U_{c(i)}$, performing the following operation for each $i = 1 \cdots m$ element at each column $j = 1 \cdots V_u$:

$$U_c(i,j) = \begin{cases} U_{uc}(i,j) & \text{if } u^{min}_{uc}(i) \leq U_{uc}(i,j) \leq u^{max}_{uc}(i) \\ u^{min}_{uc}(i) & \text{if } U_{uc}(i,j) < u^{min}_{uc}(i) \\ u^{max}_{uc}(i) & \text{if } U_{uc}(i,j) > u^{max}_{uc}(i) \end{cases} \tag{7.16}$$

At this point of the procedure, one has two inputs sets: one that represents the unconstrained control $\mathcal{U}_{uc}$ and a second one, $\mathcal{U}_c$, that is a constrained version of the former set. Therefore, a preliminary α' matrix is obtained as the element-wise division of the mentioned sets:

$$\alpha'(i,j) = U_c(i,j)/U_{uc}(i,j) \ \forall i = i \cdots m, j = 1 \cdots V_u \tag{7.17}$$

Hence, for obtaining α_{min} (diagonal matrix), it should be selected the smallest value for each row of α':

$$\alpha(i,i)_{min} = inf\{\alpha'(i,j)\} \ \forall i = 1 \cdots m, j = 1 \cdots V_u \tag{7.18}$$

Finally, a diagonal matrix of only positive values will be obtained. Recall that this result is linked with the admissible values for inputs, as well as the mapping condition for states and disturbances sets. Thus, because extreme (worst) cases are considered, it is established that all possible unconstrained control solutions are included.

7.1.3.3 Computing the ellipsoidal invariant set

For obtaining the ellipsoidal invariant set representation, it is first written the closed loop system dynamics, according to the previously exposed elements. Recall the system dynamics (7.1) and replace the input u_k as:

$$u_k = -\alpha K_u \boldsymbol{H}^{-1}\left(\boldsymbol{K_1}\tilde{x} + \boldsymbol{K_2}\tilde{\boldsymbol{d}} - \boldsymbol{H u_s}\right) \tag{7.19}$$

Replacing (7.19) into (7.1), the closed loop states expression is:

$$\begin{aligned} x_{k+1} = &\quad Ax_k - B\alpha K_u \boldsymbol{H}^{-1}\left(\boldsymbol{K_1}\tilde{x} + \boldsymbol{K_2}\tilde{\boldsymbol{d}} - \boldsymbol{H u_s}\right) + Ed_k \\ x_{k+1} = &\quad (A - B\alpha K_u \boldsymbol{H}^{-1}\boldsymbol{K_1})x_k + (E - B\alpha K_u \boldsymbol{H}^{-1}\boldsymbol{K_2}K_d)d_k - \alpha K_u \boldsymbol{H}^{-1}(\boldsymbol{K_1}x_s + \boldsymbol{K_2}K_d d_s + \boldsymbol{H u_s}) \\ x_{k+1} = &\quad \bar{A}(\alpha)x_k + \bar{E}(\alpha)d_k + \bar{\delta}(x_s, u_s, d_s, \alpha) \end{aligned} \tag{7.20}$$

with $K_d = [I_{qxq} \cdots I_{qxq}]^T$ that allows to write the relationship of the disturbance sequence in terms of its current value as $\boldsymbol{d} = K_d d_k$ and $\bar{\delta}$ gathers the reference values for states, inputs and disturbances.
Considering the values of the matrix α, it can be defined the following matrices:

$$A_1 = \bar{A}(\alpha_{min}),\ A_2 = \bar{A}(I), E_1 = \bar{E}(\alpha_{min}),\ E_2 = \bar{E}(I) \tag{7.21}$$

and the dynamics can be written in polytopic form, making $x_s = u_s = d_s = 0$:

$$x_{k+1} = A(\zeta)x_k + E(\zeta)d_k \tag{7.22}$$

where $A(\zeta) = \sum_{i=1}^{2} \zeta_i A_i$ and $E(\zeta) = \sum_{i=1}^{2} \zeta_i E_i$, with $\sum_{i=1}^{2} \zeta_i = 1$, $\zeta_i \geq 0$. In the present case, the invariant set will be computed for the polytopic system (7.22), according to the procedure introduced in Section 4.2.5. Before performing the computation of the invariant set, it should be verified that the eigenvalues of A_1, A_2 are strictly inside the unitary circle. Otherwise some work should be done with the product $\boldsymbol{H}^{-1}\boldsymbol{K_1}$, by selecting other values in the weighing matrices Q, R, S.

7.1.3.4 Obtention of the ellipsoidal invariant sets

An ellipsoidal invariant set could be obtained by finding a common Lyapunov matrix P for the polytopic system (7.22). This is possible by solving the following LMI to obtain P and the minimum value of γ:

$$\begin{bmatrix} x \\ d \end{bmatrix}^T \begin{bmatrix} A_i^T P A_i - P + I_n & A_i^T P E_i \\ E_i^T P A_i & E_i^T P E_i - \gamma^2 I_q \end{bmatrix} \begin{bmatrix} x \\ d \end{bmatrix} \leq 0, \quad i = 1, 2 \tag{7.23}$$

Considering that $d^T d \leq \bar{d}^T \bar{d}$, being $\bar{d}$ the maximum admissible absolute values of the disturbances, an invariant set for the family of systems that results after applying a constrained MPC strategy will be:

$$\bar{\Pi}_N = \{x \in \Re^n : x^T P x \leq \lambda_{max}(P)\gamma^2 \bar{d}^T \bar{d}\} \tag{7.24}$$

7.1.4 Recursive algorithm for computing the minimal robust invariant set

Following the performance analysis using invariant sets, in this section is detailed the recursive algorithm for computing the mRPI. It is analyzed the first states set for the recursive algorithm. Then, it is shown how to process the input constraints polyhedral set at every step in the recursive algorithm. The recursive algorithm is detailed and resumed in Algorithm 3 chart.

7.1.4.1 Selection of initial polyhedral set

The computation of the mRPI for the receding horizon controlled system, can use two initial polyhedral sets $\mathcal{S}(0)$: a first one given as the polyhedral approximation of the ellipsoidal set $\bar{\Pi}_N$ obtained in (7.24). The other one is a small polyhedral set, obtained from a small ball that includes the origin.
The stopping criterion for the algorithm depends relies on the initial set selected: if the initial set is $\bar{\Pi}_N$, this set is shrieked up to containing a small ball of radius ϵ. In the other case, it is applied an expanding procedure and some analysis of the norm of A^k, being k the steps can be used.

7.1.4.2 Adaptation of the constraints polyhedral set at each iteration

Because the procedure for computing the mRPI is based in the dynamical equation of the system, it is necessary to arrange the input section, that includes a saturation-like mechanism that assures the system constraints.
The following expression, based on the system dynamics (7.1) is used as the recursive expression that delivers the approximated mRPI, where $\mathcal{S}(k)$ is the states set with $\mathcal{S}(0)$ selected as suggested in Section 7.1.4.1, the disturbances set $\mathcal{D}_{max}$, formed by the extreme values as seen in (7.2) and the extended constrained inputs set $\boldsymbol{U}_c(k)$, along the matrix K_u that takes only the first elements of the latter set:

$$\mathcal{S}(k+1) = A\mathcal{S}(k) \oplus BK_u\boldsymbol{U}_c(k) \oplus E\mathcal{D}_{max} \tag{7.25}$$

However, for obtaining the set $\boldsymbol{U}_c(k)$ at $t = k$, one can use the constraints set definition definition (4.24) - (4.25):

$$L\boldsymbol{u} \leq W(x_0, u_{-1}), \text{with } W = \Delta + \bar{\xi}x_0 + \bar{\xi}_u u_{-1}$$

According to the structure of the constraints definition, L is a matrix with $r_L = rank(L)$ rows and $N.m$ columns, being N the prediction horizon and m the length of the input vector. L gives the quantity of constraints that should be accomplished by the system.
By other side, and considering that any system variable (for example, named $z \in \Re$) has a valid admissible range around the origin, not necessary symmetrical, defined as:

$$\mathcal{Z} = \{z \in \Re : z_{min} \leq z \leq z_{max}, 0 \in \mathcal{Z}\} \tag{7.26}$$

Therefore, the constraints polyhedral description has that Δ is a positive vector in $\Re^{r_L}$ that has information of the maximum admissible value of each $r_L - ith$ inequality.
Remark that for each $x_0 \in \Re^n$ and, if required, each past control vector $u_{-1} \in \Re^m$, the constraints polyhedral will change, because their mapping into the space of $\boldsymbol{u}$ affect the right side of the constraints expression. The so-mentioned mapping defines the following set:

$$\mathcal{W}_s(k) = \bar{\xi}\mathcal{S}(k) \oplus \bar{\xi}_u\mathcal{U}(k-1) \tag{7.27}$$

This Minkowski sum delivers a polyhedron of maximum $V_w = V_x.V_{u-}$ vertex, being V_x and V_{u-} the number of vertex of current states and past inputs admissible sets, respectively. Then, it is defined the following matrix Δ':

$$\Delta' = \Delta \oplus \mathcal{W}_s \tag{7.28}$$

That performs the modification of the original Δ with the mapping set $\mathcal{W}_s$. This last set is defined in the space $\Re^{r_L \times V_w}$, defining along L, at most $r_L.V_w$ constraints at each $t = k$. In fact, The following subsets can be defined:

$$\boldsymbol{U}_{c(i)}(k) = \{\boldsymbol{u} \in \Re^m : L\boldsymbol{u} \leq \Delta'_i\};\ j = 1 \cdots V_w \tag{7.29}$$

where the term Δ'_i is in fact the $i-th$ column from the set Δ'. At the end, one can obtain a constrained control polytope as the convex hull of the subsets (7.29):

$$\boldsymbol{U}_c(k) = hull\{\boldsymbol{U}_{c(i)}(k), i = 1 \cdots V_w\} \tag{7.30}$$

Nevertheless, under some particular conditions in states and/or past inputs sets, some elements of Δ'_i would be negative, making infeasible the set $\boldsymbol{U}_{c(i)}$. This would occur when part of x_0 or u_{-1} lie outside the admissible sets $\mathcal{X}$,$\mathcal{U}$, that can happen due to overshoots, wrong initialization, input saturations/disturbances, and others conditions. As consequence, the $i-th$, generally an open set, impeds the operation (7.30) in a good way.

If this happens, the following mechanism can be used with favourable results: One can create a vector $\Delta'_{def} \in \Re^{r_L}$ by taking the *maximum positive value* of each $i-th$ row of Δ', that is related as the greatest admissible inputs set that can be used in the system:

$$\Delta'_{def} \in \Re^{r_L} \text{ where } \Delta'_{def,i} = max\{\Delta'_{i,j}\}, \forall i = 1 \cdots r_L, \forall j = 1 \cdots V_w \tag{7.31}$$

And the inputs constrained set is defined in terms of this vector as:

$$\boldsymbol{U}_c(k) = \{\boldsymbol{u} \in \Re^m : L\boldsymbol{u} \leq \Delta'_{def}\} \tag{7.32}$$

The Fig 7.3 represents the mapping procedure and the selection of the right side vector Δ'_{def} (called W_{max} in the figure), with $r_L = 2$ for easy interpretation. It is seen how the Minkowski sums (7.27)-(7.28) generate a space from where the maximum size vector is taken for building the polyhedral set.

Remark: The obtained set in (7.32) is equivalent to the set obtained with (7.29). The second method selects the extreme hyperplanes for building the maximum admissible set, that is similar to the mechanism of using the convex hull of the admissible input sets. However, considering the computation time it is recommended the second method over the first one, because it takes less computational time finding the maximum values for each hyperplane of the set that performing a convex combination of multiple sets that can have a high number of vertexes.

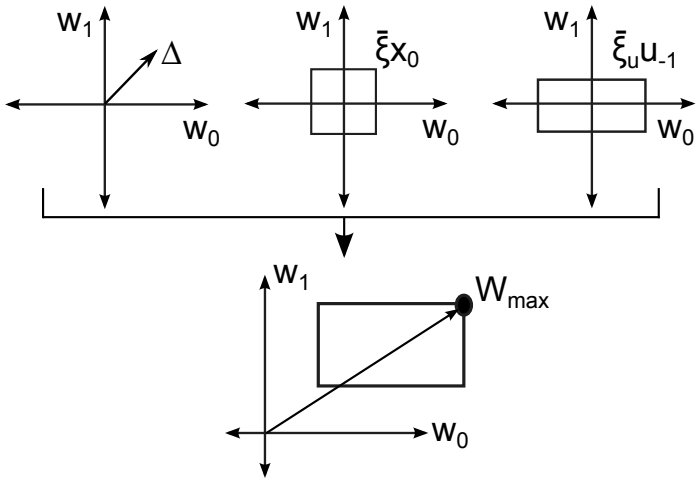

Figure 7.3: Scheme for chosing the limit vector when updating the inputs set

Remark: More precisely, each row of Δ' delivers new admissible values that can be accomplished by the $i-th$ inequality ($i = 1 \cdots r_L$) in the mapped set. Therefore, the new input set

is indeed composed by $r_L \times V_w$ hyperplanes that gather the effect of all potential points in the states and past input sets.

Considering the second condition that is *a priori* more complex, in computational terms that using the convex hull of sets, the following example is included for better interpretation.

Example 7.1. *Assume the following constraints definition for a second order system $n = 2, m = 1$ with prediction horizon $N = 2$:*

$$\underbrace{\begin{bmatrix} 1 & 1 \\ 1 & -2 \\ 1 & 0 \\ -1 & 0 \end{bmatrix}}_{L} \begin{bmatrix} u_0 \\ u_1 \end{bmatrix} \leq \underbrace{\begin{bmatrix} 1 \\ 2 \\ 1 \\ 2 \end{bmatrix}}_{\Delta} + \underbrace{\begin{bmatrix} -0.5 & -0.1 \\ 1 & 0.2 \\ 0 & 0 \\ 0 & 0 \end{bmatrix}}_{\xi} x_0$$

Now, assume the following states set:

$$\mathcal{X}_0 : \{-1 \leq x_1 \leq 1 \ ; \ -1 \leq x_2 \leq 1\}$$

Proceeding with the mapping of states, the following $\mathcal{W}_s$ is obtained, in matrix (vertex) form:

$$\mathcal{W}_s = \xi \mathcal{X}_0 = \begin{bmatrix} -0.4 & -0.6 & 0.4 & 0.6 \\ 0.8 & 1.2 & -0.8 & -1.2 \\ 0 & 0 & 0 & 0 \\ 0 & 0 & 0 & 0 \end{bmatrix}$$

Next, the Minkowski sum between $\mathcal{W}_s$ and Δ is computed:

$$\Delta' = \mathcal{W}_s \oplus \Delta = \begin{bmatrix} 0.6 & 0.4 & 1.4 & 1.6 \\ 2.8 & 3.2 & 1.2 & 0.8 \\ 1 & 1 & 1 & 1 \\ 2 & 2 & 2 & 2 \end{bmatrix}$$

Using the proposed approach, in which the maximum positive values for each row at Δ' are selected for creating Δ'_{def}, the following result is obtained for the inputs set:

$$\underbrace{\begin{bmatrix} 1 & 1 \\ 1 & -2 \\ 1 & 0 \\ -1 & 0 \end{bmatrix}}_{L} \begin{bmatrix} u_0 \\ u_1 \end{bmatrix} \leq \underbrace{\begin{bmatrix} 1.6 \\ 3.2 \\ 1 \\ 2 \end{bmatrix}}_{\Delta'_{def}}$$

In Fig. 7.4 are shown the definitive inputs sets (at right), obtained from the last set definition, as well as the input subsets obtained after using each column from Δ' with L, obtaining the sets $S1 \cdots S4$. It is seen how, effectively, the resulting input set is the convex hull of the obtained set by mapping each point of $\mathcal{X}_0$.

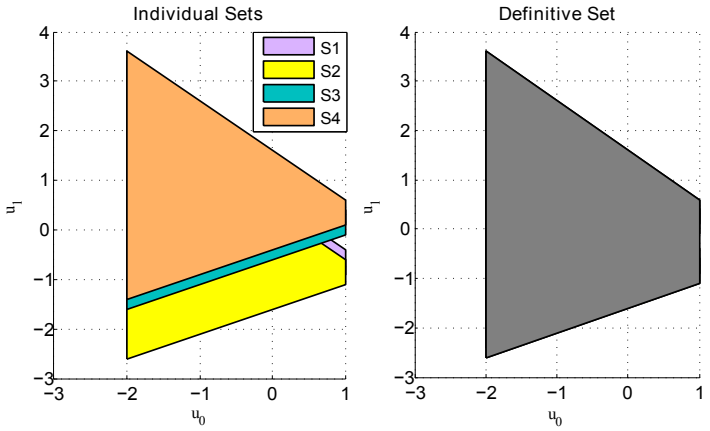

Figure 7.4: Selection of the admissible inputs set for the MPC strategy

7.1.4.3 Algorithm for computing the mRPI

The Algorithm 3 presents the procedure for computing mRPI sets approximations for receding horizon control applications. However, some aspects will be discussed next.
In first place, the following recursive equation, based in the system dynamics is used for updating the states set:

$$\mathcal{S}(k+1) = A\mathcal{S}(k) \oplus BK_u\boldsymbol{U}_c(k) \oplus E\mathcal{D}_{max} \tag{7.33}$$

In second place, the input set $\boldsymbol{U}_c(k)$ is obtained according to the procedure presented in Section 7.1.4.2. Because it is obtained a set that gathers all the control sequences for any states and last input sets, the use of K_u for only applying the first elements is used, as refereed in the MPC context.
Third, the set $\boldsymbol{U}(k-1)$ in the mapping expression (7.27) is obtained after computing the set $\boldsymbol{U}_c(k)$, multiply it by K_u and store the result for the following step.
Fourth, the initial state set $\mathcal{S}(0)$ is taken from the invariant set computed for polytopic systems $\bar{\Pi}_N$, as detailed in Section 7.1.2.

Algorithm 3 Computation of mRPI sets for constrained receding horizon controlled linear systems

Require: Discrete-time system model matrices: A, B, E, with $\|eig(A)\| < 1$ and $\|eig(E)\| < 1$
Require: Constraints polyhedral matrices $L, \Delta, \bar{\xi}, \bar{\xi}_u$, according to (4.25)-(4.26). In case of not control inputs derivative penalizations, set $\bar{\xi}_u = 0$.
Require: Computation of the ellipsoidal invariant set for the system in closed-loop (multi-system approach), according to Section 7.1.2. It is obtained $\bar{\Pi}_N$.
START
S1: Set $k = 0$. Then, select the initial states polyhedron $\mathcal{S}(0) = \bar{\Pi}_N$.
S2: Compute the constraints polyhedral set $\boldsymbol{U}_c(k)$, as exposed in Section 7.1.4.2.
S3: Obtain the states polyhedron evolution with (7.33). If required, assign $\mathcal{U}(k-1) = K_u\boldsymbol{U}_c(k)$ for the input's derivative constraints (next iteration).
if $A^k\mathcal{S}(0) \nsubseteq \mathcal{B}_\epsilon^p$ **then**
Increase $k = k+1$ and return to **S2**.
else
Return $\mathcal{S}(k)$ as the outer ϵ-approximation of the minimal Robust Invariant Set.
end if

7.1.5 Illustrative Example

Here, it is considered a second order system to illustrate the invariant set computation and the proposed coordinated control approach. Taking $T_s = 1/150s$, the dynamical model is:

$$x_{k+1} = \begin{bmatrix} 0.9667 & 0.0133 \\ -0.0067 & 0.9733 \end{bmatrix} x_k + \begin{bmatrix} -0.0333 & 0.0033 \\ 0.0333 & 0.0167 \end{bmatrix} u_k + \begin{bmatrix} -0.0067 & 0.0033 \\ 0.0013 & 0.0067 \end{bmatrix} d_k$$

The eigenvalues for this system are equal to ($\lambda_{1,2} = 0.97 \pm 0.0088j$). The following weighting matrices (P is obtained from the solution of the discrete-time LQR) and constraint vectors are used for the constrained control problem:

$$Q = \begin{bmatrix} 100 & 0 \\ 0 & 100 \end{bmatrix};\ R = \begin{bmatrix} 1 & 0 \\ 0 & 1 \end{bmatrix};\ S = \begin{bmatrix} 0 & 0 \\ 0 & 0 \end{bmatrix};\ P = \begin{bmatrix} 452.56 & 195.15 \\ 195.15 & 431.85 \end{bmatrix};\ N = 2;$$

$$x_{min} = \begin{bmatrix} -2 \\ -2 \end{bmatrix};\ x_{max} = \begin{bmatrix} 2 \\ 2 \end{bmatrix}; u_{min} = \begin{bmatrix} -3 \\ -3 \end{bmatrix};\ u_{max} = \begin{bmatrix} 3 \\ 3 \end{bmatrix}; d_{min} = \begin{bmatrix} -1 \\ -1 \end{bmatrix};\ d_{max} = \begin{bmatrix} 1 \\ 1 \end{bmatrix}$$

Using the procedure of section 7.1.2, it is verified the small gain theorem, where $\gamma_G.\gamma_K < 1$. The gain $\gamma_G = 1.5030$ is obtained after solving the LMI (7.7). On the other hand, then gain $\gamma_K = 0.0622$ is obtained from the maximum element-wise gain of the matrix K_{lw} presented in (7.9). The product $\gamma_G.\gamma_K = 0.0933 < 1$, allows to conclude that the constrained feedback is stable. Considering the model and the constrained control strategy, the following matrices can be used to describe the behavior of its equivalent polytopic model:

$$A_1 = \begin{bmatrix} 0.9467 & 0.0260 \\ 0.0051 & 0.9491 \end{bmatrix};\quad A_2 = \begin{bmatrix} 0.7622 & 0.1411 \\ 0.1082 & 0.7193 \end{bmatrix}$$
$$E_1 = \begin{bmatrix} -0.0064 & 0.0034 \\ 0.0012 & 0.0064 \end{bmatrix};\quad E_2 = \begin{bmatrix} -0.0041 & 0.0035 \\ -0.0004 & 0.0043 \end{bmatrix}$$

Thus, the matrix P which describes the common Lyapunov function and the constant γ associated for the family of the two systems are:

$$P = \begin{bmatrix} 39.5074 & -25.0582 \\ -25.0582 & 68.5678 \end{bmatrix};\ \gamma = 0.2495$$

The obtained ellipsoidal invariant set $\Pi(0)$ is depicted in Figure 7.5.

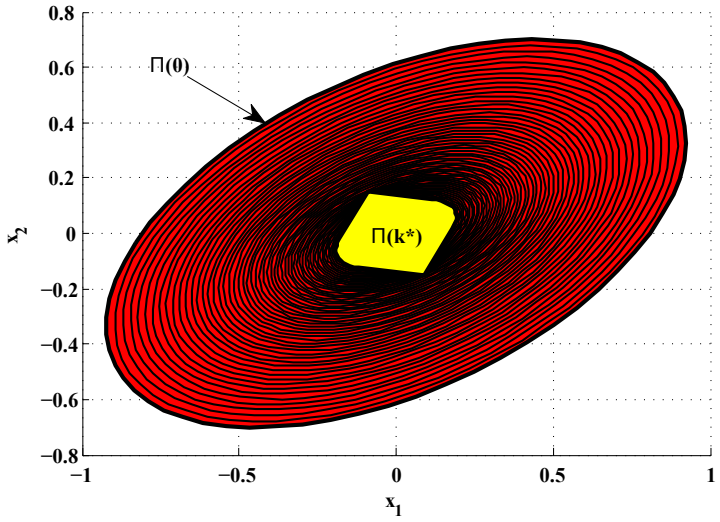

Figure 7.5: Invariant sets for evaluating the performance of a constrained control system

Outer approximation of the mRPI

Now, using as initial set an invariant polyhedral set approximation of the ellipsoidal invariant set, it is then computed an approximation of the minimal invariant set. Here, it is considered the expression (7.33). The input set is adapted at each step as indicated in Section 7.1.4.2. Because the equivalent dynamic response of the closed-loop system is slow, an ϵ-ball of radius 0.1 was used as stopping criterion for the recursive algorithm. In Figure 7.5 it is shown the ellipsoidal invariant set and the outer approximation of the mRPI set, that is obtained after $h* = 54$ iterations. This set is denoted as $\Pi(k*)$

7.2 Global Performance Analysis for a Distributed Constrained Control System with Coordination

In this section, the same invariant sets-based performance analysis, introduced in Section 7.1, will be adapted for an architecture of distributed control with the same characteristics of the *price-driven coordination* strategy shown in the Chapter 6.
The stability analysis using the small gain theorem, as well as the performance analysis of the system under coordination using invariant sets allows to determinate the behavior of a distributed system with local model predictive controllers with a coordination strategy that absorbs the local constraints. In this way, further analysis for high scale system can be developed using the same principles exposed in the dynamic system under MPC.
The computation of the invariant sets, also looking for a minimal representation, is performed in a "centralized manner". More precisely, the interactions components v_k are explicitly used in the dynamical model, using therefore a unique (centralized) expression for computing the invariant sets. However, the computational load can be high enough due to the characteristics of the states set and the interactions that should be considered for building the sets.
The results here obtained will be used in a future methodology included in Section 7.3, in which invariant sets for each subsystem are *locally* computed, while considering the coordination mechanism widely exposed in Chapter 6. In this approach, the states sets are merged, obtaining an ultimate bound that contains the invariant set.

7.2.1 System dynamics, admissible sets and control structure for the distributed coordinated control scheme

Consider the following open loop expressions for the distributed system, based in the global dynamical equation (7.1), (see Chapter 6 for more details):

$$\begin{aligned} x_{k+1} = &\quad A_d x_k + B_d u_k + E_d d_k + v_k \\ v_k = &\quad v_A x_k + v_B u_k + v_E d_k \end{aligned} \tag{7.34}$$

where A_d, B_d, E_d are the diagonal submatrices from the global system dynamics represented at (7.1), and v_k is the global interactions vector, where $v_A = A - A_d$, $v_B = B - B_d$ and $v_E = E - E_d$. From Section 6.1.2, it was obtained that one can write the predicted states and their variation for a prediction horizon N as:

$$\begin{aligned} \boldsymbol{x} &= \Omega_d \; x_0 + \Psi_d \; \boldsymbol{u_{ext}} + \Theta_d \; \boldsymbol{d} \\ \tilde{\boldsymbol{x}} &= \Omega_d \; (x_0 - x_s) + \Psi_d \; (\boldsymbol{u_{ext}} - \boldsymbol{u_{ext-s}}) + \Theta_d \; (\boldsymbol{d} - \boldsymbol{d_s}) \end{aligned} \tag{7.35}$$

and the interactions extended vector holds:

$$0 = \overline{\Psi}\boldsymbol{u_{ext}} + \overline{\Omega}\ x_0 + \overline{\Theta}\ \boldsymbol{d} \tag{7.36}$$

where $\boldsymbol{u_{ext}} = [\boldsymbol{u}^T \ \ \boldsymbol{v}^T]^T$ is the extended control vector.

Finally, the optimization problem (7.37), written in terms of two decision variables $\boldsymbol{u_{ext}}$ and $\boldsymbol{p}$, is obtained. In the optimization problem, $\boldsymbol{p}$ is a Lagrange multiplier vector for including the interactions vector in the cost function $J_{ext}(\boldsymbol{u_{ext}}, \boldsymbol{p})$ and will be used for the subsystems coordination. The matrices for the cost function are detailed in (6.22), and ones for the constraints polyhedron are defined in (6.26)-(6.27).

$$\begin{gathered} J_{ext}(\boldsymbol{u_{ext}}, \boldsymbol{p}) = \bar{V}_{ext} + \tfrac{1}{2}\boldsymbol{u_{ext}^T H_c u_{ext}} + \boldsymbol{u_{ext}^T}[\boldsymbol{K_{1c}}(x_0 - x_s) + \boldsymbol{K_{2c}}(\boldsymbol{d} - \boldsymbol{d_s}) + \boldsymbol{K_{3c}p} - \boldsymbol{H_c u_{ext_s}}] + \\ \boldsymbol{p^T}(\overline{\Omega}x_0 + \overline{\Theta}\boldsymbol{d}) \end{gathered}$$

$$\begin{gathered} \max_{\boldsymbol{p}} \min_{\boldsymbol{u_{ext}}} J_{ext}(\boldsymbol{u_{ext}}, \boldsymbol{p}) \\ \text{subject to } L_{ext}\boldsymbol{u_{ext}} \leq W_{ext} \end{gathered} \tag{7.37}$$

From (7.37) it is obtained the following unconstrained solution for $\boldsymbol{u_{ext}}$:

$$\boldsymbol{u_{ext}^{opt}} = -\boldsymbol{\varphi_1}(x_0 - x_s) - \boldsymbol{\varphi_2}(\boldsymbol{d} - \boldsymbol{d_s}) - \boldsymbol{\varphi_3 p} + \boldsymbol{u_{ext-s}} \tag{7.38}$$

that, replaced in (7.37), allows to write the optimization problem only in the variable $\boldsymbol{p}$ (the matrices are defined in (6.40)-(6.42)):

$$\begin{gathered} J_{ext} = \bar{V}_p + \tfrac{1}{2}\boldsymbol{p}^T\boldsymbol{H_p p} + \boldsymbol{p}^T[\boldsymbol{K_{1p}}\tilde{x}_0 + \boldsymbol{K_{2p}}\tilde{\boldsymbol{d}} + \boldsymbol{K_{3p}u_{ext(i)_s}}] + \boldsymbol{p}^T(\bar{\Omega}x_0 + \bar{\Theta}\boldsymbol{d}) \\ \begin{aligned} \max_{\boldsymbol{p}} \quad & J_{ext}(\boldsymbol{p}) \\ \text{subject to} \quad & L_p\boldsymbol{p} \leq W_p \end{aligned} \end{gathered} \tag{7.39}$$

After these procedures, a couple of expressions will be taken into account. The first one is the global system dynamics in terms of the interactions vector $\boldsymbol{p}$. Replacing (7.38) into (7.1), it is obtained:

$$\begin{aligned} x_{k+1} = \ & Ax_k + BK_{uext}\left(-\boldsymbol{\varphi_1}\tilde{x} - -\boldsymbol{\varphi_2}\tilde{\boldsymbol{d}} - \boldsymbol{\varphi_3 p} + \boldsymbol{u_{ext-s}}\right) + Ed_k \\ x_{k+1} = \ & (A - BK_{uext}\boldsymbol{\varphi_1})x_k + (E - BK_{uext}\boldsymbol{\varphi_2}K_d)d_k + (-BK_{uext}\boldsymbol{\varphi_3 p}) \\ & + B(K_{uext}\boldsymbol{\varphi_1}x_s + K_{uext}\boldsymbol{\varphi_2}K_d d_s + u_s) \\ x_{k+1} = \ & A_p x_k + E_p d_k + F_p\boldsymbol{p} + f_p(x_s, u_s, d_s) \end{aligned} \tag{7.40}$$

where K_{uext} is a matrix that helps to take only the first m elements from $\boldsymbol{u_{ext}}$ and $K_d = [I_{q\times q} \cdots I_{q\times q}]^T$ is a matrix for generating an N-horizon disturbance vector after the vector d_k. This expression will be useful for the stability analysis of the coordinated system.

The second expression, that is obtained is the explicit solution for the optimization problem (7.39), will be:

$$\boldsymbol{p}^*_{wc} = -\boldsymbol{H_p^{-1}}[\boldsymbol{K_{1p}}(x_0 - x_s) + \bar{\Omega}x_0 + \boldsymbol{K_{2p}}(\boldsymbol{d} - \boldsymbol{d_s}) + \bar{\Theta}\boldsymbol{d} + \boldsymbol{K_{3p}u_{ext-s}}] \tag{7.41}$$

7.2.2 Stability analysis of the distributed coordinated control scheme

As performed for the constrained receding horizon control case, in this case it is also applied the small gain theorem, exposed in Section 7.1.1, for verifying the global system stability when using the price-driven coordination strategy.

Here, the block $G(s) = x(s)/p(s)$ represents the plant in which the evolution of states x is affected by the coordination vector value $\boldsymbol{p}$. By other side, the controller block transfer function $K(s) = p(s)/x(s)$ delivers a coordination vector according to the states values. Therefore, it is obtained the closed-loop system as required for using the small gain theorem.
In this case, the gains γ_G and γ_K are computed as follows:

- For the gain γ_G, concerning the states-to-coordination vector gain, it is used the LMI presented in (7.42), applied to the dynamics (7.40). Therefore, the following LMI is solved for obtaining such gain:

$$\begin{bmatrix} x \\ \boldsymbol{p} \end{bmatrix}^T \begin{bmatrix} A_p^T P A_p - P + I_n & A_p^T P F_p \\ F_p^T P A_p & F_p^T P F_p - \gamma_G^2 I_{d_p} \end{bmatrix} \begin{bmatrix} x \\ \boldsymbol{p} \end{bmatrix} \leq 0 \tag{7.42}$$

  where $d_p = N.(n+m)$ is the product between the prediction horizon.

- For finding the value γ_K, it is used the expression of the constraints polyhedral for $\boldsymbol{p}$, originally presented in (6.26)-(6.27):

$$\begin{array}{rl} \boldsymbol{P} : \{\boldsymbol{p} \in & L_p \boldsymbol{p} \leq W_p(x_0, d_0, u_{-1})\} \\ \text{with,} & W_p = \overline{W}_p + W_{xp} x_0 + W_{dp} \boldsymbol{d} + W_{up} u_{ext-1} \end{array} \tag{7.43}$$

  It is only interesting the maximum element-wise gain (for the l_p inequalities that defines the constraints set) between the states x_k and the coordination vector $\boldsymbol{p}$, that is obtained from finding the biggest element from the gain matrix between $\boldsymbol{p}$ and x:

$$\boldsymbol{p} = L_p^{\dagger} \bar{W}_{xp} x_0 = K_{plw} x_0 \tag{7.44}$$

  After this, the gain γ_K is obtained from the following operation:

$$\gamma_K = \|\bar{\gamma}\|_\infty, \text{ where } \bar{\gamma}_i = \|K_{plw}\|_\infty \quad \text{for } i = 1 \cdots rank(K_{plw}) \tag{7.45}$$

If $\gamma_G \gamma_K < 1$ is verified, it is assured that the distributed system with the coordination mechanism provided by the price-driven based strategy is closed-loop stable, in relation with the gain matrices. Now, the performance of the closed-loop system can be evaluated as we will illustrate in the next Section.

7.2.3 Performance analysis of the distributed coordinated control using invariant sets

Here, it is presented the detailed procedure for computing the invariant set for the distributed coordinated control scheme. The basis for this analysis was presented in the case of the constrained MPC system (see Section 7.1.3).

7.2.3.1 Analysis of the closed-loop system

In the Fig. 7.4 is depicted the structure of the closed-loop configuration for the distributed and coordinated control system. Although reference values x_s, u_s, d_s are included in the expressions, it is assumed the origin as reference for the three vectors. The following elements are identified from the scheme:

- The system dynamics is influenced by the presence of disturbances d_k and current control signal u_k. The structure does not change from the standard configuration.
- The system controller has a cascade-like configuration. The inner loop controller, whose structure is given by (7.38)is formed by a state feedback part, a disturbance compensator and received the coordination vector $\boldsymbol{p}$ computed by the coordinator. This block computes the control sequence $\boldsymbol{u}_{ext}$ that respects the constraints of the global system.
- The outer control loop is located in the coordination entity. It has two blocks: one that computes an unconstrained coordination vector $\boldsymbol{p}_{uc}$ as indicated by (7.41) and a saturation block that restricts the coordination vector components according to the constraints polyhedron (4.35) and that delivers $\boldsymbol{p}$, that respects the constraints, to all the subsystems. This function can also be simplified with a saturation function, that is next analyzed.

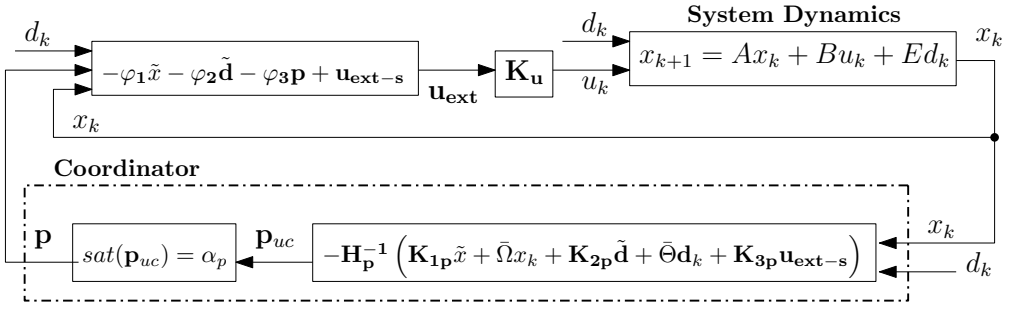

Reference values ignored in the scheme: x_s, u_s, d_s

Figure 7.6: Closed-loop system representation with constrained price-driven coordination

Considering that control signals are computed with an explicit equation and that constraints should be accomplished by the coordination vector, it is seen again that for relating the vectors $\boldsymbol{p}$ and $\boldsymbol{p}_{uc}$, one can use the following expression:

$$\boldsymbol{p} = \alpha_p \boldsymbol{p_{uc}} \tag{7.46}$$

where $\alpha_p \in \Re^{d_p \times d_p}$, with $d_p = N.(n+m)$ is a numerical matrix that accomplish the following property:

$$0_{d_p \times d_p} < \alpha_{p,min} < \alpha_p \leq I_{d_p \times d_p} \tag{7.47}$$

In this case, α_p is also a diagonal matrix that aids to write, in a polytopic fashion, the closed-loop system expressions for the coordinator case. A method for computing this matrix is here presented.

7.2.3.2 Computation of $\bar{\alpha}_{min}$ for the distributed coordinated control scheme

The computation of this matrix is not as straightforward than the case of its equivalent α_{min} for the MPC control. Remember that $\boldsymbol{p}$, used as coordination element, is indeed a Lagrange Multiplier for including some equality constraints to the optimization problem. Also and based in the duality property for solving multiparametric optimization problems [55], the problem is finally written only in $\boldsymbol{p}$.
However, the constraints are still refereed to disturbances, states and inputs values, and also the constraints polyhedral changes with the signals evolution. Thus, limits over $\boldsymbol{p}$ are time variant,

different from the well-known limits for $\boldsymbol{u}$ for the the MPC case.
However, one can use some conservative situations for computing this matrix. The hypothesis behind the method is that states, disturbances and inputs vector are included in the admissible sets $\mathcal{X}$,$\mathcal{U}$,$\mathcal{D}$. Due to the state feedback control that gives $\boldsymbol{p}_{uc}$ and the subsequent constraining operation for computing $\boldsymbol{p}$, over the same sets, there would be attenuation for some components of the coordination vector. The selection of the matrix is depicted as follows:

- First, define the sets $\mathcal{X}$,$\mathcal{U}$,$\mathcal{D}$,$\mathcal{V}$, as well as all matrices involved in the explicit $\boldsymbol{p}_{uc}$ computation, as well as the $\boldsymbol{u_{ext}}$ after computing $\boldsymbol{p}$.

- Compute the following *unconstrained coordination* set, obtained from (7.41), while setting $x_s = u_{ext-s} = d_s = 0$:

$$\boldsymbol{P}_{uc} = [-\boldsymbol{H_p^{-1}}(\boldsymbol{K_{1p}} + \bar{\Omega})]\mathcal{X} \oplus [-\boldsymbol{H_p^{-1}}(\boldsymbol{K_{2p}} + \bar{\Theta})K_d]\mathcal{D} \tag{7.48}$$

  where $\boldsymbol{d} = K_d d_k$ and $K_d = [I_{qxq} \cdots I_{qxq}]^T$.

- The set of constrained coordination vectors $\boldsymbol{P}$ can be obtained after (7.38), when answering the following question: what should be the value of the coordination vector ($\boldsymbol{P}$), for obtaining an admissible extended control set ($\boldsymbol{U}_{ext}$), when states and disturbance are in their admissible sets ($\mathcal{X}$,$\mathcal{U}$)? Then, one can obtain this set from the following expression, derived after isolating $\boldsymbol{p}$:

$$\boldsymbol{P} = (-\boldsymbol{\varphi_3}^{\dagger}\boldsymbol{\varphi_1})\mathcal{X} \oplus (-\boldsymbol{\varphi_3}^{\dagger}\boldsymbol{\varphi_2}K_d)\mathcal{D} \oplus (-\boldsymbol{\varphi_3}^{\dagger})\boldsymbol{\mathcal{U}}_{ext} \tag{7.49}$$

  , with the superindex † equivalent to the pseudoinverse matrix operation.

- Remark that both sets will be in the space of $\boldsymbol{p}$. Then, one can extract the maximum and minimum values for each dimension from the sets $\boldsymbol{P}$ and $\boldsymbol{P}_{uc}$. Expressing this sets in matrix form $P_{uc} \in \Re^{d_p \times V_{puc}}$ and $P_c \in \Re^{d_p \times V_{pc}}$, where $d_p = N.(n+m)$, V_{puc}, V_{pc} are the vertex of their respective sets.
  From these matrices, determine the extreme vectors $p_{c,min}$, $p_{c,max}$, $p_{uc,min}$, $p_{uc,max} \in \Re^{N.(n+m)}$ that are the vectors build after finding the extreme values for each dimension.

- Next, there is defined the following vectors p'_{max}, p'_{min}:

$$p'_{max}(i) = p_{c,max}(i)/p_{uc,max}(i);\ p'_{min}(i) = p_{c,min}(i)/p_{uc,min}(i)\ \forall i = 1 \cdots N.(n+m)$$

- Finally, the diagonal elements of $\bar{\alpha}_p$ are obtained by finding the smallest value between each element of p'_{max} and p'_{min}. The following vector p_α is created:

$$p'_\alpha(i) = inf\{p'_{max}(i), p'_{min}(i)\} \forall i = 1 \cdots N.(n+m)$$

  and the matrix α_p is obtained as $diag\{p'_\alpha\}$.

Although this methodology for finding α_p might be conservative, after being based in the same linear relations given by the state feedback expressions of the equivalent coordinated system, the results can be used for obtaining an invariant set approximation that could be consistent with the admissible sets.

7.2.3.3 Computing the ellipsoidal invariant set

For obtaining the ellipsoidal invariant set representation, it is first written u_k in terms of $\boldsymbol{p}$. Using the matrix K_{uext} for taking the first m elements from the extended control sequence $\boldsymbol{u_{ext}}$, the expression (7.38) becomes:

$$u_k = -K_{uext}\left(\boldsymbol{\varphi_1}\tilde{x} + \boldsymbol{\varphi_2}\tilde{\boldsymbol{d}} + \boldsymbol{\varphi_3 p} - \boldsymbol{u_{ext-s}}\right) \tag{7.50}$$

In second place, the coordination vector value $\boldsymbol{p}$ is written in terms of its unconstrained version $\boldsymbol{p}_{uc}$. The relation between the vectors is shown in (7.41) and the unconstrained coordination vector structure is shown in (7.46). Now, after replacing these expressions into (7.50) it is obtained the following structure for u_k:

$$u_k = K_{uext}\left[\zeta_x(\alpha_p)x_k + \zeta_d(\alpha_p)K_d d_k + f_p(x_s, u_s, d_s, \alpha_p)\right] \tag{7.51}$$

where $K_d = [I_{qxq} \cdots I_{qxq}]^T$ for writing $\boldsymbol{d} = K_d d_k$ and the functions ζ_x, ζ_d, f_p are defined as follows:

$$\begin{aligned} \zeta_x &= \varphi_3\alpha_p\boldsymbol{H_p^{-1}}(\boldsymbol{K_{1p}} + \bar{\Omega}) - \varphi_1 \\ \zeta_d &= \varphi_3\alpha_p\boldsymbol{H_p^{-1}}(\boldsymbol{K_{2p}} + \bar{\Theta}) - \varphi_2 \\ f_p &= (\varphi_3\alpha_p\boldsymbol{H_p^{-1}K_{3p}} + I)\boldsymbol{u_{ext-s}} - (\zeta_x - \varphi_3\alpha_p\boldsymbol{H_p^{-1}K_{1p}}\bar{\Omega})x_s - (\zeta_d - \varphi_3\alpha_p\boldsymbol{H_p^{-1}K_{2p}}\bar{\Theta})\boldsymbol{d_s} \end{aligned} \tag{7.52}$$

Replacing (7.51) in the standard system dynamics, the following closed-loop system dynamics, considering the constrained coordination is obtained:

$$\begin{aligned} x_{k+1} &= Ax_k + BK_{uext}(\zeta_x x_k + \zeta_d K_d d_k + f_p) + Ed_k \\ x_{k+1} &= (A + BK_{uext}\zeta_x)x_k + (E + BK_{uext}\zeta_d K_d)d_k + BK_{uext}f_p \\ x_{k+1} &= \bar{A}_p(\alpha_p)x_k + \bar{E}_p(\alpha_p)d_k + \bar{\delta}_p \end{aligned} \tag{7.53}$$

The last expression is suitable for obtaining an invariant set representation for the proposed coordinated control approach. As performed for the constrained MPC case, the following system and disturbance matrix can be obtained from (7.53), taking the extreme values of α_p:

$$A_{1p} = \bar{A}_p(\alpha_{p,min}),\ A_{2p} = \bar{A}_p(I), E_{1p} = \bar{E}(\alpha_{p,min}),\ E_{2p} = \bar{E}_p(I) \tag{7.54}$$

And the closed-loop coordinated system dynamics can be written in polytopic form assuming $x_s = u_s = d_s = 0$ as follows:

$$x_{k+1} = A_p(\varsigma)x_k + E_p(\varsigma)d_k \tag{7.55}$$

where $A_p(\varsigma) = \sum_{i=1}^{2}\varsigma_i A_{ip}$ and $E(\varsigma) = \sum_{i=1}^{2}\varsigma_i E_i$, with $\sum_{i=1}^{2}\varsigma_i = 1$, $\varsigma_i \geq 0$. Therefore, the methodology for computing invariant sets for polytopic systems is, again applied for (7.55), assuming that A_{1p}, A_{2p} have their eigenvalues inside of the unitary circle. If this condition is not obtained, some adaptation in the feedback matrices or even the cost matrices of the original cost functions should be adapted.

7.2.3.4 Obtention of the ellipsoidal invariant set

Solving the following LMI, for obtaining a common Lyapunov function matrix and the gain γ for defining the invariant set of the polytopic system (7.55) is sufficient for the present work.

$$\begin{bmatrix} x \\ d \end{bmatrix}^T \begin{bmatrix} A_{ip}^T P' A_{ip} - P' + I_n & A_{ip}^T P' E_{ip} \\ E_{ip}^T P' A_{ip} & E_{ip}^T P' E_{ip} - \gamma_p^2 I_q \end{bmatrix} \begin{bmatrix} x \\ d \end{bmatrix} \leq 0, \quad i = 1, 2 \tag{7.56}$$

Considering again that $d^T d \leq \bar{d}^T \bar{d}$, being $\bar{d}$ the maximum admissible absolute values of the disturbances, the invariant set for the family of systems defined by the action of the constrained coordination mechanism can be defined as follows:

$$\bar{\Pi}_P = \{x \in \Re^n : x^T P' x \leq \lambda_{max}(P')\gamma_p^2 \bar{d}^T \bar{d}\} \tag{7.57}$$

7.2.4 Recursive algorithm for computing the minimal robust invariant set

In this section are shown the elements for computing the minimal robust invariant set representation for the system under coordinated control, taking as base the procedure shown for the constrained MPC case. The Algorithm 4 chart includes an abstract of the procedure.

7.2.4.1 Selection of initial polyhedral set

Again, the initial states set $\mathcal{S}(0)$ for computing the mRPI can be chosen from two possible values: one of them is the polyhedral approximation of the ellipsoidal set $\bar{\Pi}_P$, computed from (7.57). The other option is the small ball that contains the origin. Taking one or the other, the stopping condition for the algorithm will change, aspect to be analyzed according when defining the performance test.

7.2.4.2 Adaptation of the constraints polyhedral set at each iteration

From the analysis via invariant sets for the constrained MPC strategy, it was seen that the control signal that, in this case is the coordination vector, is included in a set that evolves with the current values of states and past inputs. Therefore, some adaptation in the constraints polyhedral should be done for utilising the set $\boldsymbol{u}$ for its application in the system.
In the case of the coordinated strategy, the same procedure detailed in Section 7.1.4.2 is used. The following equation, considering reference values in the origin, is used for computing the state set evolution, that is indeed introduced in (7.40):

$$\mathcal{S}(k+1) = A_p\mathcal{S}(k) \oplus E_p\mathcal{D}_{max} \oplus F_p\boldsymbol{\mathcal{P}}(k) \tag{7.58}$$

where the set $\mathcal{D}_{max}$ is the one obtained from the extreme values of $\mathcal{D} \in \Re^q$ that does not change in the time and $\boldsymbol{\mathcal{P}}(k)$ is the coordination set computed at time $t = k$. This set is obtained after verifying the constraints (4.35) for each possible vector $\boldsymbol{p}$:

$$\begin{aligned} \boldsymbol{P} : \{\boldsymbol{p} \in \quad & L_p\boldsymbol{p} \leq W_p(x_0, d_0, u_{-1})\} \\ \text{with,} \quad & W_p = \overline{W}_p + W_{xp}x_0 + W_{dp}\boldsymbol{d} + W_{up}u_{ext-1} \end{aligned}$$

Therefore, the following set $\mathcal{W}_p$ is obtained, considering that $\overline{W}_p$ has the extreme values for system constraints and here, the disturbances values affects the topology of the constraints set:

$$\mathcal{W}_p(k) = \overline{W}_p \oplus W_{xp}\mathcal{S}(k) \oplus W_{dp}K_d\mathcal{D}_{max} \oplus W_{up}\mathcal{U}_{ext-1} \tag{7.59}$$

As done with the MPC case, the adaptation of the set $\boldsymbol{P}(k)$ can be done by merging all the subsets obtaining after the mapping procedure (each column of $\mathcal{W}_p(k)$ in matrix form, $W'_p(k)$ has limit values for the inequalities), in a way such:

$$\boldsymbol{P}_{(i)}(k) = \{\boldsymbol{p} \in \Re^{N.(n+m)} : L_p\boldsymbol{u} \leq W'_{p,i}\};\ i = 1 \cdots V_{wp} \tag{7.60}$$

where V_{wp} are the vertex obtained with the mapping operation. Then, the coordination set can be obtained as:

$$\boldsymbol{P}(k) = hull\{\boldsymbol{P}_{(i)}(k), i = 1 \cdots V_{wp}\} \tag{7.61}$$

The other method consist in found the maximum line-wise positive values of $W'_p(k)$ named $W'_{p,def}(k)$ and then, computing the set along L_p.

$$\boldsymbol{P}(k) = \{\boldsymbol{p} \in \Re^{N.(n+m)} : L_p\boldsymbol{p} \leq W'_{p,def}(k)\} \tag{7.62}$$

With this mechanism, for each iteration of the recursive algorithm, it is assured that the greatest volume coordination polyhedral set is applied for computing the states set evolution.

7.2.4.3 Algorithm for computing the mRPI

The recursive algorithm for computing the mRPI for the coordinated system is based in the expressions (7.34), where the interactions are included in explicit way in the expressions. Replacing u_k from (7.50), in the states equation at (7.34), is obtained:

$$\begin{gathered} x_{k+1} = \bar{A}_d x_k + \bar{E}_d d_k + \bar{F}_d \boldsymbol{p}_k + v_k + f_s, \quad \text{where} \\ \bar{A}_d = A_d - B_d K_{uext} \boldsymbol{\varphi}_1;\ \bar{E}_d = E_d - B_d K_{uext} \boldsymbol{\varphi}_2 K_d;\ \bar{F}_d = -B_d K_{uext} \boldsymbol{\varphi}_3; \\ f_s = B_d K_{uext} (\boldsymbol{\varphi}_1 x_s + \boldsymbol{\varphi}_2 K_d d_s + u_{ext-s}) \end{gathered} \tag{7.63}$$

and the interactions vector, also taken from (7.34) becomes:

$$\begin{gathered} v_k = \overline{v_A} x_k + \overline{v_E} d_k + \overline{v_F} \boldsymbol{p} + g_s \quad \text{, where} \\ \overline{v_A} = v_A - v_B K_{uext} \boldsymbol{\varphi}_1;\ \overline{v_E} = v_E - v_B K_{uext} \boldsymbol{\varphi}_2 K_d;\ \overline{v_F} = -v_B K_{uext} \boldsymbol{\varphi}_3; \\ g_s = v_B K_{uext} (\boldsymbol{\varphi}_1 x_s + \boldsymbol{\varphi}_2 K_d d_s + u_{ext-s}) \end{gathered} \tag{7.64}$$

At the end, the algorithm is executed as follows:

- At each iteration, compute the coordination set $\boldsymbol{\mathcal{P}}(k)$, according to the guidelines of Section 7.2.4.3.
- Then, compute the interactions set $\mathcal{V}_k$, using the following expression derived from (7.64):

  $$\mathcal{V}(k) = \overline{v_A} \mathcal{S}(k) \oplus + \overline{v_E} \mathcal{D}_{max} \oplus \overline{v_F} \boldsymbol{\mathcal{P}}(k) \oplus g_s \tag{7.65}$$

  the set g_s can be assigned equal to zero, because is considered the origin as reference value for all signals.
- The, compute the states set, using the following expression, derived from (7.63):

  $$\mathcal{S}(k+1) = \overline{A}_d \mathcal{S}(k) \oplus \overline{F}_d \boldsymbol{P}(k) \oplus \overline{E}_d \mathcal{D}_{max} \oplus \mathcal{V}(k) \oplus f_s \tag{7.66}$$

  Again, f_s can be assigned to zero, considering the references in the origin.
- Now, repeat the procedure until the ϵ-approximation is reached.

The algorithm for computing the minimal robust invariant set for the distributed coordinated closed-loop system is shown next.
Remark: In this proposed algorithm, it is considered a centralized computing structure for obtaining the minimal invariant set. The interactions and states sets are computed for the global system in distributed way, and the coordination set is computed in the same way that the coordinator does when the control scheme is applied. In the next section, a distributed computing approach for obtaining independent sets for each subsystem is presented.

Algorithm 4 Computation of mRPI for distributed coordinated systems by using the centralized model in the recursive algorithm

Require: Discrete-time system model matrices: A, B, E, with $\|eig(A)\| < 1$, $\|eig(E)\| < 1$, as well as the the interactions matrices v_A, v_B, v_E.

Require: Constraints polyhedral matrices $L_p, \overline{W}_p, W_{xp}, W_{dp}, W_{up}$, according to (4.35). In case of not using control's derivative penalizations, set $W_{up} = 0$.

Require: Small signal analysis for the dynamic system (7.40), with the constraints polyhedron (4.35), as seen in Section 7.2.2. If the system is stable, continue with the procedure. Otherwise, redefine the constraints polyhedron or the system dynamics accordingly.

START

S1: Set $k = 0$. Then, select the initial states polyhedron $\mathcal{S}(0)$, with an inner approximation of $\bar{\Pi}_P$ (Sections 4.2.2 and 7.2.3.3), or a polyhedral set approximation of a ball with small radius ($1e^{-3}$ for example). Also, define the ball $\mathcal{B}_\epsilon^p$ for stopping the recursive algorithm.

S2: Compute coordination polyhedral set $\boldsymbol{\mathcal{P}}(k) : \{\boldsymbol{p} \in L_p \boldsymbol{p} \leq W'_{p,def}(k)\}$, where $W'_{p,def}(k)$ is the longest positive vector contained in the set $\mathcal{W}_p(k)$ obtained from (7.59).

S3: Obtain the interactions polyhedral set with (7.65).

S4: Obtain the states set evolution with (7.66). If necessary, assign $\mathcal{U}_{ext}(k-1)$ for the input's derivative constraints, using a mapping version of (7.50).

if $\overline{A}_d^k \mathcal{S}(0) \nsubseteq \mathcal{B}_\epsilon^p$ **then**

Increase $k = k + 1$ and return to **S2**.

else

Return $\mathcal{S}(k)$ as the ϵ-approximation of the minimal Robust Invariant Set.

end if

7.2.5 Performance analysis for distributed non-coordinated case

There exist a particular condition when analyzing the performance of the distributed coordinated control approach: what happen when the coordination vector $\boldsymbol{p}$ is not well transmitted to the subsystems?

Having in consideration one of the main hypothesis of the subsystems behavior: *control constraints will always be respected, even when coordination is lost in some subsystem.* As seen in Chapter 6, the subsystem that losses the coordination vector passes to *local constrained control.* In other terms, the local controller assures the local stability and performance while degrading the global performance (value of the cost function). Thus, when the coordination vector is lost, the distributed control strategy passes indeed to a regime of total or partial *decentralized control* situation: the affected subsystems, by the lost of the coordination vector, will focus their local control strategy in the accomplishment of their own constraints. Therefore, a global invariant set analysis such the proposed here would not proceed.

More deeply, because the system is in fact completely different from the coordinated case, two situations can be presented regarding the subsystems:

- Some subsystems are unstable: Therefore, invariance analysis cannot be performed, because it is only devoted to stable systems.
- The subsystems are stable: considering that each system respects its constraints, then the interactions are also constrained and also worst-case analysis can be performed.

Taking into account that uncoordinated subsystems remains in admissible ranges by the effect of their internal strategies, it is proposed the following approach for building the global invariant set,

considering some systems under coordination and others with their local constrained control:

- In first place, consider the admissible input vector u_k when using the system coordination, as shown in (7.50) and call this element u_k^p. By identifying the systems affected by the coordination lost, create the following input vector:

$$u_{k,1} = \Gamma^p u_k^p \tag{7.67}$$

  where Γ^p is a diagonal matrix in $\Re^{m \times m}$, whose diagonal elements are equal to 1 if the subsystem receives the coordination vector. Otherwise, assign 0 for all inputs related to the system without coordination.

- In second place, recall from Section 6.2.1 that each subsystem is indeed a part of the decomposed global system, including its model. The local subsystem dynamics is (from (6.49)):

$$x_{(i)k+1} = A_{ii} x_{(i)k} + B_i \bar{u}_{u(i)k} + \bar{E}_{ii} \bar{d}_{(i)k}$$

  And the following local optimization problem (6.51) is obtained:

$$\begin{array}{ll} \min\limits_{\boldsymbol{u_{(i)}}} & J_{gv,uc}(\boldsymbol{u_{(i)}}) \\ \text{subject to} & L_{(i)}\boldsymbol{u_{(i)}} \leq W_{(i)}(x_{(i)}, u_{(i)}^{-1}) \end{array}$$

  After solving this problem, it is obtained the local extended control vector $\boldsymbol{u_{u(i)}}$ from where is taken the first $m_{(i)}$ elements. Then, use a vector u_k^{np} for storing the solutions for whose uncoordinated subsystems, that has a dimension lower than m.

- Create a matrix Γ^{np} such that the following operation is suitable to be done, considering the strict order of the subsystems inputs in the global inputs vector:

$$u_k^{def} = u_{k,1} + \Gamma^{np} u_{k,2} = \Gamma^p u_k^p + \Gamma^{np} u_k^{np} \tag{7.68}$$

- Considering this elements, the following states set expression will be used for performing the invariant sets computation:

$$\mathcal{S}(k+1) = A\mathcal{S}(k) \oplus \ E\mathcal{D}_{max} \oplus B\mathcal{U}(k)^{def} \tag{7.69}$$

  Where the inputs sets is derived from (7.68). Its full expression, considering the set points at the origin, has the following form:

$$\mathcal{U}(k)^{def} = \Gamma^p \mathcal{U}^p(k) \oplus \Gamma^{np} \mathcal{U}^{np}(k) \tag{7.70}$$

  For obtaining this definitive input set, it is necessary to proceed, with the constraints set, in the same introduced fashion in this chapter: obtaining the greatest volume polyhedral set and then, apply it in the mapping procedure. This should be done with the set $\boldsymbol{\mathcal{P}}(k)$ and the inputs sets for the subsystems.

7.2.6 Illustrative example

Reconsidering the same dynamic system presented in Section 7.1.5, it is proceed to perform the stability analysis via the small-gain theorem, as well as the computation of invariant sets and its approximated minimal representation for performance analysis. For simplycity is rewritten the dynamical equation, the weighting matrices and the admissible limits for all signals.

$$x_{k+1} = \begin{bmatrix} 0.9667 & 0.0133 \\ -0.0067 & 0.9733 \end{bmatrix} x_k + \begin{bmatrix} -0.0333 & 0.0033 \\ 0.0333 & 0.0167 \end{bmatrix} u_k + \begin{bmatrix} -0.0067 & 0.0033 \\ 0.0013 & 0.0067 \end{bmatrix} d_k$$

$$Q = \begin{bmatrix} 100 & 0 \\ 0 & 100 \end{bmatrix}; \; R = \begin{bmatrix} 1 & 0 \\ 0 & 1 \end{bmatrix}; \; S = \begin{bmatrix} 0 & 0 \\ 0 & 0 \end{bmatrix}; \; P = \begin{bmatrix} 452.56 & 195.15 \\ 195.15 & 431.85 \end{bmatrix}; \; N = 2;$$

$$x_{min} = \begin{bmatrix} -2 \\ -2 \end{bmatrix}; \; x_{max} = \begin{bmatrix} 2 \\ 2 \end{bmatrix}; u_{min} = \begin{bmatrix} -3 \\ -3 \end{bmatrix}; \; u_{max} = \begin{bmatrix} 3 \\ 3 \end{bmatrix}; d_{min} = \begin{bmatrix} -1 \\ -1 \end{bmatrix}; \; d_{max} = \begin{bmatrix} 1 \\ 1 \end{bmatrix}$$

Using the procedure of section 7.1.2, it is verified the small gain theorem, where $\gamma_G.\gamma_K < 1$. The gain γ_G is obtained after solving the LMI (7.7) with the proposed dynamics. It is obtained $\gamma_G = 1.5030$.
For the gain γ_K, it is obtained from the maximum element-wise gain of the matrix K_{lw} presented in (7.9). This gain is equal to $\gamma_K = 0.0622$.
The product $\gamma_G.\gamma_K = 0.0933 < 1$, shows that the constrained feedback is stable, even in critical conditions. Now, considering the model and the constrained control strategy, the following matrices could be used to define the resulted equivalent polytopic system:

$$A_1 = \begin{bmatrix} 0.7369 & -0.0105 \\ 0.2231 & 0.8561 \end{bmatrix}; \quad A_2 = \begin{bmatrix} 0.9568 & 0.0100 \\ 0.0023 & 0.9745 \end{bmatrix}$$
$$E_1 = \begin{bmatrix} -0.0040 & 0.0030 \\ -0.0014 & 0.0052 \end{bmatrix}; \quad E_2 = \begin{bmatrix} -0.0066 & 0.0033 \\ 0.0012 & 0.0069 \end{bmatrix}$$

The common Lyapunov matrix P and the constant γ associated for the family of systems are:

$$P = \begin{bmatrix} 64.0465 & -21.1863 \\ -21.1863 & 57.7698 \end{bmatrix}; \; \gamma = 0.3202$$

The figure 7.7 depicts the obtained ellipsoidal set, denoted as the set $\Pi(0)$.

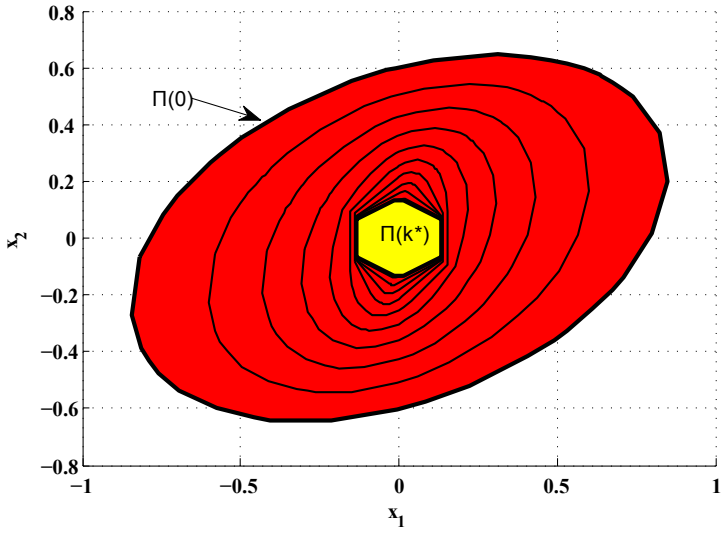

Figure 7.7: Invariant sets for evaluating the performance of the descentralized coordinated system

Outer approximation of the mRPI

An outer approximation of the invariant set for the MPC case could be obtained for the distributed coordinated system. Here, the states set evolution is computed based in (7.66) that requires updated information from the interactions set (7.65) and the coordination set. The latter is computed according to (7.59) while adapting this set following the guidelines of Sections 7.2.4.3

and 7.1.4.2.
Again, the iterative algorithm was stopped when an approximation of radius $1e^{-2}$ was obtained. used as stopping criterion for the recursive algorithm. Also in Fig . 7.7 is shown the ellipsoidal invariant set and the outer approximation of the mRPI, that is obtained after $h* = 11$ iterations, where it is represented as $\Pi(k*)$.

7.3 Global Performance analysis by distrubuted-computed invariant sets

In this section it is shown the procedure for obtaining invariant sets for each subsystem under constrained coordination. Because each subsystem has a dynamical equation with an interactions term, it is possible to compute local invariant sets, while using a coordinator that computes the constrained coordination vector $\boldsymbol{p}$ and the interactions v_k. As result, each subsystem will have its own invariant set, that will be useful for evaluating its performance in real time under coordination or even, when this information is lost.
As additional result, because all the local minimal invariant sets are orthogonal between each other, when merging all of them it is obtained an *ultimate bound* for the coordinated system. This bound is in fact an hypercube that contains the minimal invariant set computed in centralized fashion, as seen in the Section 7.2.

7.3.1 Expressions for the analysis in the distributed coordinated system

This analysis is based in the one presented at section 7.2, but is focussed in obtaining the invariant sets for each subsystem. The first element for the presented proposal considers the dynamical equation for each subsystem with the interactions vector:

$$x_{(i)k+1} = A_{ii}x_{(i)k} + B_{ii}u_{(i)k} + E_{ii}d_{(i)k} + v_{(i)k} \tag{7.71}$$

$$v_{(i)k} = \sum_{\substack{j=1 \\ j\neq i}}^{z} (A_{ij}x_{(j)k} + B_{ij}u_{(j)k} + E_{ij}d_{(j)k}) \tag{7.72}$$

Considering this structure, it can be written the local extended states vector, as function of local states, disturbance and extended local input vector, as seen in section 6.2.1, in the following form:

$$\boldsymbol{x_{(i)}} = \Omega_{(i)}x_{0(i)} + \Gamma_{(i)}\boldsymbol{\bar{u}_{ext(i)}} + \Theta_{(i)}\ \boldsymbol{\bar{d}_{(i)}} \tag{7.73}$$

Also, considering that the global cost function is decomposed for allowing the optimal constrained coordination, each subsystem has associated the following cost function, whose matrices are defined in (6.31) and (6.33):

$$J_{ext(i)} = \tfrac{1}{2}\boldsymbol{\bar{u}_{ext(i)}}^T\boldsymbol{H_{(i)}}\boldsymbol{\bar{u}_{ext(i)}} + \boldsymbol{\bar{u}^T_{ext(i)}}[\boldsymbol{K_{1(i)}}(x_{0(i)} - x_{(i)s}) + \boldsymbol{K_{2(i)}}(\boldsymbol{\bar{d}_{(i)} - \bar{d}_{(i)s}}) + \boldsymbol{K_{3(i)}p} - \boldsymbol{H_{(i)}}\boldsymbol{\bar{u}_{ext(i)_s}}] + \bar{V}_{ext(i)} \tag{7.74}$$

from this last expression, it is seen that the coordination vector $\boldsymbol{p}$ is an external element for manipulating this cost function. Finally, one can onbain the *local explicit control sequence* as:

$$\boldsymbol{\bar{u}^{opt}_{ext(i)}} = -\boldsymbol{H_{(i)}}^{-1}\left[\boldsymbol{K_{1(i)}}\tilde{x}_{0(i)} + \boldsymbol{K_{2(i)}}\tilde{\tilde{\boldsymbol{d}}}_{(i)} + \boldsymbol{K_{3(i)}p} - \boldsymbol{H_{(i)}}\bar{u}_{ext(i)_s}\right] \tag{7.75}$$

from where it is seen the dependence of the coordination vector for tuning the extended input sequence, with the objective of optimize the global cost function while respecting the global constraints.
Now, taking the first $m_{(i)}$ elements from the local control sequence with the transformation $m_{(i)}(k) = K_{u(i)}\bar{\boldsymbol{u}}^{\boldsymbol{opt}}_{\boldsymbol{ext(i)}}$, where $K_{u(i)} = [I_{m(i)\times m(i)} \quad 0_{m(i)\times(N-1)m(i)+Nr(i)}]$, as well as the local disturbance vector $\bar{\boldsymbol{d}}_{\boldsymbol{(i)}} = K_{d(i)}d(i)$ with $K_{d(i)} = [I_{q(i)\times q(i)} \cdots I_{q(i)\times q(i)}]^T$, one can write the local state vector with coordination as input in the following way:

$$\begin{gathered} x_{(i)k+1} = \bar{A}_i x_{(i)k} + \bar{E}_i d_{(i)k} - \bar{F}_i \boldsymbol{p}_k + v_{(i)k} + f_{(i)s} \\ \bar{A}_i = A_{ii} - B_{ii}K_{u(i)}\boldsymbol{H_{(i)}}^{-1}\boldsymbol{K_{1(i)}};\ \bar{E}_i = E_{ii} - B_{ii}K_{u(i)}\boldsymbol{H_{(i)}}^{-1}\boldsymbol{K_{2(i)}}K_{d(i)}; \\ \bar{F}_i = -B_{ii}K_{u(i)}\boldsymbol{H_{(i)}}^{-1}\boldsymbol{K_{3(i)}};\quad f_{(i)s} = B_{ii}K_{u(i)}\boldsymbol{H_{(i)}}^{-1}(\boldsymbol{K_{1(i)}}x_{(i)s} + \boldsymbol{K_{2(i)}}d_{(i)s}) + B_{ii}u_{(i)s} \end{gathered} \tag{7.76}$$

The structure of the local dynamical expression for computing the invariant sets is kindly similar to the global states expression under coordination as seen in (7.63), and the procedure for the algorithm is similar. Nevertheless, the verification of feedback stability for local subsystems is indeed verified with the small gain theorem in the same way as appointed in section 7.2.4, because it is necessary the global dynamical equation and constraints matrices for its computation.
In similar way, computing the ellipsoidal invariant sets for the local subsystems can be complicated. In fact, the worst case value will depend of the entire states, disturbance and input reference vectors, that requires information from the other subsystems for computing the ellipsoidal invariant set, and in the sense of interactivity between complex subsystems, the interactions vector is the only source of information that a particular subsystem possess from the other ones. For this motive, here is suggested the use of an small initial set for performing its expansion for finding the approximation to the mRPI.

7.3.2 Recursive algorithm for computing the local minimal robust invariant set

As mentioned previously, the small gain theorem is performed for the whole scale dynamical model, and the approximation to the minimal invariant set at the local systems will start with small polyhedral sets that contains the origin.
Following a similar procedure and considering the coordination of all the subsystems, by computing the local mRPI approximations, it should exist an entity that process the states sets that are computed by the subsystems and then, it calculates the *interactions vector* v_k, as well as the coordination polyhedral set $\mathcal{P}(k)$, that are used in each local iteration. In fact, the iterative algorithm, depicted in the Algorithm 5 chart, has the same structure than the coordination algorithm presented in section 6.2.2, but here re-sketched, in Fig 7.8 according to the following procedure:

- First, compute the **local states set** $\mathcal{S}_{(i)}$, by using the following equation, derived from the coordinated local dynamical equation (7.76):

$$\mathcal{S}_{(i)}(k+1) = \bar{A}_i\mathcal{S}_{(i)}(k) \oplus (-\bar{F}_i\boldsymbol{P}(k)) \oplus \bar{E}_i\mathcal{D}_{(i)max} \oplus \mathcal{V}_{(i)}(k) \oplus f_{(i)s} \tag{7.77}$$

  where $\mathcal{D}_{(i)max}$ is the local disturbance set, that is indeed contained in the global disturbance set, $\mathcal{V}_{(i)}(k)$ is the polyhedron of local interactions and $\boldsymbol{\mathcal{P}}(k)$ is the coordination set. The last two sets are sent by the *coordination entity.*

- In second place, all the subsystems should send to the *Coordinator-Like Computing Entity* their current states polyhedral sets and, if required the *local reference sets*, for computing the global interactions $\mathcal{V}(k)$ and the coordination $\boldsymbol{\mathcal{P}}(k)$ sets. But first, all the z subsystems

states polyhedral sets should be merged orthogonally for obtaining the global states sets $\mathcal{S}(k)$, that is in fact an hypercube formed by the all local sets:

$$\mathcal{S}(k) = \bigcup_{i=1}^{z} \mathcal{S}_{(i)}(k) \tag{7.78}$$

The polyhedral set $\mathcal{D}_{max}$ is also a well known hypercube, and no computational efforts should be added in each iteration.

- Now, compute the coordination set $\boldsymbol{\mathcal{P}}(k)$, following the same adaptation method for this set as detailed in Section 7.2.4.3. Once this element is computed, then compute the interactions set $\mathcal{V}(k)$ using (7.65).
- Finally, the coordination entity separates the interactions set for each subsystem, and then send them along $\boldsymbol{\mathcal{P}}(k)$ to all the subsystems, starting a new computational cycle.

With this methodology, it is assured the coordination policy while separating the computation of the states invariant set, that can be complicated for high scale systems.

Figure 7.8: Information flow for computing the local mRPI sets under the coordination scheme

Algorithm 5 Computation of an ultimate bound for distributed coordinated systems by using local invariant sets computation with a coordination-like computing entity

Require: Discrete-time system model matrices: A, B, E, with $\|eig(A)\| < 1$, $\|eig(E)\| < 1$, as well as the the interactions matrices v_A, v_B, v_E.

Require: Constraints polyhedral matrices $L_p, \overline{W}_p, W_{xp}, W_{dp}, W_{up}$, according to (7.8). In case of not using control's derivative penalizations, set $W_{up} = 0$.

Require: Small signal analysis for the dynamic system (7.40), with the constraints polyhedron (4.35), as seen in Section 7.2.2. If the system is stable, continue with the procedure. Otherwise, redefine the constraints polyhedron or the system dynamics accordingly.

START

S1: Set $k = 0$. Then, considering the dynamical matrices, separate the dynamics accordingly to each of the z subsystems, and then set $\mathcal{S}_{(i)}(0)$, as an inner approximation of $\bar{\Pi}_{(i)}$. Also, define the balls $\mathcal{B}_\epsilon^p$ for stopping the algorithm's iteration.

S2: All the subsystems sends their local states polyhedral sets $\mathcal{S}_{(i)}(k)$ to the coordination-like computing entity.

S3: The coordination entity gathers the subsystem's states polyhedrons and applies (7.78) for obtaining the hypercube $\mathcal{S}(k)$.

S4: The coordination entity computes the coordination set $\boldsymbol{\mathcal{P}}(k) : \{\boldsymbol{p} \in L_p \boldsymbol{p} \leq W'_{p,def}(k)\}$, where $W'_{p,def}(k)$ is the longest positive vector contained in the set $\mathcal{W}_p(k)$ obtained from (7.59).

S5: The coordination entity computes the global interactions polyhedral set with (7.65). .

S6: The coordinator sends to each i-subsystem, its interactions set $\mathcal{V}_{(i)}(k)$ and the coordination set $\boldsymbol{\mathcal{P}}(k)$.

S7: Obtain the local states polyhedron evolution with (7.77).

if $\overline{A}_d^k \mathcal{S}(0) \nsubseteq \mathcal{B}_\epsilon^p$, with $\overline{A}_d$ extracted from (7.63) **then**

Increase $k = k + 1$ and return to **S2**.

else

Return $\mathcal{S}(k)$ as the ϵ-approximation of the ultimate bound hypercube.

end if

7.3.3 Illustrative example

In this example, it is used the same system than the latter sections. For this algorithm, and because the goal is to compute local invariant sets, they are initialized with the small ball approximation that contains the origin. Therefore, the algorithm is based in the expansion of this initial set, until obtaining an inner approximation of the mRPI.
Thus, the recursive equation that represents each subsystem's states set is (7.77) that receives information computed by the coordination entity, which calcules the coordination set $\boldsymbol{\mathcal{P}}(k)$ and the interactions set $\mathcal{V}(k)$, based in the local informations. Remember that the coordinator receives the states information and performs the union of these orthogonal sets, obtaining at each iteration, an hypercube.
According to the procedure, the mRPI approximation from the centralized algorithm should be contained in the hypercubical approximation of the mRPI, because the latter algorithm is more conservative that the former one. Therefore, one can obtain an admissible bound for the local states, by knowing the information from the coordinator.
In Fig. 7.9 are included the sets from both dimensions (x_1, x_2)as well as the equivalent hypercubical set obtained when merging these orthogonal sets. In Fig. 7.10 a representation of the ellipsoidal

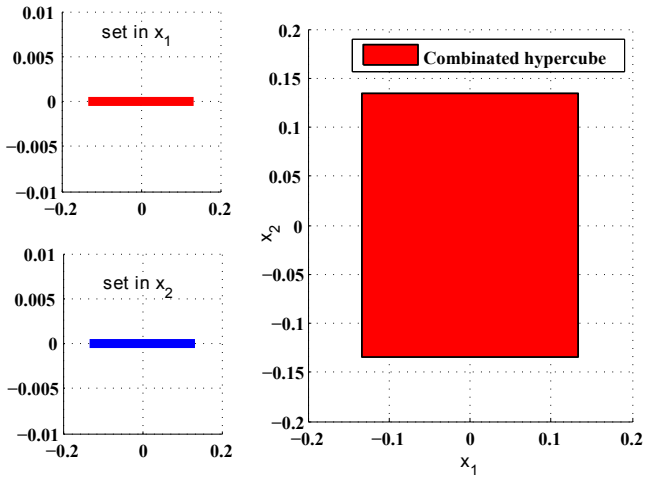

Figure 7.9: Invariant sets for evaluating the performance of the descentralized coordinated system

invariant set ("Elli. Invariant"), the outer mRPI approximation obtained in the example from the last section (see 7.2.6) ("Cent. Set") and the hypercube obtained after merging the inner mRPI approximations for each dimension, computed in distributed way ("Dist. Set"). It is seen how the hypothesis are accomplished, letting this distributed method as suitable for local(subsystems) performance analysis.

7.4 Conclusions

In this chapter was presented an approach for stability and performance analysis for constrained control systems. The approach is based on the computation of the minimal invariant sets of an equivalent polytopic system which is intended for modeling the constrained control. The stability could be established using the small gain theorem in the case of open-loop stable systems, otherwise the computation of bounded invariant sets could be used to conclude on stability of the controlled system in presence of control constraints. The approach has been applied for establishing the

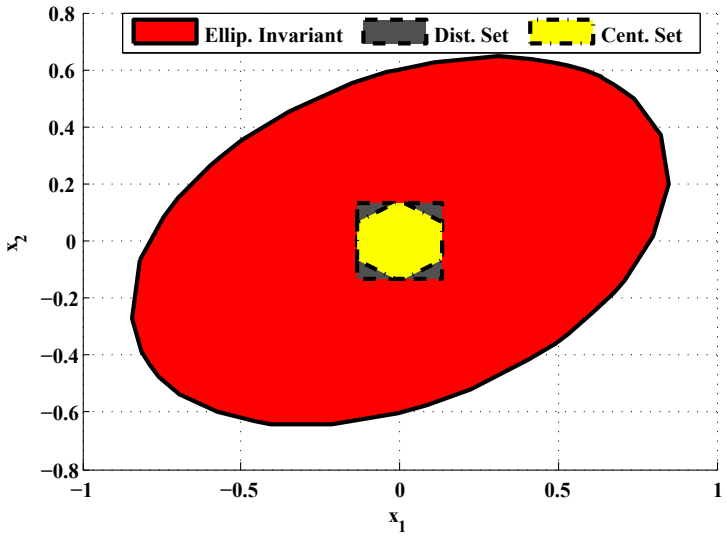

Figure 7.10: Invariant sets for evaluating the performance of the descentralized coordinated system

stability and the performance of a coordinated distributed control scheme. Finally, an alternative methodology allows the computation of local invariant sets for establishing the stability of the global system. This technique could be useful for large scale systems where *stable* decomposition and coordination control is possible. As a final conclusion, the stability of local subsystems could be ensured during coordination lost under some assumptions on the interactions terms. For instance, in presence of control and states constraints in all subsystems the interactions are bounded. Thus, when a local controlled is performed without coordination, and the states remain inside the admissible regions, then the local system remain stable. In addition, the performance of non coordinated systems could be deteriorated compared to a coordinated case where the performance has to be close to the centralized case.

Chapter 8

APPLICATION TO DISTRIBUTED POWER GENERATION CONTROL VIA SIMULATION CASE-STUDIES

Contents

8.1 Two-generator microgrid 143
8.1.1 Considered model and numerical values 145
8.1.2 Control objectives 147
8.1.3 Simulation results 148
8.1.4 Concluding remarks 151
8.2 Alternative generation-based microgrid 151
8.2.1 Dynamical model and system parameters 152
8.2.2 Control objectives 154
8.2.3 Simulation results 155
8.3 Conclusions 158

In this chapter, two case-studies are presented in order to illustrate the proposed coordination strategy and performance evaluation tools in the frame of electrical power systems.
The first example corresponds to a microgrid with two generators and a shared load. In addition,each generator has a storage unit that can deliver some energy according to the power profile, and to the power which is generated.
The second case-study is a more complex microgrid, where two generation units (photovoltaic, wind turbine and hydro electrical ones) form a network, that is itself connected to the power grid. In this case, some typical production and load profiles are adopted for a validation of the coordination strategy.

8.1 Two-generator microgrid

The system structure for this case-study is shown in Fig. 8.1. It is characterized by two power areas (Area 1, Area 2) and a shared load. The control strategy should ensure the power sharing between the units, while maintaining some variables, such as bus and battery voltages, in admissible ranges.

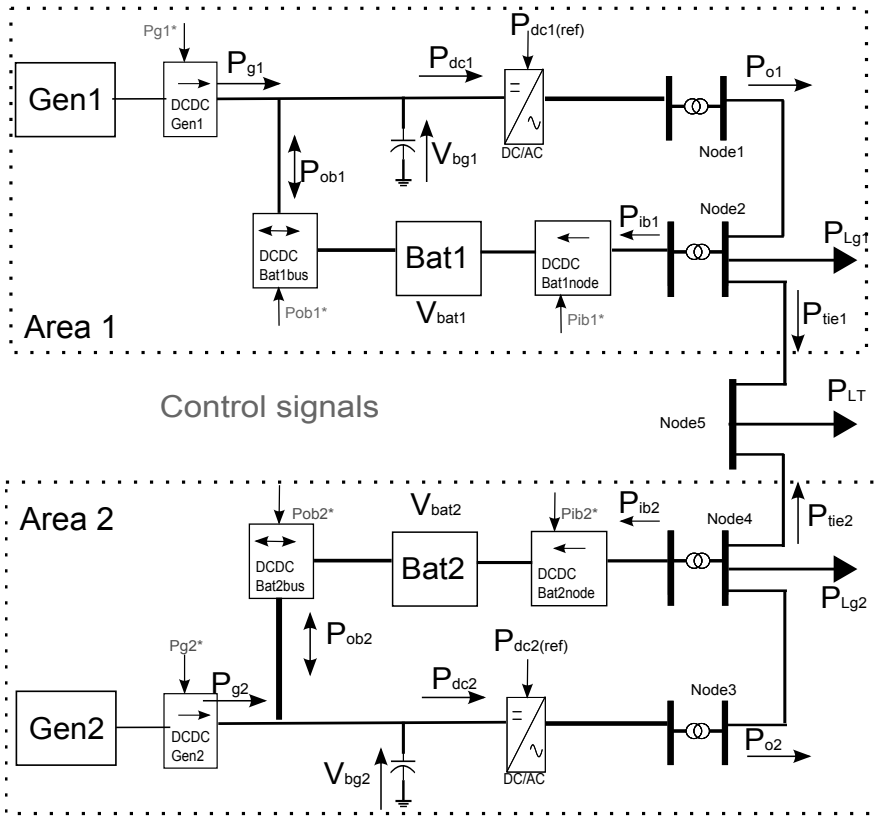

Figure 8.1: Configuration of the proposed two-source power generation system

The different parts of the power system are:

- Two power generators, *Gen1, Gen2* that deliver an amount of power to one respective DC bus, with respective voltages V_{bg1}, V_{bg2}.
- Each DC bus has a capacitor (C_{bg1}, C_{bg2}), connected to a unidirectional inverter. The buses receive the power generated by their corresponding generator $(Gen1, Gen2)$ and battery bank $(Bat1, Bat2)$.
- The equivalent AC power is injected to $Node1, Node3$ in Area 1 and Area 2, respectively. These nodes are respectively connected to $Node2$ and $Node4$ that contain local loads (P_{Lg1}, P_{Lg2}), as well as a direct path (through a rectifier) to the battery, so that this element can be used as a voltage stabilizer in cases where the loads are suddenly disconnected.
- The shared load is located in $Node5$ and is represented by P_{LT}.

In this case-study, only active power generation is considered, and transmission between subsystems is assumed to be lossless. This is motivated by two reasons: the first one is the purpose to present a methodology for obtaining a mathematical model that decouples each area dynamics, but including information from the other one in interactions terms. The second reason is that physical effects such as losses or inductive behaviors in transmission links of small scale systems can indeed be neglected [1].
As particular element for this case study, at each area a direct connection between the output node and the battery, through an unidirectional converter. The battery of each area aids to stabilize

the system and saves power in condition of overproduction of energy. In this case study, this physical disposition is indeed a challenge for the control algorithm, due to the possibility of obtaining negative reference values for this converter, that is not feasible according to the converter characteristics.

8.1.1 Considered model and numerical values

The model is based on the power flow description shown in Fig.8.1. The idea is to describe the bus capacitor and equivalent battery capacitor voltages, as well as the equivalent dynamic imposed by the inverter and its internal strategy. The instantaneous energy stored in a capacitor is expressed as follows:

$$E(t) = \frac{1}{2}CV^2(t) \tag{8.1}$$

where C is the capacitance and V is the terminal voltage of the device. Remembering that one can express any signal x as the sum of some equilibrium value X_0 and its variation $\tilde{x}$, the capacitor energy variation $\tilde{E}$ can be written as follows:

$$\widetilde{E} = CV_0\tilde{v} := K_c\tilde{v} \tag{8.2}$$

That leads to consider dynamical expressions for DC buses (C_{bg1}, C_{bg2}) energy variations, in terms of variations in power flows:

$$\begin{aligned} \dot{\widetilde{E}}_{bg1} &= \bar{K}_1(\widetilde{P}_{g1} + \widetilde{P}_{ob1} - \widetilde{P}_{o1}) \\ \dot{\widetilde{E}}_{bg2} &= \bar{K}_2(\widetilde{P}_{g2} + \widetilde{P}_{ob2} - \widetilde{P}_{o2}) \end{aligned} \tag{8.3}$$

using subindex j to denote the generation unit associated with the variable, P_{gj} for the power generated by Gen_j, $\widetilde{P}_{obj}$ for the power sent by the battery to the bus, and $\widetilde{P}_{oj}$ the power delivered to the grid, which can both be considered equal with each other due to the lossless assumption for the lines and inverter [82]. Parameters $\bar{K}_j$ normalize the expression in to use $per-unit$ in all variables [1]:

$$\bar{K}_1 = P_{o2,r}/E_{b1,max} \quad \bar{K}_2 = P_{o2,r}/E_{b2,max} \tag{8.4}$$

where $P_{oj,r}$ is the rated load and $E_{bj,max}$ is the maximum (rated) energy in the bus capacitors. It can be done the same with energy variations in the batteries:

$$\begin{aligned} \dot{\widetilde{E}}_{bat1} &= \hat{K}_1(\widetilde{P}_{ib1} - \widetilde{P}_{ob1}) \\ \dot{\widetilde{E}}_{bat2} &= \hat{K}_2(\widetilde{P}_{ib2} - \widetilde{P}_{ob2}) \end{aligned} \tag{8.5}$$

where $\widetilde{P}_{ibj}$ is the power absorbed by the battery from the output nodes and the normalization coefficients are defined as:

$$\hat{K}_1 = P_{o2,r}/E_{bat1,max} \quad \hat{K}_2 = P_{o2,r}/E_{bat2,max} \tag{8.6}$$

Let us then consider that inverters generate their active power according to some reference values $P^*_{dc,j}$ that can be measured or given by an external optimizer [82]. Thus, the output power of each unit $(\widetilde{P}_{o1}, \widetilde{P}_{o2})$, in $p.u$, is expressed as follows:

$$\begin{aligned} \dot{\widetilde{P}}_{o1} &= \tfrac{1}{\tau_{p1}}\left(-\widetilde{P}_{o1} + \widetilde{P}^*_{dc1}\right) \\ \dot{\widetilde{P}}_{o2} &= \tfrac{1}{\tau_{p2}}\left(-\widetilde{P}_{o2} + \widetilde{P}^*_{dc2}\right) \end{aligned} \tag{8.7}$$

with τ_{pj} some equivalent time constant associated to the action of the inverter control strategy, as well as any other possible filtering action on P^*_{dcj}. In the present example, those signals are

obtained from the nodes $Node2$ and $Node4$ after simple inspection, assuming $\widetilde{P}^*_{dcj} = \widetilde{P}_{oj}$:

$$\begin{array}{l} \widetilde{P}^*_{dc1} = \widetilde{P}_{ib1} + \widetilde{P}_{Lg1} + \widetilde{P}_{LT} - (\widetilde{P}_{o2} - \widetilde{P}_{ib2} - \widetilde{P}_{Lg2}) \\ \widetilde{P}^*_{dc2} = \widetilde{P}_{ib2} + \widetilde{P}_{Lg2} + \widetilde{P}_{LT} - (\widetilde{P}_{o1} - \widetilde{P}_{ib1} - \widetilde{P}_{Lg1}) \end{array} \tag{8.8}$$

Replacing expressions (8.8) in (8.7), the following output power dynamics are obtained:

$$\begin{array}{l} \dot{\widetilde{P}}_{o1} = \frac{1}{\tau_{p1}} \left(-\widetilde{P}_{o1} + \widetilde{P}_{ib1} + \widetilde{P}_{Lg1} + \widetilde{P}_{LT} + \widetilde{P}_{ib2} + \widetilde{P}_{Lg2} - \widetilde{P}_{o2} \right) \\ \dot{\widetilde{P}}_{o2} = \frac{1}{\tau_{p2}} \left(-\widetilde{P}_{o2} + \widetilde{P}_{ib2} + \widetilde{P}_{Lg2} + \widetilde{P}_{LT} + \widetilde{P}_{ib1} + \widetilde{P}_{Lg1} - \widetilde{P}_{o1} \right) \end{array} \tag{8.9}$$

Defining the following state, input and disturbance vectors (with subindex j referring to each subsystem):

$$x_{(j)} = [E_{bgj}\ E_{batj}\ P_{oj}]^T;\ u_{(j)} = [P_{gj}\ P_{obj}\ P_{ibj}]^T;\ d_{(j)} = [P_{Lgj}\ \ 0.5P_{LT}]^T \tag{8.10}$$

When the vectors are merged together, one can define a centralized model by considering the states, inputs and disturbances as follows:

$$x = [x_{(1)}\ x_{(2)}]^T;\ \ u = [u_{(1)}\ u_{(2)}]^T;\ \ d = [d_{(1)}\ d_{(2)}]^T \tag{8.11}$$

where $x \in \Re^6, u \in \Re^4, d \in \Re^2$. Considering that P_{LT} is shared, and to make the decomposition easier, for each vector $d_{(j)}$ we set $P'_{LT} := 0.5P_{LT}$. In this way, the disturbance matrix in the dynamical model can be written in square form, in terms of subsystems.
Considering the centralized-model vectors (8.11), the following continuous time model is obtained, whose matrices are defined in (8.13):

$$\begin{array}{c} \dot{x}(t) = A_c x(t) + B_c u(t) + E_c d(t) \\ \begin{bmatrix} \dot{x}_{(1)} \\ \dot{x}_{(2)} \end{bmatrix} = \begin{bmatrix} A_{11c} & A_{12c} \\ A_{21c} & A_{22c} \end{bmatrix} x(t) + \begin{bmatrix} B_{11c} & B_{12c} \\ B_{21c} & B_{22c} \end{bmatrix} u(t) + \begin{bmatrix} E_{11c} & E_{12c} \\ E_{21c} & E_{22c} \end{bmatrix} d(t) \end{array} \tag{8.12}$$

$$\begin{array}{cc} A_{11c} = \begin{bmatrix} 0 & 0 & -\bar{K}_1 \\ 0 & 0 & 0 \\ 0 & 0 & -1/\tau_{p1} \end{bmatrix} & A_{12c} = \begin{bmatrix} 0 & 0 & 0 \\ 0 & 0 & 0 \\ 0 & 0 & -1/\tau_{p1} \end{bmatrix} \\ A_{21c} = \begin{bmatrix} 0 & 0 & 0 \\ 0 & 0 & 0 \\ 0 & 0 & -1/\tau_{p2} \end{bmatrix} & A_{22c} = \begin{bmatrix} 0 & 0 & -\bar{K}_2 \\ 0 & 0 & 0 \\ 0 & 0 & -1/\tau_{p2} \end{bmatrix} \\ B_{11c} = \begin{bmatrix} \bar{K}_1 & \bar{K}_1 & 0 \\ 0 & -\hat{K}_1 & \hat{K}_1 \\ 0 & 0 & 1/\tau_{p1} \end{bmatrix} & B_{12c} = \begin{bmatrix} 0 & 0 & 0 \\ 0 & 0 & 0 \\ 0 & 0 & 1/\tau_{p1} \end{bmatrix} \\ B_{21c} = \begin{bmatrix} 0 & 0 & 0 \\ 0 & 0 & 0 \\ 0 & 0 & 1/\tau_{p2} \end{bmatrix} & B_{22c} = \begin{bmatrix} \bar{K}_2 & \bar{K}_2 & 0 \\ 0 & -\hat{K}_2 & \hat{K}_2 \\ 0 & 0 & 1/\tau_{p2} \end{bmatrix} \\ E_{11c} = E_{12c} = \begin{bmatrix} 0 & 0 \\ 0 & 0 \\ 1/\tau_{p1} & 1/\tau_{p1} \end{bmatrix} & E_{21c} = E_{22c} = \begin{bmatrix} 0 & 0 \\ 0 & 0 \\ 1/\tau_{p2} & 1/\tau_{p2} \end{bmatrix} \end{array} \tag{8.13}$$

Now, discretizing the model by Euler's method with sampling time T_s, we get:

$$x_{k+1} = Ax_k + Bu_k + Ed_k$$

$$
\begin{aligned}
A_{11} &= \begin{bmatrix} 1 & 0 & -\bar{K}_1 T_s \\ 0 & 1 & 0 \\ 0 & 0 & (1 - T_s/\tau_{p1}) \end{bmatrix} & A_{12} &= \begin{bmatrix} 0 & 0 & 0 \\ 0 & 0 & 0 \\ 0 & 0 & -T_s/\tau_{p1} \end{bmatrix} \\
A_{21} &= \begin{bmatrix} 0 & 0 & 0 \\ 0 & 0 & 0 \\ 0 & 0 & -T_s/\tau_{p2} \end{bmatrix} & A_{22} &= \begin{bmatrix} 1 & 0 & -\bar{K}_2 T_s \\ 0 & 1 & 0 \\ 0 & 0 & (1 - T_s/\tau_{p2}) \end{bmatrix} \\
B_{11} &= \begin{bmatrix} \bar{K}_1 T_s & \bar{K}_1 T_s & 0 \\ 0 & -T_s & T_s \\ 0 & 0 & T_s/\tau_{p1} \end{bmatrix} & B_{12} &= \begin{bmatrix} 0 & 0 & 0 \\ 0 & 0 & 0 \\ 0 & 0 & T_s/\tau_{p1} \end{bmatrix} \\
B_{21} &= \begin{bmatrix} 0 & 0 & 0 \\ 0 & 0 & 0 \\ 0 & 0 & T_s/\tau_{p2} \end{bmatrix} & B_{22} &= \begin{bmatrix} \bar{K}_2 T_s & \bar{K}_2 T_s & 0 \\ 0 & -T_s & T_s \\ 0 & 0 & T_s/\tau_{p2} \end{bmatrix} \\
E_{11} = E_{12} &= \begin{bmatrix} 0 & 0 \\ 0 & 0 \\ T_s/\tau_{p1} & T_s/\tau_{p1} \end{bmatrix} & E_{21} = E_{22} &= \begin{bmatrix} 0 & 0 \\ 0 & 0 \\ T_s/\tau_{p2} & T_s/\tau_{p2} \end{bmatrix}
\end{aligned} \tag{8.14}
$$

The parameters for this two-generator microgrid are given in Table 8.1, presenting the maximum values for the generated and consumed loads, as well as the admissible injected power by both, generators and batteries.

Table 8.1: Parameters for the Two-Generator Microgrid Example

PARAMETER	VALUE
Bus Capacitance (C_{bus})	100 mF
Battery Equivalent Capacitance (C_{bat})	24.5 F
Rated DC bus voltage (V_{bus0})	800 V (1 p.u)
Rated DC bus energy (E_{bus0}, $E_{b,r}$)	32 kJ (1 p.u)
Max. Battery Cap. Voltage - 90% SoC	186.3 V
Max. Battery energy 90% SoC ($E_{bat,max}$)	430 kJ
Rated Battery energy 60% SoC (E_{bat0})	77.12 kJ
Max. Generated Power ($P_{g,max}$)	10 kW (1 p.u)
Max. Power from/to Battery ($P_{ob,max}, P_{ib,max}$)	10 kW (1 p.u)
Max. Locals/shared load power ($P_{LG,max}, P_{LT,max}$)	20 kW (2 p.u)
Inverter equivalent time constants (τ_{p1}, τ_{p2})	1.0 s, 1.5 s

8.1.2 Control objectives

Considering the discrete-time model for the microgrid, with either a centralized or a distributed control strategy can be proposed, based on the control objectives that are the **regulation of the DC bus voltage** and the **regulation of the battery voltage**.
The regulation of the DC bus voltage is related to the voltage performance of the generation system. In fact, controlling this variable ensures the functionality of the inverter that requires the input voltage in some admissible range, according to the desired output voltage and the modulation index that is usually fixed [82].
Regarding the battery voltage regulation, it is directly related to its *State-of-charge* of the device, and thus to the stored energy and the amount of power that can be delivered. In fact, this variable has some range around $20\% - 90\%$ of the battery capacity: not fully discharged in order to be able to compensate some transient charge, but not fully charged either, that would prevent it for receiving excess of energy [8, 91].

Thus, considering the context of the present work, the use of receding horizon-based control strategies is adopted. The following global cost function, suitable to be properly applied for both centralized or distributed strategies is considered:

$$J_{gv} = \frac{1}{2}\left[\tilde{x}_N^T P \tilde{x}_N + \sum_{k=0}^{N-1}\left(\tilde{x}_k^T Q \tilde{x}_k + \tilde{u}_k^T R_u \tilde{u}_k + 2\tilde{u}_k^T S_u \tilde{x}_k\right)\right] + \frac{1}{2}\sum_{k=0}^{N-1}\left(\tilde{v}_k^T R_v \tilde{v}_k + 2\tilde{v}_k^T S_v \tilde{x}_k\right)$$

where weighting matrices are chosen as:

$$Q = \begin{bmatrix} Q_{(1)} & 0 \\ 0 & Q_{(2)} \end{bmatrix} \; ; \; R = \begin{bmatrix} R_{u(1)} & 0 \\ 0 & R_{u(2)} \end{bmatrix} \; ; \; S = \begin{bmatrix} S_{u(1)} & 0 \\ 0 & S_{u(2)} \end{bmatrix}$$

where the block-diagonal structure is suitable for the distributed approach, and chosen with numerical values as:

$$Q_{(1)} = Q_{(2)} = \begin{bmatrix} 10 & 0 & 0 \\ 0 & 10 & 0 \\ 0 & 0 & 10 \end{bmatrix} \; ; \; R_{u(1)} = R_{u(2)} = \begin{bmatrix} 1.5 & 0 & 0 \\ 0 & 2 & 0 \\ 0 & 0 & 5 \end{bmatrix} \; ; \; S_{u(1)} = S_{u(2)} = \begin{bmatrix} 0 & 0 & 0 \\ 0 & 0 & 0 \\ 0 & 2 & 0 \end{bmatrix}$$

$$R_{v(1)} = R_{v(2)} = 1e^5. \begin{bmatrix} 1 & 0 & 0 \\ 0 & 1 & 0 \\ 0 & 0 & 1 \end{bmatrix} \; ; \; S_{v(1)} = S_{v(2)} = 0$$

The matrix P in the cost function is computed from the discrete-time Riccati algebraic equation with Q, R and S.
About constraints, the following extremal values are considered

$$\begin{array}{ll} x_{max} = [1.02 \;\; 0.81 \;\; 1.00]^T & x_{min} = [0.98 \;\; 0.09 \;\; 0.01]^T \\ u_{max} = [0.5 \;\; 0.5 \;\; 0.5]^T & u_{min} = [0.0 \;\; -0.5 \;\; 0.01]^T \\ d_{max} = [1.0 \;\; 1.0]^T & d_{min} = [0 \;\; 0]^T \end{array}$$

where the admissible limits for bus energy, considering an initial value of 1.0, are selected so as to allow a voltage deviation lower that 2%, and the battery energy variation are set to the range $20 - 90\%$, all being here expressed in p.u.

8.1.3 Simulation results

In this section, the simulation results for this case study are presented. For this system is only considered the proposed distributed-coordinated approach. The propose is evaluate two stages of the system: the first one, the normal operation, and the second one is the lost of the coordination vector at the **Area 2** controller.

Test 1: Power System Under Proposed Coordination Approach

Here, a time window of 120 s is chosen, while initializing the states according to Table 8.1. The results for the power system controlled under the proposed distributed-coordinated approach are shown in Fig. 8.2. For this case study, the local and shared loads are modified in steps, while injecting some noise on local loads (P_{Lg1}, P_{Lg2}), according to the last chart in Fig 8.2.
The selection of power loads obeys to a premise from the grid operator's point of view, where a higher efficiency would be obtained when constant generation profiles are considered. In case of load variations, a combined action is thus desired from coordinators, ensuring in this way, a better generator performance [129].

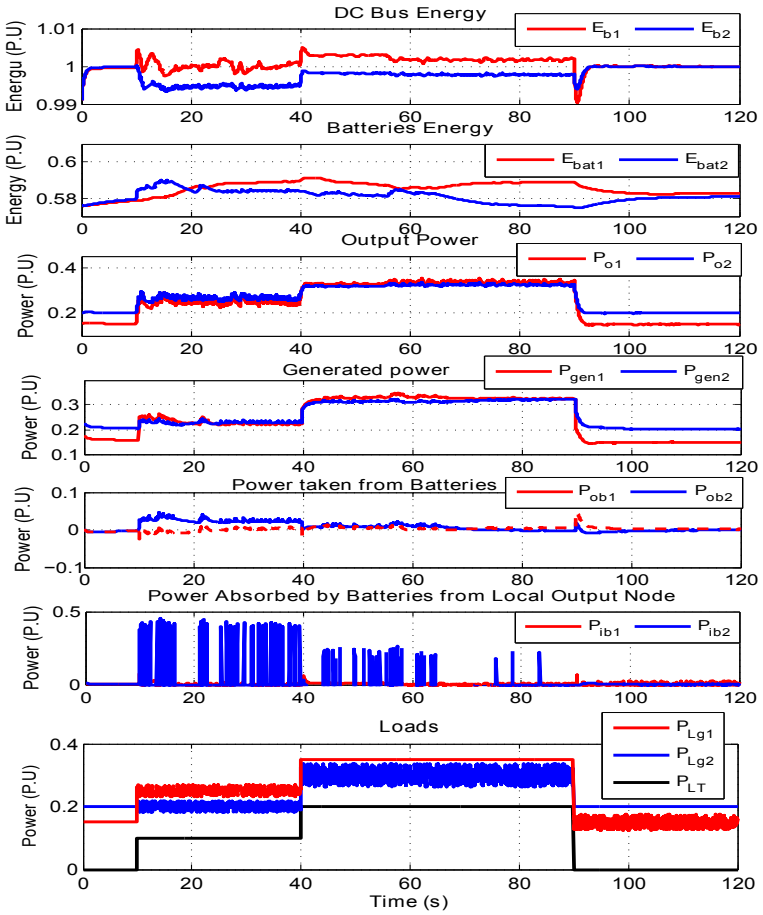

Figure 8.2: Performanace of the proposed system with the coordinated control approach in Test 1

From the results, considering the state (E_b, E_{bat}, P_o) and control $(P_{gen}, P_{ob}, P_{ib})$ evolution, one can notice:

- All system variables operate in their admissible limits, according to the chosen load profiles.
- The control signal P_{ib} helps to keep the DC bus voltage stability, as well as to limit the output power profiles. High-frequency noise at the charges can affect these variables, but absorbing the excessive-high frequency power directly to the battery, offers an interesting solution for power stabilizing, as well as SoC conservation for this class of small scale systems. This mechanism is equivalent to the provided by reactive-power controllers in grid-connected applications [130].
- Batteries are applied as support power devices. Against a sudden load power increment, they supply energy to the DC bus allowing to prevent from excessive power production by the generators. After such transients, they come back to low energy levels, or even, shut down their power production. This is obtained thanks to the weight specification for battery power generation.

As a conclusion, the coordination approach ensures the power system performance, according to the specifications, while maintaining the DC bus voltages stable.

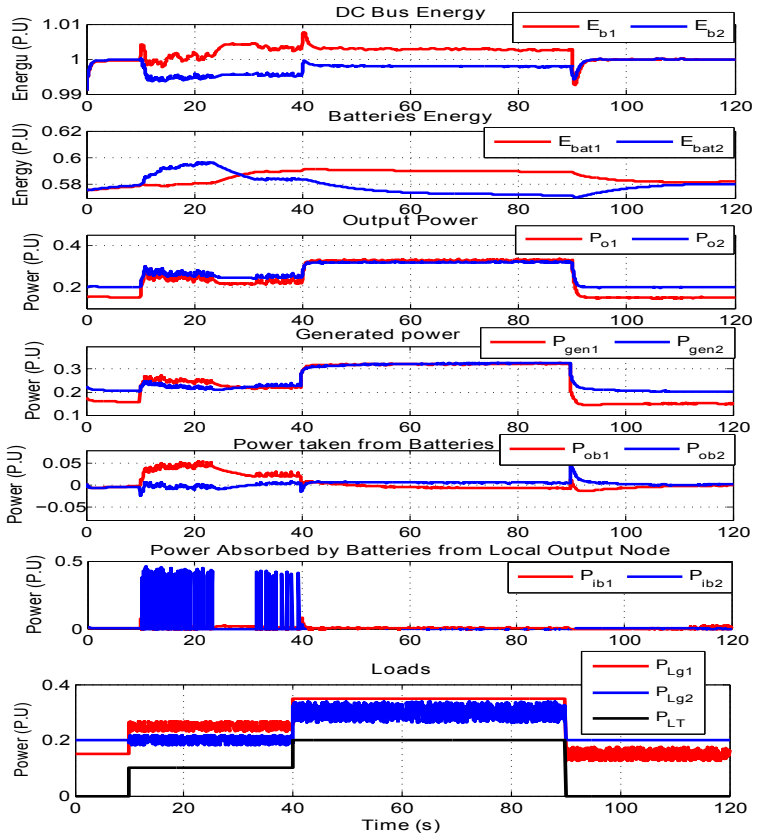

Figure 8.3: Performanace of the proposed second order system with the coordinated control approach, when subsystem 2 loses the coordination vector (Test 2)

According to the results of the first scenario for this power system, the distributed control scheme should reduce the amount of delivered power from the generator at **Area 2**, when some positive $\widetilde{P}_{ug2}$ power is injected from the external source.

Test 2: Effect of Coordination Vector Loss in Area 2

In this scenario, the same power profiles as in Test 1 are considered, with the same initialization. The system is first controlled under the coordinated scheme. Then, at $t = 40\ s$, the coordination vector is not transmitted to the control block of **Area 2**. Thus, this area changes its control policy to a *local constrained MPC*, while **Area 1** still works with coordination information.
Results of this situation are shown in Fig. 8.3, and the following can be observed:

- The battery of **Area 2** discharges more in the case when coordination is lost than before. Without loss indeed, a minimum of around 0.58 p.u for E_{bat2} is obtained, while after coordination loss, it reduces to 0.56 p.u. Therefore, the reservoir unit delivers more power when coordination is lost in order to maintain the control objectives.

- In **Area 2**, the battery power absorption capacities are reduced, giving rise to the discharge previously mentioned. Nevertheless, bus voltages are stable and the delivered output power is still smooth in this area.

Finally, those results illustrate how global performance may be reduced, here reflected by the deeper discharge event in the uncoordinated unity, while ensuring stable and constrained behaviour. From this, the coordination strategy can add robustness to the system, under conditions where communication is lost for instance.

8.1.4 Concluding remarks

This first case study of two parallel-connected generation units, although simple in conception and modeling, allows to verify the pertinence of the proposed coordination strategy. The control objectives (inner voltage bus stabilization and battery charge/discharge management) are satisfied, while respecting the operative constraints.
Moreover, the characteristics of the control scheme allows to switch to a local control strategy when data transmission from the coordinator is lost, keeping admissible operation, even though possibly degrading the global performance.
Finally, the modeling procedure here introduced is suitable to be used in any application where power electronics blocks have fast dynamical performance, in comparison with power or mechanical variables.

8.2 Alternative generation-based microgrid

This second case study is proposed inspired by the classical Load-Frequency Control (LFC) of interconnected synchronized generators [18, 39, 131, 132], giving us one structure suitable for proving the control strategies and performance evaluation tools developed in this thesis. The system is composed by two interconnected hydro-electrical generators, each of them receiving some additional power injected by an uncontrollable generator, either a photovoltaic or a wind turbine generator. In fact, in the context of modern distribution systems, main generators serve to specific areas, where decentralized generation is expected. The controllers should not only optimize the power sharing between the areas, but also must stabilize the system [130, 133, 134, 135]. Further studies and concepts of power system modeling and stabilization concepts can be consulted in [1]. In Fig. 8.4 is depicted the configuration of the considered multi-area power system, including the generators and storage units.

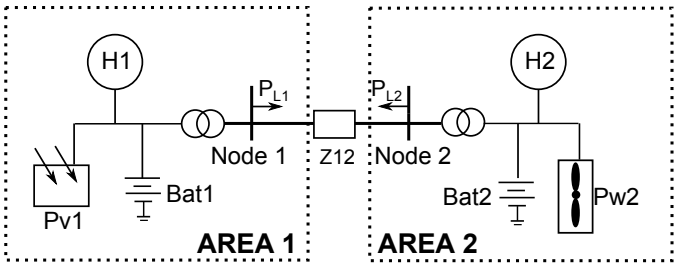

Figure 8.4: Configuration of the proposed two-area power generation system

Here, two generation areas, represented as *Area 1* and *Area 2*, are interconnected by power lines. Each area is represented by an hydroelectrical generator that includes the electric generator, as well as the governor and turbine systems, whose dynamics are lower, compared to the generators one [1]. In Fig. 8.5 it is seen how the mechanical power P_t is affected by the electrical powers P_L (the

local load), the undispatchable power power P_g injected by the alternative-based generator (PV or wind turbine) and the power injected by a *controllable back-up battery* $P_{bat} = u_2$. The governor input signal is represented by a control signal u_1, generated by the high-level control strategy that represents a *reference load value*, and a droop-frequency component, that is proportional to the frequency variation [1, 136].
The control objective for the system is to maintain the frequency close to the nominal value (50 Hz), while ensuring the load delivering and the state-of-charge of the backup battery. Also, only *active power* is considered to be controlled the system, as well as small node voltage variations.
With respect to the photovoltaic and wind turbine generators they are controlled by external strategies that ensure their optimal power production. Also, their deliverable power is lower, compared with the one delivered by their local hydroelectrical generator.

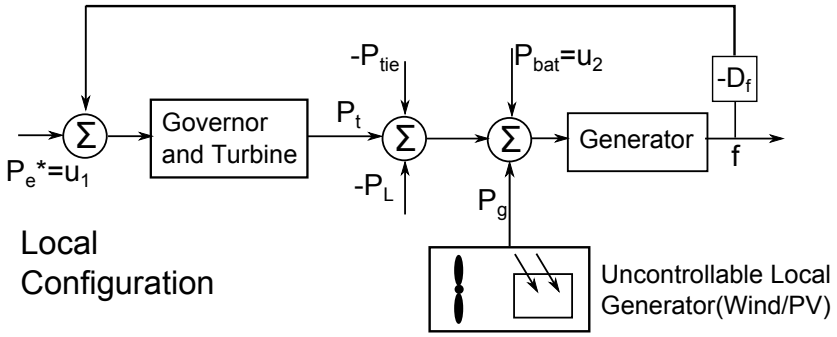

Figure 8.5: Control structure for each local power generation system

8.2.1 Dynamical model and system parameters

For the following equations, it is assumed once again that variables can be defined as $x = X_0 + \tilde{x}$, where X_0 is the equilibrium (initial) operative condition and $\tilde{x}$ is the variation around this value.

Power lines interactions

The proposed case study requires the treatment of power transmission between two nodes. Here, let us consider two nodes f and g, each one with respective voltage magnitudes V_f, V_g and angles θ_f, θ_g, as well as link impedance $Z_{fg} = i.X_{fg}$, where X_{fgj} is the power link reactance (active power lossless assumption), the following expressions describe the instantaneous active power (P_{tfg}) transmitted from node f to node g [1]:

$$P_{tfg} = \frac{V_f V_g}{X_{fg}} sin(\theta_f - \theta_g) \tag{8.15}$$

From (8.15) it can be seen how voltage magnitude and angle at each node, fix the amount of active power transmitted between them. Taking into account that nodes voltage variations are small, it can be obtained the small signal expression for the power transmitted between the two nodes, in terms of their voltage angle variations [1]:

$$\begin{aligned} \widetilde{p}_{tfg} &\simeq \frac{V_{f0} V_{g0}}{X_{fg}} cos(\theta_{f0} - \theta_{g0}).(\widetilde{\theta}_f - \widetilde{\theta}_g) \\ \widetilde{p}_{tfg} &\simeq K_{tfg}(\widetilde{\theta}_f - \widetilde{\theta}_g) \end{aligned} \tag{8.16}$$

Microgrid dynamical model

Due to the similar configuration of each generator and their identical connectivity with the other ones, a similar dynamical model represents the dynamics of each area. For a particular area i and based on the local configuration scheme included in Fig. 8.5, the following expressions are obtained (recall that u_1 is the reference power for the governor and u_2 is the injected power from the battery):

$$\begin{array}{rl} \dot{\widetilde{\theta}}_i = & 2\pi\widetilde{f}_i \\ \dot{\widetilde{f}}_i = & \frac{1}{T_{Ni}}[-\widetilde{f}_i + K_{Ni}(\widetilde{p}_{t,i} + \widetilde{p}_{g,i} + \widetilde{u}_{2,i} - \widetilde{p}_{L,i} - \widetilde{p}_{tie,i})] \\ \dot{\widetilde{p}}_{t,i} = & \frac{1}{T_{Gi}}[-\widetilde{p}_{t,i} + G_{ti}(\widetilde{u}_{1,i} - D_{fi}\widetilde{f}_i)] \\ \dot{\widetilde{soc}}_i = & -K_{si}.\widetilde{u}_{2,i} \end{array} \tag{8.17}$$

Where θ_i is the voltage angle, f_i is the frequency, $p_{t,i}$ is the transmitted mechanical power, soc_i is the state of charge, $p_{g,i}$ is the power injected by the uncontrollable generator unit, $p_{L,i}$ is the local load and $p_{tie,i}$ is the total power transmitted from the unit to the other ones. Additionally, T_{Ni} and K_{Ni} are the generator equivalent time constant and gain, T_{Gi} and G_{ti} are the time constant and the gain of the governor-turbine system and D_{fi} is the droop-frequency coefficient and K_{si} is a gain associated with the capacity of the battery.
In typical hydroelectric generators, $T_{Gi} << T_{Ni}$. Therefore, one can assume $\dot{\widetilde{p}_{ti}} \cong 0$, allowing to write the dynamical model of each area as:

$$\begin{array}{rl} \dot{\widetilde{\theta}}_i = & 2\pi\widetilde{f}_i \\ \dot{\widetilde{f}}_i = & \frac{1}{T_{Ni}}[-\widetilde{f}_i \underbrace{(1 + K_{Ni}G_{ti}D_{fi})}_{a_i} + \underbrace{K_{Ni}G_{ti}}_{b_i}\widetilde{u}_{1,i} + K_{Ni}\widetilde{p}_{g,i} - K_{Ni}\widetilde{p}_{L,1} - K_{Ni}\widetilde{p}_{tie,i}] \\ \dot{\widetilde{soc}}_i = & -K_{si}.\widetilde{u}_{2,i} \end{array} \tag{8.18}$$

Next, one can write the power transmitted from area i to area $j = 1 \cdots n, j \neq i$, where n the number of areas in the following way (based in (8.16)):

$$\widetilde{p_{tiei}} = \overbrace{\sum_{j \neq i} K_{tij}}^{g_{tij}}(\widetilde{\theta}_i - \widetilde{\theta}_j) \tag{8.19}$$

By replacing (8.19) in (8.18) one obtains the dynamical model of one particular area in terms of its own variables and also variables from other areas (interactions). The model for each area is then represented by:

$$\begin{array}{rl} \dot{\widetilde{\theta}}_i = & 2\pi\widetilde{f}_i \\ \dot{\widetilde{f}}_i = & \frac{1}{T_{Ni}}[-a_i\widetilde{f}_i + b_i\widetilde{u}_i + K_{Ni}\widetilde{p}_{gi} - K_{Ni}\widetilde{p}_{L1} - K_{Ni}g_{tij}\widetilde{\theta}_i] + \frac{K_{Ni}}{T_{Ni}}g_{tij}\widetilde{\theta}_j \\ \dot{\widetilde{soc}}_i = & -K_{si}.\widetilde{u}_{2,i} \end{array} \tag{8.20}$$

Defining the states vector $x_{(i)} = [\widetilde{\theta}_i \;\; \widetilde{f}_i \;\; \widetilde{soc}_i]^T$, control vector $u_{(i)} = [\widetilde{u}_{1,i} \;\; \widetilde{u}_{2,i}]^T$, disturbances vector $d_{(i)} = [\widetilde{p}_{Li} \;\; \widetilde{p}_{gi}]^T$ and interactions vector $v_{(i)}$, that only relies on $x_{(j)}$, the following state space model is obtained for each area i:

$$\begin{array}{rl} \dot{x}_{(i)}(t) = & A_{ii,c}x_{(i)}(t) + B_{ii,c}u_{(i)}(t) + E_{ii,c}d_{(i)}(t) + v_{(i),c}(t) \\ \dot{x}_{(i)}(t) = & \begin{bmatrix} 0 & 2\pi & 0 \\ -g_{tij}K_{Ni}/T_{Ni} & -a_i/T_{Ni} & 0 \\ 0 & 0 & 0 \end{bmatrix} x_{(i)}(t) + \begin{bmatrix} 0 & 0 \\ b_i/T_{Ni} & K_{Ni}/T_{Ni} \\ 0 & -K_{si} \end{bmatrix} u_{(i)}(t) + \\ & \begin{bmatrix} 0 & 0 \\ -K_{Ni}/T_{Ni} & K_{Ni}/T_{Ni} \\ 0 & 0 \end{bmatrix} d_{(i)}(t) + \frac{1}{T_{Ni}}\sum_{j \neq i} \begin{bmatrix} 0 & 0 & 0 \\ g_{tij} & 0 & 0 \\ 0 & 0 & 0 \end{bmatrix} x_{(j)}(t) \end{array} \tag{8.21}$$

Considering that discrete-time models are used for local MPC-based coordination, such model for each area, considering the sampling time T_s, we get:

$$\begin{aligned} x_{(i)k+1} = \;& A_{ii}x_{(i)k} + B_{ii}u_{(i)k} + E_{ii}d_{(i)k} + v_{(i)k} \\ x_{(i)k+1} = \;& \begin{bmatrix} 1 & 2\pi T_s & 0 \\ -g_{tij}K_{Ni}T_s/T_{Ni} & 1 - a_iT_s/T_{Ni} & 0 \\ 0 & 0 & 1 \end{bmatrix} + \begin{bmatrix} 0 & 0 \\ b_iT_s/T_{Ni} & K_{Ni}T_s/T_{Ni} \\ 0 & -K_{si} \end{bmatrix} u_{(i)k} + \\ & \begin{bmatrix} 0 & 0 \\ -K_{Ni}T_s/T_{Ni} & K_{Ni}T_s/T_{Ni} \\ 0 & 0 \end{bmatrix} d_{(i)k} + \tfrac{T_s}{T_{Ni}} \textstyle\sum_{j\neq i} \begin{bmatrix} 0 & 0 & 0 \\ g_{tij} & 0 & 0 \\ 0 & 0 & 0 \end{bmatrix} x_{(j)}(t) \end{aligned} \tag{8.22}$$

Numerical values

The parameters as well as initial values for voltage magnitudes and angles, obtained after a *load flow analysis*, are shown in Table 8.2, based in information taken from [1, 18].

Table 8.2: Parameters for the Two areas microgrid

PARAMETER	**VALUE** [units]
Voltages Magnitudes (V_1, V_2)	$1.00\ -0.9525$ [p.u]
Initial Voltages Angles (θ_1, θ_2)	$0.000\ -0.3094$ [rad]
Line Reactances (X_{12})	0.9 [p.u]
Equivalent Generator Gain (K_{N1}, K_{N2})	$110\ -80$
Equivalent Governor-Turbine Gain (G_{t1}, G_{t2})	$1.00\ -1.00$
Equivalent Generator Time Constant (T_{N1}, T_{N2})	$25\ -15$ [s]
Droop Frequency Gain (D_{f1}, D_{f2})	$0.25\ -0.40$ $[1/Hz]$
Max. Generated Power ($P_{T,max}$, each unit)	0.3 [p.u]
Max. Injectable Power ($P_{g,max}$, each unit)	0.25 [p.u]
Initial Injected Power $(P_{g1,0}, P_{g2,0})$	$0.00\ -0.00$ [p.u]
Max. Load Power ($P_{L,max}$, each unit)	0.5 [p.u]
Initial Local Load Powers $(P_{L1,0}, P_{L2,0})$	$0.20\ -0.20$ [p.u]

8.2.2 Control objectives

For this case study, the control strategy should minimize the frequency and state-of-charge deviations deviation, considering the injected and load power at each area, as well as minimize the voltage angle variations, with the objective of penalizing the excessive power transmitted between one area and its neighbors.
The following cost function is then chosen:

$$J_{gv} = \tfrac{1}{2}\left[\tilde{x}_N^T P \tilde{x}_N + \sum_{k=0}^{N-1}\left(\tilde{x}_k^T Q \tilde{x}_k + \tilde{u}_k^T R_u \tilde{u}_k + 2\tilde{u}_k^T S_u \tilde{x}_k\right)\right] + \tfrac{1}{2}\sum_{k=0}^{N-1}\left(\tilde{v}_k^T R_v \tilde{v}_k + 2\tilde{v}_k^T S_v \tilde{x}_k\right)$$

where weighting matrices are chosen as:

$$Q = \begin{bmatrix} Q_{(1)} & 0 \\ 0 & Q_{(2)} \end{bmatrix} \;;\; R = \begin{bmatrix} R_{u(1)} & 0 \\ 0 & R_{u(2)} \end{bmatrix} \;;\; S = \begin{bmatrix} S_{u(1)} & 0 \\ 0 & S_{u(2)} \end{bmatrix}$$

where the block-diagonal structure is suitable for the distributed approach, and chosen with numerical values as:

$$Q_{(1)} = Q_{(2)} = \begin{bmatrix} 0.1 & 0 & 0 \\ 0 & 10 & 0 \\ 0 & 0 & 2 \end{bmatrix} \; ; \; R_{u(1)} = R_{u(2)} = \begin{bmatrix} 0.1 & 0 \\ 0 & 0.5 \end{bmatrix} \; ; \; S_{u(1)} = S_{u(2)} = [0]$$

$$R_{v(1)} = R_{v(2)} = \begin{bmatrix} 1000 & 0 & 0 \\ 0 & 1000 & 0 \\ 0 & 0 & 1000 \end{bmatrix} \; ; \; S_{v(1)} = S_{v(2)} = 0$$

The matrix P in the cost function is computed from the discrete-time Riccati algebraic equation with Q, R and S. With this matrix, one can ensure that a potential centralized strategy would *a priori* stabilize the system, having in considerations the disturbance effects [41].
The admissible variables values are defined according to the values reported in Table 8.2, referred to the initial conditions. For this motive, it is seen how all of them have negative values, making the origin one admissible point in the constraints polyhedral set. The vectors are:

$$\begin{array}{llll} x_{(1),max} = & x_{(2),max} = & [\pi/4 & 2 \quad 0.4]^T \\ x_{(1),min} = & x_{(2),min} = & [-\pi/4 & -2 \quad -0.3]^T \\ u_{(1),max} = & u_{(2),max} = & [0.45 & 0.5] \\ u_{(1),min} = & u_{(2),min} = & [-0.45 & -0.5] \\ d_{(1),max} = & d_{(2),max} = & [0.8 & 0.45]^T \\ d_{(1),min} = & d_{(2),min} = & [-0.5 & -0.05]^T \end{array}$$

8.2.3 Simulation results

In this case study, it is compared two control strategies for the topology: a centralized MPC and the proposed distributed-coordinated algorithm. The idea is to analyze how different can be the proposed distributed control strategy, when compared with an MPC controller, using the same weights and objectives. After comparing the results, the construction of local invariant sets is included, only for verifying that closed loop system performance is compatible to the admissible states values.

For this system, an initial load flow analysis was performed to obtain the voltages angles for some assumed initial loads. Such initial values are included in Table 8.2, where it is seen that angles and disturbance are within the operative ranges.
Because the objective of this case study is to perform the coordination between the areas, under some uncontrollable injected power, some profiles inspired by wind power and photovoltaic power production were considered. The inclusion of batteries aids to the system stability due to their capacity to deliver/absorb power in a fast way.

Proposed distributed-coordinated approach Vs. Centralized MPC: Performance comparison

The simulations were executed for both control strategies. The results for both control algorithms are shown in Fig. 8.6, where **MPC** refers to the centralized MPC approach, while **DMPC** refers to the distributed-coordinated algorithm (see Chapter 6), in a simulation of about $450s$. The figure shows the states (angle, chart "Angles" and state-of-charge, chart "SoC"), injected power from the generators (hydroelectric power at the chart "Hydro Power", while the injected

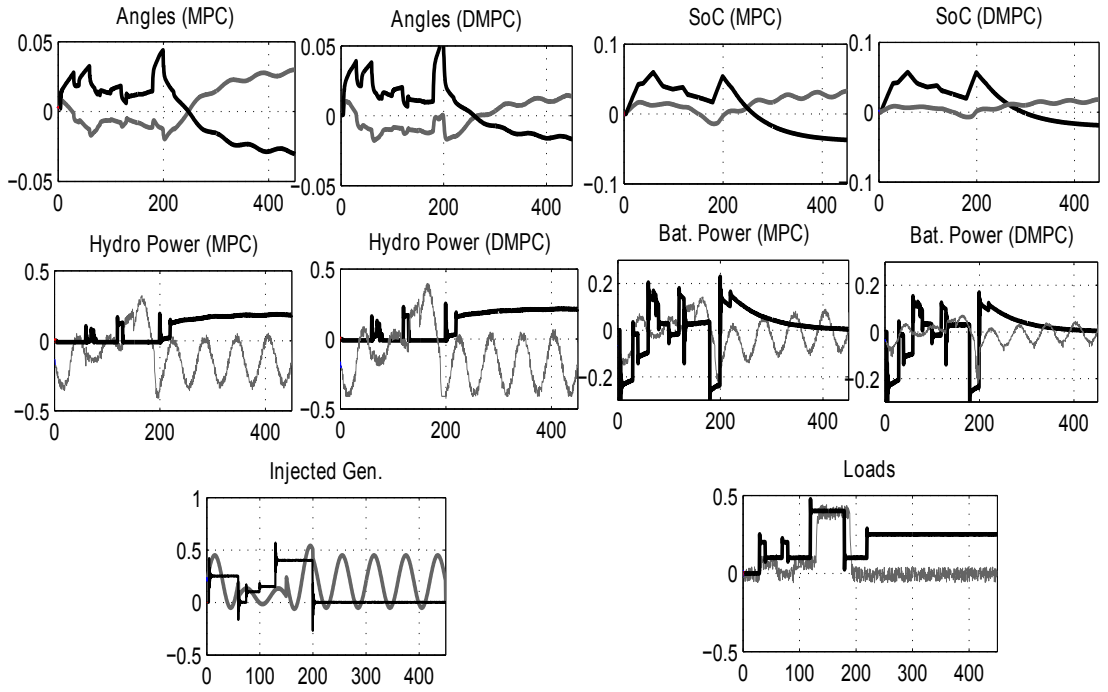

Figure 8.6: Simulation Results of Centralized MPC and Distrubuted-Coordinated Approach (DMPC) for the Multisource application (Bold: Area 1, Light: Area 2)

battery power is shown in the chart "Bat. Power"), and disturbances (local loads in the chart "Loads" and uncontrolled power generation from the alternative generator as "Injected Gen.") for both areas, according to the following line colors: Grey curves correspond to variables in **Area 1**, while black curves correspond to variables in **Area 2**. The frequency is not represented, but it is assured to have zero value (no variations around the initial value) for both scenarios.
Looking at the simulation results results, it is seen that all variables respects the constraints defined in Section 8.2.2 for this case study. Also, it is remarked how the action of hydroelectrics and batteries assures the system stability: the batteries absorb/inject enough power for maintaining the angle variations as low as possible, while the hydroelectrics deliver enough power for accomplishing the load demand. It can be that when the power demand can be covered by the injected power from the renewable source, the hydroelectric reduces its generated power.

Computation of invariant sets

It is remarked to the reader that Chapter 7 is devoted to the computation of invariant sets for constrained controlled systems, considering also the case in which the proposed coordination approach is used as control strategy.
According to the system model, from the centralized point of view, it is of order 6. Therefore, a graphical representation of the invariant set is not possible and the performance analysis would not be easy. However, the small-gain theorem and the real-bound lemma are used for concluding about the closed loop stability, considering the control structure and the disturbances.
Taking into consideration the procedure described in Section 7.2, the following results are obtained for the small-gain theorem application and the real-bound lemma:

- The small gain theorem is accomplished, due to the obtained gains $\gamma_G = 3.2$ (system gain) and , $\gamma_K = 0.02$ (controller gain). Thus, $\gamma_G.\gamma_K = 0.064 < 1$.
- Using the real-bound lemma, the matrix P, used for obtaining the approximation of the invariant set, is defined as:

$$P = \begin{bmatrix} 9.979 & 16.321 & -0.115 & -9.480 & -15.590 & 0.1763 \\ 16.321 & 65.6498 & -0.1751 & -14.998 & -51.2879 & 0.297 \\ -0.1149 & -0.1751 & 493.04 & 0.1208 & 0.2049 & 0.2548 \\ -9.4804 & -14.9979 & 0.1208 & 9.9367 & 16.6513 & -0.1668 \\ -15.5892 & -51.2879 & 0.2049 & 16.6513 & 64.5594 & -0.2698 \\ 0.1763 & 0.2972 & 0.2548 & -0.1668 & -0.2698 & 484.1835 \end{bmatrix} \tag{8.23}$$

Considering the subsystems model, weight matrices and admissible signal values, it is possible to compute inner approximation of the minimal robust invariant set, as proposed in Section 7.3. The approximations of the locals mRPI sets are shown in Fig. is suitable to this example, giving us a representation of the mRPI for each subsystem. It is seen how the critical states (angle and frequency) are indeed close to the origin, giving thus good guarantees of the power system stability for the test conditions, using the proposed distributed-coordinated approach. Evidently, if the system uses other set-point, it is necessary to recalculate the invariant sets. This aspect is to be reviewed in further works.

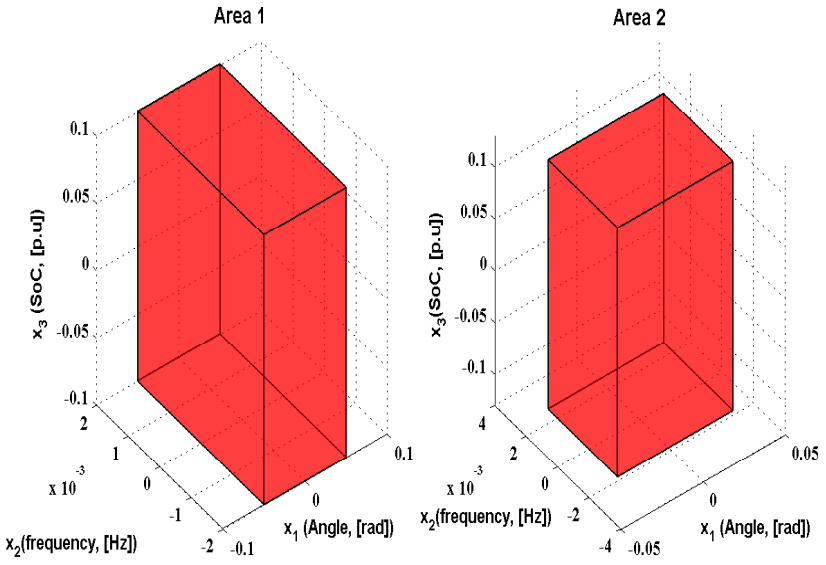

Figure 8.7: Approximations of local minimal invariant sets for the proposed microgrid

8.2.3.1 Concluding remarks

In this second part, an application of the distributed coordinated control strategy was adopted for the classical scenario of multi-area power generation system. Each area is composed by a hydroelectric generator, an uncontrollable generator, that delivers the maximum amount of available power, and a battery for injecting/absorbing power, according to the demanded by the load or the

excess injected bu the alternative generator.
The control objectives (angle variations and battery state-of-charge) were maintained in suitable levels, with both control strategies: centralized MPC and distributed-coordinated. The system constraints were also respected and the delivered power corresponds to the demanded at each area. The obtained results are in the same line than other works for the LFC problem [18, 39, 131], allowing to initially conclude that the proposed technique can be applicable in real scenarios. This is confirmed after computing the approximation of minimal invariant sets for each area, from where is inferred that states will be bounded in a small region, that includes the origin.

8.3 Conclusions

In this chapter, two illustrative case-studies were presented for evaluating the pertinence of the proposed distributed coordinated control strategy. In the first one, a two-area application with storage devices was presented. Here, the control strategy ensured the system performance by using the battery as absorbing element for high-frequency load power discharges. When coordination is lost in one unity, the system performance maintains the bounded conditions for states and inputs in both systems, although the global performance is affected.
In the second example, also a two-area scenario with hydroelectric and uncontrollable generators, along battery for each area was considered. In this example, the idea was use the distributed-coordinated strategy for a classical power system problem, and was compared with a centralized MPC approach. According to the results, the proposed methodology is suitable to be implemented ensuring both the global system performance and the constraints respect, after evaluating the approximation of the minimal invariant set, that is bounded in a small region close to the origin.

Chapter 9

CONCLUSIONS AND FUTURE WORKS

In this last chapter, a balance is made from the different conclusions given in the present manuscript, and some possible perspectives are proposed.

About the general context, let us first recall that the impact of electricity for usual development of the society, along with other sources for electricity generation or transport applications (oil, natural gas, wood), speaks in favor of the development of better strategies for the coordination of distributed power generation systems - in particular when based on renewable sources (as in the case of fuel cells, wind turbines, photovoltaic panels, hydroelectric, among other ones), and for their connexion to the grid. Due to interconnectivity and geographical disposition, such power systems can be included in the category of large-scale systems, not only considering their size, but also their dynamical modeling and performance requirements. For this reason, possible *decentralized* and *distributed* control structures were presented, beyond the *centralized* one, highlighting their advantages and restrictions.
Considering the multi-energy and spatial distribution aspects of the power sources, as well as the data interchange requirements between the elements of the control structure, a focus was even given on *distributed-coordinated* control, and more precisely with *price-driven coordination*.
About power generation systems, a special attention was paid to four of the most popular renewable-based technologies: hydroelectric, fuel cell, wind turbine and photovoltaic systems. But since the thesis was not directed to a deep study of each one of the technologies in terms of power conversion strategies, only important remarks on power production limitations, dynamical performance and conventional control strategies were presented, and a summarizing comparative chart was finally given.

About control methods, the well-known MPC (Model Predictive Control) plays a central role in the thesis, in particular owing to explicit formulation, which is of particular interest for real-time applications, in which constraints should also be considered. In that respect, the QP approach for the optimization solving, and the geometrical interpretation for constraints handling were recalled.
Finally, the theoretical principles for invariant set computation were presented, as an interesting tool for the analysis of closed-loop constrained dynamical systems subject to bounded disturbances.

Beyond those preliminary considerations, and also consequently to them, the contributions of the thesis can be summarized as follows:
First, an example of power control in a renewable-based generation system was considered, chosen here as the problem of *power production maximization with a wind turbine, in the case when no wind speed measurement is available*. For this problem, an observer-based approach was proposed, for a real-time estimation of the power characteristic of the turbine, directly related with the wind speed. On this basis, an optimal reference for the angular generator speed could be obtained,

and then used for the control strategy. This scheme was tested in simulation for measured and unmeasured wind speed cases, showing how it can offer stable operation in case of sensor damage for instance.

The second contribution was the development of a *power coordination algorithm, based on constrained MPC, for the management of power produced in a fuel-cell/wind-turbine/battery microgrid*, for low power applications. Here, the MPC problem was solved with the explicit method, and the wind turbine was considered as an non-managed power generation unit, considering that its power production was maximized by an external entity. The proposed solution shows an appropriate power management that respects the constraints imposed by the fuel cell (limited bandwidth generator) and the support battery (range of state-of-charge), for load dynamics that can be significant.

A third contribution, directed to the coordination of systems such as distributed electric power generation ones, was proposed for a distributed-coordinated control structure, under constraints, and using a price-driven coordination methodology. The idea is to distribute the control problem among subsystems, while globally taking constraints into account, so as to end up with some *explicit solution for coordinated control under constraints*. In practice, each subsystem solves an unconstrained MPC problem in order to obtain the local inputs, while receiving from the coordinator a price vector. This price is computed in such a way that its value ensures the constraints respect for all subsystems, and therefore, for the global system. The proposed control structure allows, in a possible communication loss between the coordinator and a subsystem, that the latter can switch to a local constrained control strategy, that under some hypothesis and system configuration, the constraints are respect to the subsystems, even though obviously reducing the global system performance.

A fourth contribution was the definition of an *algorithm for invariant set computation in the case of constrained MPC controlled systems*. In the MPC technique, the constraints on the control sequence can be written in terms of the current system state. For this reason, worst-case initial state trajectories are used for computing invariant sets.
First, the MPC-case was studied and the invariant set and its minimal outer approximation was computed, showing that system states can remain bounded in a region close to the origin, when a constrained MPC control and bounded disturbance are applied. This result can be useful in performance analysis of some dynamical system, by allowing to establish some settling time for test conditions for instance.
Still having the structure of MPC control in consideration, the same principles were used for the proposed distributed-coordination approach. For this case, not only the states but also the current disturbances modify the control vector, and consequently, also the coordination vector computed by the high-level agent. The most interesting result is that given the distributed structure of the problem, some ultimate bounds can be computed for each subsystem, based on the possibility to also compute the interactions among the subsystems. It was finally shown that one can compute an ultimate bound that contains a given approximation of the system invariant set, this last one being computed with an equivalent centralized model whose input is the coordination vector.

Finally, simulation results were appended to the former developments, for two case-studies, so as to better illustrate implementation aspects and some related performance on representative distributed power generation systems. A first case study includes a microgrid with a shared load and storage units, while the second one was also a two-area power system, in which synchronizing generators interact with uncontrollable power generators and batteries. The proposed control strategy responded adequately, validating in this way, its implementable capacities for real applications.

With respect to prospective developments after this thesis, the following items can be considered:

- Laboratory tests of the proposed power maximization strategy for wind turbines, with the objective of analyzing the turbine real-time behaviour, but also the applicability of the control approach, either as a reinforcement for faulty wind speed sensor events, or as an admissible general strategy.
- Extension of this proposed power maximization approach to the case with possible pitch angle action, not only to allow to work at large wind speed values, but also to allow for a more precise demanded power control.
- Further developments on the optimization problem decomposition for large scale systems, but considering the characteristics subsystems constraints, as well as a suitable structure for the coordination problem.
- Extension of the proposed coordination methodology to the case of different time scales between the coordination and generation loops, not only to ensure independence in the optimization routines, but also in order to add upper optimization layers, such as the ones related to power production according to market prices.
- Proposal of a benchmark in the sense of distributed power generation, that includes detailed models of grid elements (lines, transformers, circuit breakers, FACTS) and extended capacities for each power generation technology, and that allows different tests for control algorithms, considering centralized and distributed structures. The use of efficient and low-time demanding algorithms is an interesting challenge in this aspect.

Appendix A

Matrix Developments for the MPC and Distributed-Coordinated Strategies

In this annexe is shown the structure of each vector and matrix used in the MPC problem definition.

A.1 Matrices for the formulation of the centralized MPC problem

First, it is shown how are obtained the matrices for both, the predicted dynamic expression and the constraints definition for the centralized MPC problem.

Definition of the predicted dynamic matrices
Considering the following discrete-time state-space model:

$$x_{k+1} = Ax_k + Bu_k + Ed_k \tag{A.1}$$

where $x \in \Re^n$, $u \in \Re^m$ and $d \in \Re^q$. Define the following sequences, in the prediction horizon N, for states (x_k), inputs (u_k) and disturbance vectors (d_k), with their reference values (x_s, u_s, d_s):

$$\begin{array}{ll} \boldsymbol{x} = \begin{bmatrix} x_1 & \cdots & x_N \end{bmatrix}^T & \boldsymbol{x_s} = \begin{bmatrix} x_s & \cdots & x_s \end{bmatrix}^T \\ \boldsymbol{u} = \begin{bmatrix} u_0 & \cdots & u_{N-1} \end{bmatrix}^T & \boldsymbol{u_s} = \begin{bmatrix} u_{s0} & \cdots & u_{sN-1} \end{bmatrix}^T \\ \boldsymbol{d} = \begin{bmatrix} d_0 & \cdots & d_{N-1} \end{bmatrix}^T & \boldsymbol{d_s} = \begin{bmatrix} d_{s0} & \cdots & d_{sN-1} \end{bmatrix}^T \end{array} \tag{A.2}$$

Based in (A.1), the predicted states vector for instants $t = 1, 2 \cdots N$ is:

$$\begin{aligned} x_1 = &\quad Ax_0 + Bu_0 + Ed_0 \\ x_2 = &\quad Ax_1 + Bu_1 + Ed_1 = A^2x_0 + ABu_0 + AEd_0 + Ax_1 + Bu_1 + Ed_1 \\ &\vdots \\ x_N = &\quad A^Nx_0 + A^{N-1}Bu_0 + A^{N-2}Bu_1 + \cdots + Bu_{N-1} + A^{N-1}Ed_0 + A^{N-2}Ed_1 + \cdots + Ed_{N-1} \end{aligned} \tag{A.3}$$

With the vector sequences (A.2), one can write the predicted states vector, after (A.3) as:

$$\boldsymbol{x} = \Omega x_0 + \Gamma \boldsymbol{u} + \Theta \boldsymbol{d} \tag{A.4}$$

Where the matrices Ω, Γ and Θ are defined as:

$$\Omega = \begin{bmatrix} A \\ A^2 \\ \vdots \\ A^N \end{bmatrix} \quad \Gamma = \begin{bmatrix} B & 0 & \cdots & 0 \\ AB & B & \cdots & 0 \\ \vdots & \vdots & \ddots & \vdots \\ A^{(N-1)}B & A^{(N-2)}B & \cdots & B \end{bmatrix} \quad \Theta = \begin{bmatrix} E & 0 & \cdots & 0 \\ AE & E & \cdots & 0 \\ \vdots & \vdots & \ddots & \vdots \\ A^{(N-1)}E & A^{(N-2)}E & \cdots & E \end{bmatrix} \tag{A.5}$$

Constraints definition for the QP problem

The system constraints are expressed as follows:

$$\begin{array}{rcl} x_{min} \leq & x_k \leq & x_{max} \\ u_{min} \leq & u_k \leq & u_{max} \\ \delta u_{min} \leq & u_k - u_{k-1} \leq & \delta u_{max} \end{array} \tag{A.6}$$

The propose is write the constraints for the prediction horizon N in terms of the control sequence $\boldsymbol{u}$, given that the optimization problem searches the optimal control sequence, as seen in Section 4.1.

Before proceding individually for each constraint, first define the following admissible states, inputs and input's derivative vectors, for the prediction horizon N:

$$\begin{array}{ll} \boldsymbol{x_{max}} = \begin{bmatrix} x_{max} & \cdots & x_{max} \end{bmatrix}^T & \boldsymbol{x_{min}} = \begin{bmatrix} x_{min} & \cdots & x_{min} \end{bmatrix}^T \\ \boldsymbol{u_{max}} = \begin{bmatrix} u_{max} & \cdots & u_{max} \end{bmatrix}^T & \boldsymbol{u_{min}} = \begin{bmatrix} u_{min} & \cdots & u_{min} \end{bmatrix}^T \\ \boldsymbol{\delta u_{max}} = \begin{bmatrix} \delta u_{max} & \cdots & \delta u_{max} \end{bmatrix}^T & \boldsymbol{\delta u_{min}} = \begin{bmatrix} \delta u_{max} & \cdots & \delta u_{max} \end{bmatrix}^T \end{array} \tag{A.7}$$

States constraints

The states constraints can be written as follows:

$$x_{min} \leq x_k \leq x_{max} \tag{A.8}$$

This expression can be separated into two inequalities as follows:

$$\begin{array}{c} x_k \leq x_{max} \\ -x_k \leq -x_{min} \end{array} \tag{A.9}$$

Now, the sequence for state constraints can be obtained, in the same way that the states vector prediction (A.3) Taking the inequality $x_k \leq x_{max}$, the following predicted state constraints are obtained .

$$\begin{array}{ll} k = 1: & Ax_0 + Bu_0 + Ed_0 \leq x_{max} \\ k = 2: & Ax_1 + Bu_1 + Ed_1 = A^2x_0 + ABu_0 + AEd_0 + Ax_1 + Bu_1 + Ed_1 \leq x_{max} \\ \vdots & \\ k = N: & A^Nx_0 + A^{N-1}Bu_0 + A^{N-2}Bu_1 + \cdots + Bu_{N-1} + A^{N-1}Ed_0 + A^{N-2}Ed_1 + \cdots + \\ & +Ed_{N-1} \leq x_{max} \end{array} \tag{A.10}$$

Using (A.4) and (A.7), one can write the constraint $x_k \leq x_{max}$ for the prediction horizon N as:

$$\Gamma \boldsymbol{u} \leq \quad \boldsymbol{x_{max}} - \Omega x_0 - \Theta \boldsymbol{d_{max}} \tag{A.11}$$

A similar procedure is done with $x_{min} \leq x_k$, obtaining:

$$-\Gamma \boldsymbol{u} \leq \quad -\boldsymbol{x_{min}} + \Omega x_0 + \Theta \boldsymbol{d_{max}} \tag{A.12}$$

Defining, in this way, the state's constraints in terms of the control sequence.

Inputs constraints
The inputs constraints can be written as follows:

$$u_{min} \leq u_k \leq u_{max} \tag{A.13}$$

That can be separated into the following inequalities:

$$\begin{aligned} u_k &\leq u_{max} \\ -u_k &\leq -u_{min} \end{aligned} \tag{A.14}$$

Taking both inequalities from $k = 1 \cdots N-1$, one gets:

$$\begin{aligned} k = 0: &\quad u_0 \leq u_{max}; \quad -u_0 \leq -u_{min} \\ &\vdots \\ k = N-1: &\quad u_{N-1} \leq u_{max}; \quad -u_{N-1} \leq -u_{min} \end{aligned} \tag{A.15}$$

Therefore, one can express the inputs constraints with the inputs extreme vectors at (4.13) and the identity matrix $I_{N\times m}$, with N as the prediction horizon and m the size of the input vector, as follows:

$$\begin{aligned} I_{N\times m}\boldsymbol{u} &\leq \boldsymbol{u_{max}} \\ -I_{N\times m}\boldsymbol{u} &\leq -\boldsymbol{u_{min}} \end{aligned} \tag{A.16}$$

Considering the extended limits vectors $\boldsymbol{u_{max}} = [u_{max} \cdots u_{max}]^T$ and $\boldsymbol{u_{min}} = [u_{min} \cdots u_{min}]^T$.

Input's slew rate constraints
As made for the other constraints description, the slew rate of inputs can be specified as follows:

$$\delta u_{min} \leq u_k - u_{k-1} \leq \delta u_{max} \tag{A.17}$$

Again, the expression can be separated into two inequalities as:

$$\begin{aligned} u_k - u_{k-1} &\leq \delta u_{max} \\ -u_k + u_{k-1} &\leq -\delta u_{min} \end{aligned} \tag{A.18}$$

Performing the same procedure that for input constraints,one have:

$$\begin{aligned} k = 0: &\quad u_0 - u_{-1} \leq \delta u_{max}; \quad -u_0 + u_{-1} \leq -\delta u_{min} \\ k = 1: &\quad u_1 - u_0 \leq \delta u_{max}; \quad -u_1 + u_0 \leq -\delta u_{min} \\ &\vdots \\ k = N-1: &\quad u_{N-1} - u_{N-2} \leq \delta u_{max}; \quad -u_{N-1} + u_{N-2} \leq -\delta u_{min} \end{aligned} \tag{A.19}$$

Considering the vector of the sequence of admissible slew rate values $\boldsymbol{\delta u_{max}} = [\delta u_{max} \cdots \delta u_{max}]^T$ and $\boldsymbol{\delta u_{min}} = [\delta u_{min} \cdots \delta u_{min}]^T$, one can write the constraints at the input's slew rate as function of the previously applied input u_{-1} and the limit vectors in (4.5) as follows:

$$\begin{aligned} E_\delta \boldsymbol{u} &\leq \delta\boldsymbol{u_{max}} + E_{-1}u_{-1} \\ -E_\delta \boldsymbol{u} &\leq -\delta\boldsymbol{u_{min}} - E_{-1}u_{-1} \end{aligned} \tag{A.20}$$

with E_δ and E_{-1} defined as follows:

$$E_\delta = \begin{bmatrix} I_m & 0 & \cdots & 0 \\ -I_m & I_m & \cdots & 0 \\ \vdots & \ddots & \ddots & \vdots \\ 0 & \cdots & -I_m & I_m \end{bmatrix} \quad E_{-1} = \begin{bmatrix} I_m \\ 0 \\ \vdots \\ 0 \end{bmatrix} \tag{A.21}$$

Constraints polyhedral

The expressions (A.11), (A.16) and (A.20) let express the constraints, for the prediction horizon N in terms of the control sequence $\mathbf{u}$ as the following polyhedral:

$$L\boldsymbol{u} \leq \underbrace{\Delta + \bar{\xi}x_0 + \bar{\xi}_u u_{-1}}_{W} \tag{A.22}$$

The matrices used in (A.22) are next defined:

$$\begin{aligned} L = \begin{bmatrix} \phi \\ -\phi \end{bmatrix} \quad W = \begin{bmatrix} \bar{\Delta} \\ -\underline{\Delta} \end{bmatrix} + \begin{bmatrix} -\xi \\ \xi \end{bmatrix} x_0 + \begin{bmatrix} -\xi_u \\ \xi_u \end{bmatrix} u_{-1} \\ \text{Then,} \quad W = \Delta + \bar{\xi}x_0 + \bar{\xi}_u u_{-1} \end{aligned} \tag{A.23}$$

$$\begin{aligned} \phi = \begin{bmatrix} \Gamma \\ I_{N\times m} \\ E_\delta \end{bmatrix} \quad \bar{\Delta} = \begin{bmatrix} \boldsymbol{x_{max} - \Theta d_{max}} \\ \boldsymbol{u_{max}} \\ \boldsymbol{\delta u_{max}} \end{bmatrix} \quad \underline{\Delta} = \begin{bmatrix} \boldsymbol{x_{min} - \Theta d_{min}} \\ \boldsymbol{-u_{min}} \\ \boldsymbol{-\delta d_{min}} \end{bmatrix} \\ \xi = \begin{bmatrix} \Omega \\ 0_{N\times m} \\ 0_{N\times m} \end{bmatrix} \qquad \xi_{-1} = \begin{bmatrix} 0_{N\times m} \\ 0_{N\times m} \\ E_{-1} \end{bmatrix} \end{aligned} \tag{A.24}$$

As perform for the constrained MPC problem, the constraints are defined in terms of the control sequence.

A.2 Matrices for the formulation of the centralized MPC problem with interactions consideration

The same procedure is followed, but for the case in where interactions are considered in the dynamical model, as well as in the cost function.

Definition of the predicted dynamic matrices

Considering the following discrete-time state-space model:

$$x_{k+1} = A_d x_k + B_d u_k + E_d d_k + v_k \tag{A.25}$$

where $x \in \Re^n$, $u \in \Re^m$, $d \in \Re^q$ and $v \in \Re^r$, with $r \leq n$ according to the system configuration and interactions. Define the following sequences, in the prediction horizon N, for states (x_k), inputs (u_k), disturbance (d_k) and interactions vector (v_k), with their reference values (x_s, u_s, d_s, v_s):

$$\begin{aligned} \boldsymbol{x} &= \begin{bmatrix} x_1 & \cdots & x_N \end{bmatrix}^T & \boldsymbol{x_s} &= \begin{bmatrix} x_s & \cdots & x_s \end{bmatrix}^T \\ \boldsymbol{u} &= \begin{bmatrix} u_0 & \cdots & u_{N-1} \end{bmatrix}^T & \boldsymbol{u_s} &= \begin{bmatrix} u_{s0} & \cdots & u_{sN-1} \end{bmatrix}^T \\ \boldsymbol{v} &= \begin{bmatrix} v_0 & \cdots & v_{N-1} \end{bmatrix}^T & \boldsymbol{v_s} &= \begin{bmatrix} v_{s0} & \cdots & v_{sN-1} \end{bmatrix}^T \\ \boldsymbol{d} &= \begin{bmatrix} d_0 & \cdots & d_{N-1} \end{bmatrix}^T & \boldsymbol{d_s} &= \begin{bmatrix} d_{s0} & \cdots & d_{sN-1} \end{bmatrix}^T \end{aligned} \tag{A.26}$$

Based in (A.25), the predicted states vector for instants $t = 1, 2 \cdots N$ is:

$$\begin{aligned} x_1 = \;& A_d x_0 + B_d u_0 + E_d d_0 + v_0 \\ x_2 = \;& A_d x_1 + B_d u_1 + E_d d_1 + v_1 = A_d^2 x_0 + A_d B_d u_0 + A_d E_d d_0 + A_d v_0 + A_d x_1 + B_d u_1 + \\ & E_d d_1 + v_1 \\ \vdots \\ x_N = \;& A_d^N x_0 + A_d^{N-1} B_d u_0 + A_d^{N-2} B_d u_1 + \cdots + B_d u_{N-1} + A_d^{N-1} E_d d_0 + A_d^{N-2} E_d d_1 + \cdots \\ & + E_d d_{N-1} + \\ & A_d^{N-1} v_0 + A_d^{N-2} v_1 + \cdots + v_{N-1} \end{aligned} \tag{A.27}$$

With the vector sequences (A.26), one can write the predicted states vector, after (A.27) as:

$$\begin{aligned} \boldsymbol{x} &= \Omega_d x_0 + \Gamma_d \boldsymbol{u} + \Theta_d \boldsymbol{d} + \Lambda_d \boldsymbol{v} \\ \boldsymbol{x} &= \Omega_d x_0 + \underbrace{[\Gamma_d \ \Lambda_d]}_{\Psi_d} \boldsymbol{u_{ext}} + \Theta_d \boldsymbol{d} \end{aligned} \tag{A.28}$$

Where the matrices Ω_d, Γ_d, Θ_d and Λ_d are defined as:

$$\Omega = \begin{bmatrix} A_d \\ A_d^2 \\ \vdots \\ A_d^N \end{bmatrix} \quad \Gamma = \begin{bmatrix} B_d & 0 & \cdots & 0 \\ A_d B_d & B_d & \cdots & 0 \\ \vdots & \vdots & \ddots & \vdots \\ A_d^{(N-1)} B_d & A_d^{(N-2)} B_d & \cdots & B_d \end{bmatrix} \quad \Theta_d = \begin{bmatrix} E_d & 0 & \cdots & 0 \\ A_d E_d & E_d & \cdots & 0 \\ \vdots & \vdots & \ddots & \vdots \\ A_d^{(N-1)} E_d & A_d^{(N-2)} E_d & \cdots & E_d \end{bmatrix}$$
$$\Lambda_d = \begin{bmatrix} I & 0 & \cdots & 0 \\ A_d & I & \cdots & 0 \\ \vdots & \vdots & \ddots & \vdots \\ A_d^{(N-1)} & A_d^{(N-2)} & \cdots & I \end{bmatrix} \tag{A.29}$$

With $I \in \Re^{r \times r}$.
The same procedure is done with the interactions equation:

$$v_k = v_A x_k + v_B u_k + v_E d_k \tag{A.30}$$

The prediction of v_k between $k = 0 \cdots N-1$, using as dynamical equation (A.28) gives up:

$$\begin{aligned} v_0 = \ & v_A x_0 + v_B u_0 + v_E d_0 \\ v_1 = \ & v_A x_1 + v_B u_1 + vEd_1 = v_A A_d x_0 + vAB_d u_0 + v_A E_d d_0 + -v_A v_0 + v_1 \\ \vdots \\ x_N = \ & v_A A_d^{N-1} x_0 + v_A A_d^{N-2} B_d u_0 + A_d^{N-3} B_d u_1 + \cdots + v_B u_{N-1} + \\ & v_A A_d^{N-2} E_d d_0 + v_A A_d^{N-2} E_d d_1 + \cdots + v_E d_{N-1} - v_A A_d^{N-2} v_0 - v_A A_d^{N-3} v_1 + \cdots + v_{N-1} \end{aligned} \tag{A.31}$$

This expressions can be expressed in the following form:

$$\begin{aligned} \overline{\Lambda} \boldsymbol{v} = \ & \overline{\Gamma} \boldsymbol{u} + \overline{\Omega}\ x_0 + \overline{\Theta}\ \boldsymbol{d} \\ 0 = \ & \overline{\Psi} \boldsymbol{u_{ext}} + \overline{\Omega}\ x_0 + \overline{\Theta}\ \boldsymbol{d} \end{aligned} \tag{A.32}$$

Constraints definition for the QP problem with interactions consideration
For this system, the following constraints are obtained:

$$\begin{aligned} x_{min} \leq \ & x_k \leq \ & x_{max} \\ u_{min} \leq \ & u_k \leq \ & u_{max} \\ v_{min} \leq \ & v_k \leq \ & v_{max} \\ \delta u_{min} \leq \ & u_k - u_{k-1} \leq \ & \delta u_{max} \end{aligned} \tag{A.33}$$

where v_{max} and v_{min} are obtained from (A.30), by replacing the admissible values in states, inputs and disturbances.
The methodology applied for obtaining the constraints polyhedral in the centralized problem can be followed in this instance, for writing the constraints in terms of $\boldsymbol{u_{ext}}$. The constraints polyhedron and its matrices are here presented, in function of the matrices presented at (A.29)-(A.31):

$$\begin{aligned} L_{ext} \boldsymbol{u_{ext}} &\leq \bar{W} + W_x x_0 + W_u u_{e-1} \\ \begin{bmatrix} \phi_{ext} \\ -\phi_{ext} \end{bmatrix} \boldsymbol{u_{ext}} &\leq \begin{bmatrix} \bar{\Delta}_{ext} \\ -\underline{\Delta}_{ext} \end{bmatrix} + \begin{bmatrix} -\xi_{ext} \\ \xi_{ext} \end{bmatrix} x_0 + \begin{bmatrix} -\xi_{u-ext} \\ \xi_{u-ext} \end{bmatrix} u_{e-1} \end{aligned} \tag{A.34}$$

$$\phi_{ext} = \begin{bmatrix} \Psi_d \\ I_{N\times m} \quad 0_{N\times r} \\ 0_{N\times m} \quad I_{N\times r} \\ E_{\delta,ext} \quad 0_{N\times r} \end{bmatrix} \quad \bar{\Delta}_{ext} = \begin{bmatrix} \boldsymbol{x_{max} - \Theta d_{max}} \\ \boldsymbol{u_{max}} \\ \boldsymbol{v_{max}} \\ \boldsymbol{\delta u_{max}} \end{bmatrix} \quad \underline{\Delta}_{ext} = \begin{bmatrix} \boldsymbol{x_{min} - \Theta d_{min}} \\ \boldsymbol{u_{min}} \\ \boldsymbol{v_{min}} \\ \boldsymbol{\delta u_{min}} \end{bmatrix}$$

$$\xi_{ext} = \begin{bmatrix} \Omega_d \\ 0_{N\times m} \\ 0_{N\times r} \\ 0_{N\times m} \end{bmatrix} \quad \xi_{u-ext} = \begin{bmatrix} 0_{N(m+r)\times(m+r)} \\ 0_{Nm\times(m+r)} \\ 0_{Nr\times(m+r)} \\ E_{-1,ext} \end{bmatrix} \quad E_{\delta,ext} = \begin{bmatrix} I_m & 0_m & \cdots & 0_m \\ -I_m & I_m & \cdots & 0_m \\ \vdots & \vdots & \ddots & \vdots \\ 0_m & \cdots & -I_m & I_m \end{bmatrix}$$

$$E_{-1,ext} = \begin{bmatrix} I_m \\ 0_{(N-1)\times m} \end{bmatrix} \tag{A.35}$$

A.3 Definition of the constraints polyhedron for the coordinator optimization problem

As seen in Chapter 6, the explicit global solution for the decomposed system can be written in the following form (as in (6.39):

$$\begin{gathered} \boldsymbol{u_{ext}^{opt}} = -\boldsymbol{\varphi_1}(x_0 - x_s) - \boldsymbol{\varphi_2}(\boldsymbol{d - d_s}) - \boldsymbol{\varphi_3 p} + \boldsymbol{u_{ext-s}} \\ \boldsymbol{\varphi_1} = Y_u \widetilde{\boldsymbol{K}}_{\boldsymbol{1}}, \boldsymbol{\varphi_2} = Y_u \widetilde{\boldsymbol{K}}_{\boldsymbol{2}} Y_d^{-1}, \boldsymbol{\varphi_3} = Y_u \widetilde{\boldsymbol{K}}_{\boldsymbol{3}} \end{gathered} \tag{A.36}$$

Replacing this expression in (A.34), allows to express the constraints polyhedral in the coordination variable $\boldsymbol{p}$. It is obtained:

$$\begin{bmatrix} \phi_{ext} \\ -\phi_{ext} \end{bmatrix} [-\boldsymbol{\varphi_1}(x_0 - x_s) - \boldsymbol{\varphi_2}(\boldsymbol{d - d_s}) - \boldsymbol{\varphi_3 p} + \boldsymbol{u_{ext-s}}] \leq \begin{bmatrix} \bar{\Delta}_{ext} \\ -\underline{\Delta}_{ext} \end{bmatrix} + \begin{bmatrix} -\xi_{ext} \\ \xi_{ext} \end{bmatrix} x_0 + \begin{bmatrix} -\xi_{u-ext} \\ \xi_{u-ext} \end{bmatrix} u_{e-1} \tag{A.37}$$

Developing the expression for $\boldsymbol{p}$ and creating the following term f_s, that gathers all the set points from the original problem:

$$f_s = \boldsymbol{\varphi_1} x_s + \boldsymbol{\varphi_2 d_s} + \boldsymbol{u_{ext-s}}$$

Continuing with the developing of (A.37), it is obtained:

$$\begin{bmatrix} \phi_{ext}\boldsymbol{\varphi_3} \\ -\phi_{ext}\boldsymbol{\varphi_3} \end{bmatrix} \boldsymbol{p} \leq \begin{bmatrix} \bar{\Delta}_{ext} - \phi_{ext} f_s \\ -\underline{\Delta}_{ext} + \phi_{ext} f_s \end{bmatrix} + \begin{bmatrix} -\xi_{ext} + \phi_{ext}\boldsymbol{\varphi_1} \\ \xi_{ext} - \phi_{ext}\boldsymbol{\varphi_1} \end{bmatrix} x_0 + \begin{bmatrix} -\phi_{ext}\boldsymbol{\varphi_2} \\ \phi_{ext}\boldsymbol{\varphi_2} \end{bmatrix} \boldsymbol{d} + \begin{bmatrix} -\xi_{u-ext} \\ \xi_{u-ext} \end{bmatrix} u_{e-1} \tag{A.38}$$

From this expression, it is seen that constraints definition for the coordination problem depends now in the disturbance values, and still depends in the last applied control signal u_{e-1}. Defining the following matrices:

$$\begin{gathered} \bar{\Delta}_p = \bar{\Delta}_{ext} - \phi_{ext} f_s \quad \underline{\Delta}_p = \underline{\Delta}_{ext} - \phi_{ext} f_s \\ \xi_{xp} = \xi_{ext} - \phi_{ext}\boldsymbol{\varphi_1} \qquad \xi_{dp} = -\phi_{ext}\boldsymbol{\varphi_1} \qquad \phi_p = -\phi_{ext}\boldsymbol{\varphi_3} \end{gathered} \tag{A.39}$$

And the constraints polyhedron, for the coordination problem is:

$$\begin{bmatrix} \phi_p \\ -\phi_p \end{bmatrix} \boldsymbol{p} \leq \begin{bmatrix} \bar{\Delta}_p \\ -\underline{\Delta}_p \end{bmatrix} + \begin{bmatrix} -\xi_{xp} \\ \xi_{xp} \end{bmatrix} x_0 + \begin{bmatrix} -\xi_{dp} \\ \xi_{dp} \end{bmatrix} \boldsymbol{d} + \begin{bmatrix} -\xi_{u-ext} \\ \xi_{u-ext} \end{bmatrix} u_{e-1} \tag{A.40}$$

Appendix B

State Space Model Definition for Estimating the Parameter z to Maximize the Power Production in Wind Speed Sensorless Turbines

---

In this appendix is shown how is obtained the dynamical equation for implementing the Kalman-based observer for the wind speed sensorless wind turbine.
Let define the following parameter z, that is indeed an scaled version of the power coefficient:

$$z = C_p v_w^3 \tag{B.1}$$

where C_p is the power coefficient, that is considered constant, and v_w is the actual wind speed. Also, let assume the following structure for the wind speed:

$$\begin{aligned} v_w &= V_{w0} + \tilde{v}_w \\ \dot{\tilde{v}}_w &= -\alpha_v \tilde{v}_w + \eta_v \end{aligned} \tag{B.2}$$

where V_{w0} is the mean wind speed value (also considered constant), $\tilde{v}_w$ is the variation of the wind speed around its mean value, α_v is a coefficient that models the wind speed effective bandwidth for the turbine and η_v is a noisy component of the wind speed (zero mean).
Recall that one can write the speed variation of the generator w_e in terms of z and a control signal u (see (5.12)):

$$\dot{w_e} = \frac{K_1 z}{w_e} - K_2 w_e - K_3 u \tag{B.3}$$

Because the objective is to find the dynamical structure that will be used by the Kalman-like estimator, let us define the following states: $x_1 = w_e$ and $x_2 = z$. The derivative of x_1 is indeed (B.3), while the derivative of $x_2 = z$ is:

$$\begin{aligned} \dot{x_2} &= C_p(\dot{v_w^3}) \\ \dot{x_2} &= 3C_p v_w^2(\dot{v_w}) \\ \dot{x_2} &= 3C_p v_w^2[-\alpha_v(v_w - V_{w0}) + \eta_v] \\ \dot{x_2} &= -3\alpha_v \underbrace{C_p v_w^3}_{z} + 3\alpha_v C_p V_{w0} v_w^2 + \eta_z \\ \dot{x_2} &= -3\alpha_v x_2 + \underbrace{3\alpha_v C_p V_{w0} v_w^2}_{x_3} + \eta_z \end{aligned} \tag{B.4}$$

In the last equation of (B.4), the new state $x_3 = 3\alpha_v C_p V_{w0} v_w^2$, is created. One new derivate is done for this variable:

$$\begin{aligned} \dot{x_3} = &\quad 6\alpha_v C_p V_{w0} v_w(-\alpha_v v_w + \alpha_v V_{w0} + \eta_v) \\ \dot{x_3} = &\quad -[2\alpha_v(3\alpha_v C_p V_{w0} v_w^2)] + 6\alpha_v^2 C_p V_{w0}^2 v_w + \eta_{z3} \\ \dot{x_3} = &\quad -2\alpha_v x_3 + \underbrace{6\alpha_v^2 C_p V_{w0}^2 v_w}_{x_4} + \eta_{z3} \end{aligned} \tag{B.5}$$

In the last equation of (B.5), the new state $x_4 = 6\alpha_v^2 C_p V_{w0}^2 v_w$, is obtained. One last derivate to this term yields to:

$$\begin{aligned} \dot{x_4} = &\quad 6\alpha_v^2 C_p V_{w0}^2(-\alpha_v v_w + \alpha_v V_{w0} + \eta_v) \\ \dot{x_4} = &\quad -[\alpha_v(6\alpha_v^2 C_p V_{w0}^2 v_w)] + 6\alpha_v^3 C_p V_{w0}^3 + \eta_{z4} \\ \dot{x_4} = &\quad -\alpha_v x_4 + \underbrace{6\alpha_v^3 C_p V_{w0}^3}_{x_5} + \eta_{z4} \end{aligned} \tag{B.6}$$

The last expression of (B.6) includes the definition of $x_5 = 6\alpha_v^3 C_p V_{w0}^3$. Because it depends of constant parameters, its derivative is zero. Thus $\dot{x}_5 = 0$.
Now, let us consider the dynamic model:

$$\begin{aligned} \dot{x}(t) = &\quad A(y(t))x(t) + Bu(t) + \eta_{zobs} \\ y(t) = &\quad Cx(t) \end{aligned} \tag{B.7}$$

And assuming that $x_1 = w_e$ is the unique instrumented variable, one can write a dynamical model using expressions (B.3) - (B.6) and $\dot{x}_5 = 0$ as:

$$\begin{aligned} \dot{x}(t) = &\quad \begin{bmatrix} -K_2 & \frac{K_1}{y} & 0 & 0 & 0 \\ 0 & -3\alpha_v & 1 & 0 & 0 \\ 0 & 0 & -2\alpha_v & 1 & 0 \\ 0 & 0 & 0 & -\alpha_v & 1 \\ 0 & 0 & 0 & 0 & 0 \end{bmatrix} x(t) + \begin{bmatrix} -K_3 \\ 0 \\ 0 \\ 0 \\ 0 \end{bmatrix} u(t) + \begin{bmatrix} 0 \\ \eta_z \\ \eta_{z3} \\ \eta_{z4} \\ 0 \end{bmatrix} \\ y(t) = &\quad \begin{bmatrix} 1 & 0 & 0 & 0 & 0 \end{bmatrix} x(t) \end{aligned} \tag{B.8}$$

The model (B.8) is used for the Kalman-like observer, that delivers the estimation of z, used for the control algorithms. In further works techniques will be proposed some recommendations for the selection of the conditions V_{w0} and C_p for initializing the estimator without complications.

Bibliography

[1] P. Kundur, N. J. Balu, and M. G. Lauby, *Power system stability and control*, vol. 7. McGraw-hill New York, 1994.

[2] G. R. Walker and P. C. Sernia, "Cascaded dc-dc converter connection of photovoltaic modules," *Power Electronics, IEEE Transactions on*, vol. 19, no. 4, pp. 1130–1139, 2004.

[3] "Bp statistical review of world energy june 2014," 2014.

[4] Eurostat, "Energy, transport and environment indicators," 2014.

[5] J. Larminie, A. Dicks, and M. S. McDonald, *Fuel cell systems explained*, vol. 2. Wiley New York, 2003.

[6] J. Zárate-Florez, *Étude de Commande par Décomposition-Coordination pour l'Optimisation de la Conduite de Vallées Hydroélectriques.* PhD thesis, Université de Grenoble - École Doctorale EEATS, 2012.

[7] J. Sandoval-Moreno, G. Besançon, and J. J. Martinez Molina, "Lagrange Multipliers Based Price Driven Coordination with Constraints Consideration for Multisource Power Generation Systems," in *Proceedings of the ECC 2014*, (Strasbourg, France), pp. 1987–1992, June 2014.

[8] J. Sandoval-Moreno, G. Besancon, and J. J. Martinez Molina, "Model predictive control-based power management strategy for fuel cell/wind turbine/supercapacitor integration for low power generation system," in *Proceedings of the EPE 2013*, (Lille), 2013.

[9] J. Sandoval-Moreno, G. Besancon, and J. J. Martinez Molina, "Observer-based maximum power tracking in wind turbines with only generator speed measurement," in *Proceedings of the ECC 2013*, (Zurich, Suisse), pp. 478–483, July 2013.

[10] J. Sandoval-Moreno, J. Martínez Molina, and G. Besançon, "Optimal distributed-coordinated approach for energy management in multisource electric power generation systems," in *Topics in optimization based control and estimation* (S. Olaru, A. Grancharova, and F. Lobo Pereira, eds.), Springer Verlag, 2015.

[11] J. Sandoval-Moreno, G. Besançon, and J. J. Martinez Molina, "Stability analysis of distributed-mpc based in price driven coordination with invariant sets," *Internal Report, Gipsa Lab*, 2014.

[12] J. Sandoval-Moreno, G. Besancon, and J. J. Martinez Molina, "An observer-based method for maximizing the power production for wind speed sensorless eolian power generators," *Internal Report, Gipsa Lab*, 2014.

[13] S. Haykin and E. Moulines, "Special issue on large-scale dynamic systems," *Proceedings of the IEEE*, vol. 95, pp. 849–852, May 2007.

[14] R. Vadigepalli and F. Doyle, "Structural analysis of large-scale systems for distributed state estimation and control applications," *Control Engineering Practice*, vol. 11, no. 8, pp. 895 – 905, 2003. Process Dynamics and Control.

[15] M. Ilic, "From hierarchical to open access electric power systems," *Proceedings of the IEEE*, vol. 95, pp. 1060–1084, May 2007.

[16] S. Skogestad and I. Postlethwaite, *Multivariable Feedback Control.* Wiley, 2006.

[17] E. Camacho and C. Bordons, *Model Predictive Control.* Advanced Textbooks in Control and Signal Processing, Springer London, 2004.

[18] E. Camponogara, D. Jia, B. H. Krogh, and S. Talukdar, "Distributed model predictive control," *Control Systems, IEEE*, vol. 22, no. 1, pp. 44–52, 2002.

[19] R. Scattolini, "Architectures for distributed and hierarchical model predictive control : A review," *Journal of Process Control*, vol. 19, no. 5, pp. 723 – 731, 2009.

[20] B. T. Stewart, A. N. Venkat, J. B. Rawlings, S. J. Wright, and G. Pannocchia, "Cooperative distributed model predictive control," *Systems & Control Letters*, vol. 59, no. 8, pp. 460 – 469, 2010.

[21] M. Mesarovic, D. Macko, and Y. Takahara, *Theory of Hierarchical, Multilevel, Systems.* Academic Press, 1970.

[22] J. Venkat, A. Rawlings, and S. Wright, "Stability and optimality of distributed model predictive control," in *Proceedings of the ECC2005 and CDC2005*, 2005.

[23] G. Cohen, "Optimization by decomposition and coordination: a unified approach," *Automatic Control, IEEE Transactions on*, vol. 23, no. 2, pp. 222–232, 1978.

[24] J. Zárate-Florez, G. Besancon, J. J. Martinez Molina, and F. Davelaar, "Explicit price method for coordinated control and hydro-power production example," in *Proceedings of 8th IFAC Symposium on Power Plant and Power System Control*, (Toulouse, France), Sept. 2012.

[25] G. C. Goodwin, S. F. Graebe, and M. E. Salgado, *Control system design*, vol. 240. Prentice Hall New Jersey, 2001.

[26] G. Spagnuolo, G. Petrone, M. Vitelli, J. Calvente, C. Ramos-Paja, R. Giral, E. Mamarelis, and E. Bianconi, "A fast current-based mppt technique employing sliding mode control," *Industrial Electronics, IEEE Transactions on*, vol. PP, no. 99, p. 1, 2012.

[27] C. Ramos-Paja, C. Bordons, A. Romero, R. Giral, and L. Martinez-Salamero, "Minimum fuel consumption strategy for pem fuel cells," *Industrial Electronics, IEEE Transactions on*, vol. 56, no. 3, pp. 685–696, 2009.

[28] N. Rosero, J. M. Ramirez, and J. J. Martinez, "Minimization of water losses for optimal hydroelectric power generation," in *Control & Automation (MED), 2013 21st Mediterranean Conference on*, pp. 1322–1328, IEEE, 2013.

[29] J. Pukrushpan, A. Stefanopoulou, and H. Peng, "Control of fuel cell breathing," *Control Systems, IEEE*, vol. 24, pp. 30 – 46, apr 2004.

[30] A. E. Magri, F. Giri, A. Elfadili, and L. Dugard, "Wind sensorless control of wind energy conversion system with pms generator," in *Proc American Control Conf, Montreal Canada*, 2012.

[31] I. F. Bitterlin, "Modelling a reliable wind/pv/storage power system for remote radio base station sites without utility power," *Journal of Power Sources*, vol. 162, no. 2, pp. 906 – 912, 2006. Special issue including selected papers from the International Power Sources Symposium 2005 together with regular papers.

[32] P. Thounthong, S. Rael, and B. Davat, "Control strategy of fuel cell and supercapacitors association for a distributed generation system," *Industrial Electronics, IEEE Transactions on*, vol. 54, pp. 3225 –3233, dec. 2007.

[33] W. Greenwell and A. Vahidi, "Predictive control of voltage and current in a fuel cell/ultracapacitor hybrid," *Industrial Electronics, IEEE Transactions on*, vol. 57, pp. 1954–1963, June 2010.

[34] R. Sarrias, L. M. Fernández, C. A. García, and F. Jurado, "Coordinate operation of power sources in a doubly-fed induction generator wind turbine/battery hybrid power system," *Journal of Power Sources*, vol. 205, no. 0, pp. 354 – 366, 2012.

[35] J. Sandoval-Moreno, "Diseño, implementación y análisis de eficiencia de topologías de interconexión de pilas de combustible con sistemas de almacenamiento de energía auxiliares y cargas eléctricas," Master's thesis, Universidad del Valle, Escuela de Ingeniería Eléctrica y Electrónica, Colombia, 2011.

[36] D. Šiljak and A. Zečević, "Control of large-scale systems: Beyond decentralized feedback," *Annual Reviews in Control*, vol. 29, no. 2, pp. 169 – 179, 2005.

[37] C. Ocampo-Martinez, S. Bovo, and V. Puig, "Partitioning approach oriented to the decentralised predictive control of large-scale systems," *Journal of Process Control*, vol. 21, no. 5, pp. 775 – 786, 2011. Special Issue on Hierarchical and Distributed Model Predictive Control.

[38] H. Scherer, M. Pasamontes, J. Alvarez, J. Guzman, E. Camponogara, and J. Normey-Rico, "Distributed model predictive control for energy distribution," in *Proceedings of the ECC2013*, (Zurich), July 2013.

[39] D. Georges, "Distributed model predictive control based on decomposition-coordination and networking," in *Proceedings of the ECC*, 2009.

[40] I. Alvarado, D. Limon, D. Muñoz de la Peña, J. Maestre, M. Ridao, H. Scheu, W. Marquardt, R. Negenborn, B. D. Schutter, F. Valencia, and J. Espinosa, "A comparative analysis of distributed {MPC} techniques applied to the hd-mpc four-tank benchmark," *Journal of Process Control*, vol. 21, no. 5, pp. 800 – 815, 2011. Special Issue on Hierarchical and Distributed Model Predictive Control.

[41] G. Goodwin, M. Seron, and J. De Doná, *Constrained Control and Estimation: An Optimisation Approach*. Communications and control engineering, Springer-Verlag London Limited, 2005.

[42] P. D. Christofides, R. Scattolini, D. M. de la Peña, and J. Liu, "Distributed model predictive control: A tutorial review and future research directions," *Computers & Chemical Engineering*, vol. 51, no. 0, pp. 21 – 41, 2013.

[43] A. Rantzer, "Using game theory for distributed control engineering," *Language*, vol. 280, no. 53, p. 16, 2008.

[44] A. Rantzer, "Dynamic dual decomposition for distributed control," in *American Control Conference, 2009. ACC '09.*, pp. 884–888, June 2009.

[45] T. Mohamed, H. Bevrani, A. Hassan, and T. Hiyama, "Decentralized model predictive based load frequency control in an interconnected power system," *Energy Conversion and Management*, vol. 52, no. 2, pp. 1208–1214, 2011.

[46] W. Yan, L. Wen, W. Li, C. Chung, and K. Wong, "Decomposition coordination interior point method and its application to multi-area optimal reactive power flow," *International Journal of Electrical Power & Energy Systems*, vol. 33, no. 1, pp. 55 – 60, 2011.

[47] S. Roshany-Yamchi, M. Cychowski, R. R. Negenborn, B. De Schutter, K. Delaney, and J. Connell, "Kalman filter-based distributed predictive control of large-scale multi-rate systems: Application to power networks," *Control Systems Technology, IEEE Transactions on*, vol. 21, no. 1, pp. 27–39, 2013.

[48] R. Hermans, M. Lazar, A. Jokic, and P. van den Bosch, "Almost decentralized model predictive control of power networks," in *MELECON 2010-2010 15th IEEE Mediterranean Electrotechnical Conference*, pp. 1551–1556, IEEE, 2010.

[49] H. Ding, M. Alamir, and A. Hably, "A distributed cooperative control scheme with optimal priority assignment and stability assessment," *IFAC WC 2014*, pp. 1–8, 2013.

[50] A. Ferramosca, D. Limon, I. Alvarado, and E. Camacho, "Cooperative distributed {MPC} for tracking," *Automatica*, vol. 49, no. 4, pp. 906 – 914, 2013.

[51] A. Alessio, D. Barcelli, and A. Bemporad, "Decentralized model predictive control of dynamically coupled linear systems," *Journal of Process Control*, vol. 21, no. 5, pp. 705–714, 2011.

[52] R. R. Negenborn, P.-J. van Overloop, T. Keviczky, B. De Schutter, *et al.*, "Distributed model predictive control of irrigation canals.," *Networks and Heterogeneous Media*, vol. 4, no. 2, pp. 359–380, 2009.

[53] T. Keviczky, F. Borrelli, and G. J. Balas, "Decentralized receding horizon control for large scale dynamically decoupled systems," *Automatica*, vol. 42, no. 12, pp. 2105 – 2115, 2006.

[54] M. Farina and R. Scattolini, "Distributed predictive control: A non-cooperative algorithm with neighbor-to-neighbor communication for linear systems," *Automatica*, vol. 48, no. 6, pp. 1088 – 1096, 2012.

[55] S. Boyd, *Convex Optimization*. Cambridge, 2004.

[56] N. Sadati and M. Ramezani, "Novel interaction prediction approach to hierarchical control of large-scale systems," *Control Theory Applications, IET*, vol. 4, pp. 228–243, February 2010.

[57] P. Chawdhry and S. Ahson, "Application of interaction-prediction approach to load-frequency control (lfc) problem," *Systems, Man and Cybernetics, IEEE Transactions on*, vol. 12, pp. 66–71, Jan 1982.

[58] P.-D. Moroşan, R. Bourdais, D. Dumur, and J. Buisson, "Building temperature regulation using a distributed model predictive control," *Energy and Buildings*, vol. 42, no. 9, pp. 1445–1452, 2010.

[59] V. Y. Blouin, J. B. Lassiter, M. M. Wiecek, and G. M. Fadel, "Augmented lagrangian coordination for decomposed design problems," in *Proceedings of the 6th world congress on structural and multidisciplinary optimization, Rio de Janeiro*, vol. 30, Citeseer, 2005.

[60] M. Mahmoud, W. Vogt, and M. Mickle, "Decomposition and coordination methods for constrained optimization," *Journal of Optimization Theory and Applications*, vol. 28, no. 4, pp. 549–584, 1979.

[61] W. Qi, J. Liu, and P. D. Christofides, "A distributed control framework for smart grid development: Energy/water system optimal operation and electric grid integration," *Journal of Process Control*, vol. 21, no. 10, pp. 1504–1516, 2011.

[62] J. Zárate-Florez, J. Martinez, G. Besancon, and D. Faille, "Decentralized-coordinated model predictive control for a hydro-power valley," *Mathematics and Computers in Simulation*, vol. 91, pp. 108–118, 2012.

[63] H. Lund, "Renewable energy strategies for sustainable development," *Energy*, vol. 32, no. 6, pp. 912 – 919, 2007. Third Dubrovnik Conference on Sustainable Development of Energy, Water and Environment Systems.

[64] A. M. Omer, "Energy, environment and sustainable development," *Renewable and Sustainable Energy Reviews*, vol. 12, no. 9, pp. 2265 – 2300, 2008.

[65] H. Lund and B. Mathiesen, "Energy system analysis of 100systems—the case of denmark in years 2030 and 2050," *Energy*, vol. 34, no. 5, pp. 524 – 531, 2009. 4th Dubrovnik Conference 4th Dubrovnik conference on Sustainable Development of energy, Water & Environment.

[66] D. Burnett, E. Barbour, and G. P. Harrison, "The uk solar energy resource and the impact of climate change," *Renewable Energy*, vol. 71, no. 0, pp. 333 – 343, 2014.

[67] IDAE, "Energías renovables," 2014.

[68] D. Qian, J. Yi, and X. Liu, "Design of reduced order sliding mode governor for hydro-turbines," in *American Control Conference (ACC), 2011*, pp. 5073–5078, June 2011.

[69] T. Van Cutsem and C. Vournas, *Voltage stability of electric power systems*, vol. 441. Springer, 1998.

[70] O. Katsuhiko, "Modern control engineering," 2010.

[71] L. Scherer, C. Tischer, F. Posser, C. Franchi, and R. de Camargo, "Hybrid topology for voltage regulation applied in three-phase four-wire micro hydro power station," in *Industrial Electronics Society, IECON 2013 - 39th Annual Conference of the IEEE*, pp. 7169–7174, Nov 2013.

[72] S. Heier, *Grid Integration Of Wind Energy Conversion Systems*. Wiley, 2006.

[73] I. Munteanu, A. Bratcu, N. Cutululis, and E. Ceanga, *Optimal Control Of Wind Energy Systems: Towards a Global Approach*. Springer, 2008.

[74] F. Blaabjerg, Z. Chen, R. Teodorescu, and F. Iov, "Power electronics in wind turbine systems," in *Power Electronics and Motion Control Conference, 2006. IPEMC 2006. CES/IEEE 5th International*, pp. 1–11, 2006.

[75] E. Hau, *Wind Turbines: Fundamentals, Technologies, Applications, Economics*. Springer, 2006.

[76] K. Johnson, L. Pao, M. Balas, and L. Fingersh, "Control of variable-speed wind turbines," *Control Systems Magazine, IEEE*, vol. 26, no. 3, pp. 70–81, 2006.

[77] K. Busawon, L. Dodson, and M. Jovanovic, "Estimation of the power coefficient in a wind conversion system," in *Decision and Control, 2005 and 2005 European Control Conference. CDC-ECC '05. 44th IEEE Conference on*, pp. 3450 – 3455, dec. 2005.

[78] W. Leonhard, *Control of Electrical Drives*. Springer, 2001.

[79] L. Chen, F. Ponta, and L. Lago, "Perspectives on innovative concepts in wind-power generation," *Energy for Sustainable Development*, vol. 15, no. 4, pp. 398 – 410, 2011.

[80] R. Saidur, N. Rahim, M. Islam, and K. Solangi, "Environmental impact of wind energy," *Renewable and Sustainable Energy Reviews*, vol. 15, no. 5, pp. 2423 – 2430, 2011.

[81] M. G. Villalva, J. R. Gazoli, *et al.*, "Comprehensive approach to modeling and simulation of photovoltaic arrays," *Power Electronics, IEEE Transactions on*, vol. 24, no. 5, pp. 1198–1208, 2009.

[82] A. Yazdani, A. Di Fazio, H. Ghoddami, M. Russo, M. Kazerani, J. Jatskevich, K. Strunz, S. Leva, and J. Martinez, "Modeling guidelines and a benchmark for power system simulation studies of three-phase single-stage photovoltaic systems," *Power Delivery, IEEE Transactions on*, vol. 26, pp. 1247 –1264, april 2011.

[83] M. R. Patel, *Wind and solar power systems: design, analysis, and operation*. CRC press, 2012.

[84] R. Erickson and D. Maksimovic, *Fundamentals of Power Electronics*. Springer, 2001.

[85] E. Romero-Cadaval, G. Spagnuolo, L. Garcia Franquelo, C. Ramos-Paja, T. Suntio, and W. Xiao, "Grid-connected photovoltaic generation plants: Components and operation," *Industrial Electronics Magazine, IEEE*, vol. 7, pp. 6–20, Sept 2013.

[86] G. Petrone and C. Ramos-Paja, "Modeling of photovoltaic fields in mismatched conditions for energy yield evaluations," *Electric Power Systems Research*, vol. 81, no. 4, pp. 1003 – 1013, 2011.

[87] J. Bastidas, E. Franco, G. Petrone, C. Ramos-Paja, and G. Spagnuolo, "A model of photovoltaic fields in mismatching conditions featuring an improved calculation speed," *Electric Power Systems Research*, vol. 96, pp. 81–90, 2013.

[88] M. Orozco-Gutierrez, J. Ramirez-Scarpetta, G. Spagnuolo, and C. Ramos-Paja, "A method for simulating large pv arrays that include reverse biased cells," *Applied Energy*, vol. 123, pp. 157 – 167, 2014.

[89] M. Uzunoglu, O. Onar, and M. Alam, "Modeling, control and simulation of a pv/fc/uc based hybrid power generation system for stand-alone applications," *Renewable Energy*, vol. 34, no. 3, pp. 509–520, 2009.

[90] J.-H. Wee, "Applications of proton exchange membrane fuel cell systems," *Renewable and sustainable energy reviews*, vol. 11, no. 8, pp. 1720–1738, 2007.

[91] A. Arce, A. del Real, and C. Bordons, "Predictive control for battery performance improvement in hybrid pem fuel cell vehicles," in *Control Applications, 2008. CCA 2008. IEEE International Conference on*, pp. 696–701, Sept 2008.

[92] N. D. Benavides and P. L. Chapman, "Mass-optimal design methodology for dc-dc converters in low-power portable fuel cell applications," *Power Electronics, IEEE Transactions on*, vol. 23, no. 3, pp. 1545–1555, 2008.

[93] S. Naylor, V. Pickert, and D. Atkinson, "Fuel cell drive train topologies-computer analysis of potential systems," in *Power Electronics, Machines and Drives, 2006. The 3rd IET International Conference on*, pp. 398–403, IET, 2006.

[94] A. Emadi, Y. J. Lee, and K. Rajashekara, "Power electronics and motor drives in electric, hybrid electric, and plug-in hybrid electric vehicles," *Industrial Electronics, IEEE Transactions on*, vol. 55, no. 6, pp. 2237–2245, 2008.

[95] O. Onar, M. Uzunoglu, and M. Alam, "Modeling, control and simulation of an autonomous wind turbine/photovoltaic/fuel cell/ultra-capacitor hybrid power system," *Journal of Power Sources*, vol. 185, no. 2, pp. 1273 – 1283, 2008.

[96] J. P. Torreglosa, P. García, L. M. Fernández, and F. Jurado, "Energy dispatching based on predictive controller of an off-grid wind turbine/photovoltaic/hydrogen/battery hybrid system," *Renewable Energy*, vol. 74, no. 0, pp. 326 – 336, 2015.

[97] X. Yu, M. Starke, L. Tolbert, and B. Ozpineci, "Fuel cell power conditioning for electric power applications: a summary," *Electric Power Applications, IET*, vol. 1, pp. 643–656, Sept 2007.

[98] J. Maciejowski, *Predictive Control With Constraints*. Prentice Hall, 2002.

[99] G. K. H. Larsen, J. Pons, S. Achterop, and J. Scherpen, "Distributed mpc applied to power demand side control," in *Proceedings of the ECC 2013*, 2013.

[100] A. Bemporad, M. Morari, V. Dua, and N. Pistikopoulos, "The linear explicit quadratic regulator for constrained systems," *Automatica*, vol. 38, no. 4, pp. 3–20, 2002.

[101] M. Kvasnica, J. Hledík, I. Rauová, and M. Fikar, "Complexity reduction of explicit model predictive control via separation," *Automatica*, vol. 49, no. 6, pp. 1776 – 1781, 2013.

[102] H. Khalil, *Nonlinear Systems*. Prentice Hall, 2002.

[103] F. Blanchini, "Set invariance in control," *Automatica*, vol. 35, no. 11, pp. 1747 – 1767, 1999.

[104] S. Rakovic, E. Kerrigan, K. Kouramas, and D. Mayne, "Invariant approximations of the minimal robust positively invariant set," *Automatic Control, IEEE Transactions on*, vol. 50, pp. 406–410, March 2005.

[105] S. Olaru, J. A. De Doná, M. Seron, and F. Stoican, "Positive invariant sets for fault tolerant multisensor control schemes," *International Journal of Control*, vol. 83, no. 12, pp. 2622–2640, 2010.

[106] J. Martinez, *Commande Robuste et Tolerante aux Fautes: Application aux systèmes mécatroniques*. HDR - Université de Grenoble, 2013.

[107] C. E. de Souza and L. Xie, "On the discrete-time bounded real lemma with application in the characterization of static state feedback hinf controllers," *Systems and Control Letters*, vol. 18, no. 1, pp. 61 – 71, 1992.

[108] B. Grünbaum, *Convex Polytopes*. Graduate Texts in Mathematics, Interscience, 1967.

[109] S. Boyd, L. Ghaoui, E. Feron, and V. Balakrishnan, *Linear Matrix Inequalities in System and Control Theory*. Studies in Applied Mathematics, Society for Industrial and Applied Mathematics, 1994.

[110] A. Alessio, A. Bemporad, M. Lazar, and W. P. M. H. Heemels, "Convex polyhedral invariant sets for closed-loop linear mpc systems," in *Decision and Control, 2006 45th IEEE Conference on*, pp. 4532–4537, Dec 2006.

[111] J. Laks, L. Pao, and A. Wright, "Control of wind turbines: Past, present, and future," in *American Control Conference, 2009. ACC '09.*, pp. 2096–2103, 2009.

[112] M. Chinchilla, S. Arnaltes, and J. Burgos, "Control of permanent-magnet generators applied to variable-speed wind-energy systems connected to the grid," *Energy Conversion, IEEE Transactions on*, vol. 21, pp. 130 – 135, march 2006.

[113] L. Barote and C. Marinescu, "Modeling and operational testing of an isolated variable speed pmsg wind turbine with battery energy storage," *Advances in Electrical and Computer Engineering*, vol. 12, no. 2, pp. 81 – 88, 2012.

[114] A. Ticlea and G. Besancon, "Observer scheme for state and parameter estimation in asynchronous motors with application to speed control," *European Journal of Control*, vol. 12, pp. 1–13, 2006.

[115] G. Besancon, *Nonlinear observers and applications*. Springer, 2007.

[116] R. Stengel, *Optimal Control and Estimation*. Dover, 1994.

[117] J. Leyva-Ramos, J. Morales-Saldana, and M. Martinez-Cruz, "Robust stability analysis for current-programmed regulators," *Industrial Electronics, IEEE Transactions on*, vol. 49, pp. 1138–1145, Oct 2002.

[118] J. Sandoval-Moreno and E. Franco-Mejia, "Performance comparison between hinf and pid control strategies applied to boost power converters," in *IEEE Andescon*, 2010.

[119] Z. Gao, X. Zhang, and H. Lin, "Modeling and nonlinear control for the boost converter with constant power loads," in *Power and Energy Engineering Conference (APPEEC), 2010 Asia-Pacific*, pp. 1–4, March 2010.

[120] A. Isidori, *Nonlinear control systems*, vol. 1. Springer, 1995.

[121] J. Lagorse, D. Paire, and A. Miraoui, "Sizing optimization of a stand-alone street lighting system powered by a hybrid system using fuel cell, {PV} and battery," *Renewable Energy*, vol. 34, no. 3, pp. 683 – 691, 2009.

[122] F. Farret, *Integration of Alternative Sources of Energy*. Wiley-IEEE Press, 2006.

[123] S. Pandey, S. Mohanty, N. Kishor, and J. Catalão, "An advanced lmi-based-lqr design for load frequency control of an autonomous hybrid generation system," in *Technological Innovation for the Internet of Things* (L. Camarinha-Matos, S. Tomic, and P. Graça, eds.), vol. 394 of *IFIP Advances in Information and Communication Technology*, pp. 371–381, Springer Berlin Heidelberg, 2013.

[124] J. Van de Vegte, *Feedback control systems*. Prentice-Hall, Inc., 1993.

[125] P. Falcone, F. Borrelli, J. Pekar, and E. G. Stewart, "Reference governor for constrained piecewise affine systems. a vehicle dynamics control application," in *European Control Conference (ECC), 23-26 August 2009, Budapest, Hungary*, 2009.

[126] K. Kogiso and K. Hirata, "A reference governor in a piecewise state affine function," in *Decision and Control, 2003. Proceedings. 42nd IEEE Conference on*, vol. 2, pp. 1747–1752 Vol.2, Dec 2003.

[127] D. Q. Mayne, J. B. Rawlings, C. V. Rao, and P. O. Scokaert, "Constrained model predictive control: Stability and optimality," *Automatica*, vol. 36, no. 6, pp. 789–814, 2000.

[128] F. Borelli, A. Bemporad, and M. Morari, "Predictive control for linear and hybrid systems," 2014.

[129] D. Gayme and U. Topcu, "Optimal power flow with distributed energy storage dynamics," in *American Control Conference (ACC), 2011*, pp. 1536–1542, June 2011.

[130] J. Schiffer, T. Seel, J. Raisch, and T. Sezi, "A consensus-based distributed voltage control for reactive power sharing in microgrids," in *Control Conference (ECC), 2014 European*, pp. 1299–1305, June 2014.

[131] M. Zribi, M. Al-Rashed, and M. Alrifai, "Adaptive decentralized load frequency control of multi-area power systems," *International Journal of Electrical Power & Energy Systems*, vol. 27, no. 8, pp. 575 – 583, 2005.

[132] S. Papathanassiou, N. Hatziargyriou, K. Strunz, *et al.*, "A benchmark low voltage microgrid network," *Proceedings of the CIGRE Symposium: Power Systems with Dispersed Generation*, pp. 1–8, 2005.

[133] M. Brenna, E. De Berardinis, L. Delli Carpini, F. Foiadelli, P. Paulon, P. Petroni, G. Sapienza, G. Scrosati, and D. Zaninelli, "Automatic distributed voltage control algorithm in smart grids applications," *Smart Grid, IEEE Transactions on*, vol. 4, pp. 877–885, June 2013.

[134] T. Green and M. Prodanović, "Control of inverter-based micro-grids," *Electric Power Systems Research*, vol. 77, no. 9, pp. 1204 – 1213, 2007. Distributed Generation.

[135] K. Rudion, A. Orths, Z. Styczynski, and K. Strunz, "Design of benchmark of medium voltage distribution network for investigation of dg integration," in *Power Engineering Society General Meeting, 2006. IEEE*, pp. 6 pp.–, 2006.

[136] C. Sao and P. Lehn, "Autonomous load sharing of voltage source converters," *Power Delivery, IEEE Transactions on*, vol. 20, pp. 1009–1016, April 2005.

Résumé — Cette thèse porte principalement sur la coordination des systèmes distribués, avec une attention particulière pour les systèmes de production d'électricité multi-sources. Aux fins de l'optimalité, comme de la prose en compte de contraintes, la commande prédictive (MPC-*Model Predictive Control*) est choisie comme l'outil sous-jacent, tandis que les éoliennes, piles à combustible, panneaux photovoltaïques et les centrales hydroélectriques sont considérés comme les sources d'énergie à être contrôlées et coordonnées. En premier lieu, une application de la commande MPC dans un micro-réseau électrique est proposée, illustrant comment assurer une performance appropriée pour chaque unité de génération et de soutien. Dans ce contexte, une attention particulière est accordée à la production de puissance maximale par une éolienne, en prenant une commande basée sur un observateur quand la mesure de la vitesse du n'est pas disponible. Ensuite, les principes de contrôle distribué coordonné, en prenant une formulation à base de la commande MPC, sont considérés pour le contexte des systèmes à grande taille. Ici, une nouvelle approche pour la coordination par prix avec des contraintes est proposée pour la gestion des contrôleurs MPC locaux, chacun d'eux étant typiquement associé à une unité de génération. En outre, le calcul des espaces invariants a été utilisé pour l'analyse de la performance pour le système en boucle fermée, à la fois pour les schémas MPC centralisée et coordination par prix. Finalement, deux cas d'études dans le contexte des systèmes de génération d'électricité sont inclus, en illustrant la pertinence de la stratégie de commande coordonnée proposée.

Mots clés: Commande Prédictive Basée sur Modèle, Coordination des Grands Systèmes, Réseaux Multi-énergies, Espaces Invariants.

Abstract — This thesis is mainly about coordination of distributed systems, with a special attention to multi-energy electric power generation applications. For purposes of optimality, as well as constraint enforcement, the Model Predictive Control (MPC) is chosen as the underlying tool, while wind turbines, fuel cells, photovoltaic panels, and hydroelectric plants are mostly considered as power sources to be controlled and coordinated. In the first place, an application of MPC to a micro-grid system is proposed, illustrating how to ensure appropriate performance for each generator and support unit. In this context, a special attention is paid to the maximum power production by a wind turbine, via an original observer-based control when no wind speed measurement is available. Then, the principles of distributed-coordinated control, when taking an MPC-based formulation, are considered for the context of larger scale systems. Here, a new approach for price-driven coordination with constraints is proposed for the management of local MPC controllers, each of them being associated to one power generation unit typically. In addition, the computation of invariant sets is used for the performance analysis of the closed-loop control system, for both centralized MPC and price-driven coordination schemes. Finally, a couple of case studies in the field of power generation systems is included, illustrating the relevance of the proposed coordination control strategy.

Keywords: Model Predictive Control, Coordination of Large Scale Systems, Multienergy Networks, Invariant Sets.